Review

Not peer-reviewed version

A Technical Review of Quantum Computing Use-Cases for Finance and Economics

Manqoba Q. Hlatshwayo *, Manav Babel , Dalila Islas-Sanchez , Konstantinos Georgopoulos

Posted Date: 16 January 2026

doi: 10.20944/preprints202511.1802.v2

Keywords: quantum computing; quantum algorithms; fintech; finance; economics

Review

A Technical Review of Quantum Computing Use Cases for Finance and Economics

Manqoba Q. Hlatshwayo *, Manav Babel, Dalila Islas-Sanchez and Konstantinos Georgopoulos

National Quantum Computing Centre, UK
* Correspondence: manqoba.hlatshwayo@stfc.ac.uk

Abstract

Quantum computing has been rapidly evolving as a field, with innovations driven by industry, academia, and government institutions. The technology has the potential to accelerate computation for solving complex problems across multiple industrial sectors. Finance and economics, with many problems exhibiting computationally heavy requirements, is a high-profile sector where quantum computing could have a significant impact. Therefore, it is important to identify and understand to what extent the technology could find utility in the sector. This technical review is written for quantum applications researchers, quantitative analysts in finance and economics, and researchers in related mathematical sciences. It is divided into two parts: (i) a survey of quantum algorithms pertinent to problems in finance and economics, and (ii) mapping of several use cases in the sector to the potential quantum algorithms presented in part (i). We discuss some challenges on the pathway to achieving quantum advantage. Ultimately, this review aims to be a catalyst for interdisciplinary research that will accelerate the advent of the practical advantages of quantum technologies to solve complex problems in this sector.

Keywords: quantum computing; quantum algorithms; fintech; finance; economics

1. Introduction

Quantum computing was first theorised in the 1970s [1], and the new research field gained more momentum after Feynman's seminal talk [2]. At its core, quantum computing leverages the principles of quantum physics to process information. For problems that are intractable for classical computing, like simulation of complex quantum many-body systems, quantum computing is expected to solve them efficiently in a time frame that scales linearly with the system size [2,3]. In contrast, classical methods for such problems have computational times to solution that scale exponentially with system size. Furthermore, it was theorised that quantum computing could speed up computations for classically tractable problems like searching [4]. The landscape of proposed quantum algorithms that have speed-ups over their classical counterparts ranges from quadratic [4,5] to exponential [6,7]. Such theoretical discoveries, along with the rapid development of quantum hardware [8], have led many researchers to believe that quantum computing will have a significant impact across many disciplines and industry sectors.

In particular, in finance and economics, where complex calculations, large datasets, and optimisation problems are ubiquitous, quantum computing has the potential to improve computational efficiency for specific problem cases, provided certain conditions are met, such as efficient data loading and quantum error-correction [9]. For example, intricate models in finance for risk assessment, portfolio optimisation, fraud detection, and high-frequency trading, which generally require substantial use of high-performance computing, can potentially benefit from quantum computing. Similarly, economic modelling and simulation (particularly in macroeconomic forecasting, game theory, and

 doi:10.20944/preprints202511.1802.v2

market equilibrium analysis) could benefit from the integration of quantum processors in the computational pipeline. The expected gains with quantum computing methods are twofold: (i) large-scale, high-dimensional problems can be handled efficiently without resorting to many approximations and truncation as typically needed for classical computing approaches; and (ii) the computational time to solution can be significantly reduced, and accuracy improved for some categories of problems [10]. However, there are a few current bottlenecks in realising these potential gains, which include the challenge of efficiently loading and reading out data from a quantum computer [11,12].

This review explores some of the promising use cases in finance and economics where quantum computing could have a significant impact. We discuss the theoretical foundations of pertinent quantum algorithms, recent proof-of-concept implementations, and potential future implications. By examining these specific use cases, such as option pricing and risk management, this review highlights both the opportunities and limitations of quantum computing in the context of the aforementioned sectors. We aim to provide an objective analysis, providing a technical review of key quantum algorithms, corresponding use cases, and the overall state-of-the-art of quantum computing for finance and economics.

1.1. Motivation and Contributions

This review seeks to provide a bridge between use cases, as encountered by practitioners in finance and economics, and their potential solutions using quantum computing. This survey contributes towards stimulating interdisciplinary research to accelerate the development and demonstration of quantum computing *advantage* for applications in these sectors.

What is meant by *advantage* in quantum computing is often debated, since there is currently no unique definition for it. There are generally three terms commonly used in association with *quantum advantage*:

- *Computational Advantage* - also referred to as *Quantum Supremacy* [13], is a point where quantum computers can efficiently perform a task that is intractable for a classical computer. The task does not have to be directly useful for real-world applications, such as efficient random sampling from a particular probability distribution [14–17].
- *Quantum Utility* - a point when quantum computers can solve a problem more efficiently than classical brute force methods. This definition was first introduced by IBM Quantum in association with their work in simulating spin systems [18].
- *Practical Quantum Advantage* - a point where quantum computers can solve a problem more efficiently than the most advanced classical methods. In this case, the problem/task in question has real-world practical application(s) and impact in areas such as logistics, healthcare, finance, and economics.

Therefore, most researchers consider Practical Quantum Advantage (PQA) a monumental milestone that will unlock the benefits of quantum computing to the growth of the economy and society at large. Oxford Economics has quantified these benefits as an economy-wide productivity boost, which is projected to be up to 8.3% by 2055 in the UK, with initial gains from as early as 2034 [19]. Under reasonable assumptions, this is equivalent to each worker in the UK producing an extra one and a half weeks' worth of output annually, without putting in any additional hours [19]. Furthermore, the report estimates that by 2055, the quantum computing industry will contribute between £5.9 billion and £12.9 billion in total gross value added to the UK's GDP [19]. Globally, McKinsey [20] has projected that applications of quantum technologies in finance will contribute a total value of $622 billion by the year 2035. Hence, some analysts have predicted that the financial services sector will be one of the first industries to reap the benefits of quantum technologies [21].

Since the general expectation is that quantum computing will generate a lot of value both in the UK and globally, the key question is what is a viable path towards PQA? What are the hardware engineering and software algorithmic hurdles to overcome to achieve PQA? And what could accelerate

 doi:10.20944/preprints202511.1802.v2

the collaborative effort towards that common goal? This review seeks to contribute towards answering these questions by providing:

1. A survey of state-of-the-art quantum algorithms with potential applications in finance and economics.
2. A mathematical outline of use cases in the aforementioned sectors and viable quantum approaches towards an efficient solution. Note that this review is among the first to extend the scope of such a survey to cover use cases in economics.
3. A discussion of the technical challenges towards realising PQA of quantum computing applications in these sectors.

The following subsections outline how our contribution adds to previously published related survey reports and the benefits of the structure of this review.

1.2. Related Survey Reports

The interest in quantum computing use cases in finance is evident in the rapidly growing number of publications and investments in the field. The total number of papers, articles, and theses written on quantum computing for finance has grown from under 2,000 in 2014 to over 10,000 in recent years [22]. Commensurate with the growth of the field, regular survey reports of quantum computing in finance progressed from general overviews in the years 2019 to 2020, to specialised applications in Quantum Machine Learning and financial modelling in the years 2021 to 2024. This is a reflection of the field shifting toward practical implementations, with increasing focus on derivatives pricing, risk assessment, and quantum-enhanced financial strategies. Table 1 presents a sample list of related survey reports of quantum computing applications in finance from 2019 to 2025.

Table 1. Related survey papers on quantum computing applications in finance.

Year	First Author	Title of Publication
2019	Orús [9]	Quantum computing for finance: Overview and prospects
2020	Egger [23]	Quantum Computing for Finance: State-of-the-Art and Future Prospects
2020	Alcazar [24]	Classical versus quantum models in Machine Learning: insights from a finance application
2020	Hull [25,26]	Quantum Technology for Economists
2021	Pistoia [27]	Quantum Machine Learning for Finance ICCAD Special Session Paper
2022	García [28]	Systematic Literature Review: Quantum Machine Learning and its applications
2022	Albareti [29]	A Structured Survey of Quantum Computing for the Financial Industry
2022	Gómez [31]	A Survey on Quantum Computational Finance for Derivatives Pricing and VaR
2023	Herman [30]	Quantum computing for finance
2023	Chang [32]	The Prospects of Quantum Computing for Quantitative Finance and Beyond
2023	Naik [33]	From Portfolio Optimization to Quantum Blockchain and Security: A Systematic Review of Quantum Computing in Finance
2023	Saxena [34]	Financial modelling using quantum computing
2024	Jacquier [35]	Quantum Machine Learning and optimisation in finance
2024	Claudiu [36]	Enhancing the Financial Sector with Quantum Computing: A Comprehensive Review of Current and Future Applications
2024	Lu [37]	Quantum financing system: A survey on quantum algorithms, potential scenarios and open research issues
2024	Atadoga [38]	The Intersection of Artificial Intelligence And Quantum Computing In Financial Markets: A Critical Review
2024	Gujju [39]	Quantum Machine Learning on near-term quantum devices: Current state of supervised and unsupervised techniques for real-world applications

 doi:10.20944/preprints202511.1802.v2

Table 1. *Cont.*

Year	First Author	Title of Publication
2024	Bunescu [40]	Modern finance through quantum computing—A systematic literature review
2024	Mironowicz [41]	Applications of Quantum Machine Learning for Quantitative Finance
2024	Auer [22]	Quantum computing and the financial system
2025	Corli [42]	Quantum Machine Learning algorithms for anomaly detection: A review

Each of the survey reports above is written for a specific audience, as reflected in the depth of technical details covered and the emphasis on either quantum algorithms or financial use cases. In this review, our approach is to present the technical depth of the key quantum algorithms and the mathematical formulation of the use cases in finance and economics. We hope this approach will spur interdisciplinary collaboration that will accelerate the advent of PQA for industrial applications.

1.3. Structure of the Review

The structure of the review resembles the mapping between use cases and problem domains shown in Figure 1.

Figure 1. An overview of quantum computing use cases in finance and economics categorised by NQCC's priority problem category [43].

Thus, we have divided this report into three parts:

Part I: **Quantum algorithms** - a review of the key quantum algorithms with potential PQA in finance and economics. These are grouped into four problem domains:

(a) Simulation algorithms are presented in section (2.2), including Quantum Monte Carlo Integration and quantum solvers for Stochastic Differential Equations.

(b) Optimisation algorithms are presented in section (2.3), particularly for combinatorial and convex optimisation problems with state-of-the-art examples.

(c) Quantum Machine Learning algorithms are presented in section (2.4), which are quantum extensions of classical Machine Learning techniques for supervised, unsupervised, and reinforcement learning.

 doi:10.20944/preprints202511.1802.v2

(d) Quantum cryptography methods are presented in section (2.5), including a discussion of future expected threats to cybersecurity posed by quantum computers once the technology reaches full maturity, and some quantum-safe protocols for data encryption and communication.

The pertinent primitive algorithms that feature as subroutines to quantum algorithms in the above problem domains are outlined in section (2.1).

Part II: **Use cases in finance and economics** - a review of the mathematical formulations of potential use cases of quantum computing in finance and economics. These are grouped into three parts:

(a) Banking and Investment - presented in section (3.1), we identify some of the computational bottlenecks for classical methods in banking and investment problems, and use cases where quantum computing can potentially have an advantage. These include pricing assets and derivatives, portfolio optimisation, hedging, and arbitrage.

(b) Risk Management and Cybersecurity - presented in section (3.2), we identify some of the simulation and security challenges in risk management and cybersecurity, respectively. Similar to banking and investment, we present the technical formulations of use cases of quantum computing in this category. This includes quantum approaches for risk analysis (Value-at-Risk, credit scoring, etc.) and fraud detection.

(c) Economics - presented in section (3.3), the mathematical formulation of potential use cases of quantum technologies for problems arising in economics is outlined. These include quantum money and macroeconomic forecasting.

Part III: **Summary and outlook** - of this report is presented in section (4), in which we reiterate the benefits to financial organisations in working towards quantum readiness, and provide an outlook of one possible route towards PQA.

Note: This review is not a comprehensive review of all quantum algorithms nor use cases in finance and economics. We have selected a subset of use cases that represent areas of potential high impact with some current published research activity in the form of proof-of-concept proposals and/or demonstrations. Similarly, we have chosen to give technical details for simpler formulations of quantum algorithms for a problem domain and mention more complex approaches in passing. Furthermore, this review is also not intended as a primer on quantum computing or quantum information theory. In the quantum-specific sections, we assume a level of familiarity with quantum mechanics and related terminology, which other sources will be able to provide in more detail. In the next section, we will summarise some of the notation used in this review for the reader's convenience. Finally, we hope that financial organisations interested in incorporating quantum technologies can work with quantum applications engineers to develop relevant solutions using this survey and others as a starting point.

1.4. Notation

In this section, we summarise some of the key notation used in this review for clarity. This is not an exhaustive list, and some of the notation can be overloaded when the meaning is clear in the context. For example, in some parts of the text, the Hamiltonian may be denoted as H, and it should not be confused with the Hadamard gate. Similarly, the Big-O notation may be denoted as $O(\cdot)$ or $\mathcal{O}(\cdot)$, which both mean the same thing. Table 2 gives a sample of common notation in quantum computing and analysis of quantum algorithms that are used in this review. Since this review is not an introductory text in the field, a reader who is unfamiliar with these notations can refer to Ref. [44] for more information.

 doi:10.20944/preprints202511.1802.v2

Table 2. Common notation in quantum computing and analysis of quantum algorithms.

Symbol	Meaning	Description
$\|\psi\rangle$, $\langle\psi\|$	Dirac bra-ket notation for a general quantum state and its adjoint, respectively.	A general qubit state: $\|\psi\rangle = \alpha\|0\rangle + \beta\|1\rangle$, where $\|\alpha\|^2 + \|\beta\|^2 = 1$. Here, the basis vectors are $\|0\rangle = [1\ 0]^\intercal$, $\|1\rangle = [0\ 1]^\intercal$
$\langle\phi\|\psi\rangle$	Inner product	Measures the overlap or amplitude between two quantum states.
U	Unitary operator	Reversible transformation that preserves norm: $U^\dagger U = I$.
$\mathcal{H}$	Hamiltonian	Operator that represents the total energy of a quantum system. It determines its time evolution via the unitary $U = e^{-i\mathcal{H}t}$.
H	Hadamard gate	Puts a qubit into superposition: $H\|0\rangle = \frac{1}{\sqrt{2}}(\|0\rangle + \|1\rangle)$.
X, Y, Z, I	Pauli gates	Single-qubit gates: X (bit flip), Z (phase flip), Y (both flip), I (identity).
CX, CNOT	Controlled-NOT gate	Two-qubit gate that flips the target if control qubit is $\|1\rangle$.
T	T-gate define as $T = \begin{pmatrix} 1 & 0 \\ 0 & e^{i\pi/4} \end{pmatrix}$	A non-Clifford single-qubit gate that plays two key roles: (i) universality for the set of Clifford gates plus T-gate [44], and (ii) efficient decomposition of Toffoli gates [45] the equivalent of classical NAND gates [46].
$\otimes$, Tr	Tensor product and Trace	Combines states: $\|a\rangle \otimes \|b\rangle = \|ab\rangle$. Trace gives the sum of matrix diagonal entries; used in measurement and subsystems.
$O(\cdot)$	Big-O notation	Describes asymptotic upper bounds on complexity of an algorithm.
$\Omega(\cdot)$	Big-Omega notation	Describes asymptotic lower bounds on complexity of an algorithm.
$\Theta(\cdot)$	Big-Theta notation	Describes asymptotic average or tight (upper and lower) bounds on the complexity of an algorithm.
meas or M	Measurement	Collapses qubit to classical bit based on amplitude probabilities.

2. Quantum Algorithms

2.1. Primitive Quantum Algorithms

This section offers an introduction to a set of quantum algorithms, here referred to as primitive algorithms, that are used as the *basis* or *fundamental building blocks* from which more complex quantum algorithms, models, or frameworks are constructed [47]. As primitive algorithms do not directly solve an end-to-end problem, groups of these fundamental algorithms (also called subroutines) are needed to create a wide range of high-end quantum applications [48].

2.1.1. Quantum Phase Estimation

One of the earliest quantum algorithms to be discovered is the Quantum Phase Estimation (QPE), which was first formalised in 1995 by Kitaev[1] [50]. This subroutine has been widely used by many other

[1] Note that the idea of Quantum Fourier Transform was first used in 1994 by Peter Shor [49], but he did not explicitly formalise it into the QPE algorithm.

 doi:10.20944/preprints202511.1802.v2

algorithms, including Shor's quantum algorithm for factoring large numbers [49,51], Hamiltonian diagonalisation [52], and solving systems of linear equations [6].

QPE serves as a key building block for quantum algorithms, of which some have a potential quantum speed-up that is exponential due to it. The objective of the algorithm is the following [44]: given a unitary operator U, estimate the phase θ in the representation

$$U|\psi\rangle = e^{2\pi i\theta}|\psi\rangle . \tag{1}$$

Here $|\psi\rangle$ is an eigenvector and $e^{2\pi i\theta}$ is the corresponding eigenvalue. To implement the QPE, the quantum system needs to be separated into registers: the *state register* that contains $|\psi\rangle$ and the *phase register* that contains the encoded estimate of the phase θ. The QPE subroutine is constructed as follows:

1. **Setup:** initialise the state register with the state $|\psi\rangle$. The additional set of n qubits that form the phase register is set in state $|0^{\otimes n}\rangle$. After initialisation, the global state of the system will be:
$$|\psi_0\rangle = |0\rangle^{\otimes n}|\psi\rangle$$
2. **Superposition:** an n-bit Hadamard gate is applied on the phase register, leaving the global state as:
$$|\psi_1\rangle = \frac{1}{2^{n/2}}(|0\rangle + |1\rangle)^{\otimes n}|\psi\rangle$$
3. **Controlled Unitary Operations:** consider a controlled unitary U_C that applies the unitary operator U on the target register (i.e., the phase register) only if its corresponding control qubit is $|1\rangle$ [44]. Since U is a unitary operator with eigenvector $|\psi\rangle$ such that $U|\psi\rangle = e^{2\pi i\theta}|\psi\rangle$, it follows that:
$$U^{2^j}|\psi\rangle = U^{2^j-1}U|\psi\rangle = U^{2^j-1}e^{2\pi i\theta}|\psi\rangle = \cdots = e^{2\pi i\theta\cdot 2^j}|\psi\rangle .$$
Applying all the n-controlled operations $U_C^{2^j}$ with $0 \le j \le n-1$, and using the relation $|0\rangle \otimes |\psi\rangle + |1\rangle \otimes e^{2\pi i\theta}|\psi\rangle = (|0\rangle + e^{2\pi i\theta}|1\rangle) \otimes |\psi\rangle$, leads to the global state:
$$\begin{aligned}|\psi_2\rangle &= \frac{1}{2^{n/2}}\left(|0\rangle + e^{2\pi i\theta 2^{n-1}}|1\rangle\right) \otimes \cdots \otimes \left(|0\rangle + e^{2\pi i\theta 2^1}|1\rangle\right) \otimes \left(|0\rangle + e^{2\pi i\theta 2^0}|1\rangle\right) \otimes |\psi\rangle \\ &= \frac{1}{2^{n/2}}\sum_{k=0}^{2^n-1} e^{2\pi i\theta k}|k\rangle \otimes |\psi\rangle\end{aligned}$$
where k denotes the integer representation of n-bit binary numbers.
4. **Inverse Fourier Transform:** The Quantum Fourier Transform (QFT) maps an n-qubit input state $|x\rangle$ into:
$$\begin{aligned}\mathrm{QFT}|x\rangle = \frac{1}{2^{n/2}}\left(|0\rangle + e^{\frac{2\pi i}{2}x}|1\rangle\right) \otimes \left(|0\rangle + e^{\frac{2\pi i}{2^2}x}|1\rangle\right) \otimes \ldots \\ \otimes \left(|0\rangle + e^{\frac{2\pi i}{2^{n-1}}x}|1\rangle\right) \otimes \left(|0\rangle + e^{\frac{2\pi i}{2^n}x}|1\rangle\right).\end{aligned}$$
The expression of the global state $|\psi_2\rangle$ is the result of applying QFT on the global expression $|\psi_1\rangle$ of Step 2. Therefore, to recover the state $|2^n\theta\rangle$, an inverse Fourier transform is applied on the phase register [53]. Doing so, it is found that
$$|\psi_3\rangle = \frac{1}{2^{n/2}}\sum_{k=0}^{2^n-1} e^{2\pi i\theta k}|k\rangle \otimes |\psi\rangle \xrightarrow{\mathrm{QFT}_n^{-1}} \frac{1}{2^n}\sum_{x=0}^{2^n-1}\sum_{k=0}^{2^n-1} e^{-\frac{2\pi ik}{2^n}(x-2^n\theta)}|x\rangle \otimes |\psi\rangle$$

 doi:10.20944/preprints202511.1802.v2

5. **Measurement:** the above expression peaks near $x = 2^n\theta$. For the case when $2^n\theta$ is an integer, measuring in the computational basis gives the phase in the phase register with high probability, as the global state now is:

$$|\psi_4\rangle = |2^n\theta\rangle \otimes |\psi\rangle.$$

For the case when $2^n\theta$ is not an integer, it can be shown that the above expression still peaks near $x = 2^n\theta$ with probability at least $4/\pi^2 \approx 40\%$ [44].

Algorithm (1) summarises the key steps of the QPE subroutine which scales as $\mathcal{O}(1/\delta)$, for desired additive error δ [50]. The standard QPE circuit requires $O(2^n)$ controlled-U_C operations, which can be a resource challenge for current Noisy Intermediate-Scale Quantum (NISQ) hardware. Hence, QPE is considered a Universal Fault-Tolerant (UFT) quantum algorithm which requires Quantum Error Correction (QEC) to obtain highly accurate phase estimates. In the NISQ era, practitioners often employ approximate versions of QPE with reduced circuit depth and error mitigation methods to suppress effects of noise. These variants of QPE include the Iterative Quantum Phase Estimation (IQPE), which uses a single control qubit repeatedly and employs classical post-processing to update estimates of θ [54]. IQPE typically has the same asymptotic error scaling but requires fewer qubits [54], making it more suitable for near-term quantum devices. There have also been proposals for alternatives to QPE such as the quantum eigenvalue estimation via time series analysis [55] and the phase estimation of local Hamiltonians [56]. These methods used expectation values of the evolution operator for various times to estimate the eigenvalues of a Hamiltonian, which makes them more feasible to implement on NISQ hardware.

Algorithm 1 Quantum Phase Estimation

Initialising. Initialise the quantum system. There exist two qubit registers, the phase register initialised in state $|0\rangle^{\otimes n}$, and the state register initialised in $|\psi\rangle$.
Superposing. Apply Hadamard gates on the phase register.
Applying the unitary. Apply the controlled unitary operation as shown in the third step of the mathematical analysis.
Inverse QFT. Apply the inverse quantum Fourier transform to decode the state of the phase register.
Measure. Measure the phase register to get an approximation of the desired phase, θ.

2.1.2. Quantum Amplitude Algorithms

Another set of widely used quantum subroutines introduced by Brassard et al. [57] are the Quantum Amplitude Amplification (QAA) and Quantum Amplitude Estimation (QAE). These algorithms are an extension of the principles of Grover's search algorithm [4] to a broader range of applications.

Quantum Amplitude Amplification

The first amplitude subroutine, QAA, also used within Grover's search algorithm [4], enhances the probability amplitude of desired outcomes within a quantum algorithm. The QAA generalizes Grover's unordered search to any algorithm with a known success probability [58], enabling a potential quadratic speed-up over classical repetition strategies [57].

Consider a quantum algorithm $\mathcal{A}$ that produces a state

$$\mathcal{A}|0\rangle = |\psi\rangle = \sqrt{1-a}\,|\psi_0\rangle + \sqrt{a}\,|\psi_1\rangle\,, \tag{2}$$

where $|\psi_1\rangle$ is the 'good' subspace (desired states), a the probability of measuring a 'good' state, and $|\psi_0\rangle$ the 'bad' subspace. The amplification process is done using the Grover-like operator $\mathcal{Q}$, which acts as a rotation and is defined to be [57]

$$Q = -\mathcal{A}\mathcal{S}_0\mathcal{A}^\dagger\mathcal{S}_\chi, \tag{3}$$

 doi:10.20944/preprints202511.1802.v2

where

$$\mathcal{S}_0 = 2\,|0\rangle\langle 0| - I \quad \text{and} \quad \mathcal{S}_\chi = I - 2\,|\psi_1\rangle\langle\psi_1|\,. \tag{4}$$

The operator $\mathcal{S}_0$ reflects about the initial state, which flips the sign of the amplitudes of the good states $|x\rangle$ if and only if $|x\rangle = |0\rangle$. The operator $\mathcal{S}_\chi$ reflects about the good state $|\psi_1\rangle$ which flips the sign of $|x\rangle$ if and only if $\chi(x) = 1$. This implies that [57]

$$\mathcal{S}_\chi\,|x\rangle = -\,|x\rangle \quad \Longleftrightarrow \quad \chi(x) = 1. \tag{5}$$

The probability amplitude of the good state is $\sin^2((2m+1)\theta_a)$, where $\theta_a = \arcsin(\sqrt{a})$, with $0 < \theta_a < \pi/2$, and the optimal m number of iterations is $\lfloor \pi/(4\theta_a) \rfloor$. Applying Q iteratively to $|\psi\rangle$, the state evolves such that after m applications, the state is

$$Q^m|\psi\rangle = \sin((2m+1)\theta_a)|\psi_1\rangle + \cos((2m+1)\theta_a)|\psi_0\rangle, \tag{6}$$

Thus, Q rotates the state in the $\{|\psi_0\rangle, |\psi_1\rangle\}$ plane per each iteration. If a is known, QAA achieves a quadratic speed-up with $\Theta(1/\sqrt{a})$ applications of $\mathcal{A}$ and $\mathcal{A}^\dagger$. For unknown a, quantum search algorithms like one outlined in Section (2.1.3) use exponentially increasing numbers of iterations to find a good solution. This approach is also expected to use same $\Theta(1/\sqrt{a})$ applications $\mathcal{A}$ and $\mathcal{A}^\dagger$ if $a > 0$ [57]. Algorithm (2) summarises the QAA subroutine using the operator Q and a general $\mathcal{A}$ algorithm.

Algorithm 2 Quantum Amplitude Amplification

Initialise: Apply a quantum algorithm $\mathcal{A}$ to $|0\rangle$ to prepare the state:

$$|\psi\rangle = \sqrt{1-a}\,|\psi_0\rangle + \sqrt{a}\,|\psi_1\rangle$$

Amplify: Define the amplification operator and apply it to m number of iterations to rotate the state:

$$Q^m|\psi\rangle = \sin((2m+1)\theta_a)|\psi_1\rangle + \cos((2m+1)\theta_a)|\psi_0\rangle$$

Measure: Measure the final state $Q^m|\psi\rangle$ to obtain a good state.
Repeat: If a is unknown, use exponentially increasing m until a good state is found.

An extension of QAA, called the *variable time amplitude amplification*, which can be decomposed into multiple steps with different stopping times [59], has been applied as a subroutine that improves the complexity of Harrow et al. [6] Quantum Linear Systems Solver. Improvements to the QAA subroutine have been proposed, such as the *oblivious amplitude amplification* [60] which handles the issue that occurs when it is not possible to perform the required reflection about the state $|\psi\rangle$. Another version of QAA is the *fixed-point amplitude amplification* [61] that ensures amplitude amplification happens regardless of an unknown amplitude. These improved versions of QAA are subroutines for Quantum Singular Value Transformation (QSVT) methods [62] and have been recently compared in the Hamiltonian simulation problem [63].

Quantum Amplitude Estimation

The second amplitude subroutine, QAE algorithm first proposed by [57], is closely related to QAA and seeks to estimate the probability amplitude of a specific outcome with high precision. It is a key subroutine for a broad class of Monte Carlo-like estimation tasks [64] and offers a potential quadratic quantum speed-up [5].

The QAE can be described similarly as QAA. Consider an algorithm $\mathcal{A}$ that outputs a state given by Equation (2), the QAE seeks to produce an estimate for the amplitude a of the good state $|\psi_1\rangle$, where $a = \langle\psi_1|\psi_1\rangle$. Using the operator Q given by Equation (3), QAE estimates the value of a by using QPE to find the eigenvalues of Q [57]. Hence, both QAA and QAE use the operator Q, but the former boosts a for measurement of $|\psi_1\rangle$, while the latter quantifies a itself.

 doi:10.20944/preprints202511.1802.v2

The key idea is to assign the value of a to an angle θ so that the estimate of θ to a given precision δ using QPE gives us the estimate of a. This is done by setting $a = \sin^2(\theta)$ and then applying QPE to the controlled-Q operations, since Q acts as a rotation in $\mathcal{H}_\psi$ with eigenvalues $e^{\pm i2\theta}$. The estimate $\tilde{a}$ with M evaluations has errors bounds given by [57]

$$|\tilde{a} - a| \leq 2\pi k/\sqrt{2a(1-a)/M} + \pi k^2/M^2, \tag{7}$$

with probability at least $8/\pi^2$ for $k = 1$, and higher for $k \geq 2$. Algorithm (3) summarises the QAE that utilises QPE.

Algorithm 3 Quantum Amplitude Estimation

Initialise: Apply a quantum algorithm $\mathcal{A}$ to $|0\rangle$ to prepare the state: $|\psi\rangle = \sqrt{1-a}\,|\psi_0\rangle + \sqrt{a}\,|\psi_1\rangle$ (same as QAA).
Define: Define the amplification operator Q given by Equation (3). The eigenvalues of Q are $e^{\pm 2i\theta}$ where $a = \sin^2(\theta)$ for $\theta \in [0, \pi/2]$.
Estimate: First apply a total of M controlled-Q operations on state $|\psi\rangle$ such that

$$\sum_{k=0}^{M-1} |k\rangle\, Q^k\, |\psi\rangle\,.$$

Let $\phi = \theta/\pi$, then apply QPE to estimate the eigenphase $\tilde{\phi} \in [0, 1)$ which we use to recover the amplitude

$$\tilde{a} = \sin^2(\pi\tilde{\phi})$$

Output: Return $\tilde{a}$ as the estimate of a, with error bounds [57]:

$$|\tilde{a} - a| \leq \frac{2\pi}{\sqrt{M}}\sqrt{2a(1-a)} + \frac{\pi^2}{M^2}$$

with probability at least $8/\pi^2$ for $M \geq 1$.

This version of the QAE algorithm is relatively resource-expensive due to the use of QPE, which uses many ancilla qubits for a good estimate, multiple controlled-Q operations, and the inverse QFT. Hence, this results in deep circuits which are not feasible to run on near-term devices. Some variants of QAE that do not make use of QPE include the Maximum Likelihood Amplitude Estimation [65], Faster Amplitude Estimation [66], Iterative QAE [67], Variational QAE [68], and low depth algorithms for QAE [64] which are more feasible on near-term devices. An important application of QAE to finance is to perform Monte Carlo integration, which will be discussed in more detail in Section (2.2.1). Other applications of QAE include general numerical integration [69], estimating the probability of success of a quantum algorithm [70], and approximate counting [71].

2.1.3. Quantum Unstructured Search (Grover's Algorithm)

First proposed in 1996 by Lov Grover [4], the Quantum Unstructured Search (QUS)[2] algorithm utilises the QAA subroutine to potentially obtain a quadratic quantum speed-up over classical methods for searching an item in an unstructured dataset.

In this section, we describe the key idea behind the QUS algorithm. For a database $\mathcal{D}$ of $N = 2^n$ entries, let $\{x\} \in \mathcal{D}$ be the set of items in an array, and w the marked item (i.e., the item the routine searches for). Let f be a function such that $f(x) = 1$ if and only if $x = w$ and $f(x) = 0$ otherwise. The quantum states can be encoded as binary strings $x \in \{0,1\}^n$. One can then define the oracle U_f acting on a quantum state, $|x\rangle$, as

$$U_f\,|x\rangle \to (-1)^{f(x)}\,|x\rangle\,. \tag{8}$$

[2] Commonly known as Grover's algorithm or quantum search algorithm

 doi:10.20944/preprints202511.1802.v2

Thus, the oracle does nothing to the unmarked quantum states and negates the phase of the marked state $|w\rangle$. Geometrically, the unitary matrix of this oracle corresponds to a reflection about the origin for the marked item in an N-dimensional vector space.

The QAA subroutine provides the quadratic speed-up of QUS by amplifying the amplitude (and thus, the probability) of the target quantum state, making it more likely to appear after measurement. This procedure is summarised in Algorithm (4) and has been shown to have a query complexity of $O(\sqrt{N})$, which is a quadratic speed-up over classical brute force methods of $O(N)$ [4].

Algorithm 4 Quantum Unstructured Search (Grover's Algorithm)

Initialisation: Start with $|0\rangle^{\otimes n}$, apply Hadamard gates to create a uniform superposition:

$$|s\rangle = \frac{1}{\sqrt{N}} \sum_{x=0}^{N-1} |x\rangle.$$

Each state $|x\rangle$ has amplitude $1/\sqrt{N}$.
Oracle Application: Apply the oracle U_f, which flips the phase of solution states, such that for one solution $|w\rangle$, the state becomes:

$$U_f|s\rangle = \frac{1}{\sqrt{N}} \left(\sum_{x \neq w} |x\rangle - |w\rangle \right).$$

This marks solutions by changing their sign.
Diffusion Operator: Apply the diffusion operator $D = 2|s\rangle\langle s| - I$, where I is the identity. This reflects the state over $|s\rangle$, amplifying solution amplitudes:

$$DU_f\,|s\rangle = 2\langle s|U_f|s\rangle|s\rangle - U_f\,|s\rangle\,.$$

The action of the Grover operator $G = DU_f$ is to amplify the amplitude of the solution state.
Iteration: Repeat the Grover operator k times $G^k\,|s\rangle$ and then measure to find highest probability state $|w\rangle$. The optimal k receptions to maximise the probability of finding the target state(s) is approximately:

$$k = \frac{\pi}{4}\sqrt{\frac{N}{M}}$$

where M is the number of solutions.

Grover's algorithm has been applied as a subroutine for various applications, including speeding up nested search of structured problems [72], stochastic pure adaptive search for unconstrained global optimization [73], high-energy physics data at the Large Hadron Collider [74], image pattern matching [75], and homomorphic encryption schemes [76]. The QUS algorithm as described here is considered a fault-tolerant quantum algorithm due to the deep circuits (required to reach optimal k iterations) which are infeasible to run successfully on current NISQ hardware. Hence, similarly to the other primitives reviewed here, improvements have been suggested to the QUS to make it amenable to run on near-term quantum hardware. These include the divide-and-conquer strategy and partial diffusion operators to reduce circuit depth and error accumulation [77,78], as well as variational approaches [79,80].

2.1.4. Quantum Walks

Random walks have long served as a foundational model in the study of stochastic processes, with applications spanning physics, computer science, biology, and finance. In its classical form, a random walk describes the trajectory of a particle that takes successive steps in random directions, typically governed by a Markov process [81]. Random walks have also been generalised to graphs [82], in which case they can be viewed as finite-state Markov chains over the set of vertices [83]. A simple example is the one-dimensional symmetric random walk, where a particle at position $x \in \mathbb{Z}$ moves to $x+1$ or

 doi:10.20944/preprints202511.1802.v2

$x-1$ with equal probability at each time step. In finance, the Geometric Brownian Motion (GBM) is a widely used random walk for modelling market stochastic quantities like asset prices [84,85].

The quantum analogue of random walks, known as *quantum walks*, emerged in the early 1990s as a framework for modelling quantum dynamics and as a potential basis for quantum algorithms [86]. Unlike classical random walks, quantum walks evolve according to unitary transformations, preserving coherence and allowing for interference between paths. This leads to fundamentally different behaviour, including faster spreading and potential algorithmic advantages [87].

Two main formulations of quantum walks exist: *discrete-time* and *continuous-time*. The Discrete-time Quantum Walk (DTQW) was first formalised by Aharonov et al. [86], incorporating a coin space to account for internal degrees of freedom. In contrast, the Continuous-time Quantum Walk (CTQW), introduced by Farhi and Gutmann [88], operates directly on the graph structure without an explicit coin. In this section, we will review the key ideas behind quantum walks, beginning with their mathematical foundations and then exploring their distinctive dynamical properties, algorithmic formulations, bottlenecks, and applications.

Discrete-Time Quantum Walks

Consider a walker on a 1D line, flipping a *quantum coin* to decide whether to turn left or right at each step. This represents one of the simplest quantum walks, also referred to as a *qubit walk* on a finite cycle (with N states) in discrete time [89]. This quantum walk can be described by repeated application of a unitary evolution operator U which acts on the Hilbert space $\mathcal{H} = \mathcal{H}_C \otimes \mathcal{H}_S$ composed of the coin qubit (C) with basis $\{|\uparrow\rangle, |\downarrow\rangle\}$ and state space (S) with basis $\{|x\rangle\}$ for $x \in \{0, 1, \dots N-1\}$, respectively. The unitary U is defined as [89]:

$$U = S \cdot (C \otimes I), \tag{9}$$

where S is the conditional shift operator given by [90]

$$S = |\uparrow\rangle\langle\uparrow| \otimes S^+ + |\downarrow\rangle\langle\downarrow| \otimes S^-. \tag{10}$$

The operator $S^+ |x\rangle \to |x+1\rangle$ moves the walker one step to the right, increasing its position, and $S^- |x\rangle \to |x-1\rangle$ to the left, decreasing its position. The quantum coin operator C is can be chosen to the Hadamard gate H, such that

$$H|\uparrow\rangle = \frac{1}{\sqrt{2}}(|\uparrow\rangle + |\downarrow\rangle) \quad \text{and} \quad H|\downarrow\rangle = \frac{1}{\sqrt{2}}(|\uparrow\rangle - |\downarrow\rangle). \tag{11}$$

We note that although this coin is *unbiased*[3], the quantum walk from this coin operator ($C = H$) will be *asymmetric* with bias towards rightward paths. This is because the leftwards path (S^-) undergoes more destructive quantum interference, whereas the rightwards path undergoes more constructive quantum interference [91]. This phenomenon has no classical analogue and makes quantum walks more expressive than classical random walks [86,87]. The coin represented by the Hadamard operator alongside a step operator causes the probability amplitude to become distributed over an increasing space in discrete jumps [92]. This *asymmetry* can be overcome by choosing a *balanced* coin operator [87], for example

$$C = Y = \frac{1}{\sqrt{2}}\begin{bmatrix} 1 & i \\ i & 1 \end{bmatrix}, \tag{12}$$

which treats both $|\uparrow\rangle$ and $|\downarrow\rangle$ the same, independent of the initial coin state.

Intuitively, in each step, the qubit first 'splits' into two paths (C puts it in a superposition) and then one 'half' steps leftwards, while the other steps rightwards. This process, when repeated with T-steps, produces a probability distribution that is ballistic with standard deviation $\sigma_q \sim T$, whereas the classical random walk has a diffusive distribution with standard deviation $\sigma_c \sim \sqrt{T}$ [87]. This

[3] Meaning the states $|\uparrow\rangle$ and $|\downarrow\rangle$ of the coin are evenly distributed up to a phase factor

 doi:10.20944/preprints202511.1802.v2

implies the quantum walk propagates quadratically faster than classical walks [87], which means they can explore more of a graph in fewer steps than classical random walks [93].

Generally, quantum walks in discrete time can be viewed as a Markov chain over the edges of a graph and consist of a series of interleaved reflection operators [94,95]. This formulation of quantum walks generalises the QAA and Grover's algorithm discussed in Sections (2.1.2.1) and (2.1.3), respectively [96,97]. The bipartite character of the graph introduces the *modularity* property of quantum walks (similarly to classical random walks), which is that after an even (odd) number of steps, the probability to find the walker on odd (even) positions is always zero [98]. This property allows for simplified analysis of the performance of quantum walks, in particular, to two important metrics: the *mixing time* and *hitting time* of random walks on graphs. The mixing time of a graph is the time it takes for a random walk on the graph to become close to the stationary distribution; that is, the point where the walk "forgets" where it started and behaves as if it started from a random node [99]. The hitting time from node u to node v is the expected number of steps a random walk starting at u takes to reach v for the first time [81]. Quantum walks are shown to potentially have a polynomial quantum speed-up in mixing times [89,93,100] and hitting times for Markov-chain-based search algorithms [94,95,101–105] than their classical random walks counterpart. There have been several proof-of-concept implementations of DTQW on NISQ hardware, which include a Hadamard-based on the 4-cycle and 8-cycle [106] and extensions to multi-qubit systems [107,108].

Continuous-Time Quantum Walks

Consider an undirected graph $G(V, E)$, where V is the set of its vertices and E the set of its edges. In classical mechanics, a diffusion equation can be used, which allows probability to leak to or from neighbouring vertices. The number of neighbouring nodes equals the degree of the node j, or $\deg(j)$. This diffusion operation can be expressed as

$$\frac{\mathrm{d}}{\mathrm{d}t} p_j(t) = \sum_{k \in V} L_{j,k} p_k(t) \tag{13}$$

where t is an arbitrary continuous time parameter, p_j is a function that describes the probabilistic exchange between node j and its neighbouring nodes. The operator L is symmetric and Hermitian, called the Laplacian of G, given by

$$L_{j,k} = \begin{cases} -\deg(j) & j = k \\ 1 & (j,k) \in E \\ 0 & \text{otherwise} \end{cases}$$

Thus, since L is a Hermitian matrix, it can play the role of a Hamiltonian in Schrödinger's equation as

$$\mathrm{i}\frac{\mathrm{d}}{\mathrm{d}t} |\psi(t)\rangle = L |\psi(t)\rangle \tag{14}$$

where, for simplicity it can be assumed that $\hbar = 1$ and $|\psi(t)\rangle$ is the state of the system at arbitrary time t. First introduced by Farhi and Gutmann in [88], Equation (14) represents the Continuous-time Quantum Walk (CTQW). As evident from the above formulation, the CTQW does not need a quantum coin that drives the evolution, unlike the DTQW. This makes CTQW a construct that shares dynamics with the DTQW, but exhibits different behaviour. In contrast to the quantum coin tossing example described in Section (2.1.4.1), the walker now moves smoothly (or continuously), guided by an evolution rule (which is driven by the Hamiltonian, typically the graph Laplacian L). This evolution follows the Schrödinger Equation (14) and the walk is continuous without distinct steps. Therefore, we can summarise the fundamental differences between the two quantum walks as:

 doi:10.20944/preprints202511.1802.v2

- **State space**: CTQWs require only the vertex space, while DTQWs models need an auxiliary coin space for evolving. As described in Section (2.1.4.1), the coin operator drives the symmetry or asymmetry of the quantum walk.
- **Dynamics**: CTQWs have continuous Schrödinger evolution (via Hamiltonians), whereas discrete-time walks rely on alternating coin and shift operators per time step.

In addition, the various mixing operators used in Quantum Approximate Optimisation Algorithm, described in Section (2.3.1.4), can be viewed as CTQW connecting the feasible solutions [109]. Similarly to DTQWs, the CTQWs can showcase a quadratic advantage in terms of accelerating diffusion (i.e., spreading) compared to classical continuous-time random walks [110]. For some oracular graph problems, the CTQW can theoretically achieve exponential advantage over classical methods [111].

It was shown by Childs that CTQW can be regarded as a universal computational primitive, with any quantum computation encoded in some graph [112]. Later, Lovett et al. [113] showed that the DTQW can also achieve universal quantum computation. Hence, there have been multiple proposed unifications of quantum walks in continuous and discrete time [114,115], something that is true for the classical versions [116]. For a comprehensive review of quantum walks, see the survey in [115]; and for an overview and a discussion of connections between the various quantum-walk-based search algorithms, see the work by [103].

Quantum walks have since found applications in a variety of areas, including quantum search algorithms [97], modelling transport in biological systems [117], and many others [110]. Their utility stems from the combination of quantum superposition and interference, which enable new algorithmic paradigms not feasible in classical settings. Current research into quantum walks faces many challenges. As in any other quantum algorithm, a significant issue is implementation on NISQ devices where noise can disrupt the coherent evolution required for quantum walks. Efforts to mitigate these decoherence effects have been explored in various studies, such as [118], which simulate quantum walks of interacting particles and demonstrate topological protection against noise. However, achieving scalable quantum walks on large graphs, or lattices, remains a challenging task [110], as current hardware limitations restrict the size and duration of coherent quantum evolutions.

2.1.5. Quantum Linear System Solver

Linear systems of equations are ubiquitous in science, engineering, and mathematical fields. There are several numerical methods developed over the years for solving them efficiently on classical computers [119–121]. The general Linear Systems Problem (LSP) can be formally defines as:

Definition 1 (LSP). *Given a matrix $A \in \mathbb{C}^{N\times N}$ and a vector $b \in \mathbb{C}^N$, find a vector $x \in \mathbb{C}^N$ s.t. $Ax = b$, or indicate that the system has no solution.*

In other words, Definition (1) describes a matrix-inversion problem since the solution is given by $x = A^{-1}b$. The Quantum Linear Systems Problem (QLSP) is quantum version of the LSP, and is defined as:

Definition 2 (QLSP). *Given a matrix $A \in \mathbb{C}^{N\times N}$ and and a vector $b \in \mathbb{C}^N$, prepare the state $|\tilde{x}\rangle$ on a quantum computer with $n = \lceil \log_2 N \rceil$ qubits such that*

$$\| |\tilde{x}\rangle - |x\rangle \|_2 \leq \epsilon,$$

where ϵ is the desired precision. The target quantum state $|x\rangle = A^{-1}|b\rangle$ with

$$|b\rangle := \frac{\sum_i b_i |i\rangle}{\| \sum_i b_i |i\rangle \|_2}$$

where b_i are the i^{th} component of vector b.

 doi:10.20944/preprints202511.1802.v2

One of the key differences between the LSP and QLSP is that the former outputs the full solution vector x whilst the latter outputs a normalized vector proportional to the solution $|\tilde{x}\rangle \propto A^{-1}|b\rangle$. Table 3 shows the time complexity of the best known classical algorithm for solving the LSP, with A matrix sparse [122] and dense [123], compared with a few quantum algorithms for solving the QLSP.

Table 3. Comparison of the complexity between various algorithms for the LSP (first two rows) and QLSP. Here, N is the dimension of the system, ϵ is the desired precision, s and κ are the sparsity and condition number of the matrix A, respectively. Note that all the quantum algorithms (except one based on QSVE in the 6th row) for the QLSP have a complexity factor of $\mathcal{O}(\text{polylog}(N))$ in terms of the system size.

Assumption	Algorithm	Complexity
A is symmetric, s-sparse, and positive definite.	Conjugate Gradient [122]	$\mathcal{O}\left(Ns\sqrt{\kappa}\log\left(1/\epsilon\right)\right)$
A can be a dense square matrix	Powers of tensors [123]	$\mathcal{O}(N^{\omega})$ with $\omega < 2.3728639$
A is s-sparse, Hermitian with singular values $\in [1/\kappa, 1]$	HHL - Hamiltonian simulation with QPE [6]	$\mathcal{O}\left(s^2\kappa^2/\epsilon\right)$
Same as HHL	Variable-time amplitude amplification [124]	$\mathcal{O}\left(s^2\kappa/\epsilon\right)$
Same as HHL	Fourier or Chebyshev fitting using LCU [125]	$\mathcal{O}(s\kappa\,\text{polylog}\left(s\kappa/\epsilon\right))$
A is dense, Hermitian with eigenvalues in $[-1,-1/\kappa]\cup[1/\kappa,1]$	Quantum Singular Value Estimation [126]	$\mathcal{O}\left(\sqrt{N}\kappa^2/\epsilon\right)$
A generates Hamiltonian with spectral gap amplification constraints [127]	Adiabatic random method [128]	$\mathcal{O}((\kappa\log\kappa)/\epsilon)$
A general non-Hermitian matrix	Time-optimal adiabatic methods [129]	$\mathcal{O}(\kappa\,\text{polylog}\left(\log(\kappa/\epsilon)\right))$
Same as HHL	Zeno eigenstate filtering [130]	$\mathcal{O}(\kappa\log\left(\kappa/\epsilon\right))$
Same as HHL	Quantum discrete adiabatic theorem [131]	$\mathcal{O}(\kappa\log\left(1/\epsilon\right))$
Same as HHL	Kernel projection methods [132]	$\mathcal{O}(\kappa\log\left(1/\epsilon\right))$

HHL Algorithm In this section, we will consider the Harrow-Hassidim-Lloyd (HHL) algorithm [6] which is the first quantum algorithm for solving the QLSP. As mentioned earlier, it does not provide the whole solution vector, but a quantum state $|\tilde{x}\rangle$ proportional to the solution, which we can sample from with relatively low additional error. Given that the coefficient matrix A is sparse and well-conditioned, the quantum algorithm can potentially achieve an exponential quantum speed-up in the dimension of the matrix N compared to the best known classical algorithm [6]. However, there are caveats for this speed-up to be possible, which include [6,11] the following conditions:

1. Matrix A must be sparse or can be efficiently decomposed into a sparse form.
2. The condition number κ of A must be small and scale as $\mathcal{O}(\text{poly}(\log N))$.
3. The elements of A can be efficiently utilized via black-box oracle calls as needed.
4. The final output is the case where one does not need to know the solution $\vec{x}$ itself, but rather an approximation of the expectation value of some operator associated with $\vec{x}$, e.g., $\vec{x}^{\dagger}M\vec{x}$ for some matrix M.

It may seem that these constraints, alongside other challenges in quantum computation restricts the possibility of having a PQA as noted by Aaronson [11]. Ongoing research [133] and improved versions of HHL, such as shown in Table 3, are promising to deliver PQA.

The main steps of the algorithm are (i) phase estimation, followed by (ii) a controlled rotation, (iii) uncomputation, and, finally, (iv) measurement and post-selection [133]. A summary of the HHL

 doi:10.20944/preprints202511.1802.v2

algorithm is provided below, and for more information, the reader is referred to [6,133]. Consider the $N \times N$ matrix A that is s-sparse and Hermitian, then its spectral decomposition is given

$$A = \sum_{j=0}^{N-1} \lambda_j |u_j\rangle \langle u_j|, \qquad \lambda_j \in \mathbb{R}, \tag{15}$$

where $|u_j\rangle$ is the j^{th} eigenvector of A with respective eigenvalue λ_j. In this decomposition, the matrix inversion of A is then given by

$$A^{-1} = \sum_{j=0}^{N-1} \lambda_j^{-1} |u_j\rangle \langle u_j|. \tag{16}$$

We can express $|b\rangle$ in the eigenbasis of A as

$$|b\rangle = \sum_{j=0}^{N-1} b_j |u_j\rangle, \qquad b_j \in \mathbb{C}, \tag{17}$$

where we already have an implicit normalisation constant since we are talking about a quantum state. The goal of the HHL is to exit the algorithm with the readout register in the state approximately $|x\rangle$, which can also be expressed in the eigenbasis of A as

$$|x\rangle = A^{-1}|b\rangle = \sum_{j=0}^{N-1} \lambda_j^{-1} b_j |u_j\rangle \tag{18}$$

Therefore, the HHL algorithm encodes A into a unitary U given by

$$U = e^{iAt} := \sum_{j=0}^{N-1} e^{i\lambda_j t} |u_j\rangle \langle u_j| \tag{19}$$

Thus, by applying QPE, one can implement the mapping

$$|0\rangle |u_j\rangle \mapsto |\tilde{\lambda}_j\rangle |u_j\rangle, \tag{20}$$

where $\tilde{\lambda}_j$ is the binary representation of λ_j up to a tolerated precision. Following this, the implementation of a controlled rotation takes place conditioned on $|\tilde{\lambda}_j\rangle$. This requires an ancilla register, S, which is added to the system initialised in state $|0\rangle$. The controlled rotation is of the form of a σ_y-rotation (i.e., a rotation around the y-axis or quantisation axis) and produces a normalised state of the form.

$$\sqrt{1 - \frac{c^2}{\tilde{\lambda}_j^2}} |\tilde{\lambda}_j\rangle |u_j\rangle |0\rangle + \frac{c}{\tilde{\lambda}_j} |\tilde{\lambda}_j\rangle |u_j\rangle |1\rangle, \tag{21}$$

where c is a normalisation constant. This can be achieved through the application of the quantum operator

$$\sigma_y = e^{-i\theta} = \begin{pmatrix} \cos\theta & -\sin\theta \\ \sin\theta & \cos\theta \end{pmatrix},$$

where $\theta = \arccos c/\tilde{\lambda}$. Thus, enacting the procedure described above in the latter superposition, it is derived that

$$\sum_{j=1}^{N} b_j |\tilde{\lambda}_j\rangle |u_j\rangle \left(\sqrt{1 - \frac{c^2}{\tilde{\lambda}_j^2}} |0\rangle + \frac{c}{\tilde{\lambda}_j} |1\rangle \right).$$

 doi:10.20944/preprints202511.1802.v2

Finally, the first register is uncomputed, giving

$$|0\rangle \otimes \sum_{j=1}^{N} b_j |u_j\rangle \left(\sqrt{1 - \frac{c^2}{\tilde{\lambda}_j^2}} |0\rangle + \frac{c}{\tilde{\lambda}_j} |1\rangle \right). \tag{22}$$

Following the uncomputation, we see that the state of the system (including all the quantum registers) is $|\tilde{x}\rangle = \sum_{j=1}^{N} \tilde{\lambda}_j^{-1} b_j |u_j\rangle$, or in other words, it exists in a state that is close to the solution $|x\rangle = A^{-1}|b\rangle$. The state $|\tilde{x}\rangle$ can be reconstructed within the clock register, C, by measuring the ancilla register, S, and post-selecting on the outcome 1 modulo the constant factor of normalisation, c. The success probability of the final step can be boosted using QAA. This procedure is summarised in Algorithm (5).

Algorithm 5 Harrow-Hassidim-Lloyd algorithm for QLSP

Input. Encode the state vector $|b\rangle$ and the matrix A with oracular access to its elements. Define $t_0 = \mathcal{O}(\kappa/\epsilon)$, $T = \tilde{\mathcal{O}}(\log N s^2 t_0)$ and ϵ as the desired precision.
Initialise. Prepare the input state $|\Psi_0\rangle^C \otimes |b\rangle^I \otimes |0\rangle^S$, where $|\Psi_0\rangle = \sqrt{\frac{2}{T}} \sum_{\tau=0}^{T-1} \sin\left(\frac{\pi(\tau+1/2)}{T}\right) |\tau\rangle^C$.
Hamiltonian. Apply the conditional Hamiltonian evolution $\sum_{\tau=0}^{T-1} |\tau\rangle\langle\tau|^C \otimes e^{iA\tau t_0/T}$ following the input state.
Apply QFT to the register C, denoting the new basis states $|k\rangle$, for $k \in \{0, \ldots, T-1\}$. Define $\tilde{\lambda} := 2\pi k/t_0$.
Controlled rotation. Append the ancilla register, namely S, and apply a controlled rotation on S with C as the control register, mapping states $|\tilde{\lambda}\rangle \mapsto |h(\tilde{\lambda})\rangle$. The state $|h(\tilde{\lambda})\rangle$ is defined in such a way that it produces an output which denotes whether an inversion has occurred and if that inversion is well-conditioned or not [133].
Uncomputation. Uncompute the register C.
Measurement. Measure the register S.
Repeat. Perform $\mathcal{O}(\kappa)$ rounds of QAA on the HHL algorithm.
Output. Result is the state $|\tilde{x}\rangle$ s.t. $\| |\tilde{x}\rangle - |x\rangle \|_2 \leq \epsilon$

The HHL algorithm was the first QLSS and, as shown in Table 3, there have been many improvements on it up to the recent ones with optimal scaling in κ and ϵ [131,132]. It is worth noting these state-of-the-art quantum algorithms for the QLSS with optimal scaling for the case when A is sparse, and there have been a few proposals for the case when A is dense. For the latter case, Wossing et al. [126] utilised the Quantum Singular Value Estimation (QSVE) algorithm of [134] to achieve a polynomial speed-up over the best known classical algorithm based on powers of tensors with subcubic complexity [123]. However, as noted in [126], the classical algorithm with subcubic complexity [123] is difficult to achieve in practise hence, for the dense matrix case, the Cholesky decomposition with complexity $\mathcal{O}(N^3)$ [135] is often used. This implies that for problems with non-sparse A matrix, such as kernel methods and neural networks in machine learning [136], the potential exponential quantum advantage of HHL-type quantum algorithms is lost.

Following this, Kerenedis and Prakash generalised the QSVE-based linear systems solver to handle both sparse and dense matrices and introduced a technique for spectral norm estimation [137]. Another general framework for solving the QLSP is the Quantum Singular Value Transformation (QSVT) [138], which uses an iterative least square algorithm and has been proposed [139,140]. Although this algorithm does not have optimal scaling with κ and ϵ, it is general in the sense that it does not assume that A is invertible nor that it is a square matrix, but uses the Moore-Penrose pseudoinverse A^+[141] such that the output $\| |\tilde{x}\rangle - A^+ |b\rangle \|_2 \leq \epsilon$ is achieved efficiently [48,139,140]. Furthermore, the QSVT also provides a general framework that unifies [62] a variety of quantum algorithms, such as linear algebraic subroutines like singular-value-threshold projectors [134,138] and matrix-vector multiplication [139]. An outline of QSVT is presented in Algorithm (6).

 doi:10.20944/preprints202511.1802.v2

Algorithm 6 Quantum Singular Value Transformation

Input: A $(1, m, 0)$ block-encoding U_A of matrix A, i.e. $A = (\langle 0^m| \otimes I)\, U_A\, (|0^m\rangle \otimes I)$; a definite-parity polynomial $f : [-1, 1] \to [-1, 1]$ of degree d; and a phase sequence $\Phi = (\varphi_1, \ldots, \varphi_d)$ from polynomial synthesis.

Construct QSVT sequence: Let $Z_{|0^m\rangle} := 2|0^m\rangle\langle 0^m| - I$, and define

$$U_\Phi = \left(e^{i\varphi_1 Z_{|0^m\rangle}} U_A\right) \prod_{j=1}^{(d-1)/2} \left(e^{i\varphi_{2j} Z_{|0^m\rangle}} U_A^\dagger e^{i\varphi_{2j+1} Z_{|0^m\rangle}} U_A\right), \quad d \text{ odd},$$

$$U_\Phi = \prod_{j=1}^{d/2} \left(e^{i\varphi_{2j-1} Z_{|0^m\rangle}} U_A^\dagger e^{i\varphi_{2j} Z_{|0^m\rangle}} U_A\right), \quad d \text{ even}.$$

This yields a block-encoding of $f^{(\mathrm{SV})}(A)$ with the corresponding odd/even forms.

Linear combination: Using that $-\Phi$ implements P^*, define

$$P_{\Re}(A) = (\langle +| \otimes \langle 0^m| \otimes I)\, (|0\rangle\langle 0| \otimes U_\Phi + |1\rangle\langle 1| \otimes U_{-\Phi})\, (|+\rangle \otimes |0^m\rangle \otimes I),$$

which implements a block-encoding of $P_{\mathbb{R}}(A)$, and thus of $f^{(\mathrm{SV})}(A)$ for any definite-parity real f.

Output: $P_{\Re}(A)$ that is a $(1, m+1, 0)$ block-encoding of $f^{(\mathrm{SV})}(A)$.

While solving the QLSP does not provide classical access to the solution vector, this can still be done by utilising methods for vector-state tomography with a cost of $\mathcal{O}(N/\epsilon^2)$ samples [142]. Applying tomography would no longer allow for an exponential speed-up in the system size N [11]. However, polynomial speed-ups with tomography for some linear algebra-based algorithms are still possible for certain types of problems [48]. In addition, without classical access to the solution, certain statistics, such as the expectation of an observable with respect to the solution state, can still be obtained without losing the exponential speed-up in N [6,143]. Another current bottleneck for QLSS is loading the data of A and b into quantum gates and states, respectively [11]. In theory, this can be dealt with by using one of the two main quantum models for data access [48,139]: (i) the sparse-data access model and (ii) the quantum-accessible data structure. The sparse-data access model provides efficient quantum access to the nonzero elements of a sparse matrix. The quantum-accessible data structure, suitable for fixed-sized, non-sparse inputs, is a classical data structure stored in a quantum memory (e.g., Quantum Random Access Memory (QRAM)) and provides efficient quantum queries to its elements [139]. Considering the cost of QRAM with QEC overheads [144], the potential quantum advantage of QLSS may be reduced to polynomial at best [48] or none in the worse-case [11].

Lastly, for LSPs that involve only low-rank matrices, classical Monte Carlo methods for numerical linear algebra (e.g., the FKV algorithm [145]) can be used. These techniques have been used to produce classical algorithms that have an asymptotic exponential speed-up in dimension for various problems involving low-rank linear algebra (e.g., some machine learning problems) [146,147]. These classical quantum-inspired (dequantised) algorithms seem to have robustness issues [148], making QLSS potentially advantageous for certain cases. In addition, since these results do not apply to sparse linear systems, there is still the potential for provable speed-ups for problems involving sparse, high-rank matrices [48].

2.1.6. Variational Quantum Algorithms

Classical *variational method* is a well-established technique in quantum mechanics [149] for finding the ground state(s) of a quantum system based on the *variational principle*. The methods involve:

1. **Ansatz** - specifying some trial parametrised wavefunction $|\psi(\theta)\rangle$ where θ are the set of variational parameters.
2. **Variation** - minimising the expected energy

$$E = \langle \psi(\theta)|\mathcal{H}|\psi(\theta)\rangle \geq E_0, \tag{23}$$

 doi:10.20944/preprints202511.1802.v2

by varying the parameters θ.

Here, $\mathcal{H}$ is the Hamiltonian for the system, and by the *variational principle*, the energy E after each variation will always be bound below by the true ground state energy E_0 [149]. Hence, the set of parameters θ^* that minimizes Equation (23) results in a good approximation of the true ground-state energy E_0. In practice, there may be factors preventing the true ground state from being found, such as a failed optimisation, or an inappropriate ansatz that does not include the support basis vectors of the true ground-state [149]. In general, this task is computationally expensive for a complex many-body system with a Hilbert space that grows exponentially with system size. Hence, leveraging the high-dimensional capabilities of quantum computers to reduce the complexity of this method leads to the Variational Quantum Eigensolver (VQE) [150]. Figure 2 gives a sketch of the roles the classical and quantum computer plays in the VQE algorithm. Essentially, since the computation of the expectation value of Equation (23) is prohibitive classically, it is assigned to the Quantum Processing Unit (QPU) and the task of finding optimal parameters is assigned to the CPU [150].

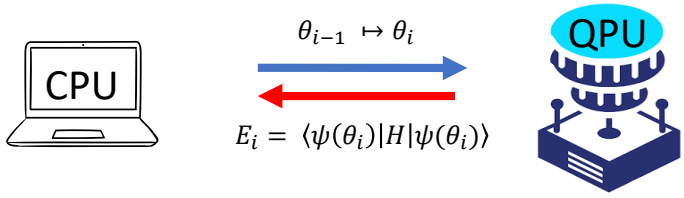

Figure 2. A sketch of classical and quantum computers' function in the VQE algorithm. The CPU sets and updates the parameters $(\theta_{i-1} \mapsto \theta_i)$ using an optimiser. The new parameters θ_i are used to prepare a quantum state $|\psi(\theta_i)\rangle$ on the QPU which is used to compute the expectation value $E_i = \langle\psi(\theta_i)|\mathcal{H}|\psi(\theta_i)\rangle$. Then the CPU takes this output E_i, and based on the energy difference $\Delta E_i = |E_i - E_{i-1}|$ decides to either terminate (convergence at $\Delta E_i \approx 0$) or continue loop with new variational parameters $(\theta_i \mapsto \theta_{i+1})$.

The choice of the VQE ansatz can have a significant effect on both the speed and quality of the solution. For example, the ansatz may be chosen to reflect a certain symmetry in the problem set up, or such that it rules out or focuses on a particular region of the Hilbert space, reflecting constraints on possible solutions [151]. Apart from the guideline of symmetry and expressiveness of the ansatz, there is no known general rule for picking the 'best' ansatz as it seems to be problem specific [152]. Another factor that impacts the quality of the solution is the performance of the classical optimiser. One common problem encountered when implementing variational algorithms is that of barren plateau [153], referring to solution landscapes that have exponentially vanishing gradients as a function of the number of qubits. This results in the optimiser being unable to efficiently find the optimal solution or being stuck in a local minimum. A lot of research has been done on the problem [154], but there is not yet a consensus on how to consistently identify or mitigate the issue [154–156].

The VQE algorithm can be considered a special cased of general Variational Quantum Algorithms (VQAs) with parametrized quantum circuits (denoted by the unitary $U(\theta)$) and a cost function given by [152]

$$C(\theta) = \sum_k f_k \Big(\mathrm{Tr}\Big[O_k U(\theta) \rho_k U^\dagger(\theta) \Big] \Big). \tag{24}$$

Here, $\{f_k\}$ is some set of functions with properties defined in [152], $\{\rho_k\}$ are input states from a training set, and $\{O_k\}$ are set of observables. The goal is to find an optimal set of parameters

$$\theta^* = \arg\min_\theta C(\theta), \tag{25}$$

by using a QPU to estimate the cost function $C(\theta)$ (or its gradient) while leveraging the efficiency of a classical optimizer to train the parameters θ. This framework naturally applies to quantum algorithms for optimisation problems [48,152,157] (see section (2.3) for more details). There have been numerous

 doi:10.20944/preprints202511.1802.v2

proposed applications of VQA which includes solving the QLSP [158,159]), PDEs) [160,161], and QML problems (section (2.4)) [162]. Although quantum computers are efficient in estimating the cost function, the general training VQAs (i.e., finding the optimal ansatz parameters) is an NP-hard non-convex optimisation problem [163,164]. Furthermore, these algorithms are heuristic with no yet provable quantum advantage in complexity of the algorithm [152], but they have empirical proof-of-concept implementations in NISQ era [48] and might obtain PQA with Mega-QuOps[4] QPUs [165].

2.1.7. Quantum Annealing

The Quantum Annealing (QAnn) algorithm [166,167] is an approach to quantum computing based on Adiabatic Quantum Computing (AQC) [168], which is an alternative to gate-based models of which all previous algorithms outlined in this section are derived from. While gate-based algorithms represent any computation as a series of gates, employing the concept of universality [44], AQC is an analogue approach that is suitable for a specific set of optimisation problems [168]. Primarily, the Quadratic Unconstrained Binary Optimisation (QUBO) problems (further discussed in section (2.3)), form the basis for a wide variety of NP-hard combinatorial optimisation problems tackled by QAnn [169].

Annealing relies on the adiabatic quantum theorem [168], which states that if the system starts in the nth eigenstate of a time-dependent Hamiltonian $\mathcal{H}(t = 0)$, and this Hamiltonian evolves *slowly enough*, the system will *remain* in the instantaneous nth eigenstate during the evolution. More specifically, during the time evolution, the parameters are changed sufficiently slowly that the system adapts to the new parameter configuration quasi-instantaneously. The length of time required for the evolution to succeed depends on the spectral properties of the Hamiltonian path and, in particular, on the minimum spectral gap [168]. For example, the change from $\mathcal{H}_0$ to $\mathcal{H}_1$ can be achieved by the Hamiltonian:

$$\mathcal{H}(t) = (1 - f(s))\mathcal{H}_0 + f(s)\mathcal{H}_1 \tag{26}$$

where $f(s) \in [0, 1]$ is the the scheduling function and $s \in [0, 1]$ is the annealing parameter. The scheduling function is chosen such that at $f(s = 0) = 0$, the system is governed by some initial Hamiltonian $\mathcal{H}_0$, and at $f(s = 1) = 1$ the final dynamics are governed by the *problem* Hamiltonian $\mathcal{H}_1$. This implies that $f(s)$ must be strictly increasing and the simplest choice $f(s) = s$ gives the vanilla AQC. If the system starts in the ground state (eigenstate with minimal energy) of $\mathcal{H}_0$ and slowly evolves, then according to the adiabatic theorem, it will remain the ground state throughout its evolution until it rests in the ground state of $\mathcal{H}_1$ [168]. This means that, to find the unknown ground state of a Hamiltonian for a hard-to-solve problem $\mathcal{H}_1$, one can start from an easy-to-solve Hamiltonian $\mathcal{H}_0$ with a known ground state and apply the QAnn algorithm.

Typically, the Hamiltonian $\mathcal{H}_0$ has the form $\mathcal{H}_0 = \sum_i \sigma_i^x$ with ground state being the equal superposition of all bit strings $\{x\}$ [166]. On the other hand, $\mathcal{H}_1$ is described by the canonical Ising model

$$\mathcal{H}_1 = \sum_i h_i \sigma_i^z + \sum_{i,j} J_{ij} \sigma_i^z \sigma_j^z. \tag{27}$$

where the biases h_i and couplings J_{ij} are determined by the problem [166]. In practice, it is very difficult to fulfil the conditions to achieve adiabaticity, mainly due to unwanted noise on NISQ hardware. Therefore, annealers forego some of the stringent theoretical conditions and heuristically repeat the annealing procedure many times, collecting several samples from which the configuration with the lowest energy can be selected as the optimal solution, but with no strict guarantee that the optimal solution will be in this sample set [48,170].

One key issue affecting annealing is the requirement that the problem is reformulated in the correct format (as it is believed the transverse-field Ising Hamiltonian is not universal [57]. For problems which have a native structure (including many graph-based problems, for example), annealing is particularly suitable [170]. For non-native problems, this reformulation may introduce a significant

[4] Quantum computers capable of performing about a million error-corrected quantum operations

 doi:10.20944/preprints202511.1802.v2

overhead, or such strenuous constraints, that annealing might fail consistently, or any potential quantum advantage might be lost [170]. There exist classes of time-dependent Hamiltonians that, through adiabatic evolution, can approximate arbitrary unitary operators applied to qubits [168,171]. Thus AQC can also realise universal quantum computation for such a class of problems. However, by polynomial equivalence to the circuit model, gate-based devices can also efficiently simulate these problems [168,170].

The main reason behind the interest in QAnn is that it provides a non-classical heuristic, tunnelling, that is potentially helpful for escaping from local minima [168]. Its closest classical analogue is simulated annealing [172], a Markov chain Monte Carlo method that was inspired by classical thermodynamics and uses temperature as a heuristic to escape from local minima. So far QAnn has demonstrated usefulness for solving QUBOs with tall yet narrow peaks in the cost function [173,174]. The overall benefit of QAnn is still a topic of ongoing research [48,170,173]. Furthermore, commercially available quantum machines that implement QAnn, from providers such as D-Wave [175], have allowed for various near-term exploration [176–179].

2.2. *Quantum Simulation*

While quantum simulation was originally envisioned as a tool for modelling quantum mechanical systems [2,3], recent advances have demonstrated its broader potential to address classical problems whose dimensional complexity renders them inefficiently solvable when tackled with conventional methods [180]. This is the case in the domain of quantitative finance, where the numerical solutions of Stochastic Differential Equations (SDEs) play a central role in modelling financial products such as pricing options [84,85]. These problems, while inherently classical, often involve high-dimensional integration and probabilistic dynamics that render them computationally intensive [181]. Quantum simulation techniques, including those adapted for solving linear systems and sampling probability distributions, provide promising pathways to address these challenges [9,31]. In the classical regime, SDEs such as those arising in the pricing of financial derivatives under the Black-Scholes-Merton or Heston models, require discretisation techniques like finite differences or Monte Carlo simulations [182]. However, the computational cost grows rapidly with the number of risk factors or underlying assets - a manifestation of the so-called *curse of dimensionality*. Quantum computing offers a potential remedy through quantum algorithms, which can achieve polynomial [5] or even exponential speed-ups over classical counterparts for problems with certain structures [183]. In this review, we will consider quantum algorithms that speed up Monte Carlo Integration (MCI) and quantum solvers for SDEs.

2.2.1. Quantum Monte Carlo

Monte Carlo methods are very commonly used to approximate solutions to equations that are difficult to solve analytically or when numerical methods scale poorly with the dimension of the problem. These include inference [184], optimisation [185], numerical integration [186], and stochastic expectation values [182]. For the latter, MCI is ubiquitously used in finance for problems such as asset pricing and risk analyses of complex investment portfolios (see use cases in sections (3.1)-(3.3)). The major advantage of MCI methods is that their scaling depends on the number of samples and not the dimension of the problem [182]. However, their downside is that they have a slow convergence since their estimation error ϵ decays as $\mathcal{O}\left(1/\sqrt{N_p}\right)$, where N_p is the number of sample paths taken [5]. Routine finance problems such as risk analysis or pricing options often require large amounts of samples to achieve a desired precision [9]. Thus, there is value in exploring and understanding any potential benefits that quantum computing could bring in this space.

QMCI Algorithm

The typical use of MCI in finance is to estimate the expected value of an unknown financial quantity (e.g., price of a financial derivative), which is a function of other nondeterministic variables (e.g., market state) [9]. The methodology, described in more detail in Section (3.1.2), generally starts with choosing a stochastic model for the underlying random variables from which samples, denoted

 doi:10.20944/preprints202511.1802.v2

as $\{X_1, \ldots, X_n\} \subseteq \Omega$, are taken. Then the corresponding value of the target quantity, denoted as $f(X_1, \ldots, X_n)$[5], is computed based on the samples drawn. The weighted average of all obtained values of the target quantity is given by the expectation [182]

$$\mathbb{E}[f(X)] = \int_\Omega p(X) f(X) dX \approx \sum_{i=1}^{n} p(X_i) f(X_i) \tag{28}$$

where $p(X)$ is the probability distribution. Note that the random variable is sampled from a space $X_i \subset \Omega$ that could be multi-dimensional. The Quantum Monte Carlo Integration (QMCI) [5] is the quantum formulation of the MCI method. Outlined in Algorithm (7), the QMCI utilises the Quantum Amplitude Estimation subroutine to compute the expectation given in Equation (28) and can potentially achieve a quadratic speed-up over classical MCI [5]. This is because the estimation error for QMCI decays as $\mathcal{O}(1/N_q)$, where N_q is the number of queries made to a quantum oracle that computes $f(X_1, \ldots, X_n)$. This is comparable to the complexity in terms of the number of samples N_p for MCI which has an error that scales as $\mathcal{O}(1/\sqrt{N_p})$. Thus, if samples are considered as classical queries, the QMCI requires quadratically fewer queries than classical MCI to achieve the same desired error.

Algorithm 7 Quantum Monte Carlo Integration

Define: Let Ω be the set of potential sample paths ω of a stochastic process that is distributed according to some probability $p(\omega)$, and $f : \Omega \to A$ is a real-valued function on Ω, where $A \subset \mathbb{R}$ is bounded.
Construct: A unitary operator P_l to load a discretised and truncated version of $p(\omega)$. The probability value $p(\omega)$ translates to the amplitude of the quantum state $|\omega\rangle$ representing the discrete sample path ω. In mathematical form, it is

$$P_l |0\rangle = \sum_{\omega \in \Omega} \sqrt{p(\omega)} |\omega\rangle \tag{29}$$

Normalise: The function f into $\tilde{f} : \Omega \to [0, 1]$, and construct a unitary P_f that computes $\tilde{f}(\omega)$ and loads the value onto the amplitude of $|\omega\rangle$. The resultant state after applying P_l and P_f is

$$P_f P_l |0\rangle = \sum_{\omega \in \Omega} \sqrt{(1 - \tilde{f}(\omega)) p(\omega)} |\omega\rangle |0\rangle + \sqrt{\tilde{f}(\omega) p(\omega)} |\omega\rangle |1\rangle \tag{30}$$

Perform: The QAE with unitary $U = P_l P_f$ and an oracle O_f that marks states with the last qubit being $|1\rangle$. See Section (2.1.2.2) for details.
Result: Will be an approximation to

$$\mathbb{E}[\tilde{f}] = \sum_{\omega \in \Omega} \tilde{f}(\omega) p(\omega)$$

This value can be estimated to a desired error ϵ utilising $\mathcal{O}(1/\epsilon)$ evaluations of U and its inverse [5].
Rescale: The output $\mathbb{E}[\tilde{f}]$ to the original bounded range (A) to obtain $\mathbb{E}[f]$.

Challenges for Quantum Advantage

At the time of this manuscript, no demonstration of quantum advantage with QMCI has been made, primarily due to the limitations of current quantum hardware and algorithmic challenges in key subroutines [12]. The former hardware limitations are due to:

1. **Clock speed**: As noted in [187], to achieve a Practical Quantum Advantage using QMCI over classical MCI, the quantum device would need to be able execute about 10^7 layers of T-gates[6] per second. This implies a required logical clock rate of about 50MHz to be competitive with current classical MCI methods. Recent methods [188] have reduced this requirement to 45MHz, which is still beyond the capabilities of current hardware.

[5] Here $f(\cdot)$ could represent the payoff function for option pricing, see Section (3.1.2.1)
[6] See Table 2 for description of T-gate.

 doi:10.20944/preprints202511.1802.v2

2. **Fault-tolerant**: The code distance for fault-tolerant implementations needs to be large enough to support 10^{10} error-free logical operations [187]. In addition, quantum algorithms with a proposed quadratic speed-up need to tackle significantly high-dimensional problems to potentially realise some advantage [46], which further complicates fault-tolerant implementations.
3. **Resource:** The estimates are high for fault-tolerant resources needed to achieve competitive performance for finance problems that are challenging for classical methods. The latest estimates for derivative pricing [188] based on Quantum Signal Processing are 4.7×10^3 logical qubits, 4.5×10^7 T-depth, and 2.4×10^9 T-count. These requirements are beyond currently available quantum hardware, and seem to be significantly higher in comparison to classical MCI, which requires 4×10^4 samples and about 10 seconds to achieve the same accuracy [48].

On the other hand, the latter algorithmic challenges are due to:

1. **Loading distribution**: The state-preparation of an arbitrary probability distribution requires exponentially large circuits in terms of the number of qubits [189], which affects the potential quantum speed-up of QMCI. The improved state-preparation algorithm by Grover–Rudolph [190] is insufficient to achieve a quantum speed-up [191]. However, for certain distributions, a quadratic speed-up is possible [95,192,193]. It is noteworthy that various non-unitary methods exist for efficient state preparation for large circuits [194,195]. However, these methods are usually incompatible with QAE because of the non-invertibility of the operations involved. Furthermore, other alternative methods have been proposed, such as Quantum Generative Adversarial Networks (QGAN) [196] and tensor networks [197].
2. **Arithmetic**: Computing coherent quantum arithmetic associated with function $f(\omega)$ can have gate complexity that is similar to classical arithmetic [48]. This step can be elevated by quantum arithmetic-free methods based on Quantum Signal Processing [192] and Fourier analysis [193,198].
3. **Estimation**: The first proposed QAE algorithm employed QPE which has a resource requirement beyond the capabilities of NISQ devices (see Section 2.1.1). However, non-QPE implementations of QAE have been proposed which can enable near-term implementations of QMCI (see Section 2.1.2.2).

As noted in [193], many other factors will drive the adoption of quantum computing in finance beyond exceeding classical performance. Some of these factors will be technical, such as ease of incorporation of QPU in a computational pipeline in finance, and others may be business and/or regulatory-related. In any case, it is important to have a well-defined framework [199] to evaluate the goal of achieving Practical Quantum Advantage. In this review, we will consider several use cases for QMCI in finance and economics, which are good candidates for obtaining a PQA in the long-run as the quantum technology matures.

2.2.2. Quantum Solvers for Stochastic PDEs

Stochastic Differential Equations (SDEs) have become fundamental tools for modelling a wide array of phenomena within finance and economics [200]. The dynamic and often unpredictable nature of financial quantities, such as asset prices, interest rates, and their derivatives, aligns naturally with the framework provided by SDEs, which explicitly incorporates stochastic elements into their structure. Unlike deterministic models based on ordinary differential equations, which yield a unique solution for a given initial condition, SDEs describe the evolution of continuous-time stochastic processes, reflecting the inherent uncertainties present in financial systems. The necessity of employing SDEs in finance arises from the fact that many financial variables exhibit diffusive dynamics, a characteristic well-captured by stochastic processes [200]. For instance, the Heath-Jarrow-Morton model [201], a cornerstone in interest rate modelling, is formulated as an SDEs. Similarly, the Heston [202] model for pricing of options under conditions of stochastic volatility, where the volatility itself is modelled as a random process, leads to a set of coupled SDEs[7].

[7] See Section (3.1.2.1) for more details

 doi:10.20944/preprints202511.1802.v2

Despite the power and versatility of SDEs in capturing the complexities of financial markets, obtaining analytical solutions to these equations is often a formidable challenge for realistic models [200,203]. This is due to various factors, which include nonlinearities in models that complicate integration and inherent high-dimensionality from multiple underlying variables [204]. There are various numerical methods for solving SDE with diverse approaches; however, in this review, we will only consider the approach of employing the Feynman-Kac formula, which gives the expectation value[8] to Equation (28) as a solution to a parabolic PDE. This will make it easier to compare with the QMCI algorithms described above.

Feynman-Kac Formula

Originally conceived within the framework of quantum mechanics by Feynman through his path integral formulation [205] and later rigorously formulated in a probabilistic context by Kac [206], this formula provides an alternative perspective for solving the expectation value given by Equation (28). Its original usage had the reverse objective to what we use it for here; that is, to solve a complex PDE with high dimensionality or non-constant coefficients by computing the expected value of a carefully constructed stochastic process [200]. However, since quantum computing is more suited to handle serious dimensional problems, it makes sense to convert expected values of stochastic processes into parabolic PDEs.

The Feynman-Kac formula [200,205–207] establishes a profound connection between parabolic partial PDEs and the expected values of certain stochastic processes. This relationship provides a conversion between the two, which can be a powerful tool for analysis and computation.

Mathematical Formulation Consider a parabolic PDE for the unknown variable $u = u(x,t) : \mathbb{R}^n \times [0,T] \mapsto \mathbb{R}$ of the form:

$$\frac{\partial}{\partial t}u + \mu \cdot \nabla u + \frac{1}{2}\mathrm{Tr}\left[\Sigma\Sigma^\intercal D^2 u\right] - Vu + f = 0 \tag{31}$$

with a terminal condition $u(x,T) = g(x)$, where $g(x)$ is the terminal payoff function. Here the known functions: $\mu = \mu(x,t)$ is a vector-valued function representing the drift, $\Sigma = \Sigma(x,t)$ is an $n \times d$ matrix representing the diffusion coefficient, $V = V(x,t)$ is a scalar potential function, and $f = f(x,t)$ is a source term. The operators: ∇u is the gradient of u, $D^2 u$ is the Hessian matrix of u, and Tr denotes the trace of a matrix. The Feynman-Kac theorem [200,207] states that the solution to the PDE in Equation (31) can be expressed as the conditional expectation:

$$u(x,t) = \mathbb{E}_Q\left[g(X_T)h(t,T) + \int_t^T f(s,X_s)h(t,r)dr \mid X_t = x\right], \tag{32}$$

where the function $h(\cdot)$ is given by

$$h(a,b) = \exp\left(-\int_a^b V(s,X_s)ds\right). \tag{33}$$

The stochastic variable X_s is the solution to the following SDE [200]:

$$dX_s = \mu(s,X_s)ds + \sigma(s,X_s)dW_s^Q \tag{34}$$

with the initial condition $X_t = x$, and W_s^Q is a d-dimensional standard Brownian motion under a probability measure Q. The expectation $\mathbb{E}_Q[\cdot]$ is taken with respect to this probability measure, conditional on the initial state $X_t = x$. Intuitively, the Feynman-Kac formula suggests [207] that the value of the function $u(x,t)$ at a point (x,t) can be seen as the expected future value, discounted by the potential V, of a stochastic process X that starts at x at time t and evolves according to the SDE

[8] This is similar to Equation (145) of Section (3.1.2)

 doi:10.20944/preprints202511.1802.v2

in Equation (34). The terminal condition $g(X_T)$ contributes at the final time T, and the source term $f(s, X_s)$ contributes along the path of the process. The function $h(a, b)$ acts as a stochastic discount factor, accounting for the accumulated effect of the potential along the random path.

Example BSM Model A classic example is the Black-Scholes-Merton (BSM) model for the vanilla European option[9], where Equation (31) can be formulated as [31]

$$\frac{\partial V}{\partial t} + rS\frac{\partial V}{\partial S} + \frac{1}{2}\sigma^2 S^2 \frac{\partial^2 V}{\partial S^2} - rV = 0, \tag{35}$$

where $V(t, S_t) \in (0, T) \times \mathbb{R}^+$ is the option expected value with the terminal condition

$$V(T, S) = f(T, S). \tag{36}$$

Here $f(\cdot)$ is the payoff function, r is the risk-free rate, and σ is the volatility of the stochastic underlying asset S_t. At the PDE of the form of Equation (35) can be solved by using quantum algorithms outlined in the ensuing sections.

Finite Difference Method

A widely used class of numerical techniques is Finite Difference Method (FDM) [208] that approximate the derivatives appearing in differential equations using differences between the values of the unknown function at discrete points in time and space. When applied to SDEs, the FDMs involves discretising both the spatial and temporal domains into a grid and replacing the continuous derivatives with their finite difference approximations [200]. Various finite difference schemes exist, including explicit and implicit methods, each exhibiting different characteristics in terms of stability and computational requirements [208]. For instance, explicit schemes are generally simpler to implement but may have stricter stability conditions, while implicit schemes, such as the Crank-Nicolson method, are known for their numerical stability, particularly for parabolic PDEs common in finance [208,209]. In situations where the financial model exhibits convection-dominated behaviour, upwind schemes are often employed to ensure numerical stability and accuracy [210].

Algorithm (8) outlines a general scheme of the FDM for solving SDEs via the Feynman-Kac formula. For every time step t_j, the problem boils down to solving a linear system of equations with dimension N that depends on the discretisation in the stochastic variable x. Therefore, assuming the matrix A in Equation (38) is well conditioned, we can employ the Quantum Linear Systems Solver discussed in Section (2.1.5) to potentially obtain an exponential speed-up [131,132]. For arbitrary cases, A is not guaranteed to be well-conditioned, and the condition number may scale as a polynomial with the dimension: $\kappa(A) \sim \mathcal{O}(\text{poly}(N))$. In such cases, both classical and quantum methods can make use of preconditioners to reduce κ before running the linear system solver algorithm. The use of preconditioners for QLSSs has been explored [183,211–213] and has shown promising results. For example, authors in [183] used a wavelet basis as an auxiliary system of coordinates in which the condition number of associated matrices is independent of N by a simple diagonal preconditioner.

[9] See Section (3.1.2) for more details.

 doi:10.20944/preprints202511.1802.v2

Algorithm 8 Finite Difference Method for solving SDEs

1. Define bounds for stochastic variable $X_t = x$ and impose appropriate boundary conditions for the expectation $u(x,t)$ [200].
2. Define the finite difference mesh by choosing two natural numbers $J > 1$ and $I > 1$.
   - the constant time step size $\Delta t = T/(J+1)$ and asset step size $\Delta x = x_\infty/(I+1)$
   - mesh nodes are $(t_j, x_i) = (j\Delta t, i\Delta x)$ where $i, j \in [0, I+1], [0, J+1]$
3. Define a suitable numerical approximation of the derivatives at each mesh node. Let $u_{ji} = u(t_j, x_i)$ the derivatives are given by [208]
$$\frac{\partial u}{\partial t} \approx \frac{u_{j+1,i} - u_{j,i}}{\Delta t}, \quad \frac{\partial u}{\partial x} \approx \frac{u_{j,i+1} - u_{j,i-1}}{2\Delta x}, \quad \frac{\partial^2 u}{\partial x^2} \approx \frac{u_{j,i+1} - 2u_{ji} + u_{j,i-1}}{(\Delta x)^2} \tag{37}$$
   where the second-order Crank-Nicolson method [208] can be used for the discretisation in time.
4. This leads to a $N = I + 1$ dimensional linear system at each time t_j given by
$$Au_j = b_j, \quad u_j, b_j \in \mathbb{R}^N \quad \text{and} \quad A \in \mathbb{R}^{N\times N} \tag{38}$$
5. Starting with $j = J + 1$, one can solve Equation (31) using either classical or quantum algorithms:
   - CG method [214] with scales as $\mathcal{O}\left(N\sqrt{\kappa}\log(\frac{1}{\epsilon})\right)$
   - QLSS [131] which scales as $\mathcal{O}\left(\log(N)\kappa\log(\frac{1}{\epsilon})\right)$

   where κ is the condition number for A and ϵ is the error tolerance.
6. Sequentially repeat step 4-6 for $j = J, J-1, \ldots, 0$.

A crucial aspect of employing FDMs for SDEs is the analysis of their stability and convergence in the presence of stochastic terms [200]. Stability ensures that any numerical errors introduced during the computation do not grow uncontrollably as the simulation progresses. Convergence analysis, on the other hand, aims to determine whether the numerical solution obtained through the FDM approaches the true solution of the SDE as the discretization step sizes in time and space are refined. In general, the convergence of numerical schemes can be characterized in two ways [208,209]: strong convergence, which focuses on the pathwise accuracy of the approximation, and weak convergence, which concerns the accuracy of the moments of the solution. These concepts of strong and weak convergence are extended to the numerical analysis of SDEs as well [200]. Therefore, it is still an active area of research [215,216] to determine how noise from quantum computing affects the stability and convergence analysis of SDEs.

Hamiltonian Simulation

The natural language of quantum computing is in terms of Hamiltonian representation [149], thus an interesting approach to solving a PDE of the form of Equation (31) is to convert it into a Schrödinger or Schrödinger-like equation. For example, in Ref. [217] showed that for the BSM model given by Equation (35), one can perform a change of variables $S = e^x$ for $x \in (-\infty, +\infty)$ and reversal of time $t \to \tau = T - t$ to reformulate Equation (35) into a Schrödinger-like equation:

$$\frac{\partial V}{\partial \tau} = i\mathcal{H}V, \tag{39}$$

where $\mathcal{H}$ is a non-Hermitian Hamiltonian given by

$$\mathcal{H} = i\frac{\sigma^2}{2}\hat{p}^2 - \left(\frac{\sigma^2}{2} - r\right)\hat{p} + ir\mathbb{I}. \tag{40}$$

 doi:10.20944/preprints202511.1802.v2

Here, $\hat{p} = -i\frac{\partial}{\partial x}$ in the momentum operator. Since the associated propagator $\hat{U}(\tau) = e^{i\tau\mathcal{H}}$ is non-unitary, the approach of [217] is to decompose $\mathcal{H}$ into a sum of Hermitian and anti-Hermitian part, $\mathcal{H} = \mathcal{H}_{\rm H} + \mathcal{H}_{\rm A}$, with

$$\mathcal{H}_{\rm H} = -\left(\frac{\sigma^2}{2} - r\right)\hat{p}, \quad \text{and} \quad \mathcal{H}_{\rm A} = i\left(\frac{\sigma^2}{2}\hat{p}^2 + r\mathbb{I}\right). \tag{41}$$

Since, the two parts of $\mathcal{H}$ commutes with each other $[\mathcal{H}_{\rm H}, \mathcal{H}_{\rm A}] = 0$, then via the Baker-Campbell-Hausdoff formula [218] the evolution operator can be written as $\hat{U}(\tau) = e^{i\tau\mathcal{H}_{\rm H}}e^{i\tau\mathcal{H}_{\rm A}}$. The non-unitary $\hat{O} = e^{i\tau\mathcal{H}_{\rm A}}$ is then embedding it into an enlarged Hilbert space requiring one additional ancillary qubit, such that the corresponding unitary evolution $\tilde{U}(\tau)$ is given by

$$\tilde{U}(\tau) = \begin{pmatrix} \hat{O} & \sqrt{1-\hat{O}^2} \\ \sqrt{1-\hat{O}^2} & -\hat{O} \end{pmatrix} \tag{42}$$

A proof-of-concept implementation using 8 qubits on a simulator got results in good agreement with analytical solutions for the BSM model[217].

The major drawback with the approach of [217] is that the embedding technique doubles the size of the problem. An alternative Hamiltonian simulation is to make an additional change of variables [216,219]:

$$\tau = \sigma^2(T-t), \quad \text{and} \quad v(x,\tau) = \exp(-ax - b\tau)V(t, S_t), \tag{43}$$

where a, b are constants given by the BSM model. This allows for the mapping of Equation (35) into the heat equation of the form [216,219]:

$$\frac{\partial v}{\partial \tau} = \frac{1}{2}\frac{\partial^2 v}{\partial \tau^2}. \tag{44}$$

A Wick rotation is performed on the time variable $\tilde{\tau} \to -i\tau$, which then can be mapped to a Schrödinger-like equation in imaginary time:

$$\frac{\partial v}{\partial \tilde{\tau}} = -\mathcal{H}_{\rm I}\, v, \tag{45}$$

where the operator $\mathcal{H}_{\rm I}$ is given by

$$\mathcal{H}_{\rm I} = -\frac{i}{2}\hat{q}^2, \quad \text{for} \quad \hat{q} = -i\frac{\partial}{\partial x}. \tag{46}$$

This simulation can be performed using the Quantum Imaginary Time Evolution (QITE), which was first proposed for quantum chemistry problems [220] but has also been applied to other quantum simulation problems [221]. State-of-the-art methods for QITE include accelerated approaches using random measurements [222], and an alternative approach that uses orthogonal basis states to efficiently express the propagated state [223]. The Schrödingerisation method of [219] can be applied to general linear differential equations, including the Fokker–Planck equation [224], which describes the time evolution of the probability density function of the velocity of a particle under the influence of drag forces and random forces. Hence, methods of solving SDE via the Fokker–Planck formulation can also be handled by the aforementioned quantum algorithm [216].

Other Approaches It is worth mentioning other quantum approaches to solving SDEs, in particular the the variational algorithm of Ref. [161]. In this approach, they first approximate the target SDE by a trinomial tree structure with discretisation to obtain a linear differential equation describing the probability distribution of SDE solutions. The resulting differential equation is then solved by formulating it as the time-evolution of a quantum state embedding the probability distributions of the SDE variables. This approach utilises the Fokker–Planck equation [224], which also gives the time

 doi:10.20944/preprints202511.1802.v2

evolution of the probability distributions of SDE solutions. A proof-of-concept implementation of this approach was shown to be in close agreement with classical methods [161], but the reported scaling of this method does not seem promising for achieving Practical Quantum Advantage for industrial-scale problems.

2.3. Quantum Optimisation

Broadly speaking, optimisation is the act of modifying a process to extremise some property, which might be the occurrence of favourable outcomes, the profit of some business model, expected returns of a portfolio, or any number of other things [225,226]. Performing an optimisation requires us to make some assumptions about the real world. For example, an investor who wishes to optimise their portfolio to maximise returns or minimise risk could begin by stating assumptions about present and future market conditions, such as risk or volatility, and comparative returns [204,227]. Since there is no way to accurately calculate these in real-time, the proper estimation of these values is vital [181,204].

In the financial sector, optimisation is the process of making a financial system more effective by adjusting the variables used for technical analysis, which might involve, for example, reducing certain transaction costs, risks, or targeting assets with greater expected returns [228]. Depending on the underlying assumptions or the target of the optimisation, there may be multiple potential optimisation procedures. The success of the chosen procedure will depend on how well one has estimated or quantified the risks, costs, and potential payouts.

Optimisation problems are, therefore, almost ubiquitous, but often very time-consuming or computationally expensive to solve given the number of variables involved [229]. Their high impact, combined with the existence and relative maturity of many quantum algorithms for solving them [150,157,230–232], means there is a lot of potential value in exploring commercially relevant applications on NISQ hardware [150,157]. Furthermore, improvements in hardware mean that the prospect of thorough and reliable benchmarking of various quantum algorithms is closer to reality. A recent paper [233] presented ten optimisation problem classes, as well as a Quantum Optimisation Benchmark Library for recording problem instances and solution track records, with standardised reporting and comparisons to the classical state of the art. This and similar efforts allow more rigorous comparison of different quantum optimisation algorithms, clarifying competing claims of suitability or performance, and enabling laypersons to more confidently explore and implement solutions.

This section discusses how such quantum algorithms may be used to solve two types of optimisation problems [152]: (i) combinatorial optimisation and (ii) convex optimisation. The former is a discrete optimisation problem, consisting of finding the optimal combination of values for some cost function, while the latter is a continuous optimisation problem involving optimising some convex cost function.

2.3.1. Combinatorial Optimisation Problems

This section presents quantum approaches for solving complex combinatorial optimisation problems which fall under the NP-hard computational class [234,235]. It is believed that there is potential for quantum advantage in this field, with quantum computers approximating solutions faster, providing higher quality solutions, or a mix of both [236]. However, this has not yet been demonstrated on large-scale real-world problems, and there remain significant theoretical and experimental challenges to overcome.

In general, combinatorial optimisation is a subfield of optimisation where the set of feasible solutions is, or can be reduced to, a discrete set. Typical combinatorial optimisation problems are the travelling salesman problem, the minimum spanning tree problem, and the knapsack problem. In many such problems, exhaustive search is not tractable, and approximation algorithms, or specialised algorithms that quickly rule out large parts of the search space, need to be used instead [236].

In the literature, combinatorial optimisation is closely interlinked with Integer Programming (IP), which concerns optimisation or feasibility problems, usually NP-hard, where some or all of the variables are restricted to be integers [235]. A specific subcategory of IP is binary problems, i.e.,

 doi:10.20944/preprints202511.1802.v2

problems in which the variables are restricted to be either 0 or 1. Trivially, all integer problems can also be represented as binary problems by expressing the integers in binary, at the cost of a logarithmic increase in problem size.

QUBO Formulation

Many IP and combinatorial optimisation problems, such as ones encountered in finance, can be reduced to a set of problems called Binary Quadratic Programming (BQP) problems with at most quadratic cost functions and constraints. By definition, a BQP can be written in the following general format:

$$\min f(x) = \sum a_i x_i + \sum b_{ij} x_i x_j \quad \text{s.t. } \sum c_i^m x_i + \sum d_{ij}^m x_i x_j + e^m \circ 0 \tag{47}$$

where x_i are binary variables, a_i and b_{ij} are the coefficients for the objective function, c_i^m, d_{ij}^m, e^m are the coefficients for the m-th constraint, and $\circ \in \{<, \leq, =, \geq, >\}$.

A Quadratic Unconstrained Binary Optimisation (QUBO) problem is a BQP with no constraints [237]. It can be written as

$$\min f(x) = \mathbf{x}^\intercal Q \mathbf{x} \tag{48}$$

where $\mathbf{x}$ is a binary vector and Q is a real symmetric matrix [237]. BQP problems can be converted to QUBOs using the Lagrangian formulation, where each constraint is converted into a penalty term with the appropriate Lagrangian parameter. This ensures that the optimal result is preserved while penalising infeasible solutions [226,238,239]. For example, if we have some constraint $Ax = b$, then the corresponding Lagrangian penalty term added to the QUBO would be $\lambda(Ax - b)^2$, which penalises infeasible solutions by an amount determined by λ.

It is known that QUBOs are very closely related (and computationally equivalent) to the Ising model, and solving them is similar to finding the ground state of the generalised Ising Hamiltonian [239]. The classical Hamiltonian of such a model is defined as:

$$\mathcal{H} = -\sum_{ij} J_{ij}\sigma_i\sigma_j - \sum_j h_j\sigma_j, \tag{49}$$

Where $J_{ij} \in \mathbb{R}$ represents the interaction between the sites i and j, and the spin variables σ_i are in the set $\{-1, 1\}$. Moreover, in the Ising model, the variables are typically arranged in a lattice where only neighbouring pairs of variables ij can have non-zero coefficients. One can then follow the substitution $\sigma_i = 2x_i - 1$ to define a QUBO cost function, similar to the form of Equation (47), thus transforming it to a classical Ising Hamiltonian.

This classical Hamiltonian can be quantised by replacing the classical variable σ_j with the Pauli-Z operator σ_j^z. Thus, finding the optimal solution for the QUBO is equivalent to finding the ground state of the corresponding Ising Hamiltonian [239]. This equivalence can be shown from Equations (47) and (49) where:

$$\begin{aligned}
\mathcal{H} &= \sum_{ij} -J_{ij}(2x_i - 1)(2x_j - 1) - \sum_j h_j(2x_j - 1) \\
&= \sum_{ij}(-4J_{ij}x_i x_j + 2J_{ij}x_i + 2J_{ij}x_j - J_{ij}) - \sum_j (2h_j x_j - h_j) \\
&= \sum_{i=1}^{N}\sum_{j=1}^{i} q_{ij}x_i x_j + C.
\end{aligned} \tag{50}$$

In the last line of Equation (50), we have used

$$q_{ij} = \begin{cases} -4J_{ij} & \text{if } i \neq j \\ \sum_{ki} 2J_{ki} + \sum_{il} 2J_{il} + 2h_i & \text{if } i = j \end{cases} \tag{51}$$

 doi:10.20944/preprints202511.1802.v2

and

$$C = -\sum_{ij} J_{ij} - \sum_{j} h_j. \tag{52}$$

As the constant C does not change the location of the optimum x, it can be neglected for optimisation and is only important for recovering the value of the original Hamiltonian [239]. In the ensuing subsections, we will review quantum algorithms for solving the optimisation problem defined by Equation (50) that are implementable in NISQ devices.

Variational Quantum Eigensolver

As discussed in Section (2.1.6), the Variational Quantum Eigensolver (VQE) is a hybrid quantum-classical algorithm that is used for optimisation problems. First proposed by Peruzzo et al. [150], and then extended and formalised by McClean et al. [240], the VQE is among the most widely used algorithms on NISQ hardware. Originally formulated to estimate the ground state of some Hamiltonian by employing the *variational method* (and more precisely in the Rayleigh-Ritz functional [241,242]), which finds an upper bound for the lowest possible expectation value of an observable with respect to a trial wavefunction. In this formulation, VQE can also be used as the first step in simulating molecules and materials, among other applications [152]. As noted in Section (2.1.6), the VQE algorithm can be used for find the optimal parameters

$$\theta^* = \arg\min_{\theta} C(\theta), \tag{53}$$

for a general cost function $C(\theta)$ generated from a parametrized circuit $U(\theta)$ [152]. This makes VQE apt for various optimisation problems.

The VQE algorithm, as illustrated in Figure 3, typically starts with a pre-processing step, defining the system whose ground state the process is trying to identify. This could include constructing the Hamiltonian and additional necessary steps (for example, encoding Pauli operators or measurement weighting [243]). The algorithm will then progress to the hybrid loop, where the classical subroutine handles the parameter updates (e.g., performing a gradient descent based on the returned values), while the quantum subroutine runs the circuit and returns the results. The hybrid loop takes a training set, a cost function, and an ansatz as input; the ansatz is the circuit used to perform the quantum mechanical estimation. visualises this process.

A key (and challenging) part of the VQE is choosing a suitable ansatz for the problem at hand. Certain ansatze are more suitable for particular problems because they take into account prior information about the ground-state wave function(s) [150]. Alternatively, evolutionary and noise-resistant techniques exist to optimise the structure of the ansatz and significantly increase the space of candidate wave functions [244]. In a recent paper [245], the authors introduced quantum variational filtering, which can be used to increase the probability of sampling low-eigenvalue states of an observable when the filtering operator is applied to an arbitrary quantum state. Their algorithm, filtering VQE, was applied to combinatorial optimisation problems and outperformed both standard VQE and QAOA [245]. Finally, the Deep VQE (DVQE) method was introduced by [246], which applies a divide-and-conquer method in order to reduce the system dimensionality and solve the effective Hamiltonian further than the approaches. In other words, the DVQE approach can provide the ground state of a given quantum system with a smaller number of qubits.

Another key problem with variational algorithms is that of barren plateaus [153]. This refers to the presence of a flattened energy landscape, with variation only in the near neighbourhood of the optimal solution. As a result, the classical optimiser is unable to converge (see Section 2.1.6). A review on barren plateaus can be found in [154] summarises the issue as arising due to the *curse of dimensionality*, where the very strength of quantum computing, the ability to manipulate and compute in a higher-dimensional space, also hinders variational algorithms. This can be circumvented using a variety of techniques, including problem-aware encodings and formulations, and specified ansatz

 doi:10.20944/preprints202511.1802.v2

architectures, but it remains an open question as to whether these further restrictions reduce the potential for quantum advantage via this algorithm [154].

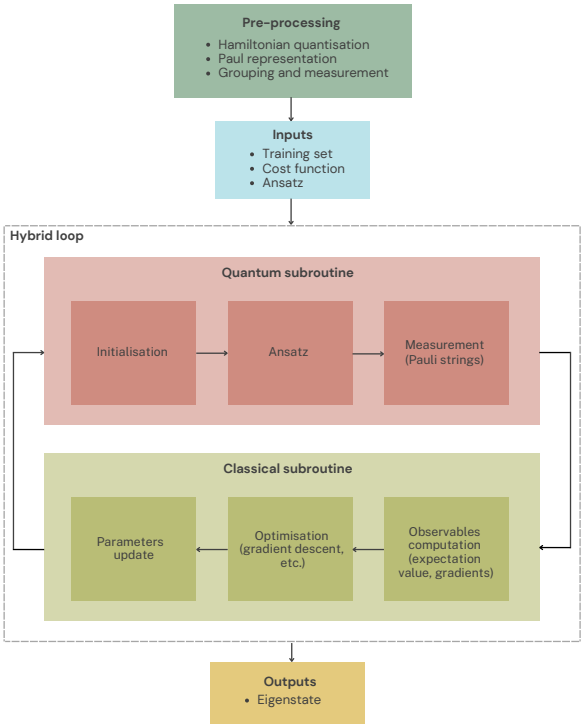

Figure 3. An overview of the main steps of the Variational Quantum Eigensolver.

Variational Quantum Imaginary Time Evolution

The classical optimisation routine for the VQE (see Section 2.3.1.2) attempting to find the ground state in a high-dimensional, non-linear parameter space has a high risk of getting stuck in a local minimum. To circumvent this, recent solutions have been using algorithms based on Quantum Imaginary Time Evolution (QITE) [194,220,245,247–250]. This method, developed by [247], can transform an arbitrary quantum state to the (almost) exact ground state by performing an approximate unitary evolution that mimics the imaginary time propagation. In other words, it is an alternative approach to preparing ground states on quantum computers.

The main idea of QITE is to represent the imaginary time propagator of a system by unitary operators via least-square fitting [194]. It has been shown that one can simulate the QITE on a quantum computer using a variational approach to find the ground state energy of the system [220]. Essentially, the energy cost function of a fixed variational ansatz is minimised following the Variational QITE (VQITE) approach [220,251]. The advantage of this method is that it can maintain a fixed circuit depth for the number of imaginary time steps, but the downside is its limited accuracy in finding the ground state. This accuracy very much depends on the variational ansatz, which can be system dependent [252,253].

Given an initial arbitrary state, $|\psi\rangle$, the normalised QITE can be defined as [220]

$$|\psi(\tau)\rangle = A(\tau)e^{-\mathcal{H}\tau}\,|\psi(0)\rangle\,, \tag{54}$$

where $\mathcal{H}$ is the Hamiltonian of the system, $|\psi(0)\rangle$ is the initial state for time $\tau = 0$, and $A(\tau) = 1/\sqrt{\|\langle\psi(0)|e^{-2\mathcal{H}\tau}|\psi(0)\rangle\|}$ is a normalisation factor. The imaginary time $\tau = it$, for $t \in \mathbb{R}$, is known as a Wick rotation transforming the evolution from relativistic Minkowski spacetime to Euclidean space. The imaginary time dynamics follow the Wick-rotated Schrödinger equation:

$$\frac{\partial\,|\psi(\tau)\rangle}{\partial\tau} = -(\mathcal{H} - E_\tau)\,|\psi(\tau)\rangle\,, \tag{55}$$

 doi:10.20944/preprints202511.1802.v2

where $E_\tau = \langle\psi(\tau)|\mathcal{H}|\psi(\tau)\rangle$ results from enforcing normalisation. The solution to Equation (55) gives the time-evolved state as $|\psi(\tau)\rangle = C(\tau)e^{-\mathcal{H}\tau}|\psi(0)\rangle$, where $C(\tau)$ is a time-dependent normalisation constant [251]. As $\tau \to \infty$, the smallest eigenvalue of the non-unitary operator $e^{-\mathcal{H}\tau}$ dominates the system so that the state approaches a ground state of $\mathcal{H}$ [220].

In the VQITE, one can use a parametrised ansatz for the time-dependent state as $|\psi(\theta(\tau)\rangle$ where the parameters $\theta(\tau)$ vary with time (i.e., $\theta_1(\tau), \theta_2(\tau), \dots$). This can then be composed with a parametrised circuit where the evolution is projected on the circuit parameters. A limitation of the variational method comes from the fact that the ansatz may not be general enough to describe all states on the desired subspace of the full Hilbert space [254]. Nonetheless, results from [220] show that this is a robust routine for energy minimisation, as long as the errors due to imperfect ansatze do not cause the routine to get trapped in local minima. In the finance sector, VQITE has been used to simulate the Feynman–Kac partial differential equation [255].

In a more recent paper, an alternative method for VQITE has been developed, which is gradient-free [194], thus avoiding expensive computations that may occur during the optimisation (such as matrix inversion or tensor computations). The VQITE can be used to solve a combinatorial optimisation problem by letting $\mathcal{H}$ encode the combinatorial cost function, in a similar manner to QAOA and VQE. It can also be used for more general optimisation problems, i.e., not only for solving QUBO. Finally, an alternative approach called Adaptive VQITE has been developed by [194], which circumvents the challenge of finding a good ansatz by iteratively expanding it along the dynamical path, keeping certain metrics (i.e., the MacLachlan distance) under a specific threshold. This ensures that the state can follow the quantum imaginary time evolution in the Hilbert space of the system rather than restricting to a fixed variational ansatz.

Quantum Approximate Optimisation Algorithm

First introduced by Farhi et al. in [157], the Quantum Approximate Optimisation Algorithm (QAOA) is a quantum algorithm for solving combinatorial problems. It is a VQA and draws inspiration from the concept of adiabatic evolution while being able to run on gate-based quantum computers (as opposed to analogue or annealing devices), characterising it as a finite, Trotterised version of annealing [157]. Hence, QAOA can solve a broader class of problems than quantum annealing, adhering to the universal quantum computation model.

The QAOA is particularly used for problems that can be cast as searching for an optimal bit string z^* such that

$$z^* = \arg\min_{z\in\{0,1\}^n} C(z), \tag{56}$$

where $C(z)$ is the cost function. The algorithm first defines a cost Hamiltonian $\mathcal{H}_C$, which encodes the solution z to its ground state. Finding this ground state is a hard problem [157]. To approximate it, the QAOA prepares an ansatz wavefunction parametrised by a parameter family $(\boldsymbol{\gamma}, \boldsymbol{\beta})$. This ansatz is embedded into a classical optimisation loop, which finds the optimal values for these parameters by utilising what is known as a mixer Hamiltonian $\mathcal{H}_B$, which 'mixes up' the quantum state to increase the space searched. It has been shown [157] that good approximate solutions to the problem can be found by preparing the variational state:

$$|\boldsymbol{\gamma}, \boldsymbol{\beta}\rangle = \underbrace{U_B(\beta_p)U_C(\gamma_p)\dots U_B(\beta_1)U_C(\gamma_1)}_{p}|s\rangle = \prod_{k=1}^{p} e^{-i\beta_k\mathcal{H}_B}e^{-i\gamma_k\mathcal{H}_C}|s\rangle\,, \tag{57}$$

where $|s\rangle$ is a suitable initial state, $U_B(\beta_k) = e^{-i\beta_k\mathcal{H}_B}$, and $U_C(\gamma_k) = e^{-i\gamma_k\mathcal{H}_C}$. In Equation (57), the variable p can be interpreted as a hyperparameter and defines the number of layers of QAOA blocks. The QAOA with p-layers, has $2p$ classical parameters to optimise over since each layer k, is characterised the set $\{\gamma_k, \beta_k\}$.

 doi:10.20944/preprints202511.1802.v2

The preparation step outlined above is followed by a measurement on the computational basis, giving a classical string z, with which one can evaluate the objective cost function $C(z)$ of the combinatorial problem. Over many repeated measurement samples, one can estimate the expectation value

$$E(\boldsymbol{\gamma}, \boldsymbol{\beta}) = \langle \boldsymbol{\beta}, \boldsymbol{\gamma} | \mathcal{H}_C | \boldsymbol{\gamma}, \boldsymbol{\beta} \rangle \,, \tag{58}$$

that is provided to the classical optimiser to update $\{\gamma_k, \beta_k\}$. Repeating this procedure will provide an optimised string z^*, with the quality of the result improving as the number of QAOA p-layers is increased [157]. In principle, assuming the absence of noise and other quantum device imperfections, the QAOA can reach the global optimum of any cost function in the limit $p \to \infty$ [157], approaching the adiabatic protocol. However, in practice, errors on NISQ devices limit the number of p-layers that can be implemented coherently. Algorithm (9) gives a concise outline of QAOA for a general combinatorial optimisation problem.

Algorithm 9 Quantum Approximate Optimisation Algorithm

Initialising Define a cost Hamiltonian $\mathcal{H}_C$, which encodes the solution to the problem as its ground state and a mixer Hamiltonian $\mathcal{H}_B$.
Construct unitaries Construct the Unitaries $U_B(\beta)$ and $U_C(\gamma)$, as defined above.
Combine unitaries Construct the unitary $U_p(\boldsymbol{\gamma}, \boldsymbol{\beta}) = \prod_{k=1}^{p} U_B(\beta_k) U_C(\gamma_k)$ for a number of layers $p \geq 1$.
Run circuit Prepare an initial state, $|s\rangle$ and apply the unitary $U_p(\boldsymbol{\gamma}, \boldsymbol{\beta})$ as defined in the previous step.
Measurement Measure the final state, estimate the expectation value, and report to the classical optimiser.
Optimisation loop Repeat the above steps while the classical optimiser optimises the parameters.
Result After many loops, the result will be an approximate solution to the optimal bit string.

The structure of the QAOA ansatz allows for finding suitable candidates for the parameters $\{\gamma_k, \beta_k\}$ purely classically for certain problem instances [157]. In general, however, finding such parameters is a challenging task as the training of VQAs is NP-hard [152,163,164]. Furthermore, just like other VQAs, the QAOA is also susceptible to barren plateaus [152,153]. However, ongoing research has uncovered promising efficient approaches for finding optimal parameters and required circuit depth estimation [256–259].

Quantum Minimum Search

It has been shown in [260] that the Quantum Unstructured Search algorithm (presented in Section (2.1.3) in the context of Grover's algorithm) can be used to find the global minimum of a function operating as a black box. The algorithm finds the index of an item whose value is smaller than the last by a particular threshold index. The resulting value is the next threshold index, and the process continues until the probability of the threshold being the global minimum is sufficiently large. Given an array of marked entries of size N, the algorithm exhibits a complexity of $\mathcal{O}(\sqrt{N})$, and at the end, will yield the index of the minimum value with a probability of at least $1/2$.

The original Quantum Minimum Search (QMS) algorithm developed by [260] is described in Algorithm (10). The probability of the algorithm can be improved by running the above routine a number of times. The authors show that by running the algorithm t times, one can obtain the minimum y with probability at least $1 - 1/2^t$.

One issue with the above algorithm is that it relies on knowledge of the answer space to formulate and solve the problem, for example, in identifying a feasible encoding into the quantum state space. Solution space knowledge tends to be unavailable for real-world problems, and finding an encoding may have to be done on a case-by-case basis. However, research by Zeng et al. [261] is aimed at alleviating these problems by introducing both a novel encoding mechanism and an adaptive algorithm used to estimate the number of solutions. These methods were demonstrated on a superconducting qubit device, making it more likely that QUS will be feasible on NISQ-era devices.

 doi:10.20944/preprints202511.1802.v2

Algorithm 10 Quantum Minimum Search

Initialising. Choose a threshold index y uniformly at random as $0 \leq y \leq N-1$.
Threshold and marking. Initialise the threshold memory as $\sum_j \frac{1}{\sqrt{N}} |j\rangle |y\rangle$ and mark every item j whose value is less than the value of y.
Quantum search. Apply the quantum search algorithm described in [262].
Update threshold. Let y' be the outcome of the previous step. Observe the outcome and if $y' < y$, then set the threshold to y'.
Repeat. Repeat for $\mathcal{O}(\sqrt{N})$ from step 2.
Measurement. Measure in order to obtain the global minimum, y, with probability at least $1/2$.

It is evident that Algorithm (10) works in a similar way to Grover's algorithm [4], providing a quadratic speed-up with the same requirements, i.e., a black box approach. The quantum oracle in this case can be described as $O_{f_y} |x\rangle = (-1)^{f_y(x)} |x\rangle$, where $f_y : \mathcal{X} \mapsto \{0,1\}$ is a classical function mapping $f_y(x)$ to 1 if $y' \leq y$ and 0 otherwise. [263] has also proposed an efficient implementation of the oracle O_{f_y}.

Quantum Annealing

As introduced above (see Section 2.1.7), Quantum Annealing (QAnn) is an approach to quantum computing that is based on the adiabatic model and is best suited to solving QUBO problems. Quantum annealers are available today from providers such as D-Wave [175], and can be used to solve several classes of optimisation problems, including a range of financial and economic optimisation problems. For example, a recent paper [264] studied the application of annealing to portfolio optimisation and found that their hybrid method outperformed a classical benchmark. A comprehensive review of annealing for random combinatorial optimisation problems is given in another paper [265].

The Quantum Annealing model consists of adiabatically evolving a system according to the transverse-field Ising Hamiltonian [166]

$$\mathcal{H}(t) = A(t)\left(-\sum_i \sigma_i^x\right) + B(t)\left(-\sum_{ij} J_{ij}\sigma_i^z\sigma_j^z - \sum_i h_i\sigma_i^z\right), \tag{59}$$

where J_{ij} are the coupling terms of an Ising Hamiltonian, h_i are magnetic field strengths, $A(t)$ and $B(t)$ are functions that control the strength of the transverse magnetic field and the terms within the parentheses are the ones defined in Section (2.1.7) as H_0 and H_1, respectively.

Annealers work by adiabatically shifting the Hamiltonian of the system from some initial H_0[10] to the problem H_1 Hamiltonian. If the system starts in the ground state of H_0, the final state will be the ground state of H_1, encoding the solution of the problem [166,167].

Since the QUBO form can be trivially mapped[11] onto the Ising problem Hamiltonian, quantum annealers (QPUs designed to perform Quantum Annealing) are the native devices for solving QUBO problems. However, there are often problem-specific challenges that must be overcome, including the presence of a too-small energy gap between the ground and excited states, causing a failure of adiabaticity [266], and the need to embed a problem on the hardware's qubit graph [267].

This latter problem, in particular, can cause issues. As the connectivity of the physical qubits in annealers is fixed, it may not directly correspond to the connectivity of the variables in the problem Hamiltonian [268]. Finding this mapping is an NP-hard problem and can be the main bottleneck in solving problems using annealing [267]. However, tools have been provided by DWave and other companies to automate this process [269], and it is a field of ongoing research.

There are peculiar advantages of quantum annealers as opposed to gate-based QPUs. Since annealers work by 'sweeping' from the initial H_0 to the problem H_1 Hamiltonian, they can execute sev-

[10] Normally chosen to have a ground state which is an equal superposition
[11] By the simple map $\{-1,1\} \mapsto \{0,1\}$ of binary Ising variables to QUBO variables

 doi:10.20944/preprints202511.1802.v2

eral hundred sweeps very rapidly, returning a set of possible solutions ready for post-processing [270]. This contrasts with gate-based methods such as VQE, which require running lengthy circuits and take much longer [152]. However, annealers are not universal quantum computers, and thus the set of algorithms they can execute is much more limited than gate-based computers, and it is an open question as to whether one technique tends to provide better solutions than the other. For example, a 2024 paper by Q-CTRL [271] claimed to demonstrate that a digitised version of annealing running on IBM devices could outperform annealing for Max-Cut and spin-glass problems in terms of probability of finding the lowest-energy state. However, a later comment by DWave [272] claimed instead that with improvements to the annealing workflow, they were able to outperform the gate-based method in both time to solution and ground state probability. As a result, it is often unclear which method is most suitable for a given problem at the current time, but it is hoped that as the field matures, the delineation will become clearer.

Separately, Quantum Annealing has inspired similar protocols for digital (gate-based) quantum computers, an example of which is the family known as Counteradiabatic Quantum Optimisation algorithms [273]. These work by adding extra terms to the cost Hamiltonian, which have the effect of suppressing excited-state transitions. The latest modification of this algorithm, Bias-Field Digitized Counterdiabatic Quantum Optimization (BF-DCQO) [274], has been used to solve Ising models [275], displaying better performance than either traditional annealing or variational methods like VQE. Another disadvantage of annealing is that it requires problems to be reduced to QUBOs, which can introduce significant overheads. The BF-DCQO algorithm has also been used to solve Higher-order Unconstrained Binary Optimisation (HUBO) problems [276] such as solving protein folding, consistently achieving optimal solutions.

2.3.2. Convex Optimisation Problems

Convex optimisation problems are those which optimise a convex function over a set of solutions that is given explicitly (i.e., through a set of constraints) or implicitly (i.e., through an oracular function) [226]. Convex optimisation is less common than combinatorial optimisation in finance and economics, but is nevertheless important, and so we provide a summary below.

Generally, the optimisation problem under consideration is NP-hard and refers to minimising a convex function $f : K \to \mathbb{R} \cup \{\infty\}$, where $K \subseteq \mathbb{R}^n$ is a convex set. If the convex function is bounded on K, one can equivalently consider the problem of minimising a linear function over a different convex set $K' \subseteq \mathbb{R}^{n+1}$. Accessing K' is easy given knowledge of f and K, and the parameters involved will be similar. Conversely, for any linear optimisation problem over an unknown convex set K, there is an equivalent optimisation problem over a known convex set with an unknown bounded convex objective function f that can be evaluated easily given access to K [226].

Quantum algorithms for convex optimisation are an active field of research. In earlier stages of the field, a study by [277] presented a quantum algorithm for minimising quadratic functions. In more recent work, there have been suggestions of potential future quantum advantage for semidefinite optimisation, an important subset of convex optimisation problems [278–281]. The quantum algorithms for these problems have been shown to have runtimes that scale polynomially with the desired precision and some geometric parameters [280,281]. In other convex problem classes, many optimisation problems can be solved classically with a logarithmic scaling complexity using interior-point methods [282]. Currently, there is one quantum speed-up which resides partially within this regime of logarithmic scaling algorithms, developed by [142] using interior-point methods and Quantum Linear Systems Solver algorithms[12] (such as improved HHL-type [131]) and tomography to accelerate the computation of the Newton linear system. Further speed-ups to semidefinite convex optimisation problems have also been proposed using multiplicative-weights methods [279,280].

Quantum algorithms have also been formulated for other classes of convex problems, such as linear programming or second-order cone programming [236]. In the former case, the algorithms include

[12] See Section (2.1.5) for more details on QLSSs algorithms.

 doi:10.20944/preprints202511.1802.v2

the quantum interior-points methodology developed by [283] and the simplex method developed by [284]. Under certain conditions, the quantum interior-points method has been shown to provide a potential polynomial speed-up for the second-order cone programming problem [285]. Finally, recent work by [279] implements subgradient approximation of convex functions via Jordan's algorithm for gradient computation [286]. This approach has quadratically better complexity than the best-known classical randomised algorithm, based on queries to the oracle [279]. However, it is an open question whether this classical quadratic bound is optimal.

2.4. Quantum Machine Learning

The field of Quantum Machine Learning (QML) is an interdisciplinary subset of quantum information that lies at the intersection of Machine Learning (ML), statistics, and quantum physics [287–289]. It seeks to utilise the power of quantum computing to potentially augment or provide improved performance over classical ML algorithms [39,290], although some of these improvements are still theoretical and not yet demonstrated experimentally [291–293]. This includes hybrid methods that involve both classical and quantum processing, where some of the classically challenging subroutines are efficiently performed on quantum computers. Developing quantum algorithms for QML is an active area of research with rapid advances in recent years [294]. In this section, we will review some of the most common quantum algorithms for supervised and unsupervised QML, and Quantum Reinforcement Learning (QRL).

2.4.1. Quantum Algorithms for Supervised ML

Supervised machine learning is a type of machine learning that uses labelled data to train algorithms that can classify data or predict outcomes [295]. In supervised learning, the algorithm learns a mapping between the input and output data. This mapping is learned from a labelled dataset, which consists of pairs of input and output data [296]. The algorithm tries to learn the relationship between the input and output data so that it can make accurate predictions on new, unseen data [289]. For example, consider a dataset of images of animals, where each image is labelled with the name of the animal it contains. A supervised learning algorithm can be trained on this dataset to recognise the animal in a new image that it has not seen before.

Supervised learning is widely used in various fields such as finance, healthcare, marketing, and more [297]. It can be used for regression or classification tasks [298], and it usually requires large amounts of labelled data to achieve high prediction accuracy in unseen input data [298]. The field of supervised machine learning is very broad, and quantum algorithms corresponding to classical ML are an active area of research [39,299,300]. Therefore, this section will not be a comprehensive review of all supervised QML algorithms but rather will present a few example algorithms that are representative of the broad field.

Quantum Classifiers

Quantum algorithms for classification problems have been an active area of research in recent years. These algorithms aim to improve the efficiency of solving classification problems in machine learning by using quantum computers. A detailed survey of recent works in this area can be found in Ref. [301]; thus, it suffices for us to outline a few common algorithms in this area.

Quantum Support Vector Machine and Kernel Methods In Machine Learning, Support Vector Machines (SVM) are supervised learning algorithms commonly used for classification and regression tasks. Given two categories (or classes) and a training set containing several data-points that are mapped to one of the classes, a SVM algorithm builds a model that assigns new data-points to either one of the two classes depending on their characteristics [302]. Figure 4 (a) is an example of binary classification, where the points that lie at the boundary of each of the margin class hyperplanes (shown with a dotted line) are called the *support vectors*, and they play a crucial role in solving the SVM

 doi:10.20944/preprints202511.1802.v2

classification problem. The black line inside the maximum margin hyperplane is the *margin normal vector* that divides the classes with the most significant possible marginal length [303].

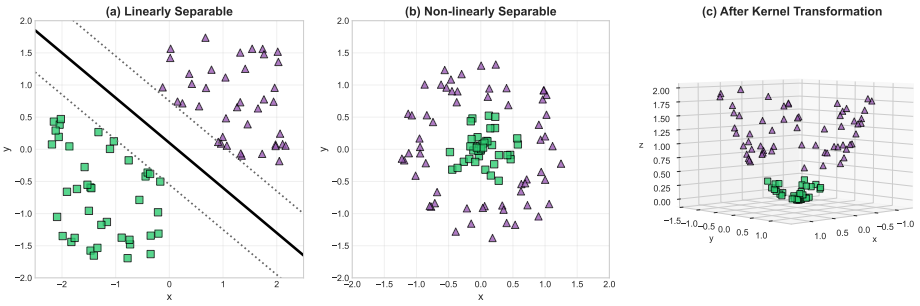

Figure 4. Example of SVM binary classification. (a) Linearly separable dataset, (b) non-linearly separable case, and (c) the same data transformed into a higher-dimensional feature space using kernel methods, where linear separation becomes possible. Adapted from [301].

The classification problem can broadly be categorised into two types, with datasets that are: (i) **linearly separable**, e.g., Figure 4 (a), and (ii) **non-linearly separable**, e.g., Figure 4 (b). For the former class, the SVM binary classification algorithm seeks to find a hyperplane that divides the data-points into two parts by maximising the distance between the support vectors and the hyperplane [303]. For the latter class, one can still use the SVM algorithm by first transforming the data into a form that can be linearly separable. This is done by using the *kernel trick*, which maps the input data set into high-dimensional feature spaces where the data can be linearly separable [304]. It is through this complex process of transforming data into higher-dimensional space and processing it that quantum computing can offer a potential computational advantage over classical techniques. Hence, various quantum algorithms for SVM have been theoretically proposed, although practical demonstrations of quantum advantage remain elusive. Below, there is a more in-depth definition of each classification.

Linear Classification: Given a linearly separable training dataset [301]:

$$\mathcal{D} = \{(\vec{x}_1, y_1), (\vec{x}_2, y_2), \ldots, (\vec{x}_M, y_M)\}, \tag{60}$$

that has M points where $\vec{x}_i \in \mathbb{R}^N$ and labels $y_i \in \{-1, 1\}$. Let the parameters $(\vec{w}, b)$ define a hyperplane in N-dimensional space such each x_i falls in either $\vec{w} \cdot \vec{x} + b \geq 1$ or $\vec{w} \cdot \vec{x} + b \leq -1$ for the $y_i = 1$ or -1 categories respectively. The goal of SVM is to find a maximum separation (marginal length) between the two classes, which means finding optimal parameters $\vec{w}^*, b^*$ that construct the decision function [301]

$$f(\vec{x}) = \text{sgn}(\vec{w}^* \cdot \vec{x} + b^*), \tag{61}$$

used to classify data-points in $\mathcal{D}$ [301]. It is common to consider the *dual problem* [226] with Lagrange multipliers which seeks to maximise

$$L(\vec{\alpha}) = \sum_{j=1}^{M} y_j \alpha_j - \frac{1}{2} \sum_{j,k=1}^{M} \alpha_j (\vec{x}_j \cdot \vec{x}_k) \alpha_k, \tag{62}$$

subject to the constraints $\sum_{j=1}^{M} \alpha_j = 0$ and $y_j \alpha_j \geq 0$ [302]. The solution to this problem leads to the construction of the optimal weights and biases in the *primal problem* given by [301]

$$\vec{w}^* = \sum_{j=1}^{M} \alpha_j^* \vec{x}_j \quad \text{and} \quad b^* = y_k - \vec{w}^* \cdot \vec{x}_k, \tag{63}$$

 doi:10.20944/preprints202511.1802.v2

for an index k corresponding to non-zero α_k^* (support vectors) [301]. Therefore, we can substitute Equation (63) into Equation (61) to obtain

$$f(\vec{x}) = \text{sgn}\left(\sum_{j=1}^{M} \alpha_j^* (\vec{x}_j \cdot \vec{x}) + b^*\right). \tag{64}$$

In general, not all datasets are linearly separable, such as the ones shown in Figure 4 (b), and thus, the SVM approach described above will not work. If the dataset is close to being linearly separable, which means it has a few outliers that do not obey the linearity, a common approach is to replace the hard-margin condition $y_i(\vec{w} \cdot \vec{x}_i + b) \geq 1$ with a soft-margin condition $y_i(\vec{w} \cdot \vec{x}_i + b) \geq 1 - \varepsilon_i$, where ε_i is the cost [305]. In practice, the soft-margin condition is more often used than the hard-margin condition because most datasets generated in the physical world are noisy [301].

Non-linear classification: For datasets that are far from linearity, one can still use SVMs to efficiently perform a non-linear classification using what is called the *kernel trick* which maps the input data set into a high-dimensional feature spaces where the data can be linearly separable [304], as shown in Figure 4 (c). Let $K(\vec{x}, \vec{y})$ be the kernel function given by [301]

$$K(\vec{x}, \vec{y}) = \phi(\vec{x}) \cdot \phi(\vec{y}), \tag{65}$$

where $\phi : \mathbb{R}^N \to \mathbb{R}^{N'}$ is the *feature map* function that maps the N-dimensional feature space to a higher N'-dimensional kernel space. The kernel function is used to compute the inner product of vectors in the kernel space [306]. Thus, ϕ does not need to be explicitly defined. Therefore, similarly to Eq.(62), one can use K to define the *dual problem* of maximising [301],

$$L(\vec{\alpha}) = \sum_{j=1}^{M} y_j \alpha_j - \frac{1}{2} \sum_{j,k=1}^{M} \alpha_j \, K_{jk} \, \alpha_k, \tag{66}$$

subject to the same constraints as Equation (62). Just like the linear SVM, one uses the optimal Lagrange multipliers $\vec{\alpha}^*$ to formulate the decision function for the *primal problem* as [301]

$$f(\vec{x}) = \text{sgn}\left(\sum_{j=1}^{M} \alpha_j^* K(\vec{x}_j, \vec{x}) + b^*\right). \tag{67}$$

Besides the Lagrange multipliers, other techniques can be applied, such as sequential minimal optimisation [306], interior-point methods [307], or gradient descent [308], which is one of the reasons SVM is popular [309]. However, these methods also face several limitations, such as the fact that it does not handle large datasets well, the computational scaling with complexity, and their dependence on kernel functions.

The Quantum Support Vector Machine (QSVM) proposed by Rebentrost, Mohseni, and Lloyd [302] was one of the first QML quantum algorithms for supervised learning. QSVM can be implemented using several approaches, for instance, using the quantum kernel method or the quantum feature mapping method. It is an extension of the least-squares version of the classical SVM algorithm [310]. In this formulation, the SVM has equality constraints with slack variable e_j instead of inequality constraints, which means the hard-margin condition can be transformed as [301]

$$y_j(\vec{w} \cdot \vec{x}_j + b) \geq 1 \quad \implies \vec{w} \cdot \vec{x}_j + b = y_j - y_j e_j. \tag{68}$$

One can then transform the associated Lagrangian of the *dual problem* into a system of linear equations [305], and then apply any Quantum Linear Systems Solver like the HHL-type algorithms described in Section (2.1.5). The QSVM algorithm uses quantum circuits to perform the classification task and has been theorised to potentially outperform classical SVMs for certain learning tasks [302]. The QSVM algorithm consists of three main components: the *quantum feature map* used to map the input

 doi:10.20944/preprints202511.1802.v2

data to a quantum state in the kernel space, the *quantum kernel* used to compute the inner product of the quantum states in the kernel space, and the *quantum classifier* used to classify the input data based on the kernel function. In a higher-dimensional space, the kernel function is assumed to be classically hard to compute, hence can be efficiently simulated on a quantum computer [302]. This leads to the idea of *covariant quantum kernels*, which have been hypothesised to potentially provide superpolynomial speed-ups for certain specialised problems [311].

Covariant Quantum Kernel: Given an efficient algorithm U_{x_i} for loading features of the sample x_i, we can define the associated quantum feature state [312]

$$\Phi(x_i) = U_{x_i} |\psi\rangle \langle\psi| U_{x_i}^\dagger = U_{x_i} V |0\rangle \langle 0| V^\dagger U_{x_i}^\dagger, \tag{69}$$

where $|\psi\rangle$ is a fiducial state generated by unitary V which depends on the learning problem and dataset. The quantum kernel for samples x_i, x_j is defined as [312]

$$K(x_i, x_j) = \mathrm{Tr}\Big(\Phi^\dagger(x_i)\Phi(x_j)\Big) = \Big|\langle 0|V^\dagger U_{x_i}^\dagger U_{x_j} V|0\rangle\Big|^2. \tag{70}$$

The kernel K can be simulated on a quantum computer using circuits U and V, and the results used in the *dual problem* to speed up the classification algorithm [311]. We note that the condition that quantum kernel methods can only be expected to do better than classical kernels if they are hard to estimate classically is a necessary but not sufficient condition for an end-to-end quantum speed-up [313]. Designing quantum kernels that exploit structure in data is a promising step toward practical applications. Quantum kernels can be optimised on a given dataset with kernel alignment that exploits group structures in the dataset [312].

At the centre of this algorithm sits a non-sparse matrix exponentiation technique for performing matrix inversion of the kernel matrix. A low-rank approximation of the kernel matrix can be used due to the eigenvalue filtering procedure of HHL [6]. In addition, classical SVMs using quantum-enhanced feature spaces to construct quantum kernels have been proposed [314].

Variational QSVM: An alternative proposition for training a QSVM variationally has been explored [314] aiming to target near- to medium-term quantum computers. Let $\{\vec{x}\}$ denote the classical training data need to be loaded into a quantum computer using a feature map $\Phi(\vec{x})$, and $W(\theta)$ be the parametrised quantum gate, and $V(\Phi(\vec{x}))$ is the embedding. The PQC can be defined in such a way that, when a measurement is applied, it returns the label $y \in \{-1, 1\}$ for each data point [314]. The PQC $|\psi(\theta)\rangle = W(\theta)V(\Phi(\vec{x}))|0\rangle$, can be trained to find good parameters θ that optimises a cost function $C(\theta)$. This cost function is constructed such that it penalises misclassified training points. Typically, a classical optimiser, such as gradient descent, is used to update the parameters θ and minimise the cost function.

In contrast to the covariant kernel approach, which optimises for the associated Lagrange multipliers, the variational classifier approach learns a boundary hyperplane by optimising the parameters θ, the quantum circuit $|\psi(\theta)\rangle$ [315,316]. Algorithm (11) summarises the general idea of the QSVM. Alternative to the above quantum algorithms for classification have been proposed, which include the quantum decision tree classifier [88,317–319], quantum nearest neighbour algorithm [299], and quantum annealing classifiers [315,316].

 doi:10.20944/preprints202511.1802.v2

Algorithm 11 Quantum Support Vector Machine

Input: Labelled dataset $\mathcal{D} = \{(\vec{x}_1, y_1), \ldots, (\vec{x}_M, y_M)\}$ with $\vec{x}_i \in \mathbb{R}^N$, $y_i \in \{-1, +1\}$
Feature Map Encoding: (a) Choose a quantum feature map $\phi : \mathbb{R}^N \to \mathcal{H}$. (b) Encode each $\vec{x}_i$ into quantum state $|\phi(\vec{x}_i)\rangle$
Kernel Evaluation: (a) For each pair $(\vec{x}_i, \vec{x}_j)$, compute kernel value $K_{ij} = \langle\phi(\vec{x}_i)|\phi(\vec{x}_j)\rangle$. (b) Use quantum circuits (e.g., swap test [320] or interference circuits) to estimate K_{ij}
Dual Optimisation: (a) Solve the dual SVM problem:

$$L(\vec{\alpha}) = \max_{\vec{\alpha}} \sum_{i=1}^{M} y_i \alpha_i - \frac{1}{2} \sum_{i,j=1}^{M} \alpha_i K_{ij} \alpha_j,$$

subject to constraints: $\sum_{i=1}^{M} \alpha_i y_i = 0$, and $\alpha_i \geq 0$. (b)Convert the dual problem into a system of linear equations which could be solved using QLSS [131] for optimal $\vec{\alpha}^*$.
Classification: Use optimal $\vec{\alpha}^*$ to compute the decision function

$$f(\vec{x}) = \text{sgn}\left(\sum_{i=1}^{M} \alpha_i^* K(\vec{x}_j, \vec{x}) + b^* \right),$$

which is used to predict the label $\hat{y} = f(\vec{x})$ for test data $\vec{x}$.

The advantage of QSVM lies in potential speed-ups for processing high-dimensional data. In particular, the proposal of [302] has a time complexity that is logarithmic in the dimension of the data N and number of data-points M, yielding a potential exponential speed-up over classical kernel methods if the data is in a coherent superposition [311,314,321]. Achieving such efficiency in processing high-dimensional data has been a motivation for continued research of QSVM. It includes searching for ways to overcome several challenges with QSVM, such as finding a practical, efficient data loading protocol, efficiently running the QLSS, and limitations of current NISQ devices [322]. These challenges are shared with general QML methods, and they would need to be addressed QSVMs can become practically useful. However, QSVM have been demonstrated in small-scale experiments[314,323–325], but large-scale implementations relevant for industrial problems still awaits maturity of quantum hardware.

Quantum Nearest Neighbour The nearest neighbour algorithm is a foundational and widely used classification technique in classical ML [326]. The algorithm works by having a large labelled dataset of examples, where each data point is represented by a feature vector. To predict the label or class of an unlabelled data point (also called a test vector or query point), the algorithm measures the distance between this query and each dataset entry. It then assigns the label or class of the closest point, often using Euclidean distance [327]. This means that data points with similar features are likely to share the same label.

Formally, given a set of training vectors or examples $\mathcal{D} = \{(\vec{x}_i, c_i)\}_{i=1}^{M}$, where each $\vec{x}_i \in \mathbb{R}^N$ is a feature vector in a N-dimensional space, and $c_i \in \mathcal{C}$ denotes the class label of the point $\vec{x}_i$. The task is to classify a new unlabelled query point q by computing its distance to each training point $\vec{x}_i$. For any two points $\vec{x}, \vec{x}' \in \mathbb{R}^N$, the Euclidean distance can be defined as [327],

$$d(\vec{x}, \vec{x}') = \sqrt{\sum_{j=1}^{N} (x_j - x'_j)^2}. \tag{71}$$

One can also use other distance measures, such as the Manhattan distance, cosine similarity, or Hamming distance, but here we will focus on the Euclidean distance as it is commonly used [328]. Using this metric, each training example $\vec{x}_i$ defines a 'neighbourhood' of nearby points, such that any

 doi:10.20944/preprints202511.1802.v2

new point $\vec{q}$ falling inside this region will be closest to $\vec{x}_i$. Hence, one needs to find the index i^* that minimises the distance [327],

$$i^* = \arg \min_{i \in \{1,\ldots,M\}} d(\vec{q}, \vec{x}_i). \tag{72}$$

Therefore, the nearest neighbour classifier (sometimes called the 1-NN rule) will label q with the label of $\vec{x}_{i^*}$, which is the class of the training sample closest to q [329]. For the simple 1-NN classifier, only the single closest neighbour is considered to assign a class. However, this approach can be sensitive to noise or outliers [308,330]. To improve robustness, it is useful to take more than one neighbour when making decisions [331].

K-Nearest Neighbour (KNN) is one of the most widely used classifiers in practice, due to its simplicity and effectiveness across a range of tasks [329]. It is 'non-parametric' and instance-based, meaning it makes no assumptions about underlying distributions and simply uses the stored training instances for decisions [332]. Instead of relying on a single nearest example, KNN considers the k closest training points to the query and bases the prediction on the most frequent class among those neighbours. The 1-NN rule described above is a special case of KNN with $k = 1$ (k is often chosen as an odd number to avoid tie votes).

KNN stores the training set in memory, and given the distance function, classifies a new point by finding the set $N_k(q)$, which is the neighbourhood of the query containing the indices of the k nearest samples to q [333]. The predicted class $\hat{y}(q)$ is then the most common label among these neighbours. If we denote by n_c the number of neighbours in $N_k(q)$ belonging to class c, the KNN classification rule can be expressed as [334],

$$\hat{y}(q) = \arg\max_{c \in C} n_c = \arg\max_{c \in C} \sum_{i \in N_k(q)} \mathbf{1}\{c_i = c\}, \tag{73}$$

meaning it selects the class c that maximises n_c, where $\mathbf{1}\{\cdot\}$ is an indicator function taking the value 1 when its argument is true, and 0 otherwise [334].

This method is intuitive but can be slow with large datasets, with time complexity that is linearly proportional to the number of data points and their dimensions [333]. A key bottleneck arises because of the distance computations between the query and all M training points, resulting in an $O(NM)$ computational cost for N-dimensional data (assuming distance calculation in $O(N)$). When M is very large (as can happen in financial applications with millions of records) or for high N (e.g., high-frequency trading data with many features), this cost becomes significant, especially if many queries need to be answered in real-time [22,29,37]. This is where quantum computing may offer a potential advantage by simultaneously calculating multiple distances using quantum parallelism [335,336]. However, this advantage is thus far theoretical and contingent upon efficient implementations of quantum data loading techniques, which are not yet practically viable [337,338].

Quantum K-Nearest Neighbour (QKNN) is the quantum version of KNN [327], it computes the distances between data points more efficiently and identifies the nearest (or K nearest) neighbours with a potential quadratic speed-up over classical methods, especially for large datasets [288]. The general approach to QKNN focuses on key components, such as quantum data encoding, distance computation, and quantum search for nearest neighbours.

To represent the data in a quantum state, there are different encoding schemes, but a common choice for distance-based algorithms is amplitude encoding [339]. For example, a data point can be encoded as [340]:

$$|\mathbf{x}\rangle = \frac{1}{\|\mathbf{x}\|} \sum_{i=1}^{N} x_i \, |i\rangle \,,$$

where $|i\rangle$ are computational basis states. Amplitude encoding is powerful because it packs N features into just $\log_2 N$ qubits by using amplitude values. However, preparing such states for arbitrary

 doi:10.20944/preprints202511.1802.v2

data can be challenging and may require Quantum Random Access Memory (QRAM)[13] or complex rotations [337,342]. Once both the query point $|\mathbf{x}_q\rangle$ and a training point $|\mathbf{x}_i\rangle$ are encoded as quantum states, the distance between them can be related to the inner product of these states. For normalised vectors, the Euclidean distance is given by [336]

$$\|\mathbf{x}_q - \mathbf{x}_i\|^2 = 2\big(1 - \langle \mathbf{x}_q | \mathbf{x}_i \rangle\big). \tag{74}$$

Thus, knowing the inner product $\langle \mathbf{x}_q | \mathbf{x}_i \rangle$ allows one to compute the distance. This overlap can be efficiently estimated on a QPU using a subroutine called the SWAP test, which measures the similarity or fidelity between two quantum states [320,343]. By repeating this test or using QAE, a good estimate of the inner product can be obtained [343].

In practice, many QKNN algorithms use the inner product as a proxy for distance. For instance, one may define a similarity score $s_i = \big|\langle x_q | x_i \rangle\big|$ for each training point i and maximise the similarity s_i, which is equivalent to minimising distance [344].

Once both the query point $|x_q\rangle$ and training points $|x_j\rangle$ are encoded, quantum circuits can be used to compute functions of their distance (via SWAP test [320] or a dedicated distance encoding routine) in superposition. One convenient choice is to produce an output state like [327]:

$$|\Psi\rangle = \frac{1}{\sqrt{N}} \sum_{j=1}^{N} |x_j, c_j\rangle \otimes \big(\alpha_j |0\rangle + \beta_j |1\rangle\big), \tag{75}$$

where c_j is the class label of the jth training point, and the amplitudes α_j, β_j depend on the distance between x_j and x_q. In an 'ideal' scenario, $\alpha_j \approx 1$ (and $\beta_j \approx 0$) for the nearest neighbours, while α_j becomes small (and the ancilla is $|1\rangle$ with high amplitude) for far-away points [344]. This way, the problem of finding nearest neighbours is encoded into quantum circuits, where the solution is identifying the basis states that have an ancilla in state $|0\rangle$ with high probability amplitude.

Once the data is encoded and distances are described in quantum amplitudes or probabilities, the next task is to actually identify the index of the k nearest neighbours, i.e., finding k index j with ancilla $|0\rangle$, meaning a small distance with high probability. One can do this by using the Quantum Unstructured Search (QUS)[14], which can find a marked item in an unsorted list of size N in $\mathcal{O}(\sqrt{N})$ steps, which is a potential quadratic speed-up over classical linear search algorithms [4]. Algorithm (12) summarises the QKNN classification procedure outlined above.

Algorithm 12 Quantum K-Nearest Neighbour

Input: Labelled dataset $\mathcal{D} = \{(\vec{x}_1, y_1), \ldots, (\vec{x}_M, y_M)\}$, query point $\vec{x} \in \mathbb{R}^N$
Encode Input Data: (a) For each $\vec{x}_i \in \mathcal{D}$, encode into quantum state $|x_i\rangle$ (b) Encode query point $\vec{x}$ as quantum state $|x\rangle$
Distance Estimation: (a) For each i, estimate distance $d(\vec{x}, \vec{x}_i) = \|\vec{x} - \vec{x}_i\|$ (b) Use a quantum subroutine (e.g., swap test) to estimate d
Nearest Neighbour Search: Use QUS to find index j^* such that $d(\vec{x}, \vec{x}_{j^*})$ is minimal
Output: Predicted label $\hat{y}$ for input $\vec{x}$

Classically, identifying k neighbours is $O(N)$ in the worst case, whereas a QKNN algorithm can potentially achieve $O(\sqrt{N})$ for fixed k or $O(\sqrt{kN})$ in general case [326]. There have been improvements on the QKNN such as a proposal for a memory-efficient quantum subroutine for distance calculation, showing a 50% reduction in qubits required [344]. Furthermore, a recent work demonstrated an efficient swap test on photonic qubits [345]. While such an experiment is not directly a QKNN implementation, the swap test [320] is a necessary component for many QKNNs and QML proposals as described here.

[13] QRAM is a mechanism to access data (quantum or classical) based on addresses which are themselves a quantum state [341].
[14] Also known as Grover's search algorithm, see Section (2.1.3)

 doi:10.20944/preprints202511.1802.v2

The QKNN has applications in finance that include economic modelling (searching historical market data to find similarities to the present), or in fraud detection pipelines, rapidly and accurately classifying transactions as likely to be fraudulent or not [33,346,347].

Quantum Decision Tree Decision trees are fundamental tools in classical ML for discovering features and extracting patterns due to their interpretability, fast inference, and natural compatibility with structured data [348]. They work by splitting data, creating a tree-like model where each branch represents a decision based on discriminant functions or decision rules [349].

A decision tree defines a function $f : \mathbb{X} \to \mathbb{Y}$ by sequentially testing feature values: at each node, an attribute A is chosen as the splitting criterion, and the dataset is divided according to A's possible values. This process continues until the subsets are homogeneous enough or other stopping criteria are met [350]. At that point, a leaf node assigns a class label (for classification), or a numerical value (for regression) [351]. In other words, the decision tree recursively partitions the feature space into regions, using decision rules at each internal node to split data, until reaching a prediction at leaf nodes [348].

To 'grow' a decision tree, the algorithm must decide which feature provides the best split at each node. This is typically done by optimising an impurity measure or information gain. A common choice is based on Shannon entropy [352]; if S is the set of training samples at a node, the entropy of S with respect to the class labels is:

$$H(S) = -\sum_{c \in \mathcal{C}} p(c) \log_2 p(c), \tag{76}$$

where $p(c)$ is the proportion of samples in S belonging to class c, and $\mathcal{C}$ is the set of class labels [353]. Here, the entropy $H(S)$ quantifies the uncertainty (impurity) in the node; it is 0 if all samples are of the same class and maximal when classes are uniformly mixed. A split on an attribute A produces child subsets S_v (for each value v of A). The information gain achieved by splitting on A is defined as the reduction in entropy:

$$\text{InfoGain}(S, A) = H(S) - \sum_{v \in \text{Vals}(A)} \frac{|S_v|}{|S|} H(S_v), \tag{77}$$

where $|S_v|$ and $|S|$ denote the cardinalities (number of samples) of the child subset S_v and the parent set S, respectively, so that $\frac{|S_v|}{|S|}$ represents the proportion of samples assigned to each branch. A high information gain means that splitting on A yields more informative subsets. At each new node, entropy is computed for that node's subset and all possible splits, and the best split is taken. This procedure stops when no attribute offers any gain (or other stopping conditions like maximum depth are reached), and then a leaf is created, which is often labelled with the majority class in that subset. Other splitting criteria can also be used, such as the Gini impurity

$$G(S) = \sum_c p(c)[1 - p(c)], \tag{78}$$

as a measure of node impurity instead of entropy, yielding a similar formula for Gini gain [348]. Regardless of the metric, the goal is to choose splits that most improve homogeneity in child nodes. This greedy heuristic approach tends to produce good results in practice, although do not guarantee to find the global optimum tree, as this is NP-hard [354,355]. The time complexity for building a classical decision tree with M samples and N features is typically $O(M, N, \log M)$ or $O(NM)$ per node [356]. In the worst case, if the tree is fully grown with M leaves, the training cost can be $O(M^2 N)$. Quantum algorithms that can improve this classical scaling have been explored [357].

The Quantum Decision Tree (QDT) algorithm [88,318] aims to enhance the decision tree induction process using quantum subroutines. As this involves encoding classical data, one common approach is to use QRAM data structure [337]; for example, if we have M data samples $(\vec{x}_i, y_i)$ where $\vec{x}_i$ are feature vectors and y_i are class labels (as shown in Section 2.4.1.1), one could prepare a state of the form:

 doi:10.20944/preprints202511.1802.v2

$$|\Psi_{\text{data}}\rangle = \frac{1}{\sqrt{M}} \sum_{i=1}^{M} |i\rangle |x_i\rangle |y_i\rangle. \tag{79}$$

A crucial part of building the tree is computing the entropy and information gain for each attribute. In the classical version, to compute the entropy $H(S)$ of a set S, the algorithm counts how many samples fall into each class [358]. A quantum algorithm can estimate these counts with potential quadratic speed-up via techniques like Quantum Amplitude Estimation (QAE) [57] (see Section 2.1.2.2). In this way, the entropy $H(S_v)$ for each branch could be obtained with fewer queries to the data [359]. Once the entropies are known, the information gain can be computed similarly to Equation (77);

$$\text{InfoGain}(S, A) = H(S) - \sum_{v} p_v H(S_v), \tag{80}$$

where P_v is the projector selecting subset S_v, $p_v = \langle \Psi | P_v | \Psi \rangle$, and $H(S_v)$ is estimated via QAE [360].

To find the optimal attribute A^* (the feature with the highest information gain) from the set of available features $F = \{A_1, A_2, \ldots, A_d\}$, one can use Quantum Maximum Search (QMxS) algorithms [360] (similar to the Quantum Minimum Search described in Section 2.3.1.5) [260] such that.

$$A^* = \arg\max_{A \in F} \text{InfoGain}(S, A). \tag{81}$$

After finding the optimal attribute A^*, the algorithm must partition the data by measuring which samples belong to each branch. Once measured, we obtain classical subsets that must be re-encoded into quantum states for processing the next level of the tree [318]. This creates a hybrid quantum-classical recursion, analogous to the classical algorithm's recursion, except that here, at each node, one relies on quantum subroutines to decide how to split. In general, the algorithm will construct the same tree as a classical greedy algorithm would, with the difference that it can potentially speed up the computation of the branch criterion [356,361]. Using the ideas above, Algorithm (13) outlines the QDT procedure.

Algorithm 13 Quantum Decision Tree

Input: Training dataset $S = \{(\vec{x}_i, y_i)\}_{i=1}^{M}$, feature set F, and optional depth limit $d_{\max}$
Initialisation: Prepare quantum state $|\Psi_{\text{data}}\rangle = \frac{1}{\sqrt{M}} \sum_{i=1}^{M} |i\rangle |x_i\rangle |y_i\rangle$ using QRAM
Homogeneity Check: (a) Estimate entropy $H(S)$ (b) If $H(S) = 0$, $F = \emptyset$, or current depth $= d_{\max}$: return a majority-class leaf
Quantum Split Evaluation: 1. For each feature $A \in F$: (a) Apply quantum predicate on A to split state $|\Psi_{\text{data}}\rangle$ via ancilla (b) Use QAE to evaluate class probabilities in each split branch (c) Compute entropy $H(S_v)$ and estimate information gain $\text{IG}(S, A)$
Optimal Split Selection: Use Quantum Maximum Search [360] to find $A^* = \arg\max_{A \in F} \text{IG}(S, A)$
Quantum Data Partitioning: (a) Measure ancilla qubit to collapse $|\Psi_{\text{data}}\rangle$ into two subsets: S_{left}, S_{right} (b) Re-normalise quantum states for each subset
Output: Associated class label

In general, for a classical node evaluation with time complexity $O(MN)$ [362,363], the quantum counterpart has a proposed complexity of $O(\sqrt{MN})$[15] [364]. For example, a quantum C5.0[16] algorithm [356] was proposed to run in time $O(D\sqrt{MN},)$ (where D is tree depth) as opposed to the classical $O(DMN)$ [356]. A recent improved QDT algorithm [361] has even potentially more significant speed-up specifically for an incremental learning scenario. By assuming that new data arrives in small batches, the algorithm can retrain a decision tree with logarithmic complexity in the number of samples $O(Dk^{2D}N\text{polylog}M)$ (where k is the number of clusters per node) [361]. This is achieved by using a

[15] This is a rough estimate; a more accurate complexity also depend on the quantum subroutines used.
[16] The C5.0 algorithm is an improved family of recursive decision tree algorithms first developed by Ross Quinlan. The "C" stands for classifier [365].

 doi:10.20944/preprints202511.1802.v2

quantum q-means algorithm [366] to find split boundaries and updating the tree, maintaining accuracy comparable to classical trees while reducing its time complexity [361]. Such results may indicate that QDT training can potentially outperform its classical counterpart for large and high-dimensional datasets.

Another source of potential advantage of QDT is when the input data itself is quantum (e.g., when quantum states need classification). In this case, one can avoid the bottleneck of reading out classical features and directly work with quantum states. An example of this is the algorithm by [367], which treats the unknown quantum state as the input and performs adaptive measurements (based on information gain) to classify the state. A QDT can thus tackle classification of quantum data in its native form, which is a potential advantage for quantum sensing or readout tasks [367].

In finance, decision trees are used for portfolio management, risk assessment, and algorithmic trading (for example, deciding whether to buy/sell based on economic indicators can be framed as a decision tree) [368–371]. A QDT can potentially handle larger feature sets and data streams in real-time, which might be useful for high-frequency trading strategies or analysing large-scale financial data for patterns [41]. The interpretability of decision trees is a plus in finance, where regulators need explanations for decisions (such as in credit approval) [372,373]. Compliance teams also often use decision trees because the resulting rules can be explained to regulators [374].

Despite the promising advantages and applications, QDTs faces several limitations and challenges. These include the bottleneck of implementing QRAM [341], and the overheads by QAE and Quantum Maximum Search subroutines. Ultimately, the output of the training is a classical decision tree even in the case where the input is quantum data. This means the potential quantum speed-up is only in training the decision tree and not in the final prediction.

In summary, QDTs promise potential polynomial speed-ups and memory advantages due to quantum subroutines like QAE. However, the quantum subroutines require advanced quantum hardware and are subject to some of the same information-theoretical limits as classical algorithms [18,375,376]. Hence, QDT are most likely to be beneficial in scenarios where data size is massive with dominating cost of processing it, or where the data is quantum mechanical in nature. As quantum technology improves, these disadvantages may be mitigated, but at present, QDTs require further research and development before achieving Practical Quantum Advantage in industrial applications such as finance and economics.

Quantum Algorithms for Regression

Regression in ML is used to solve the problem of fitting a function from the training data and identifying the relationship between independent variables and an outcome [308]. It is also used for predictive modelling to predict continuous outcomes by applying varying attributes to understand how the target value changes [377]. Many classifier algorithms, such as discussed in Section (2.4.1.1), can be adapted, with only minor modifications, for regression tasks. For example, a SVM classifier seeks a maximum-margin hyperplane for separating discrete classes, whereas its regression counterpart adjusts the objective to fit continuous targets [136]. Similarly, while a KNN classifier predicts labels by a majority vote among nearest neighbours, the regression version of KNN outputs a continuous value computed as the average of the target values of the k nearest neighbours [378]. Decision tree classifiers use impurity measures to split and assign a majority class at each leaf, whereas a regression tree uses variance-based criteria (such as minimising measures like mean squared error) to output a numeric prediction [377]. The same adjustments carry over to the quantum versions of those models.

A simple and fundamental case is linear regression [379]: given M data points $(\vec{x}_i, y_i)$ with $\vec{x}_i \in \mathbb{R}^N$ and $y_i \in \mathbb{R}$, we assume $y_i \approx x_i^\top \beta$ for some weight vector $\beta \in \mathbb{R}^N$. One wants to find β^* that minimises the sum of squared errors [380] such that

$$\beta^* = \arg\min_{\beta \in \mathbb{R}^N} \frac{1}{2} \sum_{i=1}^{M} (x_i^\top \beta - y_i)^2 \tag{82}$$

 doi:10.20944/preprints202511.1802.v2

The solution to Equation (82) is given by the *normal equation* [379]

$$X^\top X\beta = X^\top y. \tag{83}$$

This is an $N \times N$ linear system of equations. When $X^\top X$ is invertible (i.e., X has full column rank), the solution for the optimal coefficients is given in closed form by the Ordinary Least Squares (OLS) estimator:

$$\hat{\beta} \;=\; (X^\mathsf{T}X)^{-1}X^\mathsf{T}y, \tag{84}$$

where each component of $\hat{\beta}$ represents the linear effect of the corresponding feature on the outcome, holding other features fixed [381]. This solution assumes an unregularised least-squares problem. In many real-world scenarios, however, $X^\mathsf{T}X$ may be ill-conditioned or singular (e.g., when $N > M$ or features are highly correlated), which can lead to overfitting or unstable solutions [308]. Ridge regression (also called L_2-regularised linear regression) addresses this by adding a penalty on the size of coefficients [382]. The ridge estimator solves [382]:

$$\min_\beta |y - X\beta|_2^2 + \lambda|\beta|_2^2, \tag{85}$$

where $\lambda > 0$ is a regularisation parameter. Therefore, the normal equation then becomes

$$\left(X^\mathsf{T}X + \lambda I\right)\beta = X^\mathsf{T}y, \tag{86}$$

yielding the closed-form solution

$$\hat{\beta}_{\text{ridge}} = (X^\mathsf{T}X + \lambda I)^{-1}X^\mathsf{T}y. \tag{87}$$

This shrinks the regression coefficients toward zero to improve generalisation (when $\lambda = 0$ we recover OLS, and as $\lambda \to \infty$ we force $\beta \to 0$) [383].

Solving the normal equations by direct classical matrix inversion methods is $\mathcal{O}(N^3)$ in general, or $\mathcal{O}(MN^2)$ if forming $X^\mathsf{T}X$ via M data points. There exist more scalable algorithms for large M, such as iterative solvers or stochastic gradient descent [384], and the state-of-the-art classical solvers can run in time $\mathcal{O}(MN + \text{poly}(N, 1/\epsilon))$ [385]. Nonetheless, for very high-dimensional data or massive sample sizes, these computations become expensive for classical methods. This has motivated research into quantum algorithms that could potentially speed up linear regression by exploiting quantum linear algebra subroutines. In the following subsection, we will introduce some quantum algorithms for this task.

Quantum Kernel Ridge Regression One of the earliest and most famous quantum algorithms relevant to regression is the HHL algorithm [6,302] for solving systems of linear equations. Essentially, HHL can be applied to solve the normal equations of linear regression. The HHL or improved QLSS algorithm [131,132] prepares quantum circuit encoding the data, solves the normal equation via efficient quantum matrix inversion protocol, and output a quantum state proportional to the normalized $|\beta\rangle$ solution vector[17].

Subsequent research has explored variations like solving weighted least squares and introducing regularisation directly into the QLSS. For instance, quantum ridge regression can be performed by solving Equation (86) with a QLSS such as the quantum algorithm by Kerenidis et al. [134] that used this for recommendation systems with a low-rank X (thus κ small) [385]. More recently, [386] developed Quantum Regularised Least Squares (QRLS) algorithms using QSVT, achieving polynomial improvements in κ and an exponential improvement in precision for ridge regression compared to prior HHL-based methods [386]

[17] For more information see Section (2.1.5)

 doi:10.20944/preprints202511.1802.v2

While HHL tackles regression by directly solving the associated linear normal equation, an alternative quantum approach called Quantum Kernel Ridge Regression (QKRR) makes use of kernel methods to perform regression [387]. The QKRR combines the power of kernel methods (to capture non-linear relationships) with quantum computing to efficiently compute or approximate kernel functions in high-dimensional feature spaces. In classical kernel ridge regression [382,388], one maps input data points $\vec{x}$ onto a high-dimensional feature space via a feature map $\phi(\vec{x})$, and performs linear regression in that feature space with an L_2 regularisation. By the kernel trick, one avoids working explicitly with the high-dimensional $\phi(\vec{x})$, but instead the solution is obtained in terms of kernel inner products $K(\vec{x}_i, \vec{x}_j) = \langle \phi(\vec{x}_i) | \phi(\vec{x}_j) \rangle$. If K is the $M \times M$ kernel Gram matrix on the training data and y is the training target vector, the ridge regression [389] solution in dual form is

$$\vec{\alpha} = (K + \lambda I)^{-1} y, \tag{88}$$

where $\vec{\alpha}$ are the Lagrange multiplier as defined in Section (2.4.1.1). The predicted value for a new input x_* is given by [390]:

$$\hat{y}_* = \sum_{i=1}^{n} \alpha_i K(x_i, x_*). \tag{89}$$

This procedure can fit very complex functions depending on the choice of kernel, but the downside is that forming and inverting the K matrix costs $\mathcal{O}(M^3)$ classically [391]. So, for large datasets, kernel methods become computationally expensive compared to classical methods.

The quantum version of this algorithm seeks to speed up kernel evaluation and linear system solving for kernel ridge regression. The QKRR first defines a unitary $U(x)$ that prepares the state $|\phi(x)\rangle = U(x)\,|0 \cdots 0\rangle$ as an encoding of $\vec{x}$ the classical input data-point[18]. Common choices for implementing $U(x)$ include basis encoding, angle encoding, and more expressive feature maps [339,392]. The mapping should be data-efficient and ideally enhance linear separability in feature space [339]. QKRR then, estimate the kernel matrix K for all training points. In principle, one could do this by preparing $|\phi(\vec{x}_i)\rangle$ and $|\phi(\vec{x}_j)\rangle$, then performing a SWAP-test and repeating to get an estimate of the inner product. With assumptions like QRAM, quantum algorithms can access kernel matrix elements or prepare quantum states encoding kernel information, with complexity that can be sublinear in the feature dimension [134,302,393].

The output of the QPU is an estimate for K, which is inserted into Equation (88) to solve for $\vec{\alpha}$. One approach is to use a QLSS to solve Equation (88) which outputs a state proportional to the normalized solution $|\alpha\rangle$. However, this would require the ability to efficiently perform the linear operation of $K + \lambda I$ on a QPU. If K is low-rank or structured, block-encoding techniques [138] can achieve this, and if K is unitary, the LCU [48] methods can be employed.

Finally, given the solution coefficients $\vec{\alpha}$ as output from QPU, to predict on a new input x_*, one could compute $\hat{y}*$ using Equation (89). In practice, many hybrid approaches just use the QPU for estimating the kernel K and then solve the ridge regression Equation (88) on a classical computer if M is not too large. The quantum-classical computational pipeline described above can be summarised in Algorithm (14). In many implementations, Step 1 (quantum kernel computation) is executed on QPU, and Steps 2-3 are executed on CPUs. Fully quantum implementations that also solve Equation (88) might use an HHL-like QLSS in Step 2, but require K to be 'well-conditioned' and accessible as an oracle.

[18] For instance, $\vec{x}$ can be a historical price series or volatility features data-point.

 doi:10.20944/preprints202511.1802.v2

Algorithm 14 Quantum Kernel Ridge Regression

Input: Training data $\vec{x}_i, y_{i\,i=1..M}$, feature-map circuit $U(x)$ preparing $|\phi(\vec{x})\rangle$, regularisation λ.
Quantum kernel computation: Use a PQC to estimate $K_{ij} = \langle\phi(\vec{x}_i)|\phi(\vec{x}_j)\rangle$.
Solve ridge regression: Solve $(K + \lambda I)\vec{\alpha} = \vec{y}$ for $\vec{\alpha}$ (using classical or QLSS to obtain $|\alpha\rangle$).
Prediction for new input x_*: (a) Prepare state $|\phi(x_*)\rangle$ (b) compute $K(x_i, x_*)$
Output: Regression model coefficients α (classical vector).

The primary advantage of QKRR is the ability to handle extremely high-dimensional feature spaces implicitly via quantum kernel methods, which have potential speed-ups [387,394]. However, due to the current state of quantum hardware, QKRR experiments have been limited to small data sets, typically demonstrated on systems with modest qubit counts (e.g., [391,395–397]). One concern is that in practice, many proposals end up with complexity $\tilde{O}(M)$ or worse when all costs are accounted for, meaning a quantum computer might realise Practical Quantum Advantage except in special cases [11,146,398]. Another concern is that quantum kernel methods can sometimes suffer from concentration issues (be nearly uniform in high dimension), making them less useful than hoped for [399].

Despite these challenges, early demonstrations of QKRR on small systems have shown that quantum computed kernels can perform as well as classical kernels on simple tasks. For example, experiments with up to 10 qubits have used a PQC kernel to do regression on molecular data, achieving accuracy on par with classical Gaussian kernels [400].

Future research may include optimising quantum feature maps, understanding generalisation properties of quantum models, and integrating quantum kernel methods with classical frameworks. Whether QKRR can offer a decisive speed-up for practical problems remains an open challenge.

Quantum Neural Networks

Classical neural networks are function approximators composed of layers of interconnected nodes, inspired by biological neuron systems [401,402]. Each node performs an affine transformation on its inputs, followed by a non-linear activation. In a feed-forward network, the l-th layer takes an input vector $\mathbf{a}^{(l)}$, and produces an output $\mathbf{a}^{l+1}$ via:

$$\begin{aligned} \mathbf{z}^{(l+1)} &= \mathbf{W}^{(l)}\mathbf{a}^{(l)} + \mathbf{b}^{(l)} \\ \mathbf{a}^{(l+1)} &= \phi(\mathbf{z}^{(l+1)}), \end{aligned} \tag{90}$$

where $W^{(l)}$ is a weight matrix, $\mathbf{b}^{(l)}$ a bias vector (the affine transformation), and $\phi(\cdot)$ an activation function. The activation function introduces non-linearity; without it, multiple layers would collapse into an equivalent single affine layer. For example, a simple one-layer perceptron[19] with input $\mathbf{x} \in \mathbb{R}^n$ and output $y \in \mathbb{R}$ can be written as $y = \phi(\mathbf{w}^T\mathbf{x} + b)$, with trainable parameters $\mathbf{w}$ and b. Networks are trained by defining a loss function L and adjusting the weights $W^{(l)}$, $b^{(l)}$ to minimise L, typically using gradient-based optimisation [403]. Deep neural networks (many-layered) have achieved huge success in prediction tasks by learning complex hierarchical features from data [404].

A Quantum Neural Network (QNN) [405] extends the classical neural network concept by using a PQC, where the QNN 'layers' can be seen as sequential blocks of quantum gates, some of which are parametrised by adjustable angles analogous to weights. Like input layers in classical networks, QNNs begin by encoding classical data $\mathbf{x}$ into a quantum state [41]. The choice of encoding influences the QNN's expressive power[20] [406]. Encodings can be repeated throughout the circuit (data re-uploading) to form multiple 'layers', analogous to having multiple layers in a classical network [407].

[19] A perceptron is a mechanism that activates a neuron due to the input of other neurons [402].
[20] Expressive power refers to the model's capacity to represent complex functions. Different encoding strategies enable QNNs to access different regions of the quantum state space, affecting what functions can be learned.

 doi:10.20944/preprints202511.1802.v2

After encoding, the QNN applies a sequence of parametrised quantum gates $U(\boldsymbol{\theta})$ to process the state. These gates depend on a set of m trainable parameters $\boldsymbol{\theta} = (\theta_1, \theta_2, \ldots, \theta_m)$. A typical quantum layer might consist of single-qubit rotations on each qubit followed by multi-qubit entangling gates. For example, a layer on qubit j could include a rotation:

$$R_y(\theta) = \exp(-i\theta_j Y/2) = \begin{pmatrix} \cos\frac{\theta}{2} & -\sin\frac{\theta}{2} \\ \sin\frac{\theta}{2} & \cos\frac{\theta}{2} \end{pmatrix}. \tag{91}$$

These gates are analogous to weight multiplications in a classical network, with the angle θ_j as the tunable weight. In many QNN designs, one layer consists of rotations on all qubits (with independent parameters) followed by a fixed pattern of entangling gates across qubits. The combination of encoding and L layers of trainable gates produces a final quantum state:

$$|\Psi(\mathbf{x};\boldsymbol{\theta})\rangle = U(\boldsymbol{\theta})U_{\text{enc}}(\mathbf{x})|0\rangle^{\otimes n}, \tag{92}$$

where $U(\boldsymbol{\theta})$ represents the total unitary composed of all parametrised gates. This state $|\Psi(\mathbf{x};\theta)\rangle$ encodes the model's prediction in its quantum amplitudes. To extract a classical output from the quantum state (analogous to the classical output neuron activations), one measures an observable $\hat{O}$ and takes the expectation value as the model output. Then, the predicted scalar output can be written as:

$$f(\mathbf{x};\boldsymbol{\theta}) = \langle\Psi(\mathbf{x};\boldsymbol{\theta})|\hat{O}|\Psi(\mathbf{x};\boldsymbol{\theta})\rangle. \tag{93}$$

Therefore, for a binary classification, the probability of class label '0' is given by

$$\Pr(y=0|\mathbf{x}) = \frac{1+f(\mathbf{x};\theta)}{2}. \tag{94}$$

Note that the PQC, $U(\boldsymbol{\theta})$, is linear, whereas a classical neural layer is non-linear due to ϕ. The non-linearity in QNNs enters when one measures and feeds results into a classical optimiser, as the measurement probabilities have a non-linear dependence on the quantum state amplitudes [408]. Additionally, if the QNN is a hybrid network, or if intermediate measurements are performed between layers, effective non-linear transformations can be achieved [409]. In most near-term QNN implementations, a variational approach is often employed, relying on classical iterative optimisation to adjust $\boldsymbol{\theta}$ (see VQA in Section 2.1.6).

The training of a QNN involves finding the optimal parameters $\boldsymbol{\theta}$ such that the QNN's output matches the target outputs on a training dataset (same as in classical ML). This is a hybrid quantum-classical approach; the quantum circuit generates estimates of target outputs based on $\boldsymbol{\theta}_i$ and a classical optimiser updates the parameters $\boldsymbol{\theta}_i \mapsto \boldsymbol{\theta}_{i+1}$ to improve the subsequent estimate. Generally, the classical optimiser is guided by a loss function $\mathcal{L}(\theta)$, for example, the mean squared error or cross-entropy between QNN predictions $f(\mathbf{x}_i;\theta)$ and labels y_i over the dataset [407]. Hence, the parameter update can be done via gradient descent depending on estimates of $\nabla_\theta\mathcal{L}$. The gradients can be estimated on the QPU using the parameter-shift rule, an analytical quantum subroutine, or via automatic differentiation on quantum simulators [410]. The parameter-shift rule for a rotation parameter θ in a gate $R(\theta) = e^{-i\theta G/2}$ (where G is a Pauli operator) is [410]:

$$\frac{\partial}{\partial\theta}f(\mathbf{x};\boldsymbol{\theta}) = \frac{1}{2}\big(f(\mathbf{x};\theta+\tfrac{\pi}{2}) - f(\mathbf{x};\theta-\tfrac{\pi}{2})\big). \tag{95}$$

This implies we can obtain the gradient by evaluating the circuit at two shifted parameter values. This requires additional quantum evaluations for each parameter, which is a key contributor to training cost. The complete QNN training procedure is summarised in Algorithm (15).

 doi:10.20944/preprints202511.1802.v2

Algorithm 15 Training Quantum Neural Network

Input: Training samples $\{(\mathbf{x}_1, y_1), \ldots, (\mathbf{x}_S, y_S)\}$, parameters $\boldsymbol{\theta} = \{\theta_1, \ldots, \theta_M\}$, total iterations K, and error-tolerance ϵ.
Initialising: Initialise parameters $\boldsymbol{\theta}^{(0)} \sim \mathcal{N}(0, \sigma^2)$, generally randomly chosen from a normal distribution.
For $k = 1$ **to** K **do: For each training sample** $s \in \{1, \ldots, S\}$**:** (a) Prepare quantum state $U_{\text{enc}}(\mathbf{x_s}) |0\rangle^{\otimes n}$. (b) Apply PQC $U(\boldsymbol{\theta}^{(k)})$. (c) Measure observable $\hat{O}$ to obtain prediction $f_s = \langle \hat{O} \rangle$. (d) Compute sample loss $\ell_s = \ell(f_s, y_s)$ (loss for sample s).
Compute global loss: $\mathcal{L}(\boldsymbol{\theta}^{(k)}) = \frac{1}{S} \sum_{s=1}^{S} \ell_s$.
Estimate gradients for each $\theta_j \in \boldsymbol{\theta}^{(k)}$: estimate $\partial \mathcal{L}(\boldsymbol{\theta}^{(k)}) / \partial \theta_j = \frac{1}{S} \sum_{s=1}^{S} \frac{\partial \ell_s}{\partial \theta_j}$
Update parameters: $\boldsymbol{\theta}^{(k+1)} = \boldsymbol{\theta}^{(k)} - \eta \nabla_{\boldsymbol{\theta}} \mathcal{L}(\boldsymbol{\theta}^{(k)})$ where $\eta > 0$ is the learning-rate.
Terminate: if $|\mathcal{L}(\boldsymbol{\theta}^{(k+1)}) - \mathcal{L}(\boldsymbol{\theta}^{(k)})| < \epsilon$. **End for**
Output: Set of parameters $\boldsymbol{\theta}^*$ that defines a QNN for classification task.

QNNs are currently being explored theoretically and experimentally for various financial applications. For example, in financial time-series forecasting, hybrid QNNs have shown potential to capture complex temporal dependencies and outperform classical models in stock market predictions [411,412]. For fraud detection, QNN could learn subtle anomalies in large transactional data [413] by using quantum graph neural networks to flag fraudulent patterns [414]. QNNs have also been suggested for option pricing and risk modelling, where they could learn and approximate stochastic processes or option payoff scenarios that are challenging for classical networks. These applications are still in the early stages, with ongoing research assessing whether QNNs can provide better accuracy or speed compared to classical ML [415].

In theory, if each layer applies $O(n)$ single-qubit rotations and $O(n)$ two-qubit gates, the circuit depth might scale as $O(nL)$ for n qubits and L layers. This is analogous to the $O(N_{\text{params}})$ cost of evaluating a classical neural network with N_{params} weights. However, QNNs can operate in an exponentially large space of dimension 2^n, which is where the potential advantage lies. For instance, recent results [416] proved a universal approximation theorem for QNNs and derived that an $O(\lceil \log_2(1/\varepsilon) \rceil)$ number of qubits with $O(\varepsilon^{-2})$ circuit parameters can approximate functions to error ε. This suggests that to achieve high accuracy, the parameter count in a QNN might grow polynomially in $1/\varepsilon$ while the qubit count grows only logarithmically. In contrast, a classical network might require significantly more neurons to achieve the same expressive power. These are worst-case upper bounds: the actual runtime advantage of QNNs remains an open question and is likely problem-dependent. Whether they can surpass classical neural networks for real-world tasks is an active area of research [417].

A major challenge for QNNs is the barren plateau [153] phenomenon[21]. As the number of qubits or circuit depth grows, the gradients for the cost-function $\nabla_{\theta_i} C(\boldsymbol{\theta})$ can vanish exponentially, making training infeasible [153], i.e., the training landscape is almost flat in most areas. Architectures that are designed to avoid barren plateaus [418] may results to quantum circuits that can be simulated classically, hence lose quantum advantage [156]. This issue, amongst others, is a serious limitation on scaling QNN to perform large-scale classification tasks in an industrial setting [154,415].

2.4.2. Quantum Algorithms for Unsupervised ML

Building upon the foundational concepts of QML discussed in Section (2.4.1) for supervised learning, in this section, we review quantum algorithms for unsupervised ML. Unlike supervised learning, which relies on given labelled data, unsupervised methods aim to discover hidden patterns and structures within unlabelled data by themselves [403]. This attribute allows complex data analysis without requiring additional information or prior knowledge of the data, making unsupervised learning aptly tailored for real-world applications, such as in finance [42].

[21] Also discussed in Sections (2.1.6) and (2.3.1)

 doi:10.20944/preprints202511.1802.v2

To illustrate more explicitly how the unsupervised learning process works, let us revisit the animal data set example from the previous Section (2.4.1). In supervised learning, each image comes with a label indicating the type of animal: whether it is a cat, dog, or bird. The algorithm uses this label to learn a mapping function that can correctly predict new, unseen data. In unsupervised learning, however, the collection of images lacks any labels, and the algorithm might analyse intrinsic features of the images, such as colour, texture, shape, or size, to find patterns within the data. For instance, it might group cat images due to shared characteristics like pointy ears and whiskers, even though it does not know the term 'cat'. In other words, unsupervised learning aims to find a function or model that captures the patterns and structure of the data without any labels guiding the process [39].

Common ML techniques include clustering, where data points are grouped based on similarity and dimensionality reduction, which involves projecting data onto a lower-dimensional space while preserving significant features (such as Principal Components Analysis (PCA) and autoencoders) [419]. Generative models that can learn the underlying data distribution to generate new data points that resemble the training dataset. Additionally, Reinforcement Learning (RL) techniques, while traditionally categorised separately, can incorporate unsupervised elements for exploration and policy improvement without explicit labels. Extending these techniques in the context of quantum computing is particularly helpful, as they can potentially offer polynomial to exponential speed-ups over classical algorithms [420]. In the following subsections, we will review examples of these techniques and highlight how they are being adapted and implemented in quantum contexts.

Quantum Clustering

Clustering methods rely on mathematical formulations, such as distance metrics (e.g., Euclidean) or statistical models, to evaluate the relationships between data points. These formulations help identify patterns and group data points into distinct clusters by measuring how similar or different they are [39]. Quantum algorithms for clustering have been developed to improve the efficiency of classical methods [421]. Proposed quantum clustering techniques can be applied in areas like fraud detection and customer segmentation (e.g., credit scoring) [421,422]. However, practical implementations on large-scale industrial problems remain constrained by current quantum hardware and other algorithmic bottlenecks. In this subsection, we will review some of the common quantum clustering algorithms.

Quantum k-Means Clustering One of the most well-known algorithms for unsupervised learning is the k-means clustering algorithm, first introduced by Lloyd [423]. It takes as input a set of vectors $X = \{x_1, x_2, \ldots, x_M\} \subseteq \mathbb{R}^N$, where $x_i \in \mathbb{R}^N$ for $i \in \{1, \ldots, M\}$, with M being the number of data points and N the dimensionality (number of features). The aim is to place these vectors or data points in k subsets so that it minimizes the sum of the objective function f_k. This function is defined as the sum over all points of the squared Euclidean distance from a cluster centroid (subsets) to the members of the cluster [296]

$$f_k = \min_{C_1,\ldots,C_k;\mu_1,\ldots,\mu_k} \sum_{j=1}^{k} \sum_{i \in C_j} \|x_i - \mu_j\|^2, \tag{96}$$

where $C = \{C_1, C_2, \ldots, C_k\}$ are the clusters to be determined, and μ_j is the centroid of cluster C_j for $j \in \{1, \ldots, k\}$. The algorithm initialised k different centroids (often using methods like k-Means++[22] for better convergence) and iterates over two main steps until convergence. The first step involves assigning each data point x_i to the cluster with the nearest centroid, where the cluster assignment $C(x_i)$ is determined by [296]

$$C(x_i) = \arg\min_j \|x_i - \mu_j\|^2. \tag{97}$$

[22] k-Means++ is an initialisation method that selects initial centres with probability proportional to their squared distance from existing centres, improving convergence [424].

 doi:10.20944/preprints202511.1802.v2

The second step is to recompute and update the centroids as the mean of their respective clusters [425]

$$\mu_j = \frac{1}{|C_j|} \sum_{i \in C_j}^{n} x_i. \tag{98}$$

These steps are repeated until changes in the cluster assignments between iterations are sufficiently small [366]. In other words, k-means assigns each data point to the cluster whose centroid it is closest to [289].

The classical K-means clustering is a widely used clustering technique [426]; however, despite its simplicity, it suffers from several limitations. These include issues with the initialisation of centroids, which often lead to suboptimal clustering and the algorithm's complexity scaling with the number of data points and clusters. Improvements to the initialisation and optimisation stages of k-means have been proposed, such [427]. These aim to mitigate issues such as convergence to local minima and sensitivity to initial centroids, and better analysis of large-scale distributed data [428]. However, in general, the k-means clustering is an NP-Hard problem [429], hence quantum algorithms are a promising alternative to improve efficiency. Researchers have proposed multiple variants of Quantum k-Means Clustering (QkMC) [366] with potential exponential speed-ups [299,426,430]. By encoding the data into quantum states, these quantum algorithms accelerate the computationally intensive steps of the classical algorithm, typically the distance calculations [289,426].

In this review, we will introduce one variant of the QkMC based on [426]. This is a hybrid quantum-classical algorithm where the QPU handles the distance computation while the update step is done on a CPU. Similar to QML methods in Section (2.4.1), the classical data can be encoded into quantum states using amplitude encoding[23]. A sequence of controlled unitaries U prepares the state

$$U |0\rangle_a |0\rangle^{\otimes n} = \frac{1}{\sqrt{2N}} (|0\rangle_a |x\rangle + |1\rangle_a |\mu\rangle). \tag{99}$$

Here, the qubits with subscript 'a' are the ancillas and the amplitude-encoded states $|x\rangle$ and $|\mu\rangle$ are given by

$$|x\rangle = \frac{1}{\sqrt{N}} \sum_{j=1}^{N} x_j |j\rangle, \quad \text{and} \quad |\mu\rangle = \frac{1}{\sqrt{N}} \sum_{j=1}^{N} \mu_j |j\rangle, \tag{100}$$

where x_j, μ_j are the j-th feature components of data point x and centroid μ, respectively. By employing the SWAP test [320] which produces $\langle x|\mu\rangle$, the QPU efficiently estimates the Euclidean distance $d(x, \mu)$ between $|x\rangle$ and $|\mu\rangle$ given by Equation (74).

After computing the distances between the data point and all centroids, this is repeated for all $M \times k$ pairs of vectors, where M is the number of data points and k is the number of centroids. The algorithm assigns the data point to the nearest centroid as per Equation (97).

Algorithm 16 Quantum k-Means Clustering

Input: Dataset $X = \{x_1, x_2, \ldots, x_M\}$, and number of clusters k
Initialising: Select initial centroids $\mu = \{\mu_1, \mu_2, \ldots, \mu_k\}$ using k-Means++
Assignment: For each data point $x_i \in X$ and each centroid $\mu_j \in \mu$, compute distance $d(x_i, \mu_j)$ using QPU: (a) Encode x_i and μ_j as quantum states (Equation (100)). (b) Estimate distance using SWAP test [320]. (c) Assign x_i to the nearest cluster C_j.
Update: For the assigned clusters, update the estimate for the centroids given by Equation (98)
Repeat steps 3 and 4 until convergence
Output: Cluster assignments and centroids μ

[23] Some proposals to accomplish this by using Flip-Flop QRAM (FF-QRAM) [431] seemed promising but could be impractical for fault-tolerant [341].

 doi:10.20944/preprints202511.1802.v2

Examples of quantum k-means implementations include hybrid methods applied on simulators and full implementations on quantum platforms [432]. In finance, a quantum k-means pipeline is applied to cross-border payment risk supervision [433], enhancing clustering of blockchain transaction data [434]. Recent research on quantum computing for finance recognises clustering methods as one of the unsupervised learning methods applicable to finance [41,346]. Although detailed use cases are still in early exploratory stages.

Examples of quantum k-means implementations include hybrid methods applied on simulators and full implementations on quantum platforms [432]. In finance, a quantum k-means pipeline is applied to cross-border payment risk supervision [433], enhancing clustering of blockchain transaction data [434]. Recent research on quantum computing for finance recognises clustering methods as one of the supervised learning methods applicable to finance [41,346]. Although detailed use cases are still in early exploratory stages.

While quantum k-means addresses clustering through iterative centroid updates, quantum spectral clustering takes a fundamentally different approach by leveraging graph theory and eigendecomposition. Classical spectral clustering constructs a similarity graph from the data, computes the Laplacian matrix, and projects data into a lower-dimensional space defined by the smallest k eigenvectors, where traditional clustering becomes more effective, particularly for non-convex or nested structures [435,436]. The classical algorithm $\mathcal{O}(M^3)$complexity for eigendecomposition severely limits scalability [437]. Quantum spectral clustering, as proposed by Kerenidis et al. [438], attempts to accelerate this process using QPE to compute eigenvalues of the normalised Laplacian. However, this approach also requires strong assumptions, such as efficient QRAM [288] and block-encoding, and successful post-selection of the desired eigenvectors. The claimed quantum advantage remains theoretical, as the practical implementation faces significant challenges including QRAM overhead (which alone could eliminate any speed-up), the complexity of preparing the block-encoded Laplacian, and the probabilistic nature of post-selection which may require multiple runs. To date, only small proof of concept demonstrations on actual quantum hardware have been reported [439], and there is no large-scale implementations showing advantage. Recent dequantisation results suggest that classical algorithms with similar assumptions might achieve comparable performance, raising questions about whether genuine quantum advantage exists for this application.

Quantum Generative Models

Unsupervised generative models are extensively used in deep learning to generate synthetic data and new samples [30]. Classical generative models (e.g., Generative Adversarial Networks (GANs), Variational Autoencoderss (VAEs)) aim to learn a target probability distribution $\tilde{P}(\boldsymbol{x})$ over a set of possible outcomes $\boldsymbol{x} \in \Omega$. This is achieved by constructing a model distribution $P(\boldsymbol{x};\boldsymbol{\theta})$ that approximates $\tilde{P}(\boldsymbol{x})$. Despite their effectiveness, classical generative models require significant computational resources and can struggle to model complex dependencies, especially in high-dimensional spaces [440].

Quantum generative models have been proposed as alternatives to potentially address these limitations [398,441]. For instance: (i) By enabling parallel sampling from different parts of the distribution, which reduces the time required for generating new samples. (ii) Using entanglement to capture complex correlations between variables more naturally, improving the expressiveness of the model. These improvements suggest that quantum generative models could benefit tasks requiring high-dimensional data synthesis, such as generating synthetic financial data for stress testing and model validation or improving portfolio optimisation by generating diverse asset combinations [30].

The training of quantum generative models focuses on minimising a divergence or distance measure, such as the Kullback–Leibler (KL) divergence [442]. Alternatively, one may define a cost function and use maximum likelihood estimation [398] or quantum fidelity-based costs [443] to find its minimum. Below, we will highlight two major techniques: Quantum Boltzmann Machine (QBM) [444] and Quantum Generative Adversarial Networks (QGAN) [445].

 doi:10.20944/preprints202511.1802.v2

Quantum Boltzmann Machine In classical ML, a Boltzmann Machine (BM) [446] is an energy-based model that defines a probability distribution by assigning to each configuration $x \in \{0,1\}^d$ a probability [447]. This distribution is given by the Boltzmann distribution [403]:

$$P(x) = \frac{e^{-E(x)}}{Z}, \quad \text{where} \quad Z = \sum_x e^{-E(x)}, \tag{101}$$

with $E(x)$ denoting the energy of configuration x, and Z the partition function ensuring normalisation. For the standard BM, the energy function consists of pairwise interactions among units and bias terms, and can be written as [403]:

$$E(x) = -x^\top W x - b^\top x, \tag{102}$$

where W is a weight matrix and b is a bias vector.

BMs evolved from earlier energy-based models, particularly Hopfield networks[24] [448], which uses a similar energy framework but with deterministic dynamics. While Hopfield networks minimise energy through deterministic updates and can get trapped in local minima, BMs introduce stochasticity through the Boltzmann distribution in Equation (101) [449,450], allowing them to escape local minima and model probability distributions more effectively [403,451].

Training a BM is usually performed via Contrastive Divergence (CD) [452] or maximum likelihood estimation [453], which involves adjusting the weights, and is equivalent to minimising the Kullback–Leibler divergence [442] between the data distribution and the model distribution. This is typically achieved through the log-likelihood gradient, which decomposes the learning into two terms: a positive phase that increases the probability of data configurations and a negative phase that decreases the probability of configurations sampled from the model (unobserved configurations). This can be written as [454]

$$\nabla_{W_{ij}} \ell(\theta) = \langle x_i x_j \rangle_{\text{data}} - \langle x_i x_j \rangle_{\text{model}}, \tag{103}$$

$$\nabla_{b_i} \ell(\theta) = \langle x_i \rangle_{\text{data}} - \langle x_i \rangle_{\text{model}}, \tag{104}$$

where $\langle \cdot \rangle_{\text{data}}$ denotes an expectation under the empirical distribution and $\langle \cdot \rangle_{\text{model}}$ an expectation under the model distribution [403,447]. These update rules resemble Hebbian learning [455], adjusting parameters so that model statistics align with data statistics.

Through this stochastic formulation, BMs serve as generative models, since they define full probability distributions over the visible variables, and can support probabilistic inference by estimating conditional distributions. For instance, for BMs with visible and hidden units, inference includes computing $P(h \mid v)$ or $P(v \mid h)$ [403], enabling tasks such as feature extraction or generating new samples from the learned distribution. However, the computational cost of inference and learning of BMs face several challenges, such as: (i) evaluating the partition function Z requires summation over 2^d states (configurations), which is intractable for large d. (ii) approximate Markov Chain Monte Carlo (MCMC) methods such as Gibbs sampling mix slowly in practice. (iii) The CD, for a fully connected BM with n units, each Gibbs sampling requires $O(n^2)$ operations, making training computationally expensive. These limitations have motivated both architectural simplifications (e.g., Restricted Boltzmann Machines) and quantum-inspired approaches to potentially overcome classical sampling bottlenecks [456].

[24] A Hopfield network is an early energy-based model that implements associative memory by storing patterns as local minima of an energy function [448]. Boltzmann Machines extend this framework by introducing stochasticity, enabling generative modelling [447].

 doi:10.20944/preprints202511.1802.v2

In a Quantum Boltzmann Machine (QBM), the classical energy function is replaced by a Hamiltonian $\hat{H}(\boldsymbol{w})$, and the distribution is replaced by the density matrix of a thermal (Gibbs) state [444]:

$$\rho(\boldsymbol{w}) = \frac{e^{-\beta\hat{H}(\boldsymbol{w})}}{Z(\boldsymbol{w})}, \quad \text{where} \quad Z(\boldsymbol{w}) = \mathrm{Tr}\left[e^{-\beta\hat{H}(\boldsymbol{w})}\right], \tag{105}$$

and $\beta = \frac{1}{k_B T}$ is the inverse of Boltzmann constant k_B times temperature T. T As in the classical case, the learning involves adjusting the weights $\boldsymbol{w}$ so that expectation values of observables (e.g., marginal probabilities or correlation functions) under $\rho(w)$ match data statistics with model statistics. Methods include gradient-based optimisers that compute the derivative of the log-partition function and of observable expectation values, such as:

$$\frac{\partial}{\partial w} \log \mathrm{Tr}\left[e^{-\beta\hat{H}(w)}\right] \quad \text{and} \quad \frac{\partial}{\partial w} \mathrm{Tr}\left[\hat{O}\rho(w)\right]. \tag{106}$$

To perform a thermal state approximation, one approach implements $e^{-\beta\hat{H}(w)}$ via Trotterisation or variational methods [457]. The estimates of observable averages are compared with target data statistics (e.g., means, correlations), which are used to compute a cost function. Based on the gradients of the cost-function, the parameters $\boldsymbol{w}$ are updated until convergence. Algorithm (17) illustrates a typical QBM training loop using a variational approach.

Algorithm 17 Quantum Boltzmann Machine

Input: Target data statistics (means, correlations), temperature parameter, number of qubits
Initialisation: Define an ansatz for $\hat{H}(\boldsymbol{w})$ (e.g., local fields and pairwise interactions) and pick random initial $\boldsymbol{w}$
Thermal State Approximation: (a) Construct a PQC $V(\boldsymbol{\alpha})$, with randomly initialised α, to approximate $e^{-\beta\hat{H}(w)}$.
Sampling and Observables: (a) Run the circuit $V(\boldsymbol{\alpha})$ on a QPU and measure in a relevant basis (e.g., σ_z) (b) Estimate observables, such as $\langle\sigma_z^{(i)}\rangle$ or correlation $\langle\sigma_z^{(i)}\sigma_z^{(j)}\rangle$
Loss Computation: Define a loss function comparing the measured observables to the target data (e.g., least squares)
Optimisation: (a) Update $\boldsymbol{\alpha}$ to improve the approximation of the thermal state. (b) Optionally, update $\boldsymbol{w}$ to better match target statistics by adjusting the Hamiltonian terms.
Repeat until convergence or maximum iterations are reached.
Output: Hamiltonian parameters $\boldsymbol{w}^*$ that define $\hat{H}(\boldsymbol{w}^*)$

QBMs can potentially explore difficult energy landscapes more efficiently [288] through quantum effects like tunnelling and may use fewer parameters to represent certain distributions [443]. However, preparing exact thermal states remains challenging on near-term NISQ devices.

Despite their theoretical advantages, quantum generative models still have several open problems. For example, noise and decoherence limit the circuit depth on current hardware, which in turn constrains model expressivity [444]. Furthermore, the training process can face issues due to barren plateaus, especially in high-dimensional parameter spaces [454]. Researchers have achieved some promising success in mitigating these issues by employing strategies such as carefully designing ansatze, implementing layer-wise training, and using advanced initialisation methods [458]. With hardware steadily improving and novel algorithms emerging [457], quantum generative models stand as a potentially useful tool. Demonstrating a clear quantum advantage in real-world applications remains an open challenge, but progress in error mitigation, algorithm design, and hybrid frameworks is bringing these models closer to practical use.

Quantum Generative Adversarial Networks Generative Adversarial Networks (GANs) [403] are implicit generative models that learn to generate samples from a target distribution by solving an adversarial minimax game between a generator G and a discriminator D. The generator maps

 doi:10.20944/preprints202511.1802.v2

random noise $z \sim p_z$ to samples $G(z)$, while the discriminator attempts to distinguish between real data $x \sim p_{\text{data}}$ and generated samples. The objective is given by

$$\min_G \max_D V(D,G) = \mathbb{E}_{x\sim p_{\text{data}}}[\log D(x)] + \mathbb{E}_{z\sim p_z}[\log(1 - D(G(z)))]. \tag{107}$$

At equilibrium under the assumptions of infinite model capacity and an optimal discriminator, the generator distribution converges to the data distribution, i.e., $p_g = p_{\text{data}}$ [403]. In practice, however, GAN training can be unstable and is susceptible to mode collapse; variants such as the Wasserstein GAN (WGAN) improve training stability by replacing the Jensen–Shannon divergence with the Earth Mover's distance [459].

Quantum Generative Adversarial Networks (QGAN) extends this framework by parametrising the generator, discriminator, or both as Parametrised Quantum Circuits (PQCs) [445,460,461]. A typical setup employs a quantum generator, where a PQC prepares a variational state

$$|\psi(\theta)\rangle = U(\theta)\,|0\rangle^{\otimes n}, \tag{108}$$

with measurement outcomes distributed according to $p_\theta(x)$. These samples are then evaluated by either a classical discriminator (hybrid QGAN) or a quantum discriminator [460]. The adversarial loss generalises Equation (107) to the quantum–classical setting. Gradients of the quantum generator can be computed exactly for wide classes of gates via the parameter-shift rule [162,462,463], which requires multiple circuit evaluations per parameter. Training proceeds by alternating updates of the generator parameters θ and discriminator parameters ϕ, analogous to the classical setting. An outline of the QGAN training loop is shown in Algorithm (18).

Algorithm 18 Quantum Generative Adversarial Networks

Input: Dataset $\mathcal{D} = \{x\}$; prior p_z; number of qubits n; PQC ansatz $U(\theta)$; discriminator D_ϕ (classical or quantum); batch size B; shots S; learning rates η_G, η_D
Initialisation: Randomly initialise generator parameters θ and discriminator parameters ϕ
Sample real data: Draw a minibatch $\{x^{(i)}\}_{i=1}^{B} \sim p_{\text{data}}$ from $\mathcal{D}$.
Generate quantum samples: For $i = 1, \ldots, B$: draw $z^{(i)} \sim p_z$; prepare $|\psi(\theta)\rangle = U(\theta)|0\rangle^{\otimes n}$; measure in the computational basis with S shots to obtain $x_\theta^{(i)} \sim p_\theta$ (apply any required classical post-processing if modelling continuous variables).
Discriminator step: Form the (hybrid) adversarial loss (e.g., JS or Wasserstein variant)

$$\mathcal{L}_D = -\frac{1}{B}\sum_{i=1}^{B}\Big(\log D_\phi(x^{(i)}) + \log\big(1 - D_\phi(x_\theta^{(i)})\big)\Big).$$

Compute $\nabla_\phi \mathcal{L}_D$ (classical backprop if D is classical; parameter-shift or other gradient rule if D is quantum) and update $\phi \leftarrow \phi - \eta_D \nabla_\phi \mathcal{L}_D$.
Generator step: Hold ϕ fixed and define

$$\mathcal{L}_G = -\frac{1}{B}\sum_{i=1}^{B}\log D_\phi(x_\theta^{(i)}).$$

Estimate $\nabla_\theta \mathcal{L}_G$ using the parameter-shift rule [162,462,463], requiring multiple circuit evaluations per parameter, and update $\theta \leftarrow \theta - \eta_G \nabla_\theta \mathcal{L}_G$.
(Optional) WGAN variant: Replace $\mathcal{L}_D, \mathcal{L}_G$ with Wasserstein losses and include a gradient penalty term [459].
Repeat steps 3–7 for $t = 1, 2, \ldots, T$
Until convergence or maximum iterations.
Output: Trained generator parameters $\theta^\star$ (and discriminator $\phi^\star$).

QGANs have been proposed for applications in finance, particularly for learning and efficiently loading probability distributions of asset price changes [196]. Exact state preparation of arbitrary

 doi:10.20944/preprints202511.1802.v2

distributions requires $O(2^n)$ gates, but QGANs can approximate state loading with $O(\text{poly}(n))$ gates after training. Zoufal et al. demonstrate this in the context of European option pricing, where the learned generator prepares a distribution matching asset returns, enabling quantum amplitude estimation to evaluate expected payoffs more efficiently [196].

Beyond finance, QGANs have been investigated for tasks such as image [461] and molecular generation [464]. Empirically, hybrid QGANs have matched or exceeded classical baselines on specific tasks while using fewer trainable parameters in the quantum modules [464]. Theoretically, quantum sampling may enable more efficient exploration of probability landscapes [445], although such claims remain speculative.

Despite their promise, QGANs inherit both the adversarial instability of classical GANs and the limitations of NISQ hardware. Deep variational circuits are prone to barren plateaus, where gradients vanish exponentially with system size, hindering training [153,465,466]. In addition, adversarial training amplifies shot noise, requiring a large number of measurement shots to estimate gradients and loss functions accurately. The parameter-shift rule itself adds further overhead, as each parameter update requires multiple circuit evaluations [463]. Surveys of QGANs [467] emphasise that while they show strong conceptual potential for finance and other data-intensive applications, realising quantum advantage remains contingent on overcoming these limitations.

Other Approaches Several other quantum generative approaches have been developed. Such as, Quantum Circuit Born Machine (QCBM) [398,468], where a PQC directly encodes a probability distribution via the Born rule. QCBMs are also trained by minimising the KL divergence between the target and model distributions through circuit parameter optimisation.

In addition, Quantum Bayesian Network[469,470] extend classical Bayesian networks by replacing conditional probability distributions with quantum channels between nodes, enabling the representation of quantum correlations and entanglement in structured probabilistic models. While classical Bayesian network inference is NP-hard for general DAGs, QBNs may achieve polynomial speed-ups for certain network topologies through quantum amplitude amplification [469]. Recent work has also explored quantum-like Bayesian networks that use quantum probability theory for classical data, showing advantages in modelling paradoxical human decision-making and cognitive phenomena [471,472].

Quantum Dimensionality Reduction Dimensionality reduction [473] has long been an essential tool for processing large-scale datasets in ML, signal processing, and other data-driven fields. They compress high - dimensional data into lower-dimensional representations while preserving essential information. In classical frameworks, popular methods include Principal Components Analysis (PCA) [474], Singular Value Decomposition (SVD)-based approaches [475], and nonlinear manifold learning [476]. However, for extremely high-dimensional data, these techniques can become computationally expensive. In this section, we review the Quantum Principal Components Analysis (QPCA) [477] approach for QDR.

Quantum Principal Component Analysis In Quantum Dimensionality Reduction (QDR) [477], the fundamental idea is to represent high-dimensional data as quantum states and perform transformations (e.g., QPE, QSVT) that isolate essential components (principal components, singular values, etc.). Given a dataset $\{\mathbf{x}_1, \ldots, \mathbf{x}_M\}$ where $\mathbf{x}_i \in \mathbb{R}^N$, the goal is to find lower-dimensional representation $\{\mathbf{y}_1, \ldots, \mathbf{y}_M\}$ where $\mathbf{y}_i \in \mathbb{R}^d$ (with $d \ll N$) that retains most of the 'useful' structure. For instance, PCA [477] finds an orthonormal projection matrix $W \in \mathbb{R}^{N \times d}$ that minimises

$$\min_W \sum_{i=1}^{M} \left\| \mathbf{x}_i - WW^T \mathbf{x}_i \right\|^2, \tag{109}$$

 doi:10.20944/preprints202511.1802.v2

subject to $W^T W = I_d$. To employ quantum algorithms, one typically represents classical vectors as normalised quantum states. As detailed in previous sections, a frequently used technique is amplitude encoding:

$$|\psi_i\rangle = \frac{1}{\|\mathbf{x}_i\|} \sum_{j=1}^{N} x_i^{(j)} |j\rangle, \quad \text{where} \quad \|\mathbf{x}_i\| = \sqrt{\sum_{j=1}^{N} |x_i^{(j)}|^2}. \tag{110}$$

Considering a statistical mixture of states $\{|\psi_i\rangle\}$ with probabilities $\{p_i\}$ results in the density matrix:

$$\rho = \sum_{i=1}^{M} p_i |\psi_i\rangle\langle\psi_i|. \tag{111}$$

Thus QDR seeks to approximate the most significant eigenvectors or singular values of this density matrix (or a related operator) with quantum subroutines.

One of the earliest approaches of Quantum Principal Components Analysis (QPCA) was introduced by Lloyd et al. [477]. The classical data vectors are normalised and encoded into n- qubits quantum states, which are then combined into a density matrix $\rho \in \mathbb{C}^{2^n \times 2^n}$ given by Equation (111). The QPCA algorithm aims to approximate the largest eigenvalues and eigenvectors of ρ; its spectral decomposition is:

$$\rho = \sum_{k=1}^{2^n} \lambda_k |u_k\rangle\langle u_k|, \quad \text{where} \quad \lambda_1 \geq \lambda_2 \geq \cdots \geq 0, \tag{112}$$

and $\sum_k \lambda_k = 1$. The QPCA of [477] primarily utilises the QPE on an operator encoding ρ to extract eigenvalues λ_k and filter out the dominant subspace. This procedure is summarised in Algorithm (19). This algorithm potentially had an exponential speed-up in dimension compared to the best known classical algorithms at the time [288,477]. This potential speed-up, along with other QML, has since been dequantised by quantum-inspired classical methods [478]. Furthermore, to achieve an ϵ approximation eigenvalue, QPE requires $O\left(\frac{1}{\epsilon}\right)$ calls to oracle with block-encoding or QRAM access to ρ [477]. The overhead in building the necessary oracles for QPE may undermine practical quantum speed-ups. Since implementing QPE on NISQ hardware is infeasible, research has focused on alternative near-term approaches [479–481]. Another related method is tensor PCA [48,482], studied through the spiked tensor model [483] as a higher-order analogue of the spiked covariance model from matrix PCA. A quantum algorithm [482] has been proposed with provable runtime guarantees in this model, achieving a quartic speed-up over classical methods and recovering the signal at lower signal-to-noise ratios [48]. However, the spiked tensor model is not directly linked to clear practical applications and has unfavourable runtime scaling for large systems, limiting the practical impact of these results.

Algorithm 19 Quantum Principal Components Analysis

Input: Data density matrix ρ, rank cut-off r.
Data Loading: Construct or load the density matrix ρ that encodes your data distribution.
Quantum Phase Estimation: (a) Implement an oracle U_ρ (or a block-encoding of ρ) for phase estimation. (b) For each eigenstate $|u_k\rangle$, QPE encodes the eigenvalue λ_k into the phase register.
Eigenvalue Filtering: (a) Measure the phase register to approximate λ_k. (b) Post-select or project onto those eigenstates with the largest eigenvalues.
Repeat the QPE as needed to refine precision.
Output: The top r eigenvectors $\{|u_1\rangle, \ldots, |u_r\rangle\}$ (principal components) and corresponding eigenvalues.

Other Approaches Another type of approach for QDR employs Variational Quantum Algorithm [152], which are apt for NISQ devices and circumvent QPE. One popular example is the Variational Quantum Auto-Encoder (VQAE) [484], which compresses a quantum state $|\psi_i\rangle \in \mathcal{H}_N$ into

 doi:10.20944/preprints202511.1802.v2

a smaller subspace $\mathcal{H}_d$ where $d \ll N$, and then reconstructs it with minimal fidelity loss. Training involves iteratively adjusting the circuit parameters $U(\theta)$ to minimise a reconstruction-error-based cost function.

Beyond variational methods, a general method is provided by Quantum Singular Value Transformation (QSVT) [48,138], which takes a block-encoding of a matrix and a polynomial f and produces a block-encoding of the singular value transformation $f^{(\mathrm{SV})}(A)$. By interleaving applications of the block-encoding and its adjoint with phase rotations derived from a classical sequence, QSVT enables polynomial transformations of singular values and thereby encompasses a wide range of dimensionality-reduction primitives.

Quantum dimensionality reduction holds promise for tackling large-scale data challenges. While algorithms like QPCA, Variational Quantum Autoencoders, and QSVT show asymptotic advantages, major issues, like data loading, hardware noise, and circuit complexity, make it difficult to achieve definitive quantum advantage in real-world scenarios.

2.4.3. Quantum Reinforcement Learning

Reinforcement Learning (RL) [291,485] is an area of Machine Learning that aims to train models or *agents* via the notion of actively taking actions in an *environment* that maximises the reward. It is one of the three fundamental ML paradigms, alongside supervised and unsupervised learning [486]. It is used to find the optimal behaviour or policy within a specific environment to achieve a long-term goal.

One of the main differences of RL compared to other ML paradigms is that it eliminates the need for labelled input/output pairs. Instead, the agent learns from scalar reward signals, emphasising the exploration-exploitation trade-offs [487]. This makes it suitable for problems where optimal actions are not known a priori. Additionally, there is no need for sub-optimal actions to be explicitly corrected. The focus is on finding a balance between discovering new policies within an environment (exploration) while effectively using current knowledge (exploitation) [488]. RL can include approaches such as value-based, policy gradient and model-based methods. In this section we will focus on the first two: value-based and policy gradient methods.

The main points in RL can be identified as follows:

- **Input:** the initial state[25] of the model.
- **Training:** based upon the input, the model will follow (or evolve) through a sequence of events and produce an output. Based on the output, the model will receive a reward or penalty signal.
- **Output:** an action selected from possible actions, aiming to maximise cumulative reward over time. The best solution or policy is decided based on maximising the expected return.

Basic RL is modelled as a discrete-time, finite-state Markov Decision Process (MDP)[26] [489]. Such an MDP contains a set of environment and agent states S, a set of actions, A, and the one-step dynamics of the environment [485]. The probability of transition at time t from state $s \in S$ to $s' \in S$ under action $a \in A$ [485] can be defined as

$$P_a(s'|s,a) = \Pr\{S_{t+1} = s', R_{t+1} = r|S_t = s, A_t = a\}. \tag{113}$$

Over an episode (a sequence of interactions terminating in a terminal state), the agent accumulates a sequence of rewards [485]. The return from time t is defined as the total discounted reward:

$$G_t = \sum_{k=0}^{\infty} \gamma^k, R_{t+k+1}, \tag{114}$$

[25] The 'state' refers to all the information available to the model/agent, defined by the environment.

[26] When an environment is an MDP, it means that only the current state contains all the information needed to predict the future, not the entire history of states and actions that came before [485]. This property is called the *Markov property*.

 doi:10.20944/preprints202511.1802.v2

which the agent aims to maximise, where $\gamma \in [0,1]$ is a discount factor, and R_{t+k+1} denotes the reward at time step $t+k+1$.

An RL agent interacts with its environment in discrete time steps [485]. At each time, t, it receives the current state $S_t \in S$ and a reward R_t. Following this, it chooses an action $A_t \in A$ which evolves the environment to a new state S_{t+1} and generates a new reward R_{t+1}. The reward is computed according to the function $R_a(s,s')$ and depends on the transition $R_{t+1} : (S_t, A_t) \to S_{t+1}$. The set of successive decisions creates a history [487] within the MDP model as $h_n = (S_0, A_0, S_1, A_1, \ldots, S_{n-1}, A_{n-1}, S_n)$.

A policy π is a strategy defining the agent's behaviour, mapping states to a probability distribution over actions [490]. Under a given policy π, the state-value function $V_\pi(s)$ is the expected return when starting from state s and following π thereafter [485,490,491]. Similarly, the action-value function (Q-function) $Q_\pi(s,a)$ is the expected return starting from state s, taking action a, and then following π. The goal of RL is to learn a mapping from states to actions that maximise the expected cumulative reward [485,491], or in mathematical terms, learn a policy $\pi : S \times A \to [0,1]$,

$$V_\pi(s) = \sum_{a \in \mathcal{A}} \pi(a|s) \left[R_a(s) + \gamma \sum_{s' \in \mathcal{S}} P_a(s'|s,a) V^\pi(s') \right], \tag{115}$$

where V^π is the state-value function under policy π, and $\pi(a|s)$ defines the probability of the agent selecting action a at state s according to π.

RL can be applied to applications within finance, such as pricing, hedging, portfolio or investment allocation [492–494], managing asset liability, or exploring and optimising tax revenues and their implications.

Value-Based Methods form a fundamental class of RL algorithms. These methods learn to estimate the value of states or state-action pairs, then derive optimal policies from these learned values. This approach transforms the control problem into a value estimation problem.

The core of value-based methods is Q-learning [485], which aims to learn the optimal action-value function $Q_*(s,a)$. In its tabular form, the learning update rule is:

$$Q(s,a) \leftarrow Q(s,a) + \alpha \Big[r + \gamma \max_{a'} Q(s',a') - Q(s,a) \Big], \tag{116}$$

where α is the learning rate, r is the immediate reward, γ is the discount factor, and s' is the next state.

Deep Q-Learning (DQL) extends Q-learning to high-dimensional state spaces using neural networks [496]. The network $\hat{Q}(s,a;\theta)$ approximates the optimal action-value function, according to the Bellman optimality equation [485]:

$$Q_*(s,a) = \mathbb{E}[R_{t+1} + \gamma \max_{a'} Q_*(S_{t+1}, a') | S_t = s, A_t = a], \tag{117}$$

where $Q_*(s,a)$ represents the maximum expected return achievable from state-action pair (s,a), following the optimal policy. At time t, the agent observes state $S_t \in \mathcal{S}$, selects action $A_t \in \mathcal{A}$, receives reward R_{t+1}, and transitions to new state S_{t+1}. The network parameters θ are optimised by minimising the loss:

$$L(\theta) = \mathbb{E}\Big[\big(y - \hat{Q}(s,a;\theta) \big)^2 \Big], \tag{118}$$

where $y = r + \gamma \max_{a'} \hat{Q}(s',a';\theta^-)$ and θ^- are the parameters of a target network that is periodically updated from θ to stabilise training [496].

Despite the success of these algorithms, classical value-based methods face several scalability challenges. Tabular Q-learning becomes intractable for large state spaces, requiring memory and updates proportional to $|S| \times |A|$, making it impractical for continuous or high-dimensional domains [485]. Even with function approximation, Q-learning with non-linear approximators can diverge due to the deadly triad of off-policy learning, bootstrapping, and function approximation [497]. Sample inefficiency plagues both approaches; Q-learning requires visiting each state-action pair multiple times

 doi:10.20944/preprints202511.1802.v2

for convergence, while DQL often needs millions of frames despite using experience replay [496]. Some of these limitations motivate exploring quantum computing approaches that could potentially provide a polynomial or exponential speed-up.

Recent advances in QML come in the form of hybrid quantum-classical machine learning systems [498]. These hybrid QML models use PQCs with a few qubits that can be trained to solve certain benchmarking environments, exploring whether PQCs might provide advantages for specific learning tasks.

In [499], it was proposed to represent the state set with a quantum superposition state; the eigenstate obtained by randomly observing the quantum state is the action. The probability of the action is determined by the probability amplitude, which is updated in parallel according to the rewards. The probability of the 'good' action is amplified by using iterations of Grover's algorithm (see Section 2.1.3). In addition, they showed that the approach makes a good trade-off between exploration and exploitation using the probability amplitude, and could potentially speed up learning. In [500], it was shown that the computational complexity of a projective simulation can be quadratically reduced for specific problem instances [404]. This speed-up applies to particular structured environments rather than providing a general advantage.

Quantum Deep Q-Learning (Q-DQL) replaces the neural network in DQL with a PQC. The quantum circuit takes the classical state s as input (encoded into a quantum state $|\psi(s)\rangle$ via amplitude encoding, basis encoding, or other quantum state preparation methods) and outputs expectation values corresponding to Q-values for each action. For each action a, the Q-value is obtained by measuring an appropriate observable $\hat{O}_a$ on the quantum state $|\psi(s;\theta)\rangle$ [501]:

$$Q_\theta(s,a) = \langle\psi(s;\theta)|\hat{O}_a|\psi(s;\theta)\rangle. \tag{119}$$

where $\hat{O}_a$ is the observable for action a [501].

The parameters θ are updated using gradient-based optimisation, where gradients $\nabla_\theta Q_\theta(s,a)$ can be estimated using the parameter-shift rule [498,502]. For each parameter θ_i, the circuit is evaluated at $\theta_i \pm \frac{\pi}{2}$ to obtain derivative estimates. This hybrid learning loop is analogous to training a classical neural network in DQL [501].

Below is a more detailed version of the hybrid Q-DQL process, Algorithm (20). The quantum circuit replaces the classical neural network in computing the approximate Q-values.

Algorithm 20 Quantum Deep Q-Learning

Input: A PQC Q_θ, learning rate α, discount factor γ, replay buffer $\mathcal{D}$
Initialise: Environment, circuit parameters θ, target parameters θ^-, and observe initial state s
Encode state: (a) Encode s into quantum state $|\psi(s)\rangle$ via chosen encoding scheme (b) Measure observables $\{\hat{O}_a\}$ to obtain $Q_\theta(s,a)$ for all actions a (c) Select action a using ϵ-greedy policy based on $Q_\theta(s,\cdot)$ (d) Execute a in the environment, observe reward r and next state s' (e) Store transition (s,a,r,s') in replay buffer $\mathcal{D}$
Sample a mini-batch from $\mathcal{D}$: (a) Compute target values Equation (118) (b) Update θ via gradient descent using parameter-shift rule (c) Periodically update target parameters: $\theta^- \leftarrow \theta$ (d) Set $s \leftarrow s'$
Output: Trained quantum circuit parameters θ.

Ref. [502] demonstrated Q-DQL on grid-world environments using quantum devices. They achieved comparable performance to classical methods for small problems. Ref. [495] applied PQCs to Atari games, showing that data re-uploading encoding can match classical performance with fewer parameters.Ref. [503] implemented Q-DQL on real quantum hardware, achieving learning despite hardware noise.

Although quantum methods offer potential polynomial speed-up for search within value iteration [499,504], actual performance benefits remain heavily contingent on hardware capabilities and problem structure [501,505]. The prospective advantages include enhanced function approximation

 doi:10.20944/preprints202511.1802.v2

and potential polynomial or exponential speed-ups in very specific scenarios [443,499]. However, most implementations show no advantage over classical methods on current hardware [506].

Policy Gradient Methods take a fundamentally different approach from value-based methods. Rather than learning value functions and deriving policies, these methods directly parametrise and optimise the policy $\pi(a|s;\theta)$ [507]. This direct optimisation often provides better convergence properties for continuous action spaces.

The core idea is to maximise the expected return:

$$J(\theta) = \mathbb{E}_{\tau\sim\pi_\theta}\left[\sum_{t=0}^{T}\gamma^t r_t\right], \tag{120}$$

where τ denotes a trajectory sampled from policy π_θ.

The policy gradient theorem provides the gradient [485]:

$$\nabla_\theta J(\theta) = \mathbb{E}_{\pi_\theta}\left[\sum_{t=0}^{T}\nabla_\theta \log \pi_\theta(a_t|s_t)G_t\right], \tag{121}$$

where $G_t = \sum_{k=0}^{T-t}\gamma^k r_{t+k}$ is the return from time step t.

REINFORCE The REINFORCE algorithm [508] is one of the most commonly used policy gradient algorithms. It implements Equation (121) using neural networks to parametrise the policy [408]. The main idea is to modify the policy to favour sequences of actions that led to high returns, and those actions are more likely to happen in the future [509]. The update rule is:

$$\Delta\theta = \eta\sum_t \nabla_\theta \log \pi_\theta(a_t|s_t)G_t, \tag{122}$$

where η is the learning rate [408].

Policy gradient methods suffer from high variance in gradient estimates [507]. Sample efficiency is poor, as thousands of trajectories may be needed for reliable gradient estimation [510]. The variance results in unstable policy updates, which increase convergence time [408]. Credit assignment is challenging when rewards are sparse or delayed [511]. Neural network policies face vanishing gradients in deep architectures [512].

Following the approach of replacing neural networks with PQCs demonstrated in hybrid quantum-classical RL [498], the REINFORCE algorithm can be adapted as follows.

The quantum policy is defined as:

$$\pi_\theta(a|s) = \frac{e^{\beta\langle O_a\rangle_{s,\theta}}}{\sum_{a'} e^{\beta\langle O_{a'}\rangle_{s,\theta}}}, \tag{123}$$

where $\langle O_a\rangle_{s,\theta}$ is the expectation value of observable O_a for state s and parameters θ. The inverse temperature β controls exploration [498].

The state s is encoded into the circuit through data re-uploading or amplitude encoding [513]. For discrete actions, $\lceil \log_2 |A| \rceil$ qubits represent the action space [514]. Continuous actions can be represented through expectation values parametrising distributions.

The gradient $\nabla_\theta \log \pi_\theta(a|s)$ is computed using the parameter-shift rule:

$$\frac{\partial}{\partial\theta_i}\langle O_a\rangle = \frac{1}{2}\left(\langle O_a\rangle_{\theta_i+\pi/2} - \langle O_a\rangle_{\theta_i-\pi/2}\right). \tag{124}$$

The above procedure is summarised in Algorithm (21).

 doi:10.20944/preprints202511.1802.v2

Algorithm 21 REINFORCE with Parametrised Quantum Circuit

Input: Episodes N, learning rate η, discount γ
Initialise: PQC parameters θ
For episode = 1 to N_{episodes}: (a) Initialise s_0 (b) Collect trajectory $\tau = \{(s_0, a_0, r_0), ..., (s_T, a_T, r_T)\}$:
For $t = 0$ to T: (a) Encode s_t into a quantum state via the chosen encoding (b) Measure PQC to sample $a_t \sim \pi_\theta(\cdot|s_t)$ (c) Execute a_t, observe r_t, s_{t+1}
Policy gradient update: For each (s_t, a_t, G_t) in trajectory, (a) Compute $\nabla_\theta \log \pi_\theta(a_t|s_t)$ via parameter-shift rule (b) Update: $\theta \leftarrow \theta + \eta \nabla_\theta \log \pi_\theta(a_t|s_t) G_t$
Output: Optimised PQC parameters θ.

While replacing a classical neural network with an PQC in quantum algorithms is a conceptually straightforward extension, it introduces profound practical challenges that go beyond standard hardware limitations. Such as the known difficulties of training variational quantum circuits (e.g., barren plateaus and the high cost of gradient estimation) [466,515] which, in an agent-environment feedback loop, inaccurate Q-value or policy gradient creates a vicious cycle where errors are constantly amplified. Or the fact that there is no canonical way to encode a classical state s and action a into a quantum circuit. The choice of encoding scheme (e.g., amplitude encoding, angle encoding, or more complex data re-uploading techniques) determines the model's expressive power and its ability to generalise [516].

For these reasons, while early theoretical work suggested potential quadratic speed-ups in idealised settings [517,518], the path to a Practical Quantum Advantage in Quantum Reinforcement Learning is exceptionally challenging. Progress will require not only better quantum hardware but also fundamental breakthroughs in noise-resilient and stable training techniques specifically designed for a dynamic quantum-classical feedback loop.

2.5. Quantum Cryptography

Modern classical encryption methods rely on the difficulty of solving certain mathematical problems [519]. They are time-tested and regularly updated to account for new attacks or increased computational power. However, quantum algorithms exist that can efficiently solve these problems, breaking the protocols that rely on them [520]. While quantum computers large and powerful enough to implement these algorithms do not yet exist, data is still vulnerable through so-called "harvest now, decrypt later" attacks [521], where it is scooped up *en masse* for decryption when quantum computers are more powerful in what is now known as *Q-day* [522]. In this section, we will review some of the basic concepts for classical encryption protocols, simple quantum algorithms that can break these protocols, and a brief outlook on post-quantum cryptography and quantum secure communications. For a comprehensive review of quantum cryptanalysis and resource estimation, see [48].

2.5.1. Classical Protocols

Classical encryption protocols are used for a wide range of applications, from securing communications to digitally signing files, which confirms their authenticity. They rely on several different problems in mathematics, such as prime factorisation, and discrete logarithms [519]. In this section, we review two common protocols: the Rivest-Shamir-Adleman (RSA) [523] and Diffie-Hellman Key Exchange (DHKX) protocol [524,525].

Rivest-Shamir-Adleman (RSA)

The RSA is one of the most famous and widespread families of encryption algorithms [519,526]. The RSA is a public-key encryption protocol used for both secure one-way communication and digitally signing files to prove authorship [523,526]. The basic formulation is outlined in Algorithm (22), and consists of a *private* and *public* key for encryption and decryption. The RSA protocol can be implemented in two ways:

 doi:10.20944/preprints202511.1802.v2

- Allow the sender to encrypt messages using the public key to the holder of the private key, so that only the receiver can decrypt them, enabling secure one-way communication.
- The holder of the private key can encrypt data and release it so that anyone can decrypt it with the public key, thus digitally signing the message as proof that it has not been tampered with.

The basic encryption and decryption of RSA uses modular exponentiation [519]. The encryption function for some message m using the public key (n, e) is

$$c(m) = m^e \bmod n. \tag{125}$$

While the decryption function for some ciphertext c using the private key d is

$$m(c) = c^d \bmod n. \tag{126}$$

The values of the public key and private key are computed according to the RSA Algorithm (22). The most commonly-chosen value is $e = 2^{16} + 1$, since smaller values of e make the algorithm faster but sometimes less secure [526] .

Algorithm 22 The RSA Algorithm

Randomly choose two large secret prime numbers p and q.
Compute $n = pq$, which is used as the modulus. Its length in bits is the *key length*.
Compute $\lambda(n) = \text{lcm}(p-1, q-1)$, where lcm is the least common multiple.
Choose an integer e such that $1 < e < \lambda(n)$ and e and $\lambda(n)$ are coprime.
Calculate d such that $de \equiv 1 \bmod \lambda(n)$
Output *public key* (n, e) and *private key* is d

To break the RSA encryption, one needs to factor the public key n into the two randomly chosen primes (p, q). From this, an attacker could compute the secret d and decrypt the message. The RSA is thought to be secure for large enough n because the factorisation problem is believed to be intractable for classical computation [27] [519,523]. Brute-force methods to break RSA are possible, for example, in 2010, a team of researchers factorised a 768-bit number over about 2000 core-years [528]. However, current recommended bit lengths are at least 2048, rendering the protocol theoretically secure from classical brute-force methods [526].

Diffie-Hellman Key Exchange (DHKX)

The DHKX protocol [524,525] was proposed earlier than RSA and aimed at bootstrapping a secure communications channel. In the early days of cryptography (stretching back to antiquity), establishing such a channel required the presence of a pre-existing one. For example, to send secure letters, the parties involved would need to meet in person to decide on the security protocol to use. How, then, could a secure channel be established without having a second one to decide on the security of the first? The key innovation of DHKX is to allow two parties to set up an informationally secure channel over a physically insecure one [524]. The algorithm provides both parties with a private key, which is used to encrypt messages. The parties communicate in such a way that even if an eavesdropper intercepts all communications, they will be unable to deduce the private key.

The DHKX protocol, which has since been improved manifold times [529], is presented in Algorithm (23) and also illustrated in Figure 5. Using this protocol, Alice and Bob can send each other a secure key s in the presence of an eavesdropper (Eve) with access to the public information $\{A, B, p, g\}$. This is because for Eve to obtain the shared key

$$s = A^b \bmod p = B^a \bmod p, \tag{127}$$

[27] Meaning no polynomial-time method for factoring large numbers has been found, and there is no proof that none exist [519, 527].

 doi:10.20944/preprints202511.1802.v2

they would have to solve for a in

$$g^a \bmod p = A \tag{128}$$

which is a discrete logarithm problem [530]. Just like the aforementioned prime factorisation problem, the discrete logarithm problem is intractable; there is no known efficient classical algorithm that can solve it in polynomial time [530,531]. As a result, Alice and Bob have collaboratively constructed a shared secret over an insecure channel.

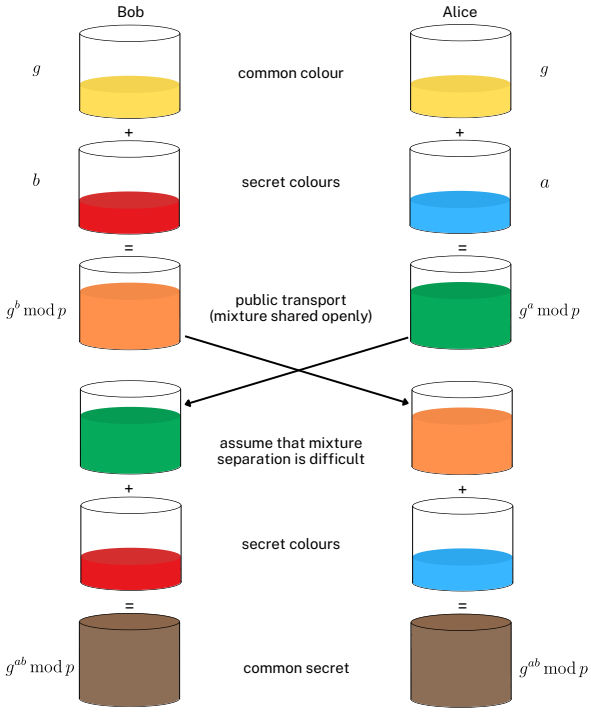

Figure 5. The DHKX protocol, illustrated with mixing paint, which represents the numbers Alice and Bob send between themselves to arrive at a shared secure key.

Algorithm 23 Diffie-Hellman Key Exchange

The two parties, Alice and Bob, publicly (insecurely) agree on two numbers, a modulus p and a base g.
Alice chooses a secret integer a, and then insecurely sends Bob $A = g^a \bmod p$.
Bob chooses a secret integer b, and then insecurely sends Alice $B = g^b \bmod p$.
Both parties compute the secret key s:

- Alice computes it via $s = B^a \bmod p$
- Bob computes it via $s = A^b \bmod p$

Now s can be used to encrypt and decrypt messages, establishing a secure channel.

2.5.2. Quantum Attacks

Several quantum algorithms exist that can efficiently solve the mathematical problems on which some classical cryptographic protocols depend. These include:

- **Shor's algorithm** (Algorithm 24), which can efficiently factorise numbers and breaks RSA (Algorithm 22) and DHKX (Algorithm 23) [51,532].
- **Grover's algorithm** (Algorithm 4), which can efficiently search unstructured lists and drastically decreases the time taken to brute-force symmetric-key encryption schemes [533,534].
- **Quantum annealing**, which supports various algorithms that could also be used to break encryption, but as yet has only been demonstrated on particularly small problems with foreknowledge of the solution [535,536].

Here, we give a brief outline of the key ideas behind Shor's factoring algorithm and quantum annealing-based approaches for breaking classical encryption.

 doi:10.20944/preprints202511.1802.v2

Shor's Algorithm

The mathematician Peter Shor first proposed the *quantum factoring algorithm* [51], now know as Shor's algorithm. It one of the well-known quantum algorithms with a concrete theoretical advantage over classical computers [10]. In the abstract, it can solve the hidden subgroup problem, of which prime factorisation and discrete logarithms are instances, in polynomial time [10,537]. It is a hybrid algorithm: mainly classical, with a quantum subroutine which provides the speed-up. Algorithm (24) outlines Shor's algorithm for factoring N (odd, composite large number).

Algorithm 24 Shor's algorithm

Pick a random number $1 < a < N$.
Calculate $K = \gcd(a, N)$, where $\gcd(\cdot)$ is the greatest common divisor.
If $K \neq 1$, then we are done.
Otherwise, use a quantum subroutine, Quantum Phase Estimation (see Section 2.1.1) to find the order r of a modulo N, i.e.: $a^r \equiv 1 (\bmod N)$
If r is odd or $a^{r/2} \equiv -1 (\bmod N)$, return to step 1.
Calculate $g = \gcd(N, a^{r/2} - 1)$ and $g = \gcd(N, a^{r/2} + 1)$.
If $g \neq 1$, we are done. Otherwise, return to step 1.

The various conditional branches are due to the implied properties of the calculated numbers. For example, if the calculated r were odd, then $a^{r/2}$ would not be an integer, and so the algorithm would not work. For a more in-depth explanation of the algorithm, see [44,51,532]. The quantum subroutine, QPE, provides an exponential speed-up in solving the following problem [44,51]: given coprime integers a, N, find the order r of a mod N, which is the smallest positive integer such that $a^r \equiv 1 \bmod N$. However, as of writing, Shor's algorithm has only been implemented and used to factor very small primes [538–540] due to the large quantum resource requirements of QPE (see Section 2.1.1). Early fault-tolerant estimates for factoring a 2048-bit number required about 20 million physical qubits running over eight hours, depending on the chosen Quantum Error Correction code [541]. This estimate has recently been improved to less than 1 million physical qubits running over a week [542]. This large physical qubit requirement and error correction quality assumptions are significant beyond current state-of-the-art, hence the projected timelines are very uncertain, ranging from around 2030 [543] to 2039 and beyond [544]. Thus, while it is unlikely that Shor's algorithm will be used relatively soon to break modern encryption (based on major hardware providers' technology roadmaps), there is ongoing research and infrastructure preparations for alternative encryption that is safe from quantum attacks (see Section 2.5.3).

Quantum Annealing

Due to some of the limitations of Shor's algorithm, particularly the large quantum resource requirements for QPE, alternative quantum-based approaches to integer factorisation have been developed [48]. Quantum Annealing (QAnn) (see Section 2.1.7) has emerged as a promising alternative [545], with a recent demonstration of factorisation of an 80-bit number, the largest yet [546]. While this is still orders of magnitude away from any practical application, this result demonstrates some of the key advantages QAnn holds over traditional gate-based quantum algorithms, especially in the NISQ era. While Shor's algorithm requires thousands of logical qubits, translating to millions of physical qubits (as described in Section 2.5.2.1), QAnn requires far fewer qubits, scaling at most as $O(\log^2(N))$ with the integer N [545]. However, QAnn requires statistical sampling and has an unknown time complexity, while Shor offers time complexity guarantees in finding the solution [10,545,546].

In this section, we will outline one of the simplest applications of QAnn for factorisation: By reformulating the problem as an optimisation problem in QUBO form as shown in [547]. In this approach, the problem of factorising $N = pq$ into the primes p, q can be phrased as the problem of minimising the cost function

$$C(p, q) = (N - pq)^2, \tag{129}$$

 doi:10.20944/preprints202511.1802.v2

where p, q are represented in binary. After adding auxiliary variables to convert the quartic into a quadratic cost function, the authors in [547] were able to factorise $N = 4137131$ into $p = 2029$ and $q = 2039$ using 93 variables. Alternative approaches that have been proposed range from implementing full-adder circuits [548] to integrating annealing into a hybrid workflow [546]. The latter approach was used to achieve the current record-breaking result above of factorising an 80-bit integer.

Significant challenges remain to be solved, such as algorithmic development for efficient implementation and connectivity of annealing hardware, before QAnn-based approaches become a viable method of solving the factorisation problem [546,548]. Nevertheless, the advantages of annealing-based approaches mean it is possible that it might be the first to factor 1024 or 2048-bit RSA. Hence, alongside Shor's algorithm, organisations should also monitor progress on algorithmic and hardware advances in Quantum Annealing.

2.5.3. Post-Quantum Cryptography

In response to the growing threat of a future quantum computer that renders modern encryption insecure, there has been a huge amount of research and development into so-called Post-Quantum Cryptography (Post-QC), which refers to classical encryption protocols that aim to be secure against both classical and quantum attacks [549–552]. This has culminated in the 2024 announcement by the US National Institute of Standards and Technology (NIST) of a set of three standard Post-QC protocols recommended for use in key establishment and digital signing [553–555]. Even before this, however, post-quantum protocols were beginning to be adopted by large technology companies, notably Google [556] and Apple [557]. As a result, there is not only a large body of literature and code available for easy implementation, but a number of organisations providing Post-QC as a service, minimising the need for customised (and therefore potentially unsafe) implementations. The details of these protocols are outside the scope of this paper, but we present below a brief list of the key families as a guide to further perusal:

- Lattice-based [558] which employs difficult lattice problems such as the Shortest Vector Problem.
- Code-based [559], which uses error-correcting codes to encrypt data.
- Multivariate [560], which is based on the hard problem of solving multivariate polynomials over finite fields.
- Hash-based [561,562], which utilises the hard problem of reverse-engineering hash functions that map arbitrary inputs to fixed-length outputs.

These algorithms are generally complex, and it is not recommended that each organisation implement their own version themselves, but rather partner with a trusted provider. The UK's National Cyber Security Centre has published a migration roadmap for Post-QC [563] which has estimated completion between 2031 and 2035. These timelines are in line with estimates of Q-day happening between 2030 and 2039 [522,543,544]. Financial organisations should therefore proactively work on the migration to Post-QC encryption.

2.5.4. Quantum Communications

An important issue with cryptography protocols is that there is every chance that new algorithms, either quantum or classical, will be created that can break them. For example, the Supersingular Isogeny Key Encapsulation (SIKE) algorithm [564,565] was considered secure for more than a decade[28] before it was broken in 2022 by a team of researchers using a legacy Intel chip [567]. Of course, the same potential for new algorithms also exists for classical cryptographic protocols, but the novelty of quantum protocols means they have had less time to be tested.

This uncertainty in encryption implies that existing communication networks can always be intercepted, and encrypted data stored in anticipation of novel decryption attacks in the future. Thus, it is desirable to have an alternate way of encrypting data by generating and distributing a secret key

[28] SIKE was a finalist in NIST's competition for post-quantum protocols [566].

 doi:10.20944/preprints202511.1802.v2

in a way that is inherently protected by the laws of physics. This is what is achieved by the Quantum Key Distribution (QKD) which was first proposed by Charles Bennett and Gilles Brassard in 1984 [568], forming what is now known as the BB84 protocol [569]. The security of the protocol can be formally established under the assumption of an idealized, error-free quantum communication channel. The theoretical proof relies on two foundational premises: (1) the quantum-mechanical principle that any attempt to extract information from non-orthogonal states necessarily perturbs the signal[29], consistent with the no-cloning theorem [570]; and (2) the availability of an authenticated, publicly accessible classical communication channel [569].

The key idea of the BB84-QKD is to send a secure key encoded into quantum states in a way that it would be impossible for an eavesdropper to copy it without being detected. The information is exchanged as outlined in Algorithm (25), is encoded in polarised states of photons, and the measurement basis is given by:

$$M+ = \begin{cases} |0\rangle & \text{horizontal} \rightarrow \\ |1\rangle & \text{vertical} \uparrow, \end{cases} \tag{130}$$

for the rectilinear basis and

$$M\times = \begin{cases} |+\rangle = \frac{|0\rangle+|1\rangle}{\sqrt{2}} & \text{north-east} \nearrow \\ |-\rangle = \frac{|0\rangle+|1\rangle}{\sqrt{2}} & \text{south-east} \searrow, \end{cases} \tag{131}$$

diagonal basis. Alice chooses a random binary key, encodes it into the polarisation of photons prepared in a randomly chosen basis, and sends it to Bob via a public quantum communication channel (assumed to be error-free). Bob measures these photons in his own randomly chosen set of measurement bases to generate a set of bit strings. Alice and Bob then communicate via a classical (potentially insecure) channel to compare their chosen set of preparation and measurement basis. They sift out the results of the cases where the preparation and measurement basis differ and keep the rest. In principle, assuming an error-free quantum channel and no eavesdropper (Eve), the remaining set of bit strings would be almost identical (possibly with some very small errors). However, if Eve has intercepted their message by measuring the photons in a random basis and then sending 'spoof' photons prepared in that basis to Bob, there would be a significant Quantum Bit Error Rate (QBER) rate given by [568]

$$\text{QBER} = \frac{\text{Number of mismatched bits}}{\text{Total compared bits}}. \tag{132}$$

There is a threshold for statistically acceptable QBER, for BB84 is about 11%, thus anything above it would mean Eve has listened to the message. For Eve to be undetected, she would need to have a device that makes exact copies of the photon states without measurements, which is forbidden by the no-cloning theorem [570]. If the QBER is below the BB84 threshold (meaning no eavesdropper in the quantum channel), then Alice and Bob can proceed to use classical information reconciliation and privacy amplification techniques to construct a shared private key [568,571].

The BB84 protocol is one of the simplest QKD, and more sophisticated methods exist utilising quantum superposition and entanglement to increase fidelity and decrease the number of photons which need to be sent [569]. In particular, the 1991 protocol by Ekert [572] (known as E91) uses entangled Bell states to create a more secure QKD. Implementations of such QKD already exist and are available commercially; for a review of the progress and state-of-the-art of the field see Refs. [573–575].The relative lack of widespread quantum network channels means their use is limited to local communications and research. However, an example of a fully-realised implementation is the quantum network in the Chinese city of Hefei, which allows for secure QKD over 4,600 kilometres [576].

[29] In other words, there is no physical process that can clone a quantum state; see Section (3.3.1) for more details.

 doi:10.20944/preprints202511.1802.v2

It is built with a combination of fibre-optics and ground-to-satellite links and is currently the largest of its kind in the world [576].

Algorithm 25 BB84 - Quantum Key Distribution

Goal: Alice to send to Bob a key to encrypt data via a public channel that could be intercepted by an eavesdropper, Eve.
Preparation: Alice generates a random set of $\{K_A, M_A\}$ of a key of binary n bits string $K_A \in \{0,1\}^n$ and measurement basis $M_A \in \{M+, M\times\}^n$. The random key K_A is encoded into n photon states polarised as either $\{|\uparrow\rangle, |\rightarrow\rangle\}$ if $M_A = M+$ or $\{|\nearrow\rangle, |\searrow\rangle\}$ if $M_A = M\times$.
Transmission: Alice sends to Bob this sequence of n photons via a public channel.
Measurement: Bob generates a random sequence of measurement basis $M_B \in \{+, \times\}^n$ and measures each photon to obtain a key $K_B \in \{0,1\}^n$.
Sifting: Alice and Bob share via a public channel their randomly chosen measurement basis M_A and M_B, respectively. They sift out the results of bits that were measured on the wrong basis as they were prepared and keep the matching k basis set $M_{AB} = M_A \cap M_B$ where $k < n$.
Error checking: Alice randomly chooses $k/2$ bit strings of the set M_{AB} and shares the values with Bob who does the same via a public channel. They use these values to compute an estimate of the QBER given by Equation (132). If the QBER is above some tolerant threshold ($\sim 11\%$ for BB84), they both abort or try again afresh another time because it is highly likely that Eve is listening to their communication.
Key Distillation: If QBER is below the threshold, they then use classical post-processing (error correction and privacy amplification) [569] to generate the final shared key.
Output: Shared private key between Alice and Bob K_{AB} that can be used to encrypt their messages.

Another related set of quantum communication protocols is *quantum money* [26,577] (see Section 3.3.1). A recent experimental implementation reported a quantified time advantage over optimal classical cross-checking protocols for secure financial transactions [578]. This advantageous verification speed-up of *quantum money* and security of QKD could potentially fuel rapid industrial adoption for applications requiring high security, privacy, and minimal transaction times, like financial trading and network control. However, the pace of widespread adoption of QKD schemes will also be dependent on the rate at which quantum-capable network infrastructure is built, which involves government regulations.

2.5.5. Quantum Random Number Generation

Random Number Generators (RNGs) are vital in not only many cryptographic protocols, but also in wider areas of fintech, including blockchain technologies and smart contracts [579–581]. True RNG can be achieved via random physical processes, such as inter-event times in atomic decay, voltmeter readings, and semiconductor thermal noise [582]. However, this physical approach has two sets of problems:

- **Provable Distribution**: The generated sequence must approximate independent, uniformly distributed variables. In bit-stream implementations, this entails equal probability for 0 and 1, alongside bitwise independence. Since such statistical properties cannot typically be proven, validation relies on empirical statistical testing to assess conformity with the desired distribution and independence criteria [582].
- **Impractical**: Connecting computational algorithms to physical RNGs is generally more costly and slower (less rapid generation of samples) than *pseudo*-RNGs [583].

Pseudo-RNG are chaotic (but deterministic) functions which generate sequences of samples that are independent and identically distributed (i.i.d.), and uniformly distributed over the interval (0, 1)[584]. They take a seed (sometimes a random input such as movements of a computer mouse) and generate a sequence of samples that are difficult to distinguish from true random numbers. The difficulty in predicting the pattern of pseudo-RNGs depends on whether the seed is known and properties of the pseudo-random functions [584]. In general, if the seed is not known, then many pseudo-random functions produce samples that are almost impossible to predict their pattern. Hence, some RNGs

 doi:10.20944/preprints202511.1802.v2

uses a physical process for a true random seed and proceeds to generate pseudo-random numbers that are 'unpredictable' [582]. More formally, a cryptographically secure pseudo-RNG is believed to be unpredictable if it passes the next-bit test[30] introduced by Blum and Micali [585]. However, just like other cryptography protocols, the unpredictability of pseudo-RNG depends on some hardness assumption which has not been proven [582].

There is a further serious issue when there is a lack of trust in the output of a RNG; it is impossible to look at a sequence of bits and be certain as to whether it is random or not [582,586]. In a zero-trust environment (such as communicating over the internet), there must be a way to certify randomness to all parties involved. Quantum technologies offer alternative sources of randomness which are certified by the laws of quantum physics [587,588]. In particular, there are proposed protocols for Quantum Random Number Generator (QRNG) certified by Bell's inequality violation [587,589]. However, as pointed out in [590], these protocols have a limitation in that they cannot circumvent the need to trust a third party to faithfully implement all their requirements. A recent alternative approach proposed by Aaronson and Hung [588] re-purposes the random circuit sampling experiments [14] to construct a certified randomness protocol employing the Linear Cross-Entropy Benchmark threshold. Generating random numbers from a random circuit sampling distribution with entropy above this entropy threshold is computationally hard classically, but is possible using quantum computing. This is what guarantees that the output is truly generated from a QPU, not a pseudo-classical simulator, provided you can efficiently verify these distributions. As noted in [588], the drawback of this approach is that it requires a classical computer to perform the verification at a cost that scales exponentially with the number of qubits used. This limits its practical implementations to about $n \sim 60$ qubits [588]. A recent experiment [590] based on this entropy verification has certified over 70 000 bits using 56 qubits of a trapped-ion QPU. This is the largest experiment of its kind, and more research in quantum verification is needed to lower the computational costs [591–593]. Furthermore, the limited adversarial model and protocol assumptions make them not yet ready for industrial deployment [590], but are a promising stepping stone towards more secure future communications and cryptography protocols.

3. Use Cases in Finance and Economics

3.1. Banking and Investment

The financial services sector has undergone a profound transformation over the last two decades [594], driven by technological advancements, the proliferation of data, and the increasing demands for efficiency and scalability [595]. Central to this evolution is the integration of computational tools, which include Machine Learning (ML) algorithms, Artificial Intelligence (AI) models for big data, and blockchain technologies [596,597] that are reshaping the landscape of banking and asset management [595,598]. These tools enable financial institutions to handle vast amounts of data, make more informed decisions, and provide personalised services at scale. Even though these classical methods have delivered significant positive results in the sector, they still face computational bottlenecks for certain hard-problems which quantum computing can potentially overcome [9,10,30]. According to a 2023 study by McKinsey [20], quantum computing use cases in banking and asset management are projected to generate a value of about 302 billion[31] USD and 80 billion USD, respectively, by the year 2035. These two categories represent a combined 61% of the total projected value of 622 billion USD by year 2035 [20]. In this section, we will give a technical overview of some of the use cases that can benefit from quantum computing in finance that approximately fall under the two categories of banking and investment.

[30] Given the first k bits of its output, no polynomial-time algorithm can predict the next bit with probability significantly better than 0.5 [585].

[31] The total figure is composed of 190 billion USD in corporate, 90 billion USD in retail, 20 billion USD in investment banking, and 2 billion USD in operations.

 doi:10.20944/preprints202511.1802.v2

3.1.1. Asset Pricing

In finance, the accurate pricing of traded assets is a fundamental problem with significant implications for risk management, investment strategies, and regulatory compliance [599]. Asset pricing involves determining the value of different types of financial instruments, such as stocks, bonds, and derivatives. According to Cochrane [181], asset pricing theory seeks to explain why assets that offer uncertain future payments have the prices they do, and why some offer higher returns than others. The theory can be used both to describe how prices work in real-world markets (positively) and to suggest what prices should be if markets were perfectly rational (normatively) [181]. When actual prices don't match the theory's predictions, it could mean the model needs improvement, or that the market is mispricing the asset, creating opportunities for smart investors [600]. The theory is also useful for pricing assets whose values are not directly observable, such as new projects, private investments, or complex financial products, helping guide both private and public financial decisions [181].

The growing complexity of modern financial products, including exotic options, structured derivatives, and interest rate instruments, has necessitated the use of advanced computational techniques to obtain reliable asset pricing [601]. The non-linearity, path-dependence, and high dimensionality inherent in these instruments make asset pricing a challenging task for classical computing. A growing number of practitioners are exploring the use of quantum computing to alleviate some of the computational bottlenecks of traditional classical methods [12,602].

In this section, we present the mathematical formulation of asset pricing models and describe some computational methods that include quantum algorithms. Many of the quantum algorithms employed for these use cases are described in more detail in Part I of this review and cited papers, hence to make the connection at the problem formulation level. In a similar spirit, this review will not be a comprehensive exegesis of finance models but will present pertinent information to make the case for the potential benefit of using quantum computing.

Pricing Models

There are different approaches to developing robust pricing models, which we will not discuss here. For this review, we will follow the approach of Cochrane [181] and formulate the asset pricing problem in terms of stochastic discount factors of the expected asset payoff. This is summarised by the formula

$$p_t = \mathbb{E}(m_{t+1} \cdot x_{t+1}), \tag{133}$$

where p_t and x_{t+1} is the asset's price and payoff at times t and $t+1$, respectively. The stochastic discount factors at time $t+1$ are given by

$$m_{t+1} = f(\text{data}, \text{parameters}) \tag{134}$$

where $f(\cdot)$ is an economic model of the market. These economic models are generally based on two main pricing principles [181]: (i) general equilibrium asset pricing and (ii) rational asset pricing. The former focuses on asset pricing through supply and demand, whereas the latter principle assigns derivative prices such that they are arbitrage-free with respect to more fundamental securities prices. Irrespective of which economic model you choose for $f(\cdot)$, the task of selecting the type of empirical representation for Equation (133) is separate and can be reformulated in terms of returns, price-dividend ratios, expected return-beta relationships, moment conditions, and the distinctions between continuous- and discrete-time frameworks. Essentially, the main benefit of this approach is that it provides a single theoretical framework that covers a variety of cases. Table 4 outlines examples of how Equation (133) translates to different pricing problems.

 doi:10.20944/preprints202511.1802.v2

Table 4. Examples of how the general asset pricing problem of Equation (133) translates to other pricing problems. Here, d_{t+1} is the stock dividend, and other variables are explicitly defined in [181].

Asset	Price p_t	Payoff x_{t+1}
Stock	p_t	$p_{t+1} + d_{t+1}$
Return	1	R_{t+1}
Price-dividend ratio	$\frac{p_t}{d_t}$	$\left(\frac{p_{t+1}}{d_{t+1}} + 1\right)\frac{d_{t+1}}{d_t}$
Excess return	0	$R^e_{t+1} = R^a_{t+1} - R^b_{t+1}$
Managed portfolio	z_t	$z_t R_{t+1}$
Moment condition	$\mathbb{E}(p_t z_t)$	$x_{t+1} z_t$
One-period bond	p_t	1
Risk-free rate	1	R^f
Option	C	$\max(S_T - K, 0)$

The ability to switch between different representations helps in understanding empirical results, as many seemingly distinct approaches are deeply connected. Using discount factors often simplifies analysis compared to a portfolio-based approach [181]. For instance, it's easier to verify the existence of a positive discount factor than to compare all possible portfolios. Discount factors also shift the perspective from mean-variance geometry to state-space geometry, which Cochrane [181] highlights as a key intuition behind many traditional results. Because of these advantages, the discount factor framework and state-space view are widely used in academic research and advanced financial practice.

Computational Methods

The approach of Cochrane [181] decomposes the asset pricing problem into three parts:

1. Choosing a model for simulating the payoff x_{t+1}, which is a function of underlying stochastic variables. For example, the payoff for option pricing depends on the spot value S_t of the underlying asset, which can be modelled using the Black-Scholes-Merton (BSM) [84,85] or its variants.
2. Choosing a model of simulating the discount factors m_{t+1}, which are functions of market data and model parameters which incorporates the risks associated with the asset. For example, option pricing has discount factors depending on the filtration $\mathcal{F}_t$ which represents the market information assumed to be known until time t (see Section 3.1.2.1).
3. Computing the expectation $\mathbb{E}(\cdot)_{t+1}$ which is conditional on information at time t.

This abstraction of the problem makes it easy to see where the root of the computational bottlenecks associated with asset pricing lies, and where a quantum algorithm offers an advantage. In the case where part (2) is 'easy', that is, a standard model with parameters fitted on historic data accurately describes the discount factors, then part (3) can be tackled by common computational methods such as Monte Carlo Integration to simulate many paths for the stochastic variables (like consumption, returns, or prices) using random draws and computing sample averages [181,203,603]. The benefit is that MCI is generally flexible, easy to implement, and can handle high-dimensional problems since its accuracy is independent of the problem dimension [182]. The main downside is that it has a slow convergence and needs a large number of samples for accurate simulations [5]. This challenge can be alleviated by employing Quantum Monte Carlo Integration which, as discussed in Section (2.2.1), can potentially have a quadratic speed-up over MCI methods [5].

In the case where part (2) is 'hard', that is, standard models do not accurately capture the discount factors, then ML techniques can be used to learn from historic market data. Examples include the use of Recurrent Neural Networks (RNN) to run time series predictions [604,605]. However, RNNs are computationally intensive, especially in complex scenarios, QML techniques are being considered as potentially more efficient alternatives [9,30,35,41]. A natural approach would be to extend to quantum Recurrent Neural Networks (RNN) as shown in [606] where the learning is performed by parametrised quantum circuits. This approach has demonstrated comparable accuracy in preliminary tests with

 doi:10.20944/preprints202511.1802.v2

small datasets; however, its effectiveness at scale remains to be fully validated. Other classical ML techniques for asset pricing have shown great potential to improve the accuracy of learning from historic market data. For example, the authors in [604] studied a collection of ML methods, including linear regression, generalised linear models, principal component regression, and neural networks. An equivalent study of QML for quantitative finance problems, which includes asset pricing, was done by [41]. A notable example is Quantum Generative Adversarial Networks (QGAN) which can be trained to learn the conditional probability distributions of the asset's value from historical market data [196]. A proof-of-concept implementation of QGAN for the option pricing problem was done by [196,607] using log-normal probability distributions. However, training QGANs can be time-consuming for industrial applications, hence some quantum-inspired methods, such as tensor networks, can be a more efficient alternative [197]. The research is still ongoing, and the solution is likely to be a hybrid quantum-classical approach for the case of asset pricing.

Quantum Assets

Thus far, we have considered classical assets (described by real values) traded in a classical market (described by real-valued functions). A quantum solution to the asset pricing problem is the real-valued output of a quantum algorithm that embeds the classical variables into quantum states and associated probability amplitudes. An interesting recent theoretical work by Bao and Rebentrost [608] has shown that it is possible to define assets that are quantum in nature, referred to as *quantum assets*, as shown in Figure 6(**a**). These are described by quantum states/density operators in a Hilbert space. Furthermore, asset pricing theorems for quantum assets can be derived analogously to the classical asset pricing theorem [608].

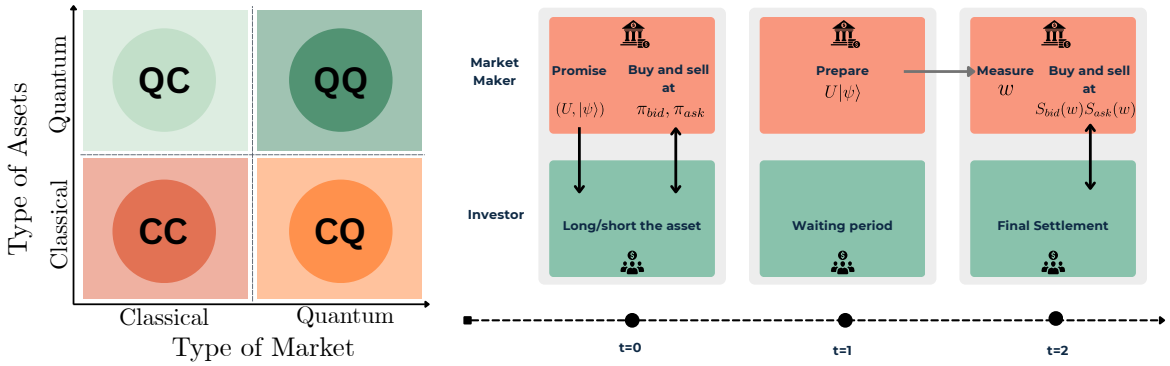

(**a**) A generalisation of types of assets and markets. (**b**) A toy model of how quantum assets can be traded in a *quantum market* discussed in the text.

Figure 6. The results in this section are based on QQ in (a), and the trading toy model (b) for quantum assets. Both figures are adapted based on [608].

Mathematical Formulation Assume the market is *quantised*, meaning stochastic events are described by probabilities associated with quantum states in the Hilbert space. A quantum asset class, which sits under QQ in Figure 6(**a**), can be defined as follows [608]:

Definition 3 (Quantum Asset). *Given a Hilbert space $\mathcal{H}$, with $dim(\mathcal{H}) = N$, a quantum asset is a positive semidefinite Hermitian matrix $\mathcal{A} \in \mathbb{C}^{N\times N}$, such that for all $|\psi_{t+1}\rangle \in \mathcal{H}$, the future payoff is given by*

$$x_{t+1} = \langle \psi_{t+1}|\mathcal{A}|\psi_{t+1}\rangle \geq 0 \tag{135}$$

The quantum asset can be bought/sold at a price $p_t = \pi > 0$, computed using Equation (133) in a quantum market. It follows that a given a classical asset $\mathcal{A}_{\text{cl}} \in \mathbb{R}^N$, its quantum asset embedding is the diagonal matrix $\mathcal{A} = \text{diag}(\mathcal{A}_{\text{cl}}) \in \mathbb{R}^{N\times N}$. A quantum asset assumes a diagonal form in its

 doi:10.20944/preprints202511.1802.v2

eigenbasis, a structure that naturally lends itself to financial interpretation [608]. Within this framework, each eigenstate may be regarded as a fundamental event specific to the quantum asset, distinct from the elementary events defined in a classical probability finite sample space Ω. The associated eigenvalues represent the respective outcomes or payoffs realised when these corresponding events occur. Figure 6(**b**) illustrates a reasonable trading scenario in a quantum market with a market maker (top panels) with access to a quantum computer interacting with an investor (bottom panels). The toy model, shown in Figure 6(**b**), has the following interactions [608]:

t=0 : The market marker announces the following:

1. A n-qubit state $|\psi\rangle = \sum_{i=0}^{2^n-1} \alpha_i |w_i\rangle$ and unitary $U \in \mathbb{C}^{N\times N}$ where $N = 2^n$.
2. The initial bid and ask prices denoted by π_{bid} and π_{ask}, respectively.
3. Two function $\mathcal{S}_{\text{bid}}(w)$ and $\mathcal{S}_{\text{ask}}(w)$ that will determine the bid and ask prices at $t = 2$, where $w \in \{0,1\}^n \subset \Omega$ and $\mathcal{S}_{\text{bid}}, \mathcal{S}_{\text{ask}} : \Omega \mapsto \mathbb{R}_+$.

t=1 : The market marker uses a quantum computer to prepare the state $|\psi\rangle$ and then evolves it by the unitary U to get the final unobserved quantum state $U|\psi\rangle$.

t=2 : The market marker measures the final quantum state in the computational basis of $|\psi\rangle$ to get measurement outcome w occurring with probability $|\langle w|U|\psi\rangle|^2$.

The asset pricing problem involves computing expectations of the form of Equation (133). An equivalent expectation for the quantum asset $\mathcal{A}$ at time $t = 1$ viewed at $t = 0$ is given by

$$\mathbb{E}_\rho[\mathcal{A}] = \text{Tr}\{\rho\mathcal{A}\}, \tag{136}$$

where the final quantum state is described by the density operator $\rho = U|\psi\rangle\langle\psi|U^\dagger$. Note that in this formulation ρ becomes associated with the probability measure that Bao and Rebentrost [608] use to propose the *fundamental theorem of quantum asset pricing*, which is analogous to the first fundamental theorem of asset pricing based on arbitrage theory [181]. They also describe a path to formulate *quantum derivative* assets and equivalent pricing scheme [608].

Similar ideas of a quantum market have also been considered in [609], and stochastic finance based on quantum mechanics has been explored in [610]. As quantum technologies advance, we may see practical implementation and adoption of such defined quantum financial instruments[32]. However, the research in this field is still in its infancy; we can only speculate that if quantum assets are practically demonstrated and adopted, they will most likely be a relatively small but significant part of the global financial economy, similar to cryptocurrencies.

3.1.2. Derivative Pricing

Derivatives are financial instruments whose value is derived from the performance of underlying assets, indexes, interest rates, or other financial variables [204]. Common examples of underlying assets include stocks, bonds, currencies, and commodities. Derivatives allow investors to hedge risks, speculate on price movements, or access assets and markets that might otherwise be difficult or costly to trade. Common types of derivatives include the following [204]:

1. Options Contracts: These contracts give the buyer the right (but not the obligation) to buy (call option) or sell (put option) an asset at a predetermined price before or at expiration.
2. Credit Derivatives: These are used to transfer credit risk. A common type is the Credit Default Swap (CDS), where the buyer pays a premium for protection against a credit event like a default.
3. Swaps: Contracts in which two parties agree to exchange streams of cash flows over a set period. For example, an interest rate swap involves exchanging fixed-rate interest payments for floating-rate ones.
4. Futures Contracts: Agreements to buy or sell an asset at a predetermined price at a specific time in the future.

[32] This may include quantum money described in Section (3.3.1).

 doi:10.20944/preprints202511.1802.v2

5. Forward Contracts: Similar to futures but traded over-the-counter instead of on exchanges, providing more flexibility in terms and conditions.

Efficient pricing of derivatives represents a significant opportunity for improvement in financial operations. The projected size of the global derivatives market by 2033 is $64.24 billion [611], which coincides with predicted time-lines for Universal Fault-Tolerant quantum computing [20]. This is a growth from $30.57 billion in 2024 at an CAGR of 8.6% during the forecast period from 2025 to 2033 [611]. According to Business Research Insights [611], the projected growth of the derivatives market is attributed to various factors which includes: (1) growing demand for price volatility, (2) increasing changes in demand and supply which influence product demand, (3) rapid industrialisation of many underdeveloped countries, and (4) rising technological developments in financial sectors of which quantum computing may play a significant role.

In this section, we will review some of the use cases of quantum computing for derivative pricing. In particular, we will focus on the computational methods for pricing options, colleteralised debt obligations, and swap netting.

Option Pricing

Options are financial derivatives that provide the holder with the right, but not the obligation, to buy or sell an underlying asset at a predetermined price (the strike price) before or at the expiration date [601]. Option pricing is the process of determining the fair value of an option [612–614], which depends on various factors such as the underlying asset's price, volatility, time to expiration, and risk-free interest rate. The pricing of options is critical for investors and traders as it helps make informed decisions about hedging, speculation, and portfolio management [204].

According to the Futures Industry Association (FIA)[33] worldwide volume of Exchange-Traded Derivatives (ETDs)[34] has been on the order of 10 billion contracts in recent years. Figure 7 lists some of the most traded ETDs and their relative percentage volumes in 2025. Note that these data do not include the Moscow Exchange and its volume and open interest history [615]. This data is presented to underscore the potential opportunity space for quantum computing for efficient pricing of options contracts.

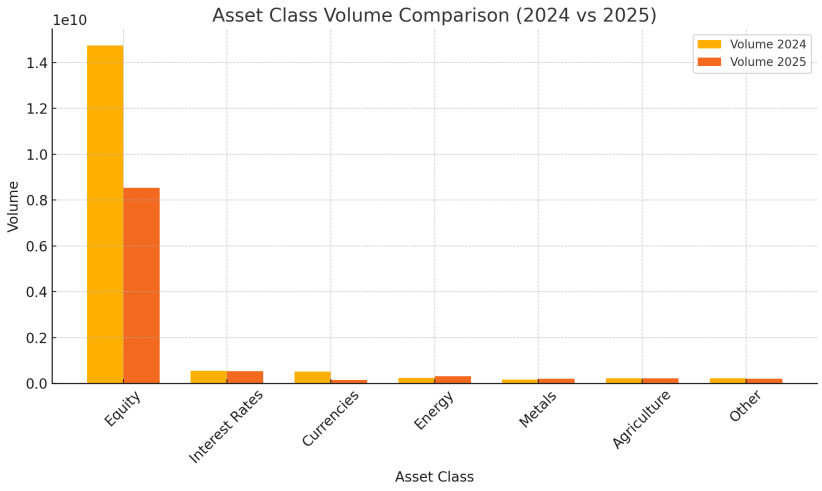

Figure 7. FIA ETD data of asset class trading volume of futures and options in January 2024 and 2025 [615]. Although there was a decline of nearly 40% from 2024 to 2025, the total volume is still in the order of billions of trades per year, of which more than 80% are based on underlying equity assets.

[33] FIA is a prominent global trade organisation that represents the interests of the futures, options, and derivatives markets, including futures commission merchants and principal traders.

[34] An ETD is a financial contract that is listed and traded on a regulated exchange. In other words, these are derivatives that are traded in a regulated environment.

 doi:10.20944/preprints202511.1802.v2

Options represent a versatile class of financial instruments, structured as contracts between a buyer and a seller. The buyer compensates the seller with a premium in exchange for specific contractual rights [204]. *Call options* confer upon the holder the right, but not the obligation, to purchase an underlying asset at a predetermined price within a specified period. Conversely, *put options* grant the holder the right to sell the asset under similar conditions. Each call option transaction involves a bullish buyer and a bearish seller, whereas put options feature a bearish buyer and a bullish seller [616]. Market participants engage in options trading for various strategic purposes. Speculative trading enables investors to leverage their positions in an asset at a lower capital outlay compared to direct ownership of the underlying security. Additionally, options serve as a risk management tool, allowing investors to hedge against portfolio volatility [204]. In some instances, option holders can generate income by purchasing call options or assuming the role of an options writer [617]. Furthermore, options provide a direct mechanism for investing in commodities such as oil.

For options traders, three critical metrics serve as key indicators for making informed investment decisions: fair value, daily trading volume, and open interest [617]. It is with the efficient computing of the fair value of an option that quantum computing can potentially make a difference. In this subsection, we will describe the mathematical formulation of the option pricing problem by following the workflow illustration in Figure 8. First, we describe some different types of options with their payoff. Second, we consider some traditional models for underlying assets such as the BSM and Heston model. Lastly, we outline some quantum algorithms for option pricing, which include QMCI and quantum solvers for Stochastic Differential Equation (SDE).

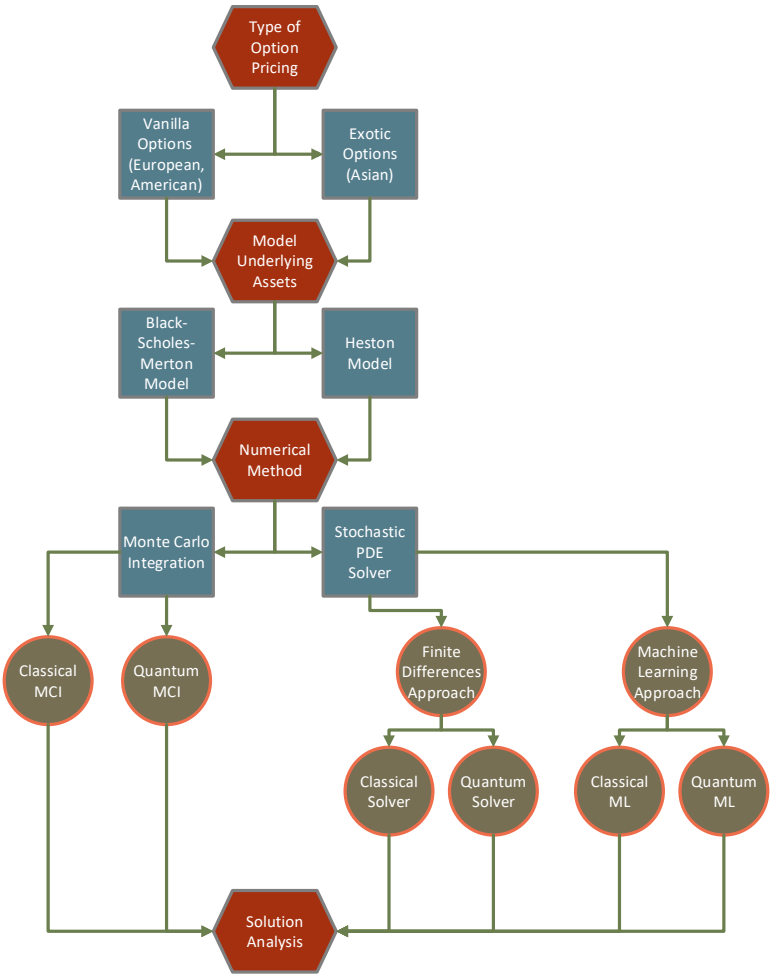

Figure 8. An illustrative workflow of option pricing which involves: (1) choosing the type of option, (2) selecting an appropriate model of the underlying assets, and (3) choosing a numerical method for the computation. Quantum algorithms have the potential to improve the efficiency of classical numerical methods.

 doi:10.20944/preprints202511.1802.v2

Types of Options Options, also known as contingent claims or non-linear derivatives, are financial instruments whose payoffs exhibit a non-linear relationship with the value of the underlying asset [181,204]. The options pricing problem generally falls into two classes: Vanilla Asset Pricing and Exotic Asset Pricing. The option value corresponds to the premium that the buyer must pay to acquire the rights conferred by the option contract. In derivative pricing, mathematical models establish the relationship between the underlying asset and the fair value of the option, which makes both the option seller and buyer break even [181,204].

Definition 4 (Vanilla Asset Pricing)**.** *Let v_t and S_t denote the value of the option and the underlying asset at time t, respectively. At the expiring date T of the option contract, or before under certain circumstances, the option holder receives a payment, referred to as the payoff, given by*

$$v_t = h(T, S_T) \tag{137}$$

where h is a non-linear function of T and value of underlying asset S_T at expiration.

European Option on an underlying asset grants the holder the right, but not the obligation, to purchase or sell the asset at a predetermined future date, referred to as the expiry date (T), and at a specified price, commonly known as the strike price (K) [181,204]. The payoff for the option is given by [181]:

$$c_T = \max(S_T - K, 0) \quad \text{and} \quad p_T = \max(K - S_T, 0), \tag{138}$$

Where c_T and p_T are *call* and *put* values at maturity. For the call option, we say that [204]:

$$c_T \text{ is } \begin{cases} \textit{in the money}, & \text{if} \quad S_T > K \\ \textit{out the money}, & \text{if} \quad S_T < K \\ \textit{at the money}, & \text{if} \quad S_T = K \end{cases} \tag{139}$$

This similarly applies to the put option. Since the strike price K is fixed for the duration of the contract, the option pricing problem is to calculate the fair value of the contract at the pricing date $t = 0$ given the expected value S_T at maturity under certain assumptions about the market [181].

Definition 5 (General Asset Pricing)**.** *Let v_t and S_t denote the value of the option and the underlying asset at time t, respectively. At any-time $0 < t < T$, the option value is given by*

$$v_t = V(t, S_t) \tag{140}$$

where V is a non-linear function of t and value of underlying asset S_t.

American Option on an underlying asset grants the holder the right, but not the obligation, to exercise the buy (sell) at the asset at a strike price K at any time $t_e \in [0, T]$ and receive a payoff of [601]:

$$c_{t_e} = \max(S_{t_e} - K, 0) \quad \text{or} \quad p_{t_e} = \max(K - S_{t_e}, 0), \tag{141}$$

for a call and a put option, respectively. Other exotic options include the Asian option, where the payoff is based on the average value of the underlying asset over specific discrete times or within a defined period [181,204,601].

Models for Underlying Assets Derivative pricing largely depends on the chosen stochastic model for the underlying asset, which takes into account many dynamic factors that affect the price of the asset [181]. In this report, we give the mathematical description for two traditional models: Black-Scholes-Merton (BSM) model [84,85] and Heston model [202]. These models compute the value

 doi:10.20944/preprints202511.1802.v2

of the option price $v_t = V(t, S_t)$ at time t based on the value of the underlying asset S_t at that time. They both assume that S_t follows a Geometric Brownian Motion (GBM) with a probability measure P defined in the filtered probability space [618]. These give rise to SDEs given in Table 5 where the variable are defined to be [84,85,202]:

$$\begin{array}{ll} S_t - \text{underlying asset value} & \nu_t - \text{instantaneous variance} \\ \mu - \text{drift parameter} & \kappa - \text{mean reversion speed} \\ \sigma - \text{asset volatility} & \chi - \text{volatility of the volatility} \\ \theta - \text{long-term variance} & dW_t^{S,\nu} - \text{increment of Wiener/Brownian motion} \end{array} \tag{142}$$

Table 5. Traditional models: BSM and Heston for the stochastic dynamics of the value of the underlying asset S_t.

	BSM	Heston
Assumption	constant volatility σ	stochastic volatility $\sqrt{\nu_t}$
SDE	$dS_t = \mu S_t dt + \sigma S_t dW_t^S$	$dS_t = \mu S_t dt + \sqrt{\nu_t} S_t dW_t^S$ $d\nu_t = \kappa(\theta - \nu_t)dt + \chi\sqrt{\nu_t} S_t dW_t^\nu$

For the Heston model, the Brownian motions W_t^S and W_t^ν are correlated as [202]

$$dW_t^S dW_t^\nu = \rho dt \tag{143}$$

where ρ is the correlation coefficient that captures the dependency between asset value and variance. Since these models must be arbitrage-free, one has to ensure that the discounted prices satisfy the Martingale property under the risk-neutral probability measure Q [181,204]. Combining the Martingale property with Itô's lemma[35], we obtain the *vanilla European option* value v_t as a conditional expectation given by [204,618]:

$$v_t = V(t, S_t) = e^{-r(T-t)} \mathbb{E}_Q[h(T, S_T)|\mathcal{F}_t], \tag{144}$$

where r is the risk-free/discounting rate that replaces the drift μ in Table 5 and $\mathcal{F}_t$ is the filtration which represents the market information assumed to be known until time t. Similarly, the *American option* is given by the conditional expectation [204,618]:

$$v_t = V(t, S_t) = \max_{\tau \in [t,T]} e^{-r(T-\tau)} \mathbb{E}_Q[h(\tau, S_\tau)|\mathcal{F}_t], \tag{145}$$

where τ denotes the stopping time when the option is exercised.

These models are typically solved (v_t computed) using numerical methods, and in this review, we will focus on QMCI techniques and quantum solvers for SDEs described in the ensuing subsections.

Quantum Monte Carlo Integration A very common approach to computing the expectation of Equations (144) and (145) is to rewrite them as an integral and employ the classical MCI. In particular, the risk-neutral valuation of Equation (144) is given by [181,618]:

$$V = e^{-r(T-t)} \int_{\mathbb{R}} h(T, y) g(y|\mathcal{F}_t) dy, \tag{146}$$

[35] Itô's lemma or Itô's formula is an identity used in stochastic calculus to find the differential of a time-dependent function of a stochastic process. It serves as the stochastic calculus counterpart of the chain rule.

 doi:10.20944/preprints202511.1802.v2

where $g(\cdot)$ is the conditional probability density function of the underlying asset value S_t. In general, the problem of evaluating Equation (146) can be reduced to computing the discretised integral expectation of the form [618]:

$$\mathbb{E}[f(x)] = \int_\Omega p(x)f(x)dx \approx \sum_i p(x_i)f(x_i), \tag{147}$$

where $f(x)$ and $p(x)$ are the general payoff functions and conditional probability distribution, respectively. The random variable $x \in X$ (corresponding to the asset value S_t) is sampled from a space $X \subset \Omega$ that could be multi-dimensional.

Since Equation (147) is the same as Equation (28), we can employ the Quantum Monte Carlo Integration described in Algorithm (7) on a quantum computer. Note that we can rescale the function f to output values between $[0, 1]$ as required by qubit systems, and by linearity of expectation values, we can rescale back at the end of the computation [31].

The pricing of vanilla European options is one of the most straightforward applications implemented on quantum hardware. In the literature, they are often regarded as an initial benchmark or, more precisely, a proof of concept demonstration on quantum computers. Examples include Refs. [619–622] where implementations on either quantum simulators or hardware were made. Recent approaches include the QMCI engine [193], which is a modular, extendable, and general quantum algorithm for numerical integration [69].

Stochastic PDE An alternative approach is to reformulate Equations (144) and (145) into PDEs using the Feynman–Kac formula [207] as shown in Section (2.2.2). For example, the value of the European option in the BSM model can be written as [31]:

$$\frac{\partial V}{\partial t} + rS\frac{\partial V}{\partial S} + \frac{1}{2}\sigma^2 S^2 \frac{\partial^2 V}{\partial S^2} - rV = 0, \tag{148}$$

where $V(t, S_t) \in (0, T) \times \mathbb{R}^+$ with the terminal condition

$$V(T, S) = h(T, S). \tag{149}$$

Hence, the PDE of the form of Equation (148) can be solved by using quantum algorithms as discussed in Section (2.2.2). In this review

Finite Difference: A widely used method for solving PDEs is the *finite differences* methods described in Algorithm (8). The above BSM example of solving Equation (148) requires defining bounds for the underlying asset and imposing boundary conditions depending on the specific payoff. For instance, one can choose the bounds $S_t \in [0, S_\infty]$ where $S_\infty = 4K$ and boundary conditions [31]:

$$V_{j,I+1} = S_\infty - e^{-r(T-t_j)}K, \qquad \text{where} \quad V_{j,0} = 0. \tag{150}$$

Following Algorithm (8), the problem boils down to solving a $N = I + 1$ dimensional linear system at each discretised time-point t_j given by [31]:

$$AV_j = b_j, \qquad \text{where} \quad V_j, b_j \in \mathbb{R}^N \quad \text{and} \quad A \in \mathbb{R}^{N\times N}. \tag{151}$$

Here, the mesh nodes are $(t_j, S_i) = (j\Delta t, i\Delta S) = \left(j \cdot \frac{T}{(J+1)}, i \cdot \frac{S_\infty}{(I+1)}\right)$ for $i, j \in [0, I+1], [0, J+1]$. The user-chosen natural numbers $J > 1$ and $I > 1$ define the mesh-size. Generally, the finer the mesh-size, the more accurate the calculation, but this also increases the computational cost since it results in a high-dimensional linear system of equations. This is where quantum computing can potentially make the computational pipeline more efficient. By employing the Quantum Linear Systems Solver (QLSS), the theoretical speed-up can be up to exponential in terms of the size of the linear system N [6,131].

 doi:10.20944/preprints202511.1802.v2

However, as discussed in Section (2.1.5), the QLSS has challenges of efficient data-loading on and read-out from a quantum computer, which might limit its Practical Quantum Advantage [11].

Hamiltonian Simulation: Another approach is to reformulate Equation (148) into a Schrödinger or Schrödinger-like equation as discussed in Section (2.2.2). These methods perform a carefully chosen change of variables that transform the problem into:

- Performing non-unitary Hamiltonian simulation using embedding techniques [217].
- Performing imaginary-time evolution of the heat equation [219,614].

The advantage of these methods is that they can circumvent the mesh discretisation issues of finite difference methods, whilst also having the same potential exponential quantum speed-up due to quantum Hamiltonian simulation [31,48]. The drawback is that the quantum resource estimates are so high for Universal Fault-Tolerant implementations [48], the use of quantum analogue systems has shown promising results [216,219].

Quantum Machine Learning: Another interesting approach is to reformulate the problem of solving linear PDEs of the form of Equation (148) into a learning problem that can be solved using deep learning techniques [623,624]. This can be translated to the variational QML technique for solving PDEs [625]. However, unlike the previous methods, this approach does not have a known theoretical quantum speed-up and may have empirically determined efficiency just like other VQA methods discussed in Section (2.1.6).

Collateralised Debt Obligations

A Collateralised Debt Obligation is a complex financial product backed by a pool of loans and other assets and sold to institutional investors [626]. The utility of the tool is to free up capital and shift risk. A typical CDO pool is divided into three categories, otherwise called tranches [626]: junior, mezzanine, and senior. The tranches of CDOs are named to reflect their risk profiles. The senior tranches are generally safest because they have the first claim on the collateral, but they offer the lowest interest rates, with the opposite being true for junior tranches. Although the senior tranche is protected from loss, other default events can cause the CDO to collapse, such as events that caused the 2008 financial crisis [627].

Mathematical Formulation The goal is to compute a fair price of a CDO where the return is consistent with the expected loss for investors of each tranche (denoted by k). Following the notation in [627], let L denote the total loss for the portfolio and L_k denote the loss suffered by the holders of tranche k. Denote the lower and upper attachment point for tranche k by K_{L_k} and K_{U_k}, respectively. When defaults occur, the buyer of the tranche k will bear the loss in excess of K_{L_k}, and up to $K_{U_k} - K_{L_k}$. It follows that

$$L_k = \min\left[K_{U_k} - K_{L_k}, \max\left(0, L - K_{L_k}\right)\right] = h(L) \tag{152}$$

where $h(\cdot)$ is an non-linear function of L similar to the payoff function in Equation (137) for the vanilla option pricing. Investors care about the fair spread r_k of each tranche given by [626,627]:

$$r_k = \frac{1}{N_k}\mathbb{E}[L_k = h(L)], \tag{153}$$

where $N_k = K_{U_k} - K_{L_k}$ is the notional value of the trance k of the portfolio. Since a fair price of a CDO is consistent with the expected losses at each tranche, the fair spread r_k is considered the expected return for a chosen tranche.

Models for Total Loss Analogous to the option pricing problem where models are based on Geometric Brownian Motion for the stochastic value of the underlying asset S_t, the total loss L for a CDO is computed based on the *Conditional Independence Approach* [628]. Conditional independence models [628] are often used for estimating the chances of parties defaulting on the credit in the CDO pool. In such models, given the systemic risk z, the default risks $\{X_1, \ldots, X_n\}$ of the assets involved

 doi:10.20944/preprints202511.1802.v2

are independent. z is then used as a latent variable to introduce correlations between the default risks. The distributions of the default risks and the systemic risk are usually either Gaussian [628] or normal-inverse Gaussian [629]. In particular, for a CDO comprising of n assets with correlated default events, the total expected loss is [626,627]:

$$\mathbb{E}[L] = \int_{\infty}^{\infty} \sum_{i=1}^{n} \lambda_i p_i(z) f(z) dz, \tag{154}$$

where λ_i is the loss that would incur for asset i with probability $p_i(z)$ under systematic risk level z with probability density function $f(z)$. In practice, one integrates z from -3σ to $+3\sigma$, which covers 99.73% of a Gaussian distribution with a variance σ [627]. The expected loss in Equation (154) can then be used to compute the fair spread in Equation (153).

Quantum Approach The MCI is generally the most preferred method for computing expectations of the form in Equation (154) since its scaling does not depend on the dimension of the problem but the number of samples used. As noted in Section (2.2.1), the QMCI can potentially have a quadratic speed up of this computation [5,193]. A small-scale proof-of-concept implementation of CDO on IBM quantum computers was performed in Ref. [627]. As quantum computers scale up, some improved versions of QMCI may deliver Practical Quantum Advantage.

Swap Netting

In general, a swap is a derivative contract between two parties who exchange sequences of monetary flows for a set period of time [630]. One of the most common types of swaps is the interest rate swap, where institutions exchange fixed and floating interest payments to either hedge against interest rate fluctuations or take advantage of market movements [630,631]. Usually, at the time the contract is initiated, at least one of these flows is determined by a random or uncertain variable, such as an interest rate, foreign exchange rate, equity price, or commodity price. Swap netting involves netting the present values of cash flows that two parties owe each other under swap contracts, so that only the net amount is exchanged. There are two main categories of swaps [632]:

1. Settlement netting – netting the periodic cash flows due on the same date.
2. Close-out netting – netting all current and future obligations in the event of a default.

Swap netting is a method of reducing credit, settlement, and other risks of financial contracts by reducing them into a net obligation [630]. When a financial institution has thousands to millions of swaps with multiple counterparties, calculating net exposures across all these positions can be computationally demanding. This is because each swap may have different tenors (lengths), currencies, payment schedules, interest rate indices, optionality (e.g., callable swaps), etc [630]. This leads to high-dimensional cash flow matrices represented as a complex graph problem [633].

Mathematical Formulation Let the $\mathcal{S}$ be the set of swaps for a given counterparty with the clearing house. We can introduce a partition $\mathcal{P}$ on $\mathcal{S}$ such that [634]:

$$\mathcal{S} = \cup_{k=1} M_k, \quad \text{where} \quad M_k \in \mathcal{P} \subset \mathcal{S}. \tag{155}$$

The elements of each M_k will be swaps that are similar enough to be netted with each other. In a fine-grained partition, these may be swaps with identical economic terms. However, the general problem is to consider partitioning into a smaller number of larger subsets to select nettable groups within them [634]. Assuming there are n swaps in each M_k, we denote notional of swap $i \in \{1, 2, \ldots, n\}$ by $\mathcal{N}_i$ and define the direction d_i such that

$$d_i = \begin{cases} +1 & \text{if the clearing house pays the counterparty} \\ -1 & \text{if the counterparty pays the clearing house} \end{cases} \tag{156}$$

 doi:10.20944/preprints202511.1802.v2

where a fixed cash flow payment is between the two parties. The objective is to select subsets of M_k with a maximum notional that can be netted, such that within each subset, the fixed legs and float legs are similar to each other. This is an optimisation problem that is solved by numerical methods.

Quantum Approach Mapping the problem of swap netting to a quantum computer was first proposed in Ref. [634]. The authors define a binary decision variable x_i for each swap i, which has a value of one if the corresponding swap is in the chosen group of swaps to be netted and zero otherwise. The optimisation problem for choosing the swaps to be netted can be formulated as a QUBO given by [634]:

$$x = \max_{x_i \in \mathbb{B}^N} \left[\sum_{i \in M} x_i \mathcal{N}_i - \alpha \left(\sum_{i \in M} x_i d_i \mathcal{N}_i \right)^2 - \beta \sum_{i,j \in M} x_i x_j I_{ij} \right]. \tag{157}$$

The first term aims to maximise the total notional value of swaps within each group. The second term introduces a penalty for groups whose notional amounts deviate significantly from offsetting each other. The third term applies a penalty based on the incompatibility between pairs of swaps. This pairwise incompatibility, denoted as I_{ij}, must be precomputed for every swap pair and is non-negative. The incompatibility function can also be interpreted as a way to prioritise different attributes (like interest rate, duration, etc.) and can be weighted according to the priorities set by the clearing house [634]. The constants α and β control the relative weighting of these terms and can be set either manually using theoretical insights or calculated using methods such as sub-gradient descent. This process, defined for the general component M, is applied to each M_k within the partition $\mathcal{P}$ to generate netting proposals for the group and then aggregating all the outputs for each subset k into a final netting for the full set $\mathcal{S}$.

As noted in [634], similar but non-identical swaps may not be fully netted due to factors like coupon blending, which can produce interest rates diverging from market values. Furthermore, different partitioning strategies and tuning of constants α and β can yield multiple netting proposals. The QUBO of Equation (157) can be solved using quantum algorithms described in section (2.3) on a quantum annealer, which may also generate various solutions for a subset, allowing selection of the proposal that best aligns with market conditions.

3.1.3. Investment Optimisation

Portfolio Optimisation

Portfolio optimisation is one of the most common optimisation problems in fintech. It is the process of choosing and weighting assets to hold in a portfolio such that some given objective is achieved. This problem has a huge amount of flexibility, but the canonical model was proposed in 1952 by Markowitz [228], wherein the most common objectives are to maximise returns for a given level of risk, or vice versa. This trade-off between risk and return is due to the asset volatility: a volatile asset can increase in price dramatically, providing a high return, or it may drop precipitously, losing money. The trade-off is characterised by a curve known as the *efficient frontier* [228].

The above is of course a simplification, and in the decades since the Markowitz model was proposed, a vast number of additional variables and constraints have been taken into account, including transaction costs, dynamic optimisation (where the portfolio is rebalanced regularly), liquidity, time to maturity, asset class (e.g. stocks, bonds, futures, options), regulatory and compliance requirements, and so on [635]. The resulting optimisation problem can be of staggering complexity and very difficult to solve using traditional computational methods.

Mathematical Formulation We consider a simplified portfolio optimisation problem to illustrate the formulation and solution approach. Given a pool of assets, with some expected returns μ_i (mean of historical returns) and risk σ_i (variance of historical returns), combine them to either maximise return

 doi:10.20944/preprints202511.1802.v2

for some level of risk, or minimise risk for some level of return, creating a optimised static portfolio[36]. There are now two main approaches [636]: optimising weightings, where the problem is to pick the right amount (either continuous or discrete) of each asset, or optimising inclusion, where we specify an amount of each asset and simply choose whether to include it or not. In the case of maximising return for a given level of risk R by optimising the weightings x_i, the optimisation problem would be [636]:

$$\max \sum_i \mu_i x_i \quad \text{such that} \quad \sum_i \sigma_i x_i = R. \tag{158}$$

While in the case of minimising risk for a given level of return P by optimising inclusion, it would be [636]:

$$\min \sum_i \sigma_i w_i b_i \quad \text{such that} \quad \sum \mu_i w_i b_i = P, \tag{159}$$

where w_i is the amount of each asset, and b_i is the binary variable determining whether or not it is included in the portfolio. Instead of just choosing or weighting assets, it is also possible to choose whether to hold long or short positions, in a technique known as long-short minimum risk parity optimisation [637]. Briefly, this is where the decision to go long or short (buy or sell) assets is optimised in the interest of minimising risk. This is prioritised over maximising return as the shorting strategy can lead to theoretically unlimited losses, which must be mitigated against.

Depending on the formulation, there are numerous classical techniques for solving this problem, which include convex [228] or mixed-integer programming [638,639], meta-heuristic methods [640], principal component-based methods [641], or genetic algorithms [642]. These methods have varying degrees of efficiency and accuracy, but all face computational bottlenecks as optimisation problems with many variables and constraints [229]. Hence, quantum computing has the potential to offer efficient computation of approximate solutions, higher quality solutions, or some mix of both [236].

Quantum Approach There are various quantum algorithms, discussed in section (2.3), that can be used to solve this problem. The constrained optimisation problems above can be reformulated as a QUBO, allowing the application of Quantum Annealing [643] and variational gate-based methods [644]. Such approaches can also account for additional constraints [645,646] via, for example, using mixing operators (see Section 2.3.1.4). Other approaches utilise an adaptation of Grover's algorithm [263], exhibiting the expected quadratic speed-up over analogous classical techniques, while yet more [647,648] formulate the problem as dynamic in time, making decisions for the same portfolio as it evolves in time.

Quantum walks may also be used. There has been a proposition in [646] where an algorithm based on a Continuous-time Quantum Walk (CTQW) structure is used in the context of portfolio optimisation. This Quantum Walk Optimisation Algorithm (QWOA) uses a CTQW Hamiltonian defined by a graph adjacency matrix [88,649] to evolve the system. The advantages of QWOA for the portfolio optimisation problem lie in its flexibility in 'connecting' only the solutions in the valid subspace, the ability to eliminate degenerate portfolio states (thus significantly reducing the search space), and complete global symmetry amongst valid solutions (eliminating the bias of one valid solution over another due to mixing asymmetry) [646]. This latter is compared positively to approaches like QAOA in [650], which retain this bias in the mixing operator over non-trivial feasible solutions. The results from numerical simulations show that the QWOA for portfolio optimisation leads to an improved performance by reducing the asset search space by a significant factor while also showcasing a higher convergence rate and solution quality [646].

Hedging

A special case of portfolio optimisation is *hedging*, which is a strategy that seeks to reduce risk in a portfolio by ensuring that changes in the value of some assets are countered by opposite changes

[36] Static means we ignore the possibility of time-varying allocations.

 doi:10.20944/preprints202511.1802.v2

in the values of other assets [651]. The most common method of hedging is through derivatives, which are securities whose value depends on some function of the values of one or more underlying assets (see Section 3.1.2). Hedging strategies are fundamental in financial risk management, providing mechanisms to mitigate exposure to adverse market movements [652].

Mathematical Formulation Consider a portfolio with value V exposed to market risk. The investor has access to a set of hedging instruments with return vector $\mathbf{r} = (r_1, r_2, \ldots, r_n)$ and wishes to determine the position vector $\mathbf{w} = (w_1, w_2, \ldots, w_n)$ to minimise risk. A classical variance-based formulation of the hedging problem is [228,653]:

$$\min_{\mathbf{w}} \ \mathrm{Var}(V + \mathbf{w}^\top \mathbf{r}). \tag{160}$$

Assuming the return vector $\mathbf{r}$ has covariance matrix Σ, the problem simplifies to:

$$\min_{\mathbf{w}} \ \mathbf{w}^\top \Sigma \mathbf{w} \quad \text{subject to} \quad \mathbf{w}^\top \mathbf{p} = C, \tag{161}$$

which are linear budget constraints. Here, $\mathbf{p}$ is the price vector of the hedging instruments and C denotes the total capital allocated for hedging. This is a combinatorial optimisation problem with a quadratic risk term determined by the covariance matrix Σ, which is computed using historical pricing information [652].

Quantum Approach To solve the hedging problem on a quantum computer, the general approach is to reformulate it as a QUBO by first discretising the continuous decision variables $\mathbf{w}$ [654]. Let each w_i be expressed in binary form as:

$$w_i = \sum_{k=1}^{K} 2^{k-1} x_{ik}, \quad \text{where} \quad x_{ik} \in \{0, 1\}. \tag{162}$$

The variance minimisation objective becomes [654]:

$$\min_{\mathbf{x} \in \{0,1\}} \ \mathbf{x}^\top T^\top \Sigma T \mathbf{x}, \tag{163}$$

where T is a transformation matrix mapping binary vectors $\mathbf{x}$ to real-valued weight vectors $\mathbf{w}$. We can incorporate the budget constraint within the QUBO framework by introducing a penalty term: $\lambda(\mathbf{p}^\top T\mathbf{x} - C)^2$, where λ is a Lagrange multiplier regulating the constraint's influence. The final QUBO formulation is [654]:

$$\min_{\mathbf{x} \in \{0,1\}} \ \mathbf{x}^\top T^\top \Sigma T \mathbf{x} + \lambda(\mathbf{p}^\top T\mathbf{x} - C)^2. \tag{164}$$

Various quantum algorithms can be used to solve (164), as discussed in section (2.3). One approach, presented in [654], is to map the solution to finding a maximum-independent set in a specially constructed graph. In this graph, the vertices represent assets with significant correlations amongst them being represented by the connecting edges. In order to solve the problem, the authors use two methods. In the first instance, the asset exhibiting minimal risk is picked by finding a maximum-independent set in the above graph in similar terms to Equation (164). The second method proposes a modified solution to the optimisation problem through a graph colouring formulation [654], finding a colouring minimising the edge weights connecting same-colour nodes.

Settlement

In finance, settlement (or transaction settlement) is the process by which a set of securities (be it assets, bonds, or derivatives) is exchanged for a form of compensation [655]. The problem is to settle as many transactions as possible in a complex graph of transactions, using the minimum amount of resources (such as time, number of transactions, individual communications, and so on) [656]. It is

 doi:10.20944/preprints202511.1802.v2

a challenging problem due to the constraints posed by legal requirements, as well as the complexity added by further parameters that need to be taken into account (i.e., collateralised assets or credit information). However, an optimal solution results in the least expenditure of resources, which, if performed at a large organisation like a central bank, can be a significant saving.

Mathematical Formulation For the settlement optimisation problem, one needs to maximise the weighted sum S of settled transactions [657]:

$$S = \max_{\vec{x}} \sum_{i=1}^{T} w_i x_i, \tag{165}$$

where T is a set of transactions, x_i is a binary variable indicating that the transaction is being settled, and w_i is the weight for each transaction i that reflects the total monetary value of the transaction. If, instead of maximising the total value of transactions settled, we wish to settle the total *number* of transactions, we can set $w_i = 1\ \forall i$. In the first instance, the optimisation of equation (165) is subject to the inequality constraint

$$\vec{b}_p + \sum_{i \in \Gamma_p} x_i \vec{v}_{ip} \geq \vec{l}_p, \quad \forall p, \tag{166}$$

where P is the number of parties that take part in the T transactions, the ith transaction involves a party p and is described by the vector $\vec{v}_{ip}$, Γ_p is the set of transactions of party p and $\vec{b_p}$ is a balance vector, which encodes the securities and currencies that party p owns before any transactions settle [657].

In practise, the inequality constraints of equation (166) can be transformed to equality constraints by defining the settlement optimisation as [658]:

$$S = \max_{\vec{x}} \sum_{i=1}^{T} w_i x_i, \quad \text{subject to} \quad \vec{b}_p + \sum_{i \in \Gamma_p} x_i \vec{v}_{ip} = \vec{l}_p + \vec{s}_p, \quad \forall p, \tag{167}$$

where $\vec{s}_p \in \mathbb{R}_{\geq 0}$ is a vector including slack variables.

Quantum Approach It has been shown [658] that well-known quantum methods, such as VQE or QAOA, can be extended to solve problems that reside within the Mixed Binary Optimisation (MBO) class, which combines binary and continuous variables. The work proposes hybrid quantum-classical heuristics to address the problem of settlement optimisation, allowing the modelling of the constraints and options described above.

The constrained optimisation problem in equation (167) can be mapped to a QUBO by transforming the equality constraint into a quadratic penalty term scaled by a penalty coefficient $\lambda > 0$ [658]:

$$\max_{\vec{s_p} \geq 0, \vec{x}} \left[\sum_{i=1}^{T} w_i x_i - \lambda \sum_{p=1}^{P} \left(\vec{b}_p + \sum_{i \in \Gamma_p} x_i \vec{v}_i - \vec{l}_p - \vec{s}_p \right)^2 \right]. \tag{168}$$

In this final form, one can solve the transaction settlement optimisation problem using any of the QUBO-solving techniques mentioned above, such as Quantum Annealing or QAOA. For example, the aforementioned study, as well as a second [659], approach the problem using QAOA, and are able to find the optimal solution for the problems under consideration by running on real QPUs. However, as in many of the other use cases in this paper, constraints include noise and limitations on qubit number and circuit depth, which prevent competitive comparisons with state-of-the-art classical solvers on real-world problems.

Arbitrage

Arbitrage refers to the exploitation of market inefficiencies, such as trading the same asset in different markets to take advantage of different prices [660]. Such assets might include securities,

 doi:10.20944/preprints202511.1802.v2

currencies, or commodities. Arbitrage tends to be more speed-reliant than other trading strategies: as the act of trading influences prices, being faster than competitors to identify and exploit an opportunity leads to much better returns [661]. For example, an FCA report in 2020 highlighted that races between different firms to exploit an arbitrage opportunity can be over in a matter of tens of milliseconds [662].

In general, arbitrage can be far more complex, involving multiple interconvertible assets across multiple markets, potentially over an extended period, and allowing for complications such as fees, regulatory requirements, and liquidity [663]. Identifying optimal strategies faster than competitors is a crucial and high-impact problem, as the very act of exploiting an opportunity causes it to lessen. Apart from the potential profitability, an accurate and rapid analysis of market distortions causing arbitrage opportunities can also provide a significant amount of information about other potential opportunities.

Mathematical Formulation One formulation of the problem of finding an optimal arbitrage strategy is described in [664] and summarised below. We have a set of assets represented as nodes of a graph. There are several directed edges between the nodes, representing potential conversions, with edge weights $\log c_{ij}$, where c_{ij} represents how many units of asset j a unit of asset i can be converted to.

To find the most profitable arbitrage opportunity, we want to maximise the product of the conversion rates in the cycle. We define x_{ij} as the binary variable for including the ij edge in the final cycle. Thus, the profit of a given cycle can be written as $\sum x_{ij} \log c_{ij}$, ignoring constants, where the logarithm accounts for converting a product to a sum. For conceptual simplicity, we will consider only cyclical strategies, where we start and end with the same asset. To enforce this, we need two constraints: that all nodes have the same number of entrances as exits, and that all nodes are passed through exactly once, represented as [664]:

$$\sum_{(i,j)\in E} x_{ij} = \sum_{(j,i)\in E} x_{ji} \quad \text{and} \quad \sum_{(i,j)\in E} x_{ij} \leq 1, \qquad \forall i \in V. \tag{169}$$

From here, it is also easy to add a risk constraint by adding a risk penalty for each conversion, to limit cycle length, or to enforce certain transaction structures.

There exist classical algorithms (such as Bellman-Ford's algorithm [665] and Floyd-Warshall's algorithm [666]) which run in polynomial time and return the first viable cycle they find, but the problem of finding the *optimal* cycle is NP-hard [667]. As mentioned above, arbitrage is a particularly competitive strategy, and so successfully implementing an algorithm to reduce the time taken would be a significant prize.

Quantum Approach In a graph-based formulation, the problem lends itself to being converted to a QUBO and solved using any of the aforementioned quantum methods, such as variational (QAOA/VQEs) or annealing methods. For example, one study [668] formulated the objective function and penalties as a QUBO, and solved using both QAnn and simulated QAOA. They found that the QAnn formulation returned the optimal result, while QAOA often did not return feasible solutions to the problem. Like many other current approaches, the feasibility and advantage of a quantum approach will become more visible as hardware improves, but promising results in proof-of-concept studies like the above suggest this is a worthwhile field of study.

However, it is important to note that such quantum approaches are unlikely to be suitable for the most rapid trades or short-lived opportunities in liquid markets such as oil. Calls to quantum hardware take tens of milliseconds at the very least, stretching to hours if queuing times are included [669], which is a significant speed disadvantage compared to state-of-the-art classical methods. As mentioned before, this is one field where the time to solution is vital, meaning such latency is fatal. While it is possible that, as quantum hardware improves and becomes more widespread, this speed disadvantage will decrease, the greater potential of quantum computing for arbitrage is for slower trades in less liquid markets, and the aforementioned ability to glean information about market distortions from the results.

 doi:10.20944/preprints202511.1802.v2

Natural Language Processing

Natural Language Processing (NLP) is now widely used in many sectors, especially those driven by large volumes of unstructured textual data (e.g., press releases, regulatory filings, social media sentiment, or financial news) [670]. Its uses range from short-term trading algorithms to option pricing models (see Sections 3.1.1 and 3.1.2). NLP aims to interpret and extract key text information, enabling better understanding and generation of human language.

Mathematical Formulation Natural language can be modelled as a sequence of tokens $X = (w_1, w_2, \ldots, w_n)$ from a vocabulary V, each token $w_i \in V$ is represented as a vector in $\mathbb{R}^d$ via an embedding function $E : V \to \mathbb{R}^d$. Distributional semantics states that words appearing in similar contexts have similar meanings [671], which embedding methods implement by mapping such words to nearby vectors [672], which are often compared using measures like the dot product $w_i^\intercal w_j$ [673]. For example *word2vec* [674–676] training optimises word vectors so that the inner product $\langle E(w), E(w') \rangle$ is high if w and w' share contextual neighbours [677]. Thus, semantic similarity is quantified geometrically (e.g., via cosine similarity) in the embedding space. Embeddings can be static (each word has a single vector) or contextual. In contextual embeddings, introduced by transformer-based models like Bidirectional Encoder Representations from Transformers (BERT) [678] or Generative Pre-trained Transformers (GPT) [679], the representation of a word depends on its surrounding words. A contextual embedding is a function F mapping the whole sequence X to context-aware vectors $(h_1, \ldots, h_n)$, where $h_i = F_i(X) \in \mathbb{R}^d$ encodes the meaning of w_i in context. These embeddings capture both semantics and syntax by encoding word order and co-occurrence patterns from large collections of text data.

Syntactic structure is often modelled by formal grammars or parse trees. In a parse tree T for sentence X, words are leaves and nonterminal nodes represent phrase constructs (such as noun phrases, verb phrases) with a root of type 'sentence'. Transformers achieve this through self-attention mechanisms: given token w_i with an associated query vector q_i and other tokens w_j with keys k_j, the attention weight from w_i to w_j is $\text{Softmax}(q_i \cdot k_j / \sqrt{d_k})$ [677]. This attention weight determines how much information from token j's value vector contributes to w_i's new representation.

Mathematically, a transformer layer updates the sequence representation by a function,

$$h_i^l = \sum_{j=1}^{n} \alpha_{ij} (W_V h_j), \tag{170}$$

where $\alpha_{ij} = \text{Softmax}_j((W_Q h_i) \cdot (W_K h_j)/\sqrt{d_k})$ are attention weights and W_Q, W_K, W_V are learned projection matrices. Through layered feed-forward networks, transformers produce rich contextual embeddings that encode semantic relations and syntactic structure [677].

Classical Methods The process of NLP has undergone significant developments due to the advancements in the area of deep learning [680]. Deep neural networks can be used to create complex language models [681–683] that benefit tasks such as, such as market sentiment analysis, event-driven forecasting, and credit risk assessment [684]. However, large models (including RNNs, and GPTs) demand substantial computational resources to develop and train [685,686], resulting in high energy usage and limited scalability. Hence, significant challenges remain in terms of bias, energy consumption, computational resources, or environmental and societal impact [687].

Quantum Approach One way to construct a model for NLP is by combining meaning and grammar into a single language model (which can then be represented in a diagrammatic framework [37] [689]), known as Distributional Compositional Categorical (DisCoCat). It has also been shown that this very framework can be used by categorical quantum mechanics [690,691] and can be represented

[37] Diagrammatic structure is a graphical high-level representation of how meanings and grammatical structures interact to form the meaning of a sentence, see [688] for a detailed description.

 doi:10.20944/preprints202511.1802.v2

by quantum circuits utilising ZX-calculus [692]. This makes the model 'quantum-native', meaning it can naturally be run on a quantum computer via quantum circuits. In [672], the grammatical structure is explicitly encoded into a quantum circuit provide a structured way to interpret how word meanings combine to form sentence-level sentiment. This is a difference from other large language models, which learn these relationships implicitly from vast amounts of data.

Alternative approaches to NLP arise from QNNs and enhancing the capacity of current NLP models' neural architectures [346,606,693]. QNN-based approaches replace parts of existing deep learning architectures with quantum subroutines, offering a potential solution to some of NLP's scalability and efficiency issues. This intersection is often referred to as Quantum Natural Language Processing (QNLP) [690]. Experiments have been carried out in NISQ devices for a variety of simple NLP tasks [677,694–699], such as topic classification using single-qubit rotations and entangling gates or encoding Word2Vec embeddings [674] in a QRAM with a 'modest' number of qubits. These experiments suggest QNLP can in principle perform NLP tasks, although noise and limited circuit depth in NISQ devices are currently a key challenge [677,690,700].

While classical deep learning still dominates NLP in both research and industry, there has been growing interest in exploring QNLP methods [672,699,701], particularly for applications like sentiment analysis in finance [672]. For instance, one can use these methods to perform sentiment analysis to predict market trends, analyse investor sentiment, and improve decision-making in trading. This usually involves extracting positive, neutral, or negative sentiments from financial text data.

Moreover, a potential advantage of QNLP (especially in scaling to more complex datasets) relies on faster and more efficient data processing compared to classical NLP approaches [677]. This is very important in finance, as timely analysis of massive amounts of textual data can provide a competitive advantage [702]. The aim is that this explicit approach might eventually lead to more robust or efficient models for specific financial NLP tasks. If scaled up, QNN-based NLP could add new capabilities to classical models [690]; however, demonstrating a clear quantum advantage in NLP financial tasks remains an ambitious goal. Further development in encoding schemes, possibly leveraging dimensionality reduction or hybrid classical-quantum architectures, as well as more stable qubits and error-corrected quantum systems are crucial to fully realise the potential of QNLP in finance.

3.2. Risk Management and Cybersecurity

In modern finance, risk management and cybersecurity have become foundational pillars for sustaining operational integrity, client trust, and regulatory compliance [703]. Financial institutions face a complex landscape of threats ranging from credit and market risk to sophisticated cyberattacks targeting digital infrastructure. As the financial sector becomes increasingly digitised and interconnected, safeguarding assets and ensuring resilience against uncertainties has transcended from a compliance necessity to a strategic imperative [704].

Risk management entails identifying, assessing, and mitigating potential financial losses arising from market volatility, operational failures, credit defaults, and systemic crises [705]. An effective risk management framework enables firms to allocate capital efficiently, optimise portfolio returns relative to risk exposure, and maintain solvency under stress conditions. Concurrently, cybersecurity protects the confidentiality, integrity, and availability of financial data and systems against malicious activities such as hacking, ransomware, and insider threats [706]. Failures in either domain can result in catastrophic financial loss, reputational damage, and systemic contagion effects that extend beyond individual institutions. The increasing reliance on automated trading, cloud-based infrastructures, and real-time payment systems has further amplified vulnerabilities, necessitating advanced and proactive defences. Financial institutions are faced with two kinds of limitations: on one hand, classical computational methods for risk assessment often rely on complex simulations and/or optimisation algorithms which have several bottlenecks related to problem dimensionality and computation time [707]. Quantum computing has the potential to alleviate these bottlenecks as it can naturally perform computations in a high-dimensional Hilbert space. On the other hand, classical cryptographic methods (e.g., RSA) depend on the computational difficulty of problems like integer factorisation and discrete logarithms,

 doi:10.20944/preprints202511.1802.v2

which are theoretically vulnerable to advances in quantum computing (see Section 2.5). Therefore, the inevitable solution is to incorporate cryptographic systems that are quantum-safe.

In this section, we will consider some use cases of quantum technologies in risk-management and cybersecurity. According to a study by McKinsey [20], the projected value of quantum technology applications for risk-management and cybersecurity will be about $80 billion by 2035. Hence, strategic investments in quantum research and early adoption frameworks will likely define the resilience and competitiveness of financial institutions in the coming decades.

3.2.1. Value at Risk and CVaR

Risk analysis in finance can be either quantitative or qualitative [708]. Under quantitative risk analysis, a risk model is built using simulation or deterministic statistics to assign numerical values to risk. Inputs that are mostly assumptions and random variables are fed into a risk model. For any given input range, the model generates a range of outputs or outcomes [708]. The model's output is analysed using graphs, scenario analysis, and/or sensitivity analysis to make decisions to mitigate and deal with the risks. On the other hand, qualitative risk analysis [709] is an analytical method that does not identify and evaluate risks with numerical and quantitative ratings. Qualitative analysis involves a written definition of the uncertainties, an evaluation of the extent of the impact (if the risk ensues), and countermeasure plans in the case of a negative event occurring [709]. Risk assessment enables corporations, governments, and investors to assess the probability that an adverse event might negatively impact a business, economy, project, or investment.

One of the most important metrics for quantitative risk assessment are the Value-at-Risk (VaR) and Conditional Value at Risk (CVaR) [710–714]. The VaR is a measure of the worst expected loss on a portfolio of instruments resulting from market movements over a given time horizon and a pre-defined confidence level [715]. This metric is most commonly used by investment and commercial banks to determine the extent and occurrence ratio of potential losses in their institutional portfolios. Risk managers can use VaR to measure and control the level of risk exposure for compliance. For example, the Basel III regulations require banks to perform stress tests using VaR [716]. The associated metric CVaR, also known as the *Expected Shortfall*, is a measure of the average of all potential losses exceeding the VaR at a given confidence level. This risk assessment measure quantifies the amount of tail risk an investment portfolio has. The metric is derived by taking a weighted average of the "extreme" losses in the tail of the distribution of possible returns, beyond the VaR cutoff point. CVaR is used in portfolio optimisation for effective risk management [717].

Mathematical Formulation Consider a portfolio with uncertain future profit/loss L, then we can define the VaR as:

Definition 6. *Given a confidence level $\alpha \in (0,1)$, the portfolio Value-at-Risk is*

$$VaR_\alpha = \inf\{l \in \mathbb{R} : \mathbb{P}(L \leq l) \geq \alpha\} = \inf\{l \in \mathbb{R} : F_L(l) \geq \alpha\}, \tag{171}$$

where $F_L(l) = \mathbb{P}(L \leq l)$ is the is the Cumulative Distribution Function (CDF) of L.

In other words, the VaR is the smallest number l such that the probability the loss exceeds L is at most $1-\alpha$. In practise, $\alpha = 0.999$, thus VaR is the loss level that will not be exceeded with 99.9% confidence. As outlined in Algorithm (26), the VaR can be computed using MCI [717,718]. However, as discussed in Section (2.2.1), the MCI methods have a slow convergence, hence quantum algorithms that have a potential quadratic speed-up are desirable.

 doi:10.20944/preprints202511.1802.v2

Algorithm 26 Computation of VaR via Monte Carlo Simulation

Require: Number of simulations M, portfolio value V_0, model parameters (e.g., μ, σ), confidence level α
Ensure: Estimated Value-at-Risk VaR_α
1: **for** $i = 1$ to M **do**
2: Simulate one portfolio return r_i based on the assumed distribution (e.g., normal: $r_i \sim \mathcal{N}(\mu, \sigma^2)$)
3: Compute simulated profit and loss: $L_i = V_0 \times r_i$
4: **end for**
5: Sort $\{L_i\}$ in ascending order
6: Find the $(1-\alpha)$ quantile of the sorted $\{L_i\}$
7: Set $\text{VaR}_\alpha = -\text{Quantile}(L, 1-\alpha)$
8: **return** VaR_α

We can also define the CVaR based on the VaR:

Definition 7. *Given the profit-loss variable L that is integrable and continuous CDF, then the CVaR at confidence level $\alpha \in (0,1)$ is defined as*

$$CVaR_\alpha = \mathbb{E}[L | L \geq VaR_\alpha] = \frac{1}{1-\alpha} \int_\alpha^1 VaR_u \, du. \tag{172}$$

This shows CVaR as an average of VaRs beyond the quantile α [717] and can be computed using MCI.

Quantum Approach The most straightforward quantum approach to employ the QMCI for computing the VaR and CVaR. As shown in Section (2.1.2), the QAE has two loading operators:

$$\mathcal{P}_l \left|0\right\rangle_n = \left|\psi\right\rangle_n = \sum_{i=0}^{N-1} \sqrt{p_i} \left|i\right\rangle_n, \quad \text{with} \quad \sum_{i=0}^{N-1} p_i = 1, \tag{173}$$

which prepares the initial state with discretised probabilities p_i using n qubits, where $N = 2^n$. The second operator F_l which applies the function $f : \{0, \ldots, N-1\} \mapsto [0,1]$ on corresponding states as:

$$\mathcal{F}_l \left|i\right\rangle \left|0\right\rangle = \left|i\right\rangle \left(\sqrt{1 - f(i)} \left|0\right\rangle + \sqrt{f(i)} \left|1\right\rangle \right). \tag{174}$$

These operators combine to give

$$\mathcal{F}_l \mathcal{P}_l \left|0\right\rangle_n \left|0\right\rangle = \sum_{i=0}^{N-1} \sqrt{p_i} \sqrt{1 - f(i)} \left|i\right\rangle \left|0\right\rangle + \sum_{i=0}^{N-1} \sqrt{p_i} \sqrt{f(i)} \left|i\right\rangle \left|1\right\rangle, \tag{175}$$

thus by measuring the probability of the last qubit $|1\rangle$ we get an estimate for the expectation value $\mathbb{E}[f(X)] = \sum_{i=0}^{N-1} p_i f(i)$, where X is mapped into $\{0, \ldots, N-1\}$. In Ref. [710], this method is extended by defining a function

$$f(i) = \begin{cases} 1 & \text{if} \quad i \leq l \\ 0 & \text{otherwise} \end{cases} \tag{176}$$

where $l \in \{0, \ldots, N-1\}$. Therefore, Equation (175) reduces to:

$$\mathcal{F}_l \mathcal{P}_l \left|0\right\rangle_n \left|0\right\rangle = \sum_{i=l+1}^{N-1} \sqrt{p_i} \left|i\right\rangle \left|0\right\rangle + \sum_{i=0}^{l} \sqrt{p_i} \left|i\right\rangle \left|1\right\rangle. \tag{177}$$

The probability of measuring the last qubit $|1\rangle$ is given by $\sum_{i=0}^{l} p_i = \mathbb{P}[X \leq l]$. The authors in [710] then use a bisection search over l to find the smallest level l_α, which corresponds to the $\text{VaR}_\alpha(X)$, such that $\mathbb{P}[X \leq l_\alpha] \geq \alpha$ in at most n steps. Similarly, an appropriate function $f(\cdot)$ for CVaR can be defined,

 doi:10.20944/preprints202511.1802.v2

and then the same procedure is followed. This quantum algorithm has an error that scales as $\mathcal{O}(1/M)$, which is a quadratic speed-up over MCI described in Algo. (26). A proof-of-concept implementation of this QMCI for VaR and CVaR on quantum computers was performed in [710,719]. Additionally, Ref. [719] offers estimates for the total number of qubits needed, the anticipated circuit depth, and how these factors relate to the expected runtime, assuming reasonable projections for future fault-tolerant quantum hardware.

3.2.2. Credit Risk Analysis

Credit risk analysis is a fundamental discipline in finance concerned with the assessment of the likelihood that a borrower will default on contractual debt obligations [720]. It plays a critical role not only in individual lending decisions but also in the strategic management of financial institutions' portfolios and the determination of necessary capital reserves [720]. With the globalisation of financial markets and the increasing complexity of credit products, the methodologies for assessing, pricing, and managing credit risk have evolved substantially.

The two major branches of credit risk analysis are: the quantification of Economic Capital Requirement (ECR) and the development of robust credit scoring systems. The ECR refers to the amount of capital a financial institution needs to ensure that it stays solvent with a high degree of confidence over a specified time horizon [721]. Credit scoring, on the other hand, operationalises credit risk evaluation at the transaction level by using statistical and machine learning techniques to predict a borrower's probability of default [722]. Credit scoring models are essential not only for underwriting but also for regulatory compliance, particularly under frameworks like Basel II and III, which link credit risk quantification directly to minimum ECR [716]. Traditional models such as logistic regression remain prevalent [722,723], although recent advancements have integrated ensemble methods and deep learning to improve predictive performance [724,725].

However, classical computational bottlenecks arise in these systems due to the increasing size and complexity of datasets, the non-linear interactions between multiple risk factors, and the need for real-time or near-real-time analytics [726]. Given these limitations, researchers have been exploring how quantum computing can offer speed-ups, accuracy, and efficiency [727]. In this section, we will state the mathematical formulations of these credit risk analyses and outline some proposed quantum computation approaches to these problems, which may potentially offer an advantage.

Economic Capital Requirement

As described above, the ECR is an important risk metric that quantitatively captures the amount of capital required to remain solvent at a given confidence level [716,721]. It captures unexpected losses arising from credit events and serves as a buffer against adverse outcomes. Institutions allocate economic capital across their credit portfolios based on internal models that estimate the distribution of potential losses, taking into account default probabilities, loss given default, and exposure at default [728]. The result reflects the amount of capital that the firm should have to support any risks that it takes on its investment portfolio. The measurement process for economic capital involves converting a given risk into the amount of capital that is required to support it. The calculations are based on the institution's financial strength (or credit rating) and expected losses. Financial strength is the probability of the firm not becoming insolvent over the measurement period and is otherwise known as the confidence level in the statistical calculation [728].

Mathematical Formulation Let $L_{\mathbf{x}}$ denote the random variable representing the total *loss* of the institution's portfolio of K assets, denoted by $\mathbf{x} = (x_1, \ldots, x_K) \in \mathbb{R}^K$, over a fixed time horizon (typically one year). The distribution of $L_{\mathbf{x}}$ is characterised by its CDF $F_{L_{\mathbf{x}}}(l) = \mathbb{P}(L_{\mathbf{x}} \leq l)$ as described in Section (3.2.1). The ECR is commonly defined as the difference between the VaR and the expected loss [721]:

$$\mathrm{ECR}_{\alpha}[L_{\mathbf{x}}] = \mathrm{VaR}_{\alpha}(L_{\mathbf{x}}) - \mathbb{E}[L_{\mathbf{x}}], \tag{178}$$

 doi:10.20944/preprints202511.1802.v2

where $\mathbb{E}[L_{\mathbf{x}}]$ denotes the expected (mean) loss of the portfolio. Alternatively, in more robust risk management frameworks [729] , the CVaR can be use to define ECR as:

$$\mathrm{ECR}_{\alpha}[L_{\mathbf{x}}] = \mathrm{CVaR}_{\alpha}(L_{\mathbf{x}}) - \mathbb{E}[L_{\mathbf{x}}]. \tag{179}$$

In practice, institutions seek to allocate their portfolio of assets denoted to minimise the ECR, subject to regulatory, liquidity, and investment constraints. A general optimisation problem can be stated as [730,731]:

$$\begin{aligned} \min_{\mathbf{x}\in\mathbb{X}} \quad & \mathrm{ECR}_{\alpha}[L_{\mathbf{x}}] \\ \text{subject to} \quad & g_i(\mathbf{x}) \leq 0, \quad i = 1, \ldots, m, \\ & h_j(\mathbf{x}) = 0, \quad j = 1, \ldots, p, \end{aligned} \tag{180}$$

where $\mathbb{X}$ is the feasible set determined by internal risk policies and external regulations, and:

- $g_i(\mathbf{x})$ are inequality constraints representing risk limits (e.g., sector exposure caps, maximum portfolio volatility, leverage restrictions).
- $h_j(\mathbf{x})$ are equality constraints ensuring portfolio balance (e.g., full investment constraint $\sum_{k=1}^{K} x_k = 1$, or specific regulatory ratios).

Quantum Approach We see that the problem of ECR is two fold:

1. First, for a given portfolio of assets $\mathbf{x}$, compute the associated $\mathrm{ECR}_{\alpha}[L_{\mathbf{x}}]$ by modelling its total loss $L_{\mathbf{x}}$ using *Gaussian conditional independence models*[38] [732] such as discussed in Section (3.1.2.2) for Collateralised Debt Obligations. The problem is solved in three-steps:
   (a) Compute $\mathbb{E}[L_{\mathbf{x}}]$, which is the same form as Equation (154), and thus it has been shown by [627] that this can be efficiently performed on a quantum computer using QMCI algorithm.
   (b) Compute the $\mathrm{VaR}_{\alpha}(L_{\mathbf{x}})$ just as in Section (3.2.1) using QMCI algorithm [710,719].
   (c) Combine the above to compute the $\mathrm{ECR}_{\alpha}[L_{\mathbf{x}}]$ by using Equation (178).
2. Second, repeat the above to find an optimal portfolio $\mathbf{x}^* \in \mathbb{X}$ that solves the optimisation problem (180). This can be done by converting the problem into a QUBO and solve it using quantum algorithms described in section (2.3).

A proof-of-concept computation of ECR using QMCI on quantum computers was performed in [719] with comparative accuracy to classical methods. Additionally, [719] offers quantum resource estimates for future fault-tolerant quantum hardware. However, unlike the pipeline described above, the authors in [719] used classical numerical integration for computing $\mathbb{E}[L_{\mathbf{x}}]$ and did not proceed to solve the optimisation problem (180). Therefore, to the best of our knowledge, there is still an opportunity for researchers to explore the benefits of the end-to-end pipeline involving multiple quantum algorithms.

Credit Scoring

The process of credit scoring, otherwise called defining creditworthiness, is one of the most difficult problems in finance due to the large amount of data necessary to determine key independent features that can influence the end result [722,724,725]. Credit scoring can be identified as a potential use-case both for quantum optimisation as well as Quantum Machine Learning techniques. A typical credit score is influenced by payment history, accounts owed, length of credit history, new credit, and credit mix [733]. For business credit, this information can be gathered from historical business data, public filings, and payment collections. Currently, credit scores are often predicted by using classical regression models or machine learning algorithms [734,735]. In order to get more accurate results, it is helpful for the machine learning algorithms to train on more data; however, this process

[38] This scheme resembles the one employed for regulatory purposes in the Internal Ratings-Based approach to credit risk under Basel II and subsequent frameworks.

 doi:10.20944/preprints202511.1802.v2

is computationally intensive. Some researchers are exploring the potential for QML to be able to efficiently resolve critical features to determine a person's creditworthiness.

Mathematical Formulation One approach of credit scoring is to reformulate it as a combinatorial optimisation problem aiming to select the most influential (or highly affecting) features for identifying creditworthiness [736]. In this approach, one considers a dataset of past credit applicants represented by a matrix $U \in \mathbb{R}^{m\times n}$:

$$U = \begin{bmatrix} u_{11} & u_{12} & \cdots & u_{1n} \\ u_{21} & u_{22} & \cdots & u_{2n} \\ \vdots & \vdots & \ddots & \vdots \\ u_{m1} & u_{m2} & \cdots & u_{mn} \end{bmatrix} \tag{181}$$

Each row represents an applicant, and each column a feature. The outcome vector $V \in \{0,1\}^m$ represents credit decisions:

$$V = \begin{bmatrix} v_1 \\ v_2 \\ \vdots \\ v_m \end{bmatrix} \tag{182}$$

where $v_i = 0$ indicates acceptance and $v_i = 1$ indicates rejection. Suppose we begin with n original features and aim to identify a subset of K features to guide our credit decision-making process[39]. To avoid introducing bias in the selection, we desire an exhaustive yet efficient search. However, the number of possible subsets of size K is combinatorial, given by $C(n,K)$. Even with early pruning, the search space remains prohibitively large, necessitating a strategy that prioritises promising candidate subsets [736]. The aim is to select columns from the data matrix U that exhibit strong correlation with the target vector V, while being mutually uncorrelated among themselves. We assume a correlation metric yielding values in the range $[-1,1]$ is available. In practice, "correlation" may encompass domain-specific rules, such as mandatory inclusion of certain features, that go beyond simple statistical association [736].

Let ρ_{ij} denote the correlation between the i-th and j-th columns of U, and let ρ_{V_j} be the correlation between the j-th feature and the target V. We introduce binary variables $x_j \in \{0,1\}$ to indicate whether feature j is selected:

$$x_j = \begin{cases} 1, & \text{if feature } j \text{ is selected} \\ 0, & \text{otherwise} \end{cases} \tag{183}$$

We thus define the objective function [736]:

$$f(\mathbf{x}) = -\left[\alpha \sum_{j=1}^{n} x_j |\rho_{V_j}| - (1-\alpha) \sum_{j=1}^{n} \sum_{\substack{k=1 \\ k\neq j}}^{n} x_j x_k |\rho_{jk}|\right] \tag{184}$$

where $\alpha \in [0,1]$ is the parameter that balances influence and independence such that: $\alpha = 0$ and $\alpha = 1$ prioritise the independence and influence that features have on the marked class, respectively [736].

Quantum Approach Let $\mathbf{x} = (x_1, \ldots, x_n)$ be a collective vector of the binary variables, and by using the property $x_j x_j = x_j$, the objective function in Equation (184) can be expressed as a quadratic form:

$$f(\mathbf{x}) = -\mathbf{x}^\top Q \mathbf{x} \tag{185}$$

[39] There are several motivations for feature reduction [736]: financial costs associated with data collection, the presence of redundant information, and features so weakly associated with the target outcome that they behave like noise.

 doi:10.20944/preprints202511.1802.v2

The optimal subset $\mathbf{x}^*$ is given as a QUBO:

$$\mathbf{x}^* = \arg\min_{\mathbf{x}} \left(-\mathbf{x}^\top Q \mathbf{x} \right) \tag{186}$$

This problem can then be solved using quantum optimisation techniques for QUBOs described in section (2.3). A proof-of-concept implementation on a QAnn using German credit data was shown to yield comparative accuracy as traditional feature selection methods [736]. In addition, the QUBO feature selection framework in [736] yielded a smaller feature subset with no loss of accuracy compared to common classical methods like recursive feature elimination. This paves the way for leveraging quantum computing to systematically reduce the dimensionality of large feature sets, particularly as QPUs become more advanced.

Other more common proposals for credit scoring on quantum computers are based on QML includes *systemic quantum score* using quantum kernels [737], a hybrid quantum-classical neural network approaches [738,739], and a quantum-inspired evolutionary method for feature selection [740]. Although still in its early stages and constrained by current quantum hardware limitations and theoretical hurdles, the findings to date highlight the promising potential of quantum computing for efficient credit scoring. Improvements in accuracy, processing speed, inclusivity, and feature optimisation point to a promising future for quantum-enhanced credit risk assessment in finance [737]. As quantum technology advances, continued progress in algorithm development, data representation, and hybrid quantum-classical methods will be essential to achieving Practical Quantum Advantage and integrating these innovations into the financial industry.

3.2.3. Fraud Detection

Fraud detection is a mission-critical function in financial institutions, safeguarding against losses and ensuring regulatory compliance. It refers to identifying events such as transactions or withdrawals that are likely to be fraudulent, based on data about them. Fraud poses a huge threat to economic systems - the UK Finance Annual Fraud Report recorded more than $1.5 billion fraud-related losses in the United Kingdom alone in 2023, while total global losses were estimated at approximately $485.6 billion [741]. To crack down on this, the UK Economic Crime and Corporate Transparency Act 2023 and other similar legislation are imposing more responsibilities on various financial organisations to combat fraud [742]. Currently, classical machine learning techniques are used to detect and prevent fraud, but they often suffer from problems including a high false positive rate reaching 80% [743], and long inference times. Given the high impact of even small improvements in terms of time and money saved, organisations are turning to more advanced algorithms, including quantum computing, to boost performance.

Classical Methods Classical machine learning techniques have high performance variability due to the model used, apart from other factors such as data selection, formatting, and preprocessing, model choice, and hyperparameter fixing. Some particular models and algorithms are popular due to their interpretability, robustness, and computational efficiency. Logistic regression is suited to binary classification tasks like credit scoring, and is easy to set up and use [744]. Decision trees are useful for providing transparency into decisions, although they may be prone to overfitting (where models generalise insufficiently) [745]. This may be overcome using random forests, which are ensembles of decision trees and aggregate multiple tree outcomes [746]. Finally, support vector machines [747] and k-Nearest Neighbors [331] can be computationally expensive, but can identify subtle patterns associated with fraud. Each method has a range of benefits and drawbacks, enumerating which is outside the scope of this paper, and correct model selection and preparation are vital in setting up a functioning and high-performing fraud detection pipeline. A recent survey paper [748] summarises developments in both types of fraud, and in the ML pipelines used to detect them. In particular, it appears deep learning techniques, including Convolutional Neural Networks (CNNs) and ensemble

 doi:10.20944/preprints202511.1802.v2

methods, have experienced a surge in popularity due to their greater robustness and more rapid classification [749,750].

Quantum Approaches Quantum approaches to fraud detection can be split into two domains: quantum algorithms applied to classical data, and those applied to data that has been loaded into a quantum format. For the former, the data are simply a table of numbers, which may refer to observed, calculated, or encoded properties of a particular transaction. Quantum k-means and spectral clustering algorithms are known to be potentially more efficient over classical counterparts [420] (see Section 2.4.2.1). A recent hybrid quantum-classical framework implements classification through QRAMs enhanced by quantum feature selection, demonstrating improved accuracy through complementary exploration of the feature space [751]. These implementations are conceptually simple as the data remain unchanged, necessitating little novel pre-processing. A simple example of this is quantum neural networks was demonstrated in Ref. [752]. In the report, they constructed a classical deep neural network, and replaced one of the layers with a Parametrised Quantum Circuit. This enabled them to achieve similar accuracy scores on the same data, using fewer parameters, resulting in a more performant pipeline [752].

For fully quantum implementations, the data must be encoded in a quantum format. There are a number of ways to do this; one common method is using Quantum Generative Adversarial Networks (QGAN) [753]. A GAN is a combination of a generator and a discriminator model. The generator takes as input a noise vector and outputs a data vector, while the discriminator attempts to distinguish the real and generated data. Over the course of training, the generator learns the data's underlying distribution. The quantum version of this uses a QNN (see Section 2.4.1.3) in place of the generator. In essence, it takes an equal superposition of qubits and learns the circuit parameters to convert this into a quantum-encoded datapoint. Thus, the data are indirectly encoded into a quantum format. This enables the method to potentially exploit a quantum advantage in sampling efficiency: classically sampling from a complex probability distribution is computationally expensive, while the quantum version is far easier [445,467,754]. The aforementioned study [753] reported results that achieve performance on par with currently existing classical methods, while potentially circumventing their key drawbacks of training instabilities and sampling inefficiency. Additional approaches include QAE for density-estimation based anomaly detection, quantum-enhanced kernels for clustering methods [755], and Quantum Boltzmann Machine [444].

Although there is some optimism about these quantum methods, a recent study [415] raised doubts about the proper benchmarking of these quantum approaches. The authors developed a benchmarking suite and used it to compare classical and quantum ML algorithms; they found that out-of-the-box classical models tended to outperform quantum ones on the small datasets used. On the other hand, it is known that results from small amounts of data do not necessarily hold for larger amounts, due to the properties of deep learning techniques [415]. Thus, it is possible that as the scale increases, the benefits of the quantum approach become apparent. As a result, it is still an open question as to the precise benefit that is to be gained from a quantum approach to fraud detection.

3.2.4. Quantum Safe Cryptography

One very frequent and important vulnerability that financial services companies tend to have is a reliance on legacy software, with commensurate security issues and time-consuming patches and upgrades, which includes the security of that software [756]. A key problem exposed by this is the need to upgrade security to Post-QC protocols[40] before quantum computers capable of breaking current encryption algorithms become feasible [563]. The expected delay before this occurs may tempt organisations to put off this transition. However, waiting for malicious actors to pose a present risk by possessing quantum computers is highly dangerous, not only due to the risk of being caught off-guard,

[40] These are quantum-safe protocols, and some are outlined in Section (2.5.3).

 doi:10.20944/preprints202511.1802.v2

but due to the threat from 'harvest-now decrypt-later' attacks where information is gathered and held until it can be decrypted [521].

Given the complexity of the field, attempts to enact this transition entirely internally are likely to lead to substandard and insecure implementations. The simplest path is to rely on recommendations from national or international bodies, including NCSC [563], NIST [757], ETSI [758], and the IETF [759], which are actively working on developing and disseminating such standards. However, as mentioned above, Post-QC is still a relatively novel field, and while roll-out has begun on a large scale, there is every chance that novel attacks will be developed that can break these protocols. One must therefore balance the potential risk of a switch with the likelihood of harvest now/decrypt later attacks. Furthermore, security is a weak-link problem: any system is only as secure as its most insecure point, and for cryptography, that point is human error. Post-QC protocols cannot be seen as a panacea, and must be implemented in tandem with rigorous and regular training and testing of personnel. If this is carried out, organisations' data stands a good chance of remaining secure against hostile actors equipped with quantum computers.

3.3. Economics

Economics, at its core, is the study of how individuals, firms, and societies allocate scarce resources to meet their needs and desires [760]. The field spans microeconomic inquiries into individual behaviour and market mechanisms to macroeconomic studies of national income, inflation, and employment. Central to economics is the development and analysis of models that help explain complex systems, predict outcomes, and inform policy. The key objectives of the field include efficiency in resource allocation, economic growth, equitable distribution of wealth, and the stabilisation of economies through informed decision-making [25,760–763].

To achieve these objectives, economists rely heavily on mathematical modelling, statistical analysis, and computational simulations [764]. These tools are vital in forecasting market trends, understanding consumer behaviour, optimising financial portfolios, and solving general equilibrium models. However, as datasets grow larger and models become more sophisticated, especially in areas like game theory [765], and agent-based modelling [766,767], limitations of classical computing become apparent. For example, in supply chain economics [768], solving for the optimal allocation of resources in real-time can be computationally expensive, especially as the number of variables increases. Quantum technologies offer a potential efficient alternative for economic modelling [25]. In this section, we will outline some of the potential use cases of quantum computing in economics, which include quantum money and economic modelling.

3.3.1. Quantum Money

The concept of quantum money, first introduced by Stephen Wiesner in the 1980s [577], represents one of the earliest applications of quantum information to cryptography. At its core, quantum money exploits the *no-cloning theorem*, which asserts that it is fundamentally impossible to create an exact copy of an arbitrary unknown quantum state [570]. This property provides a natural basis for unforgeability, a critical requirement for any monetary system. Quantum money has become a foundational example of how quantum information can provide security guarantees impossible in classical systems.

Wiesner Private-Key Quantum Money

In Wiesner's original formulation [577], a quantum banknote is a tuple $(s, |\psi_s\rangle)$, where:

- $s \in \{0,1\}^m$ is a classical serial number.
- $|\psi_s\rangle \in \mathcal{H}^{\otimes n}$ is an n-qubit quantum state.

Each qubit is chosen from one of two mutually unbiased bases:

$$\{|0\rangle, |1\rangle\} \quad \text{(computational basis)}, \quad \{|+\rangle, |-\rangle\} \quad \text{(Hadamard basis)}, \tag{187}$$

 doi:10.20944/preprints202511.1802.v2

where $|+\rangle = \frac{1}{\sqrt{2}}(|0\rangle + |1\rangle)$ and $|-\rangle = \frac{1}{\sqrt{2}}(|0\rangle - |1\rangle)$. The specific choice of basis and value for each qubit is known only to the issuing bank and stored in a secure database indexed by the serial number s. The bank randomly selects: A basis $b_i \in \{Z, X\}$ for each qubit, and a bit $v_i \in \{0, 1\}$ indicating the qubit value in that basis. It then generates the full state as:

$$|\psi_s\rangle = \bigotimes_{i=1}^{n} |\phi_i\rangle, \quad \text{where} \quad |\phi_i\rangle \in \{|0\rangle, |1\rangle\} \quad \text{or} \quad \{|+\rangle, |-\rangle\}. \tag{188}$$

The bank maintains a secret mapping:

$$\text{DB}[s] = ((b_1, v_1), \ldots, (b_n, v_n)). \tag{189}$$

To verify a note, the bank measures each qubit in the basis b_i and checks whether the outcome matches v_i. Any discrepancy leads to rejection.

The security of Wiesner's scheme stems from the no-cloning theorem, which can be formally stated as follows:

Theorem 1 (No-Cloning Theorem [570]). *There does not exist a unitary operator U and a fixed state $|e\rangle$ such that:*

$$U(|\psi\rangle \otimes |e\rangle) = |\psi\rangle \otimes |\psi\rangle$$

for all $|\psi\rangle \in \mathcal{H}$.

The implication is that any adversary who tries to duplicate an unknown quantum state $|\psi_s\rangle$ without knowledge of the preparation bases will likely alter it irreversibly. Measuring a qubit in the wrong basis yields a random result, destroying the original state and producing a statistically distinguishable forgery[41].

However, Wiesner's quantum money has at least three notable limitations [25]. First, it requires verification through an online authority, reducing its practicality compared to traditional cash. Second, it is based on a private-key scheme, meaning the issuer must keep certain verification details secret. Third, the scheme is technologically difficult to implement, given its quantum memory and hardware requirements. Hence, the ensuing section will describe modern approaches to quantum money that have a decentralised verification protocol, which in principle addresses the first two challenges with Wiesner's protocol.

Modern Public-Key Quantum Money

To overcome the limitations of Wiesner's quantum money, the concept of public-key quantum money emerged, aiming to create a system where anyone could verify the validity of a quantum banknote without needing to consult the issuing authority [25]. These development represents a significant step towards realising a more practical and widely usable form of quantum currency. The concept of *publicly verifiable quantum money* was first proposed by Aaronson [769] and later developed in [770–772] and other works, which provided schemes where the authenticity of a quantum banknote can be verified without access to a secret database. These schemes typically have the following design:

- A key generation algorithm $\text{Gen}() \to (pk, sk)$,
- A quantum state generator $\text{Mint}(sk) \to |\psi\rangle$,
- A verification procedure $\text{Verify}(pk, |\psi\rangle) \in \{0, 1\}$.

Here, the pair of generated keys (pk, sk) is the public-key and secret-key, respectively. The security of such schemes is often based on computational assumptions resistant to quantum attacks, such as the hardness of lattice problems or quantum-secure hash functions [772,773]. An alternative approach is the work of Zhandry [774], who has proposed a public-key quantum money scheme based on

[41] See Section (2.5.4) where a similar idea is used for Quantum Key Distribution

 doi:10.20944/preprints202511.1802.v2

abelian group actions. The key idea is to create quantum states (called 'bolts') that are unclonable and non-reproducible, even by the entity that generated them — a stronger notion than traditional quantum money. This can be formalised as:

- Bolt Generation: **Gen()** $\mapsto \{|\psi_s\rangle, s\}$ which that outputs a quantum state $|\psi_s\rangle$ ('bolt') and serial number s.
- Verification: **Ver**$(|\psi_s\rangle) \mapsto s$ or $\perp$, which returns the serial number if valid or rejects, respectively.

The security of the *quantum lightning* is that no efficient quantum adversary can create two bolts $\{|\psi_1\rangle, |\psi_2\rangle\}$ such that both verify to the same serial number [773]. This goes beyond the no-cloning theorem and ensures computational unclonability even with access to the generation process. Making bill serial numbers public and unique allows anyone to verify the total money supply, offering transparency. Unlike physical cash, where a central bank could secretly print duplicates, this system prevents such manipulation. It reduces the need to fully trust central banks, which is especially useful in countries with a history of inflation.

There are currently a variety of proposed quantum money schemes, which can be categorised by the type of money:

1. **Quantum Bill** - Identifiable quantum money units with unique serial numbers, traceable across transactions (less anonymous) [577,769,771,775].
2. **Quantum Coins** - Indistinguishable quantum money units that offer user anonymity (untraceable) [776–779].
3. **Quantum Bolts** - Public quantum money with the additional guarantee that even the issuer cannot create duplicates with the same serial number [772,774,780,781].
4. **Quantum Smart Contracts**[42] - hybrid classical-quantum payment system based on classical blockchains capable and public-key quantum money quantum bolts (decentralised) [783,784].

Most of the modern constructions aim to preserve the physical unforgeability offered by quantum mechanics while enabling decentralised verification, a crucial property for practical deployment. However, some of these protocols are insecure [770] due to many factors, which include information leakage from the verification procedure, which can allow attackers to learn enough to forge the quantum money [772], unrealistic hardness assumptions (e.g., hidden subspace problems) [771], or inadequate modelling of adversaries especially quantum-capable ones [775].

On one hand, theorists continue to perform rigorous cryptanalysis of such proposed schemes, i.e., Bilyk et al. recently showed that Zhandry's quantum bolts scheme may be insecure [785]. On the other hand, experimentalists are performing proof-of-concept demonstrations of quantum money using coherent states of light [786,787] and quantum S-tokens, which eliminate reliance on quantum memories and long-distance quantum communication [578,788]. The latter approach by [578] has reported a quantified time advantage over optimal classical cross-checking protocols for transactions. This could potentially be adopted for applications requiring high security, privacy, and minimal transaction times, like financial trading and network control [578].

Quantum money presents a compelling blend of quantum physics and cryptography, where fundamental quantum principles like measurement uncertainty and the no-cloning theorem enforce properties that are otherwise unattainable in classical systems. The ongoing research into publicly verifiable schemes [25,26] may result in practical quantum-secure finance.

3.3.2. Economic Forecasting

Economic forecasting is the process of attempting to predict the future condition of the economy using a combination of widely followed indicators [789]. Government officials and business managers use economic forecasts to determine fiscal and monetary policies and plan future operating activities, respectively. In this section, we were explore some of the potential quantum computing use cases

[42] A smart contract is, in essence, a mechanism that enables parties to deposit funds and automatically release them once certain algorithmically verifiable conditions are met [782]. This makes it a formal tool for enforcing monetary incentives.

 doi:10.20944/preprints202511.1802.v2

for economic forecasting areas which includes time series analysis, synthetic data generation, and predicting financial disasters.

Time Series Analysis

Time series analysis, a fundamental pillar of quantitative analysis in economics and finance, involves examining sequences of data points collected over time to discern patterns, understand underlying dynamics, and ultimately forecast future values [790]. This methodology plays a crucial role for financial analysts in making informed investment decisions by providing insights into historical trends and enabling the prediction of future movements in key variables such as quarterly sales figures and daily asset returns. The consistent collection of data points at defined intervals allows for the observation of how variables evolve, revealing critical information about market behaviour and economic activity.

In contemporary financial and economic landscapes, the sheer volume and intricate nature of data present significant analytical challenges. Modern markets are characterised by non-linear relationships, high volatility, and complex interdependencies that often strain the capabilities of traditional computational methods [791]. This increasing complexity necessitates the exploration of novel computational paradigms capable of handling these intricate datasets and extracting meaningful insights with greater efficiency and accuracy. Given the inherent computational intensity of advanced time series analysis in finance and economics, quantum computing presents a compelling avenue for exploration [792].

First, let us introduce some key concept in time series analysis before describing the associated quantum algorithms that can potentially provide a performance boost. A time series is considered *covariance stationary* if its statistical properties, including the expected value (mean), the variance, and the covariance between values at different time points (autocovariance), remain constant over time [791]. Many time series encountered in economics and finance are non-stationary, meaning their statistical properties change over time, often exhibiting trends or seasonality [793]. In such cases, it is often necessary to transform the series into a stationary one, for example, by using techniques like differencing, before applying certain time series models [790,791]. Other key concepts include *seasonality* (patterns that repeat over a period), *trends* (general upwards or downward direction over time), and *noise* (random ups and downs) [791]. There are various models time series models that work better for some data-sets depending on their feature. In this review, we will outline a few classical models and associated quantum approaches for time-series analysis.

Classical Time Series Models A wide variety of time series forecasting models exist, utilising different mathematical approaches and varying in complexity. Among the most commonly used are the Auto-Regressive Integrated Moving Average (ARIMA) and Smoothing model families. In this review, we will outline the ARIMA models which is a is a class of models that predicts the future values of a given time series based on its own past values (lags) and the lagged forecast errors [794].

First, the Auto-Regressive (AR) models of order p, denoted as AR(p), posit that the current value of a time series is linearly dependent on its p most recent past values, along with a constant term and a random error term. Mathematically, this can be expressed as:

$$y_t = c + \sum_{i=1}^{p} \phi_i y_{t-i} + \epsilon_t \tag{190}$$

where y_t is the value at time t, c is a constant, ϕ_i are the auto-regressive parameters, and ϵ_t is the error term.

 doi:10.20944/preprints202511.1802.v2

Second, the Moving Average (MA) models [794] of order q, denoted as MA(q), suggest that the current value of the time series is a linear combination of the past q error terms and the current error term. The general equation for an MA(q) model is given by:

$$y_t = \mu + \sum_{i=1}^{q} \theta_i \epsilon_{t-i} + \epsilon_t \tag{191}$$

where μ is the mean of the series, θ_i are the moving average parameters, and ϵ_t represents the error term at time t.

Third, Auto-Regressive Moving Average (ARMA) models [794] of order (p, q), denoted as ARMA(p, q), combine the auto-regressive and moving average components to model stationary time series. An ARMA(p, q) model can be written as:

$$y_t = c + \sum_{i=1}^{p} \phi_i y_{t-i} + \sum_{i=1}^{q} \theta_i \epsilon_{t-i} + \epsilon_t, \tag{192}$$

encompassing the dependencies on both past values of the series and past error terms.

Fourth, for time series that exhibit non-stationarity, the ARIMA model of order (p, d, q) is widely used [795]. The 'Integrated' (I) part, denoted by d, refers to the number of times the raw observations are differenced to achieve stationarity. The ARIMA model essentially fits an ARMA(p, q) model to the d-th difference of the series. Using the backshift operator B, where $B^k Y_t = Y_{t-k}$, the general form of an ARIMA(p, d, q) model is [795]:

$$\phi_p(B)(1 - B)^d Y_t = \theta_q(B) a_t, \tag{193}$$

where

$$\phi_{(p,q)}(B) = 1 - \phi_1 B - \cdots - \phi_{(p,q)} B^{(p,q)} \tag{194}$$

are the auto-regressive p and moving average q polynomials in the backshift operator, respectively, and a_t is the white noise error term.

Fifth, to model the time-varying volatility often observed in financial time series, the Generalized Autoregressive Conditional Heteroskedasticity (GARCH) model of order (p, q) is employed [796]. The GARCH(p, q) model posits that the conditional variance of the error term at time t, denoted by σ_t^2, depends on the q most recent lagged squared error terms (ARCH terms) and the p most recent lagged conditional variances (GARCH terms) [796]. The mathematical formulation for the conditional variance is [796]:

$$\sigma_t^2 = \omega + \sum_{i=1}^{p} \alpha_i \epsilon_{t-i}^2 + \sum_{j=1}^{q} \beta_j \sigma_{t-j}^2, \tag{195}$$

where ω is a constant, α_i are the coefficients for the ARCH terms, and β_j are the coefficients for the GARCH terms

Sixth, the Kalman Filter provides a different framework for time series analysis by employing a state-space representation to estimate unobserved variables [797]. It is a recursive algorithm that operates through prediction and update steps based on a system's dynamic model and noisy measurements. The core of the Kalman Filter lies in two key equations: the *state transition equation* and *measurement equation* given by [797]

$$x_{k+1} = \Phi x_k + w_k \quad \text{and} \quad z_k = H x_k + v_k, \tag{196}$$

which describes how the system's state evolves over time and relates the measurements to the system's state, respectively. Here, x_k is the state vector, Φ is the state transition matrix, w_k is the process noise, z_k is the measurement vector, H is the measurement matrix, and v_k is the measurement noise.

The increasing volume of financial and economic data, coupled with the need to analyse high-dimensional time series (i.e., series with many variables observed over time), poses significant com-

 doi:10.20944/preprints202511.1802.v2

putational demands and scalability issues for classical methods. As the number of data points and the number of variables increase, the computational time and resources required for parameter estimation, forecasting, and validation can grow substantially, potentially hindering real-time analysis and decision-making [792]. Hence, quantum computing approaches have become attractive to many researchers and practitioners.

Quantum Approach There has been numerous proposals for performing time-series analysis on a quantum computer. A quantum analogue to the classical ARIMA model is proposed in [798] where the potential speed-up comes from employing the QFT as a subroutine (see Section 2.1.1). However, most proposals for time series analysis on quantum computers are based on QML methods discussed in section (2.4). In particular, QNN which can be designed with fewer parameters than their classical counterparts while potentially achieving comparable or even improved accuracy, especially for complex time series signals such as explored in [799]. Proof-of-concept time series predictions of important economical factors such as the amount of rainfall fall and electric load power were implemented using QNN in [792] and the reported results were comparable to classical methods used in the study. Another variant of QML methods are approaches are based on quantum RNN explored in [800] where they also reported comparative results to classical methods when trained on real-world data.

One may ask the question: how do these QML models compare with classical methods for time series forecasting. An answer is found in a benchmarking study [801] where they found that in overall, state-of-the-art classical models currently outperforms their counterpart quantum models. However, most of the quantum models were able to achieve comparable results to classical methods, and for one data set two quantum models outperformed the classical ARIMA model [801]. These benchmarking results highlight the need for more research to develop better quantum models so that as quantum hardware increases in capabilities they may have a good chance to achieve Practical Quantum Advantage.

Synthetic Data Generation

Synthetic Data Generation (SDG) has become a vital tool for training ML models [802], particularly in fields like finance where access to sensitive data is limited. SDG allows for ML practitioners to generate artificial datasets that resemble real-world data while avoiding many of the regulatory and logistical challenges associated with accessing sensitive financial information [803]. Banks and financial institutions, for example, can benefit from larger and more diverse datasets for risk modelling [804] and stress testing [805], especially when relevant data are scarce or do not reflect rare market events [804]. Customer behaviour analysis can also become less constrained by strict data protection rules and avoid exposing sensitive consumer information since artificial datasets preserve important statistical relationships. Therefore, researchers and regulators often use synthetic datasets to compare or benchmark different predictive models, enabling a more transparent comparison of outcomes.

Mathematical Formulation Most SDG techniques focus on learning the underlying distribution $p(\mathbf{x})$ of real data samples $\mathbf{x}$ [802,806] (e.g., multiple financial variables such as asset prices or macroeconomic indicators), and construct a model $G_\theta(\mathbf{z})$ (generative model) which transforms variables $\mathbf{z}$ from a known prior distribution $p(\mathbf{z})$ [803], such as a Gaussian or uniform distribution into synthetic samples $\widehat{\mathbf{x}} = G_\theta(\mathbf{z})$ [804]. The objective is typically to minimise a discrepancy measure between the real data distribution $p(\mathbf{x})$ and the synthetic distribution $q_\theta(\mathbf{x})$ (see section 2.4.2.2). In finance, this typically means learning a high-dimensional distribution that captures complex patterns, such as correlations across multiple assets[807] or autocorrelations in time series [808]. Additionally, financial use cases often involve constraints; for instance, a synthetic dataset used in stress testing needs to accurately reflect tail risk behaviour; this can be encouraged by the use of penalty functions or regularisers [809–811].

 doi:10.20944/preprints202511.1802.v2

Classical Method GANs have been the leading choice for these tasks [812], using a generator to create artificial data and a discriminator to distinguish between genuine and synthetic samples [813]. Over the past decade, various extensions of GANs have improved performance. However, challenges such as training instability [814] and the considerable computational resources required to handle large-scale data persist [804,815]. VAEs have also been explored, showing promise in producing correlated asset returns and improve model's interpretability [816]. However, they can sometimes struggle with retaining sharp details of complex distributions [804].

Quantum Approach More recently, researchers have been exploring quantum computing for synthetic data generation [817]. For example, the use of QGANs [818] to reduce mode collapse and can potentially capture intricate financial patterns more fully. Other approaches, such as Quantum Boltzmann Machines, rely on quantum Hamiltonians to define their energy landscapes [819], which can help to explore complex financial dependencies more efficiently than classical methods. Quantum Annealing-based is also explored by using quantum tunnelling to sample from distributions that reflect realistic market conditions [9,820]. Despite promising theoretical insights, practical applications remain limited by hardware constraints and the often difficult task of mapping financial data to the relevant quantum models.

A proof-of-concept demonstration can be found in [196], where they used a QGAN framework to learn and approximate classical probability distributions, such as log-normal or bimodal distributions (which are commonly used in financial modelling) to load these distributions into quantum circuits efficiently. This approach can significantly reduce the resource overhead required for data loading (which is a bottleneck in quantum algorithms). The QGAN framework prepares quantum states that approximate these distributions with high fidelity by learning a quantum representation of the target probability distribution [818]. The main application involves pricing financial derivatives, specifically European call options [181], by integrating the learned quantum states that represent the learned asset price distribution into a QAE algorithm. This integration shows a potential pathway for quantum computing to transform computationally intensive financial tasks, providing faster and more accurate derivative pricing and risk management methods, even with near-term quantum devices [702]. However, as with other quantum-based models, current NISQ hardware limitations and the complexities of scaling remain a challenge [821].

Despite these challenges, quantum computing could improve SDG for finance as quantum technology improves [822]. Progress in QEC and hardware scalability may facilitate the development of more powerful quantum models that can handle large-scale financial data. This might deliver improvements in areas such as high-frequency trading, stress testing, and modelling rare but critical market behaviour [805].

Predicting Financial Crises

A financial crisis is often associated with a panic or a bank run, during which investors sell off assets and withdraw cash from savings accounts, because they fear the value of those assets will drop, or the bank will collapse, respectively [823]. In such a crisis, asset prices see a steep decline in value, businesses and consumers are unable to pay their debts, and financial institutions experience liquidity shortages [824]. Other situations that may be labelled a financial crisis include the bursting of a speculative financial bubble, a stock market crash, a sovereign default, or a currency crisis [824]. A crisis may be limited to banks or spread throughout a single economy, the economy of a region, or economies worldwide.

The problem of predicting crises is therefore of great importance, and can be approached using a number of techniques, from modelling the evolution of markets, to detecting outlier events or identifying inconsistencies in the equilibrium of market values [824]. Mathematical models for predicting crises typically involves non-linear terms and interactions between many components [825]. These non-linear terms make prediction the behaviour difficult and computationally demanding for

 doi:10.20944/preprints202511.1802.v2

traditional classical methods. Below, we outline one promising approach that can be naturally mapped onto Quantum Annealing to potentially achieve a computational advantage [826].

Mathematical Formulation The problem of predicting financial crises can be represented by a financial network graph [825] where nodes represent entities and the edges represent how the worth of each entity is connected or depends upon other entities (see example in Figure 9). Analysing such networks is invaluable for predicting financial crises.

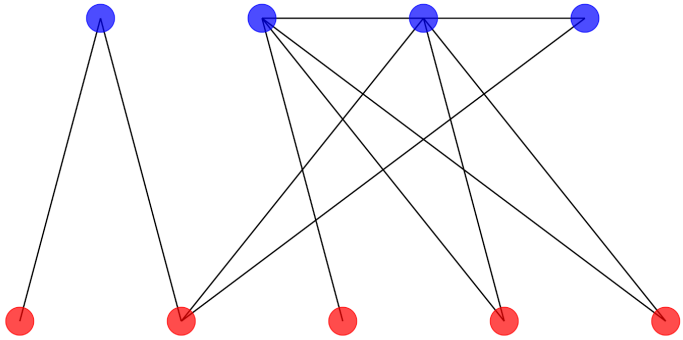

Figure 9. An example of a random financial network with 4 institutions (blue/top-row) and 5 assets (red/bottom-row).

Following the formulation in [346,825], we assume a financial network that has E entities and A assets. Let the vector $\vec{w}_e \in \mathbb{R}^A_{\geq 0}$ denote the worth of each asset that the entity $e \in [0, E-1]$ owns. We also assume assets in A are co-owned by multiple entities and a matrix $D \in \mathbb{R}^{E\times A}_{\geq 0}$ containing the percentage of ownership by an entity E of a co-owned asset. Furthermore, entities can have cross-holdings in other financial entities in the network, represented by a matrix $C \in \mathbb{R}^{E\times E}_{\geq 0}$ and the self-ownership of an entity can be found via the diagonal matrix $\tilde{C}$ such that $\tilde{C}_{jj} := I - \sum_i C_{ij}$. From the above definitions, it follows that one can define the market valuations for the assets associate with an entity as [825]:

$$\vec{v} = \tilde{C}(I - C)^{-1}(D\vec{w} - \vec{\lambda}(\vec{v}, \vec{w}))., \tag{197}$$

where $\vec{\lambda}$ is the *failure vector* that models a drop in the equity valuation including effects beyond a certain critical point. When such a failure occurs, there is generally loss of investor confidence as the entity is unable to cover operating costs. Hence, the goal is to find an equilibrium value for $\vec{v}$ where the entity is considered stable, which has been shown to be an NP-Hard optimisation problem [825] as the inter-dependencies of the network can be very complex for a large financial network.

Quantum Approach The first proposal to tackle this problem on quantum computers was by Orus et al. [827] where they reformulated it as a QUBO. First, they define a cost function:

$$F(\vec{v}) \equiv \left[\vec{v} - \tilde{C}(I - C)^{-1}\Big(D\vec{w} - \vec{\lambda}(\vec{v} - \vec{w})\Big)\right]^2 \geq 0. \tag{198}$$

which is strictly larger than zero away from equilibrium and zero (i.e., minimum) at equilibrium value of $\vec{v}$. Hence, the classical cost function $F(\vec{v})$ will be minimised when the vector $\vec{v}$ is at equilibrium. One can approximate the values of the vector by binary variable $v_i \approx \sum_{k=-q}^{q} 2^k x_{i,k}$ with $2q+1$ classical bits. It is straightforward to define an associated binary vector $\mathbf{x}^*$ that gives the minimum for the following Higher-order Unconstrained Binary Optimisation (HUBO) cost function [827]:

$$f_Q(\mathbf{x}) = \mathbf{x}^T Q \mathbf{x} = \sum_{i=1}^{n}\sum_{j=1}^{n} Q_{ij} x_i x_j, \tag{199}$$

 doi:10.20944/preprints202511.1802.v2

where Q incorporates all the non-linear constraints. As shown in [827], Equation (199) can then be approximated by Pauli-z matrices and two-qubit interactions[43] which reduces the problem into a QUBO that can be run on a QAnn to predict a potential massive failure of financial institutions after a small shock to the system. Ding et al. [826] also experimentally implemented this approach for assessing financial equilibrium but not the crash itself. Fellner et al. [828] formulated the problem in a similar way to Equation (199), but instead use gate-based computers and QAOA to solve it. The current bottleneck for these quantum methods is mapping the HUBO problem to available quantum hardware that is small in scale [826,828], hence we expect that future implementations to be different as the hardware scales up.

4. Summary and Outlook

In this review, we have surveyed some use cases of quantum computing for finance and economics. Our approach is to first outline the technical constructions of the quantum algorithms in four problem domains that are relevant for finance and economics, namely: simulation, optimisation, machine learning, and cryptography. Following, we review the mathematical formulation of the use cases (i.e., computational problems encountered in finance and economics) and map their quantum computing solution(s) to the quantum algorithms described in the first part. This is summarised in Figure 10, where the four problem categories (top row) are mapped to several use cases (middle row), which are then mapped to pertinent quantum algorithms (bottom row). The benefit of this structure is that it makes it easier to work out the technical details of the use-case formulation/solution and quantum algorithm separately. This allows one to easily spot opportunities of reformulating the use-case into another problem class, and thus utilising a different quantum algorithm. For example, the option pricing problem is often formulated as computing an expectation value, which makes Quantum Monte Carlo Integration suitable as a solver. However, as discussed in Section (3.1.2.1), the same problem can be formulated as a Stochastic Differential Equation, which can be solved by quantum solvers for PDEs, which includes Hamiltonian simulation. Furthermore, we hope this structure will help experts in other technical fields, i.e., with little or no background in quantum computing, to collaborate and contribute in improving quantum algorithms and application so that we can achieve Practical Quantum Advantage (PQA). In the ensuing section, we will discuss a potential path to achieving PQA.

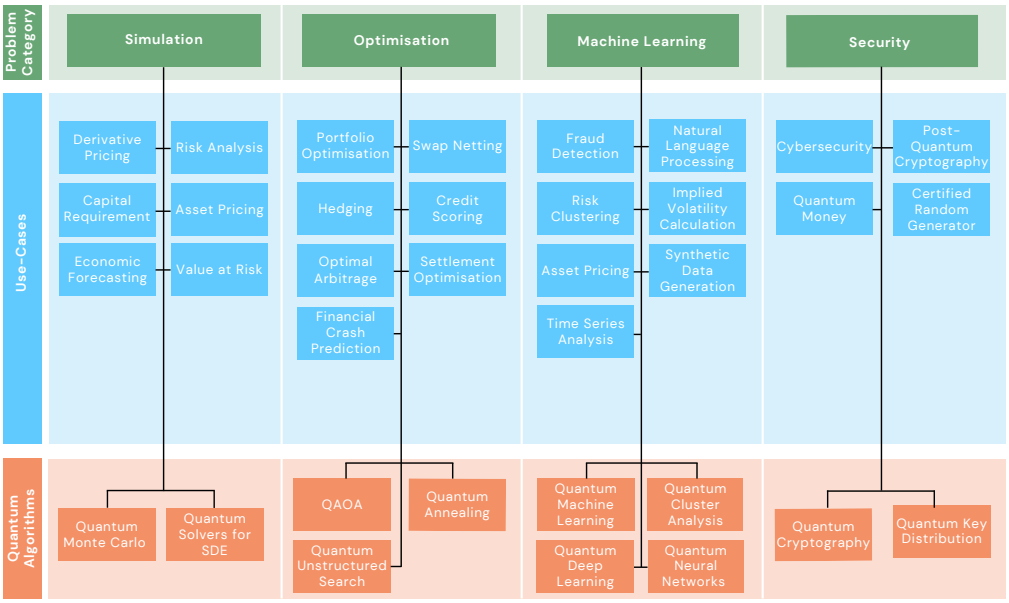

Figure 10. A mapping between use cases and applications for each of the main problem categories in quantum finance and economics.

[43] The goal is to find an effective Hamiltonian with the same low-energy subspace and at most two-qubit interactions [827].

 doi:10.20944/preprints202511.1802.v2

4.1. Path Towards Practical Quantum Advantage

The definition for PQA and related concepts is given Section (1.1). Here, we give an overview of some of the key ingredients towards achieving the goal of PQA in finance and economics. While about to complete this manuscript, we were made aware of Ref. [199] that proposes overlapping ideas for the path to PQA as described below.

4.1.1. Scaling Quantum Hardware

The core limiting factor towards PQA is the scale and noise-tolerance of quantum hardware. A lot of hardware engineers, physicists, quantum theorists, control system specialists and application engineers are working to solve this challenge. The NQCC hosts an annual *Quantum Computing Scalability Conference* [829] which discusses various aspects of this challenge, including Quantum Error Correction (QEC), qubit and gate performance, integrated photonics & qubit addressability, cryo-engineering technology, control systems, and quantum computing networking. It is an incredible challenge to scale up quantum hardware to meet the requirements of practical applications, albeit significant progress has been made thus far.

Many hardware manufacturing companies, especially ones with full-stack services, have made their development road map public. Most of the gate-based companies anchor their targets towards achieving Universal Fault-Tolerant (UFT) with net-positive QEC. The idea of QEC comes from the *quantum threshold theorem* (or quantum fault-tolerance theorem), which states that a gate-based quantum computer with a physical error rate below a certain threshold can, through application of QEC schemes, suppress the logical error rate to arbitrarily low levels [830–832]. This has been the foundational theory for why quantum computers can be made fault-tolerant, which is analogous to von Neumann's threshold theorem for classical computation [833]. Hence, for such systems, an important milestone in the NISQ era is proof-of-concept demonstrations of QEC, where a net positive benefit has already been achieved in small-scale experiments [834–838].

The next major milestone is for these systems to scale up to MegaQuOp machines capable of performing a million coherent operations [165]. This is along the path from NISQ-era to UFT. The ambitious goal of the UK's National Quantum Strategy Mission 1 is to have TeraQuOp quantum machines that are capable of performing a trillion coherent operations by the year 2035 [839]. If that is achieved, the resulting productivity gains could provide significant economy-wide boosts, as projected by Oxford Economics [19]. Along with key progress in the quantum stack, such milestones will more likely meet or exceed McKinsey's $622 billion projected value generated by quantum computing in finance by year 2035 [20].

Although other non-gate-based quantum computers do not have the same qubit-based road-maps, they still have scalability challenges. For example, photonic QPUs seek to scale *measurement based quantum computing* with large error-corrected cluster states [840]. Irrespective of the QPU modality, the scaling of quantum hardware and error correction are expected to be the keys that unlock Practical Quantum Advantage.

4.1.2. Application Benchmarks

In the meantime, while we still do not have UFT quantum computers or large-scale Quantum Annealing, what will speed up the advent of PQA is having readily accessible Up-to-date Application Benchmarks (UAB). As quantum computers are advancing, so are classical systems and associated algorithms. In some instances, where a quantum advantage has been claimed over the best known classical algorithm, researchers may find a classical method that achieves better results than originally compared to. A notable example is Ewin Tang's quantum-inspired classical algorithm for recommendation systems [146], which showed that the previously claimed quantum exponential speed-up by Kerenidis and Prakash [134] is no longer valid compared to her new algorithm. A similar case exists for practical applications benchmarks, when certain performance achievements are claimed by a quantum method, there may exist better classical implementations that achieve equal or better performance. A

 doi:10.20944/preprints202511.1802.v2

recent example is the ML vs QML benchmarking in [415], which found that across all experiments in that case, the out-of-the-box classical models systematically outperformed the quantum models considered.

Therefore, it would be beneficial for speeding up research if there were central repositories with UAB for classical, hybrid, and quantum methods. We note that there are sites that have some benchmarking problems like Kaggle data-sets [841] for ML, sparse-matrix collections that arise in real-world applications [842,843], and published benchmark papers for optimisation problems [233,236]. However, to the best of our knowledge we have not yet seen sites/publications with UAB that provides both problem data and state-of-the-art performance metrics for classical, hybrid, and quantum algorithms. This remains a gap in the community which if filled, would spur progress towards achieving PQA sooner than otherwise.

4.1.3. Quantum Middleware

The term Quantum Middleware (QM) refers to the middle layers of the quantum computing stack, sitting between quantum hardware (which occupies the bottom of the stack) and quantum applications (which sit at the top) [844–846]. It is generally comprised of software packages that provide layers of abstraction which enable applications engineers to focus on developing solutions using quantum algorithms while masking hardware complexities.

In the path towards PQA, QM will become very important in the quantum ecosystem as it can potentially speed up and simplify the process of developing industry applications. Some key desirable features for QM are:

1. Tools for minimising quantum computation errors which include quantum error suppression, quantum error-mitigation, and Quantum Error Correction.
2. Circuit compilation tools that perform optimal circuit compression and embedding to specific quantum hardware.
3. Heterogeneous computation [847] which involves the use of different types of computing hardware such as CPUs, GPUs, and QPUs. The QM will essentially be an orchestrator that manages the execution of tasks on distributed computing resources.
4. Application libraries for various classes of problems with state-of-the-art algorithms.

As use cases become increasingly complex and quantum hardware becomes more sophisticated, most applications engineers will rely on QM to speed-up the development process.

4.2. Quantum Algorithms

In this review, we discussed the technical details of quantum algorithms in four problem domains: simulation, optimisation, machine learning, and cryptography. Here, we summarise and give key takeaways from these quantum algorithms.

4.2.1. Quantum Simulation

Originally developed for solving problems that are quantum in nature [2,3], i.e., they can be expressed as Hamiltonian dynamics in Hilbert space, quantum simulation is a useful tool for non-quantum problems [180]. In section (2.2), we focused on two classes of algorithms: QMCI and quantum solvers for SDE.

Quantum Monte Carlo Integration This is the quantum analogue of the classical Monte Carlo Integration which has the potential of a quadratic speed-up over its classical counterpart [5,193]. In general, the MCI is favoured in many industry applications, especially in finance and economics because they can better handle non-linear and high-dimensional problems as they scale independently of the problem size. However, as discussed in Section (2.2.1), MCI has a slow convergence, requiring a large number of samples for accuracy, which can be computationally intensive and time-consuming. Thus, the potential quadratic speed-up offered by QMCI is attractive to researchers, albeit it is not

 doi:10.20944/preprints202511.1802.v2

trivial to realise it practically. There are hardware and algorithmic challenges with QMCI, discussed in Section (2.2.1), which must be solved in order achieve PQA.

Quantum Solvers for SDEs The fields of finance and economics uses Stochastic Differential Equations to model quantities affected by randomness such as stock prices and economic crises. In Section (2.2.2) we discussed how SDEs can be reformulated as PDEs via the Feynman-Kac formula. Quantum solvers for PDEs can then be used such as ones based on finite-difference methods [848]. We also outlined more sophisticated methods of mapping the PDE to a Schrödinger-like equation [219] and then solving it via Hamiltonian simulation methods. It is currently not fully known if such methods can realise a PQA, especially for real-world problems [48], hence research and proof-of-concept demonstrations are ongoing.

4.2.2. Quantum Optimisation

Quantum Optimisation, explored in section (2.3), is another widely-studied application domain of quantum computing, with a huge diversity of use cases across a range of industrial sectors [236]. A subset relevant to finance and economics is discussed in sections (3.1-3.3), which includes portfolio optimisation, optimal arbitrage identification, and others. Quantum algorithms such as the QAOA and VQE, as well as Quantum Annealing, are common choices due to their flexibility, as well as their suitability for running on NISQ hardware. Similarly to the above, several recent papers have proposed a theoretical quantum advantage [236,849], but limitations posed by current hardware, as well as improving classical algorithms, have prevented incontrovertible proof of an empirical advantage. There also remain some open problems in the field, including dealing with barren plateaus [154] and ensuring constraint satisfaction [236].

4.2.3. Quantum Machine Learning

As explored in section (2.4), QML shows promise across different ML paradigms, from supervised classification and regression to unsupervised clustering and reinforcement learning.

A significant limitation in many QML algorithms is the assumption of efficient data loading into quantum states through QRAM to provide rapid access to large volumes of classical data [11,337]. While algorithms such as quantum k-means [299] and quantum nearest neighbour [327] report polynomial or even exponential speed-ups under QRAM assumptions [11], no fault-tolerant, scalable QRAM has yet been realised [341]. This could change as researchers collaboratively work on the development of QRAM [850]. Moreover, data encoding (e.g., amplitude or angle encoding) is non-trivial and may negate any theoretical speed-up if performed inefficiently [477]. Another challenge is the limitations of current hardware, with short coherence times, gate errors and highly affected by noise.

Adding to this is the lack of consistent algorithm and application benchmarks (such as UAB described above) for assessing quantum advantage in QML. Many QML demonstrations are on synthetic or contrived datasets with idealised assumptions about data encoding or oracle access [415,801]. Without consistent/accepted benchmarks, it remains challenging to ascertain whether demonstrated improvements reflect a genuine quantum advantage or merely misrepresents results. Nonetheless, identifying problem setups/formulations/types where quantum computing could provide an advantage, and the associated assumptions, is beneficial in-and-on itself both for problem/algorithm selection and bottlenecks identification.

4.2.4. Quantum Cryptography

Cryptography and cybersecurity are one of the most well-known sectors of impact by quantum computing, with Shor's algorithm - see Section (2.5.2.1) - being widely discussed and researched since it was conceived [540]. As discussed in section (2.5), most modern encryption relies on hard mathematical problems being intractable on classical computers. However, some of these problems are theoretically solvable on a fully fault-tolerant quantum computer in a reasonable amount of time. As a result, multiple national agencies and technology companies are performing intensive research into

 doi:10.20944/preprints202511.1802.v2

new and updated *quantum-safe* protocols which are resistant to such attacks [706]. This has culminated in the recent release of a few standard algorithms, which many organisations have already started incorporating [553–555]. Given the current resource estimates of quantum hardware requirements to execute known quantum decryption algorithms (in terms of number of qubits, gate depth, and the likely requirement for QEC [542]), it seems unlikely that a cryptographically relevant decryption will happen in the next few years [543,544]. However, financial institutions that generally deal with sensitive data should plan for a migration of their systems to quantum-safe protocols [563]. An earlier migration will lower the risk of *harvest now, and decrypt later* type of security attacks [521].

4.3. Use Cases

This technical review is dedicated to use cases of quantum computing in finance and economics. These can be broadly categorise into use cases that: (i) have a potential advantage, and (ii) a speculative adoption.

4.3.1. Potential Advantage

Most of the quantum algorithms examined here exhibit theoretical speed-ups or potential better performance compared to current classical algorithms. Therefore, organisations or practitioners may find it optional to use quantum or hybrid quantum-classical approaches for their computational needs. If quantum computing is incorporated, the sector stands to benefit from two kinds of quantum advantage:

- *Speed-up*: we can broadly classify use cases that depend of quantum simulation and quantum optimisation as top candidates to realise faster runtimes; see sections (2.2) and (2.3). These include use cases in option pricing, portfolio optimisation, hedging, economic forecasting, etc; see sections (3.1) to (3.3). It should be noted that the analysis performed in this review does not take into account delays caused by internal processes and regulatory requirements. It might be possible that for some of these use cases the difference in potential speed-up is not significant enough to matter when all the non-computational factors are considered. However, we expect that large organisations with global operations or companies with large-scale portfolios will need quantum solutions to remain competitive in fast-changing markets.
- *Accuracy*: in general, use cases based on QML may have the benefit of better accuracy of model predictions compared to classical models; see section (2.4). This has a huge impact on use cases like fraud detection, where the classification accuracy of the model is far more important than the speed of training [851]. The same rationale applies to risk analysis, economic forecasting, etc, see sections (3.2) and (3.3).

However, as noted in Section (4.1), both quantum hardware and algorithms would need to significantly improve to realise these benefits. Hence, in the long term, quantum computing is expected to provide direct computational advantages and also to deliver substantial indirect benefits by accelerating the development of novel computational methods and inspiring new insights in classical algorithm development.

Speculated Adoption

In this review, we also considered use cases of quantum computing whose adoption can only be speculated at this point. These use cases include:

- *Quantum Money* [26] - a form of currency that is extremely difficult or even impossible to forge due to security guarantees from quantum mechanics.
- *Quantum Assets* [608] - a class of assets that are quantum in nature and traded in a quantum market enabled by quantum computers.

These use cases represents the potential transformative impact of quantum computers beyond speed-up and accuracy benefits. The former use-case, quantum money, has a long history dating back to 1980s when Stephen Wiesner proposed the first formulation of private-key quantum money [577]. As

 doi:10.20944/preprints202511.1802.v2

discussed in Section (3.3.1), the field has grown over the years to the point that there now exist several experimental proof-of-concept demonstrations of quantum money [578,786–788]. A notable recent experiment is that of Jiang et al. [578], where they reported a time advantage over optimal classical cross-checking protocols for transactions over significantly long inter-city distances. If these results are reproducible, they will stand as one of the first realisation PQA in finance and economics. This is because, the protocol of could potentially be used for applications requiring high security, privacy and minimal transaction times, like financial trading and network control [578].

Therefore, one might speculate that quantum money might create a niche market of specialised usage. In the medium-term quantum money might become like crypto-currencies in the sense that it will only be utilised by a small fraction of the global market. However, irregardless of adoption to the economy, we expect that the concepts of both quantum money and quantum assets will feature directly or indirectly in many other technological advancements. For example, the authors in [783] have shown how quantum money can be coupled with blockchain technologies like Bitcoin to enhance the formation of smart contracts. Therefore, we predict that there is a significant chance of unforeseeable breakthroughs that would make these proposals become mainstream use-case in the global economy, and we are optimistic of such a line of research.

4.4. Further Research Directions

Given the findings and use cases discussed, several important research directions seem promising for future exploration. For example, quantum computing methods for predicting financial crises [824,826] seem feasible in near-term quantum hardware and could have a significant impact. Furthermore, as global markets are becoming more interconnected, classical methods may soon reach the limit of what they can simulate in a reasonable time when considering large data sets and a huge number of constraints for optimisation problems.

Other interesting long-term use cases are quantum money [25] and quantum assets [608]. While practical implementations of these use cases are still in their infancy, their theoretical frameworks and/or experimental advancements are promising and certainly an area for further exploration.

The pace of the field is exemplified by the fact that while this manuscript was under internal review, some papers showing promising progress were published which include quantum enhanced computation of institutional algorithmic bond trading [852], sampling-based VQA for portfolio construction [853], regulatory considerations of quantum computing applications in financial services [854], a new record two-qubit gate fidelity of 99.99% by a trapped-ion quantum computer [855], and a claim by Google and collaborators of a Practical Quantum Advantage [856]. All these recent developments, including this year's Nobel Prize award in physics [857], being related to experiments that have contributed to quantum hardware, attest to the optimism that quantum computing will deliver real-world value. However, we still maintain, as recently noted by Eisert and Preskill [858], that the field still has some major gaps to fill in the space between NISQ and future fault-tolerant application-scale quantum computers that will unlock widespread Practical Quantum Advantage.

Author Contributions: Konstantinos Georgopoulos (KG) conceived the work and its structure, and carried out an initial survey of the landscape for fintech problems with potential solutions in quantum computing. The landscaping was then continued and completed by Manqoba Hlatshwayo (MQ), Manav Babel and Dalila Islas-Sanchez. MQ led the delivery of the technical content. All authors contributed equally to the writing of the manuscript. KG was responsible for overall supervision of the work. The manuscript was then proof-read and revised by all authors.

References

1. Phys, N.R. 40 years of quantum computing. *Nature Reviews Physics* **2022**, *4*, 1–1.
2. Feynman, R.P. Simulating physics with computers. *International Journal of Theoretical Physics* **1982**, *21*, 467–488.
3. Lloyd, S. Universal Quantum Simulators. *Science* **1996**, *273*, 1073–1078.

 doi:10.20944/preprints202511.1802.v2

4. Grover, L.K. A fast quantum mechanical algorithm for database search. In Proceedings of the Proceedings of the twenty-eighth annual ACM symposium on Theory of computing, 1996, pp. 212–219.
5. Montanaro, A. Quantum speedup of Monte Carlo methods. *Proceedings of the Royal Society A: Mathematical, Physical and Engineering Sciences* **2015**, *471*, 20150301.
6. Harrow, A.W.; Hassidim, A.; Lloyd, S. Quantum Algorithm for Linear Systems of Equations. *Phys. Rev. Lett.* **2009**, *103*, 150502.
7. Berry, D.W. High-Order Quantum Algorithm for Solving Linear Differential Equations. *Journal of Physics A: Mathematical and Theoretical* **2014**, *47*, 105301.
8. QUANTUMPEDIA – The Quantum Encyclopedia. A Brief History of Quantum Computing. Accessed 2025-07-15.
9. Orús, R.; Mugel, S.; Lizaso, E. Forecasting financial crashes with quantum computing. *Phys. Rev. A* **2019**, *99*, 060301.
10. Aaronson, S. How Much Structure Is Needed for Huge Quantum Speedups? *arXiv* **2022**.
11. Aaronson, S. Read the fine print. *Nature Physics* **2015**, *11*, 291–293.
12. Bouland, A.; van Dam, W.; Joorati, H.; Kerenidis, I.; Prakash, A. Prospects and challenges of quantum finance, 2020.
13. Preskill, J. Quantum computing and the entanglement frontier. *arXiv preprint* **2012**.
14. Arute, F.e.a. Quantum supremacy using a programmable superconducting processor. *Nature* **2019**, *574*, 505–510.
15. Zhong, H.S.; Wang, H.; Deng, Y.H.; Chen, M.C.; Peng, L.C.; Luo, Y.H.; Qin, J.; Wu, D.; Ding, X.; Hu, Y.; et al. Quantum computational advantage using photons. *Science* **2020**, *370*, 1460–1463.
16. Madsen, L.S.; Laudenbach, F.; Askarani, M.F.; Rortais, F.; Vincent, T.; Bulmer, J.F.F.; Miatto, F.M.; Neuhaus, L.; Helt, L.G.; Collins, M.J.; et al. Quantum computational advantage with a programmable photonic processor. *Nature* **2022**, *606*, 75–81.
17. Gao, D.e.a. Establishing a New Benchmark in Quantum Computational Advantage with 105-qubit Zuchongzhi 3.0 Processor. *Physical Review Letters* **2025**, *134*, 090601.
18. Kim, Y.; Eddins, A.; Anand, S.; Wei, K.X.; van den Berg, E.; Rosenblatt, S.; Nayfeh, H.; Wu, Y.; Zaletel, M.; Temme, K.; et al. Evidence for the utility of quantum computing before fault tolerance. *Nature* **2023**, *618*, 500–505.
19. Oxford Economics. Ensuring that the UK can capture the benefits of quantum computing, 2025. Commissioned by IBM and Oxford Quantum Circuits.
20. Gschwendtner, M.; Morgan, N.; Soller, H. Quantum technology use cases as fuel for value in finance, 2023. Last accessed: 14-10-2024.
21. Ménard, A.; Ostojic, I.; Patel, M.; Volz, D. A game plan for quantum computing. *McKinsey Quarterly* **2020**.
22. Auer, R.A.; Angela, D.; Leonardo, G.; Joon, S.P.; Koji, T.; Andras, V. *Quantum computing and the financial system*; Number no 149 in BIS papers, BIS, Bank for International Settlements, **2024**.
23. Egger, D.J.; Gambella, C.; Marecek, J.; McFaddin, S.; Mevissen, M.; Raymond, R.; Simonetto, A.; Woerner, S.; Yndurain, E. Quantum Computing for Finance: State-of-the-Art and Future Prospects. *IEEE Transactions on Quantum Engineering* **2020**, *1*, 1–24.
24. Alcazar, J.; Leyton-Ortega, V.; Perdomo-Ortiz, A. Classical versus quantum models in machine learning: insights from a finance application. *Machine Learning: Science and Technology* **2020**, *1*, 035003.
25. Hull, I.; Sattath, O.; Diamanti, E.; Wendin, G. Quantum Technology for Economists. *arXiv* **2020**.
26. Hull, I.; Sattath, O.; Diamanti, E.; Wendin, G. *Quantum Technology for Economists*; Contributions to Economics, Imprint: Springer: Cham, **2024**.
27. Pistoia, M.; Ahmad, S.F.; Ajagekar, A.; Buts, A.; Chakrabarti, S.; Herman, D.; Hu, S.; Jena, A.; Minssen, P.; Niroula, P.; et al. Quantum Machine Learning for Finance ICCAD Special Session Paper. In Proceedings of the 2021 IEEE/ACM International Conference On Computer Aided Design (ICCAD). IEEE, **2021**.
28. García, D.P.; Cruz-Benito, J.; García-Peñalvo, F.J. Systematic Literature Review: Quantum Machine Learning and its applications. *arXiv* **2022**.
29. Albareti, F.D.; Ankenbrand, T.; Bieri, D.; Hänggi, E.; Lötscher, D.; Stettler, S.; Schöngens, M. A Structured Survey of Quantum Computing for the Financial Industry. *arXiv* **2022**.
30. Herman, D.; Googin, C.; Liu, X.; Sun, Y.; Galda, A.; Safro, I.; Pistoia, M.; Alexeev, Y. Quantum computing for finance. *Nature Reviews Physics* **2023**, *5*, 450–465.

 doi:10.20944/preprints202511.1802.v2

31. Gómez, A.; Leitão, A.; Manzano, A.; Musso, D.; Nogueiras, M.R.; Ordóñez, G.; Vázquez, C. A Survey on Quantum Computational Finance for Derivatives Pricing and VaR. *Archives of Computational Methods in Engineering* **2022**, *29*, 4137–4163.
32. Chang, Y.J.; Sie, M.F.; Liao, S.W.; Chang, C.R. The Prospects of Quantum Computing for Quantitative Finance and Beyond. *IEEE Nanotechnology Magazine* **2023**, *17*, 31–37.
33. Naik, A.S.; Yeniaras, E.; Hellstern, G.; Prasad, G.; Vishwakarma, S.K.L.P. From portfolio optimization to quantum blockchain and security: a systematic review of quantum computing in finance. *Financial Innovation* **2025**, *11*, 88.
34. Saxena, A.; Mancilla, J.; Montalban, I.; Pere, C. *Financial modeling using quantum computing*, 1st ed. ed.; Packt Publishing, **2023**.
35. Jacquier, A.; Oleksiy, K. *Quantum machine learning and optimisation in finance*, second edition. ed.; Packt Publishing Ltd.: Birmingham, UK, **2024**.
36. Claudiu, B.; Cosmin, E.; Otniel, D.; Andrei, A., Enhancing the Financial Sector with Quantum Computing: A Comprehensive Review of Current and Future Applications. In *Proceedings of 22nd International Conference on Informatics in Economy (IE 2023)*; Springer Nature Singapore, **2024**; pp. 195–203.
37. Lu, Y.; Yang, J. Quantum financing system: A survey on quantum algorithms, potential scenarios and open research issues. *Journal of Industrial Information Integration* **2024**, *41*, 100663.
38. Atadoga, A.; Ike, C.U.; Asuzu, O.F.; Ayinla, B.S.; Ndubuisi, N.L.; Adeleye, R.A. The Intersection of AI And Quantum Computing In Financial Markets: A Critical Review. *Computer Science; IT Research Journal* **2024**, *5*, 461–472.
39. Gujju, Y.; Matsuo, A.; Raymond, R. Quantum machine learning on near-term quantum devices: Current state of supervised and unsupervised techniques for real-world applications. *Physical Review Applied* **2024**, *21*, 067001.
40. Bunescu, L.; Vârtei, A.M. Modern finance through quantum computing—A systematic literature review. *PLOS ONE* **2024**, *19*, e0304317.
41. Mironowicz, P.; H., A.S.; Mandarino, A.; Yilmaz, A.E.; Ankenbrand, T. Applications of Quantum Machine Learning for Quantitative Finance. *arXiv* **2024**.
42. Corli, S.; Moro, L.; Dragoni, D.; Dispenza, M.; Prati, E. Quantum machine learning algorithms for anomaly detection: A review. *Future Generation Computer Systems* **2025**, *166*, 107632.
43. Georgopoulos, K. Fintech Use-case Library, Quantum Readiness Delivery. Internal NQCC Report.
44. Nielsen, M.A.; Chuang, I.L. *Quantum Computation and Quantum Information: 10th Anniversary Edition*; Cambridge University Press, **2010**.
45. Selinger, P. Quantum circuits of T-depth one. *Physical Review A* **2013**, *87*, 042302.
46. Babbush, R.; McClean, J.R.; Newman, M.; Gidney, C.; Boixo, S.; Neven, H. Focus beyond Quadratic Speedups for Error-Corrected Quantum Advantage. *PRX Quantum* **2021**, *2*, 010103.
47. Arnault, P.; Arrighi, P.; Herbert, S.; Kasnetsi, E.; Li, T. A typology of quantum algorithms, **2024**.
48. Dalzell, A.M.; McArdle, S.; Berta, M.; Bienias, P.; Chen, C.F.; Gilyén, A.; Hann, C.T.; Kastoryano, M.J.; Khabiboulline, E.T.; Kubica, A.; et al. Quantum algorithms: A survey of applications and end-to-end complexities, **2023**.
49. Shor, P.W. Algorithms for quantum computation: discrete logarithms and factoring. In Proceedings of the Proceedings of the 35th Annual Symposium on Foundations of Computer Science (FOCS). IEEE, **1994**, pp. 124–134.
50. Kitaev, A.Y. Quantum measurements and the Abelian Stabilizer Problem, **1995**.
51. Shor, P.W. Polynomial-Time Algorithms for Prime Factorization and Discrete Logarithms on a Quantum Computer. *Society for Industrial and Applied Mathematics* **1997**, *26*, 1484–1509.
52. Abrams, D.S.; Lloyd, S. Quantum Algorithm Providing Exponential Speed Increase for Finding Eigenvalues and Eigenvectors. *Physical Review Letters* **1999**, *83*, 5162–5165.
53. Griffiths, R.B.; Niu, C.S. Semiclassical Fourier Transform for Quantum Computation. *Physical Review Letters* **1996**, *76*, 3228–3231.
54. Dobšíček, M.; Johansson, G.; Shumeiko, V.; Wendin, G. Arbitrary accuracy iterative quantum phase estimation algorithm using a single ancillary qubit: A two-qubit benchmark. *Phys. Rev. A* **2007**, *76*, 030306.
55. Somma, R.D. Quantum eigenvalue estimation via time series analysis. *New Journal of Physics* **2019**, *21*, 123025.
56. Clinton, L.; Bausch, J.; Klassen, J.; Cubitt, T. Phase estimation of local Hamiltonians on NISQ hardware. *New Journal of Physics* **2023**, *25*, 033027.
57. Brassard, G.; Høyer, P.; Mosca, M.; Tapp, A. Quantum amplitude amplification and estimation, **2002**.

 doi:10.20944/preprints202511.1802.v2

58. Høyer, P. Arbitrary phases in quantum amplitude amplification. *Physical Review A* **2000**, *62*.
59. Ambainis, A. Variable time amplitude amplification and quantum algorithms for linear algebra problems. In Proceedings of the 29th International Symposium on Theoretical Aspects of Computer Science (STACS 2012); Dürr, C.; Wilke, T., Eds., Dagstuhl, Germany, **2012**; Vol. 14, *Leibniz International Proceedings in Informatics (LIPIcs)*, pp. 636–647.
60. Berry, D.W.; Childs, A.M.; Cleve, R.; Kothari, R.; Somma, R.D. Exponential Improvement in Precision for Simulating Sparse Hamiltonians. In Proceedings of the Proceedings of the forty-sixth annual ACM symposium on Theory of computing, New York, NY, USA, **2014**; STOC '14, p. 283–292.
61. Yoder, T.J.; Low, G.H.; Chuang, I.L. Fixed-Point Quantum Search with an Optimal Number of Queries. *Physical Review Letters* **2014**, *113*, 210501.
62. Martyn, J.M.; Rossi, Z.M.; Tan, A.K.; Chuang, I.L. Grand Unification of Quantum Algorithms. *PRX Quantum* **2021**, *2*, 040203.
63. Toyoizumi, K.; Yamamoto, N.; Hoshino, K. Hamiltonian simulation using the quantum singular-value transformation: Complexity analysis and application to the linearized Vlasov-Poisson equation. *Physical Review A* **2024**, *109*, 012430.
64. Giurgica-Tiron, T.; Kerenidis, I.; Labib, F.; Prakash, A.; Zeng, W. Low depth algorithms for quantum amplitude estimation, **2020**.
65. Suzuki, Y.; Uno, S.; Raymond, R.; Tanaka, T.; Onodera, T.; Yamamoto, N. Amplitude estimation without phase estimation. *Quantum Information Processing* **2020**, *19*.
66. Nakaji, K. Faster Amplitude Estimation. *Quantum Information & Computation 2020* **2020**, *20*, 1109–1123.
67. Grinko, D.; Gacon, J.; Zoufal, C.; Woerner, S. Iterative quantum amplitude estimation. *npj Quantum Information* **2021**, *7*.
68. Plekhanov, K.; Rosenkranz, M.; Fiorentini, M.; Lubasch, M. Variational quantum amplitude estimation. *Quantum* **2022**, *6*, 670.
69. Shu, G.; Shan, Z.; Xu, J.; Zhao, J.; Wang, S. A general quantum algorithm for numerical integration. *Scientific Reports* **2024**, *14*.
70. Rotello, C. Quantum algorithm for approximating the expected value of a random-exist quantified oracle. *arXiv* **2024**.
71. Aaronson, S.; Rall, P., Quantum Approximate Counting, Simplified. In *Symposium on Simplicity in Algorithms*; Society for Industrial and Applied Mathematics, **2020**; pp. 24–32.
72. Cerf, N.J.; Grover, L.K.; Williams, C.P. Nested quantum search and structured problems. *Physical Review A* **2000**, *61*, 032303.
73. Bulger, D.; Baritompa, W.P.; Wood, G.R. Implementing Pure Adaptive Search with Grover's Quantum Algorithm. *Journal of Optimization Theory and Applications* **2003**, *116*, 517–529.
74. Armenakas, A.E.; Baker, O.K. Application of a Quantum Search Algorithm to High- Energy Physics Data at the Large Hadron Collider. *arXiv* **2020**.
75. Tezuka, H.; Nakaji, K.; Satoh, T.; Yamamoto, N. Grover search revisited: Application to image pattern matching. *Physical Review A* **2022**, *105*, 032440.
76. Fernández, P.; Martin-Delgado, M.A. Implementing the Grover algorithm in homomorphic encryption schemes. *Physical Review Research* **2024**, *6*, 043109.
77. Zhang, K.; Rao, P.; Yu, K.; Lim, H.; Korepin, V. Implementation of efficient quantum search algorithms on NISQ computers. *Quantum Information Processing* **2021**, *20*.
78. Zhang, K.; Yu, K.; Korepin, V. Quantum search on noisy intermediate-scale quantum devices. *Europhysics Letters* **2022**, *140*, 18002.
79. Liu, C.Y. Practical Quantum Search by Variational Quantum Eigensolver on Noisy Intermediate-Scale Quantum Hardware. In Proceedings of the 2023 International Conference on Computational Science and Computational Intelligence (CSCI). IEEE, **2023**, pp. 397–403.
80. Piron, R.; Goursaud, C. Hybrid Grover Search for AUD on a NISQ Device. In Proceedings of the 2024 32nd European Signal Processing Conference (EUSIPCO), **2024**, pp. 2102–2106.
81. Spitzer, F. *Principles of random walk*, 2. ed., 1. softcover printing ed.; Number 34 in Graduate texts in mathematics, Springer: New York, NY, **2001**. Literaturverz. S. [395] - 402.
82. László, L. Random Walks on Graphs: A Survey, Combinatorics, Paul Erdos is Eighty. *Bolyai Soc. Math. Stud.* **1993**, *2*.
83. Norris, J.R. *Markov Chains*; Cambridge Series in Statistical and Probabilistic Mathematics, Cambridge University Press, **1997**.

 doi:10.20944/preprints202511.1802.v2

84. Black, F.; Scholes, M. The Pricing of Options and Corporate Liabilities. *Journal of Political Economy* **1973**, *81*, 637–654.
85. Merton, R.C. Theory of Rational Option Pricing. *The Bell Journal of Economics and Management Science* **1973**, *4*, 141.
86. Aharonov, Y.; Davidovich, L.; Zagury, N. Quantum random walks. *Physical Review A* **1993**, *48*, 1687–1690.
87. Kempe, J. Quantum random walks - an introductory overview. Contemporary Physics, Vol. 44 (4), p.307-327, **2003**.
88. Farhi, E.; Gutmann, S. Quantum computation and decision trees. *Physical Review A* **1998**, *58*, 915–928.
89. Ambainis, A.; Bach, E.; Nayak, A.; Vishwanath, A.; Watrous, J. One-Dimensional Quantum Walks. In Proceedings of the Proceedings of the Thirty-Third Annual ACM Symposium on Theory of Computing, New York, NY, USA, **2001**; STOC '01, p. 37–49.
90. Douglas, B.L.; Wang, J.B. Efficient quantum circuit implementation of quantum walks. *Phys. Rev. A* **2009**, *79*, 052335.
91. Krovi, H. Symmetry in quantum walks, **2007**.
92. Georgopoulos, K.; Emary, C.; Zuliani, P. Comparison of quantum-walk implementations on noisy intermediate-scale quantum computers. *Physical Review A* **2021**, *103*.
93. Aharonov, D.; Ambainis, A.; Kempe, J.; Vazirani, U. Quantum Walks on Graphs. In Proceedings of the Proceedings of the Thirty-Third Annual ACM Symposium on Theory of Computing, New York, NY, USA, **2001**; STOC '01, p. 50–59.
94. Magniez, F.; Nayak, A.; Roland, J.; Santha, M. Search via Quantum Walk. *SIAM Journal on Computing* **2011**, *40*, 142–164.
95. Szegedy, M. Quantum speed-up of Markov chain based algorithms. In Proceedings of the 45th Annual IEEE Symposium on Foundations of Computer Science, **2004**, pp. 32–41.
96. Ambainis, A.; Kempe, J.; Rivosh, A. Coins Make Quantum Walks Faster. In Proceedings of the Proceedings of the Sixteenth Annual ACM-SIAM Symposium on Discrete Algorithms, USA, **2005**; SODA '05, p. 1099–1108.
97. Shenvi, N.; Kempe, J.; Whaley, K.B. Quantum random-walk search algorithm. *Phys. Rev. A* **2003**, *67*, 052307.
98. Reitzner, D.; Nagaj, D.; Bužek, V. Quantum Walks. *Acta Physica Slovaca. Reviews and Tutorials* **2011**, *61*.
99. Levin, D.A.; Peres, Y.; Wilmer, E.L. *Markov chains and mixing times*; American Mathematical Society: Providence, Rhode Island, **2009**.
100. Moore, C.; Russell, A. Quantum Walks on the Hypercube. In Proceedings of the Randomization and Approximation Techniques in Computer Science; Rolim, J.D.P.; Vadhan, S., Eds., Berlin, Heidelberg, **2002**; pp. 164–178.
101. Ambainis, A. Quantum Walk Algorithm for Element Distinctness. *SIAM Journal on Computing* **2007**, *37*, 210–239.
102. Ambainis, A.; Gilyén, A.; Jeffery, S.; Kokainis, M., Quadratic Speedup for Finding Marked Vertices by Quantum Walks. In *Proceedings of the 52nd Annual ACM SIGACT Symposium on Theory of Computing*; Association for Computing Machinery: New York, NY, USA, **2020**; p. 412–424.
103. Apers, S.; Gilyén, A.; Jeffery, S. A Unified Framework of Quantum Walk Search, **2019**.
104. Childs, A.M.; Eisenberg, J.M. Quantum Algorithms for Subset Finding. *Quantum Info. Comput.* **2005**, *5*, 593–604.
105. Somma, R.D.; Boixo, S.; Barnum, H.; Knill, E. Quantum Simulations of Classical Annealing Processes. *Phys. Rev. Lett.* **2008**, *101*, 130504.
106. Razzoli, L.; Cenedese, G.; Bondani, M.; Benenti, G. Efficient Implementation of Discrete-Time Quantum Walks on Quantum Computers. *Entropy* **2024**, *26*, 313.
107. Chawla, P.; Singh, S.; Agarwal, A.; Srinivasan, S.; Chandrashekar, C.M. Multi-qubit quantum computing using discrete-time quantum walks on closed graphs. *Scientific Reports* **2023**, *13*.
108. Nandi, B.; Singha, S.; Datta, A.; Saha, A.; Chakrabarti, A. Robust implementation of discrete-time quantum walks in any finite-dimensional quantum system. *Modern Physics Letters A* **2025**, *40*.
109. Ruan, Y.; Marsh, S.; Xue, X.; Li, X.; Liu, Z.; Wang, J. Quantum approximate algorithm for NP optimization problems with constraints, **2020**.
110. Qiang, X.; Ma, S.; Song, H. Quantum Walk Computing: Theory, Implementation, and Application. *Intelligent Computing* **2024**, *3*.
111. Childs, A.M.; Cleve, R.; Deotto, E.; Farhi, E.; Gutmann, S.; Spielman, D.A. Exponential Algorithmic Speedup by a Quantum Walk. In Proceedings of the Proceedings of the Thirty-Fifth Annual ACM Symposium on Theory of Computing, New York, NY, USA, **2003**; STOC '03, p. 59–68.

 doi:10.20944/preprints202511.1802.v2

112. Childs, A.M. Universal Computation by Quantum Walk. *Physical Review Letters* **2009**, *102*, 180501.
113. Lovett, N.B.; Cooper, S.; Everitt, M.; Trevers, M.; Kendon, V. Universal quantum computation using the discrete-time quantum walk. *Physical Review A* **2010**, *81*, 042330.
114. Childs, A.M.; van Dam, W. Quantum algorithms for algebraic problems. *Rev. Mod. Phys.* **2010**, *82*, 1–52.
115. Venegas-Andraca, S.E. Quantum walks: a comprehensive review. *Quantum Information Processing* **2012**, *11*, 1015–1106.
116. Klebaner, F.C. *Introduction to Stochastic Calculus with Applications*, 3rd ed.; Imperial College Press, **2012**.
117. Mohseni, M.; Rebentrost, P.; Lloyd, S.; Aspuru-Guzik, A. Environment-assisted quantum walks in photosynthetic energy transfer. *The Journal of Chemical Physics* **2008**, *129*.
118. Giri, M.K.; Mandal, S.B. Realizing topological quantum walks on NISQ digital quantum computer. *Physica Scripta* **2025**, *100*, 035111.
119. Spedicato, E. *Computer Algorithms for Solving Linear Algebraic Equations*; Number v.77 in Nato asi Subseries F: Ser., Springer Berlin / Heidelberg: Berlin, Heidelberg, **1991**.
120. Allgower, E.L.; Georg, K., Introduction to Numerical Continuation Methods; Society for Industrial and Applied Mathematics, **2003**; chapter 4, pp. 28–36.
121. Gould, N.I.M.; Scott, J.A.; Hu, Y. A numerical evaluation of sparse direct solvers for the solution of large sparse symmetric linear systems of equations. *ACM Transactions on Mathematical Software* **2007**, *33*, 10.
122. Shewchuk, J.R. An Introduction to the Conjugate Gradient Method Without the Agonizing Pain. Technical report, Carnegie Mellon University, USA, **1994**.
123. Le Gall, F. Powers of tensors and fast matrix multiplication. In Proceedings of the Proceedings of the 39th International Symposium on Symbolic and Algebraic Computation. ACM, **2014**, ISSAC '14, pp. 296–303.
124. Ambainis, A. Variable time amplitude amplification and a faster quantum algorithm for solving systems of linear equations, **2010**.
125. Childs, A.M.; Kothari, R.; Somma, R.D. Quantum Algorithm for Systems of Linear Equations with Exponentially Improved Dependence on Precision. *SIAM Journal on Computing* **2017**, *46*, 1920–1950.
126. Wossnig, L.; Zhao, Z.; Prakash, A. Quantum Linear System Algorithm for Dense Matrices. *Phys. Rev. Lett.* **2018**, *120*, 050502.
127. Somma, R.D.; Boixo, S. Spectral Gap Amplification. *SIAM Journal on Computing* **2013**, *42*, 593–610.
128. Subaşı , Y.; Somma, R.D.; Orsucci, D. Quantum Algorithms for Systems of Linear Equations Inspired by Adiabatic Quantum Computing. *Phys. Rev. Lett.* **2019**, *122*, 060504.
129. An, D.; Lin, L. Quantum linear system solver based on time-optimal adiabatic quantum computing and quantum approximate optimization algorithm. *ACM Transactions on Quantum Computing 3, 2, Article 5 (June 2022)* **2019**, *3*, 1–28.
130. Lin, L.; Tong, Y. Optimal polynomial based quantum eigenstate filtering with application to solving quantum linear systems. *Quantum* **2020**, *4*, 361.
131. Costa, P.C.; An, D.; Sanders, Y.R.; Su, Y.; Babbush, R.; Berry, D.W. Optimal Scaling Quantum Linear-Systems Solver via Discrete Adiabatic Theorem. *PRX Quantum* **2022**, *3*, 040303.
132. Dalzell, A.M. A shortcut to an optimal quantum linear system solver, **2024**.
133. Dervovic, D.; Herbster, M.; Mountney, P.; Severini, S.; Usher, N.; Wossnig, L. Quantum linear systems algorithms: a primer, **2018**.
134. Kerenidis, I.; Prakash, A. Quantum Recommendation Systems, **2016**.
135. Dabrowski, A., Ed. *2013 signal processing: algorithms, architectures, arrangements, and applications (SPA)*; IEEE: Piscataway, NJ, **2013**.
136. Geron, A. *Hands-on machine learning with Scikit-Learn, Keras, and TensorFlow*, third edition ed.; Data science / machine learning, O'Reilly: Beijing, **2023**.
137. Kerenidis, I.; Prakash, A. Quantum gradient descent for linear systems and least squares. *Phys. Rev. A* **2020**, *101*, 022316.
138. Gilyén, A.; Su, Y.; Low, G.H.; Wiebe, N. Quantum Singular Value Transformation and beyond: Exponential Improvements for Quantum Matrix Arithmetics. In Proceedings of the Proceedings of the 51st Annual ACM SIGACT Symposium on Theory of Computing, New York, NY, USA, 2019; STOC **2019**, p. 193–204.
139. Chakraborty, S.; Gilyén, A.; Jeffery, S. The Power of Block-Encoded Matrix Powers: Improved Regression Techniques via Faster Hamiltonian Simulation. In Proceedings of the 46th International Colloquium on Automata, Languages, and Programming (ICALP 2019); Baier, C.; Chatzigiannakis, I.; Flocchini, P.; Leonardi, S., Eds., Dagstuhl, Germany, **2019**; Vol. 132, *Leibniz International Proceedings in Informatics (LIPIcs)*, pp. 33:1–33:14.

 doi:10.20944/preprints202511.1802.v2

140. Gribling, S.; Kerenidis, I.; Szilágyi, D. Improving quantum linear system solvers via a gradient descent perspective, **2021**.
141. Barata, J.C.A.; Hussein, M.S. The Moore–Penrose Pseudoinverse: A Tutorial Review of the Theory. *Brazilian Journal of Physics* **2011**, *42*, 146–165.
142. Kerenidis, I.; Prakash, A. A Quantum Interior Point Method for LPs and SDPs. *ACM Transactions on Quantum Computing* **2020**, *1*.
143. Kiani, B.T.; De Palma, G.; Englund, D.; Kaminsky, W.; Marvian, M.; Lloyd, S. Quantum Advantage for Differential Equation Analysis. *Physical Review A* **2022**, *105*, 022415.
144. Hann, C.T.; Lee, G.; Girvin, S.; Jiang, L. Resilience of Quantum Random Access Memory to Generic Noise. *PRX Quantum* **2021**, *2*, 020311.
145. Frieze, A.; Kannan, R.; Vempala, S. Fast Monte-Carlo Algorithms for Finding Low-Rank Approximations. *J. ACM* **2004**, *51*, 1025–1041.
146. Tang, E. A Quantum-Inspired Classical Algorithm for Recommendation Systems. In Proceedings of the Proceedings of the 51st Annual ACM SIGACT Symposium on Theory of Computing, New York, NY, USA, **2019**; STOC 2019, p. 217–228.
147. Chia, N.H.; Gilyén, A.; Li, T.; Lin, H.H.; Tang, E.; Wang, C., Sampling-Based Sublinear Low-Rank Matrix Arithmetic Framework for Dequantizing Quantum Machine Learning. In *Proceedings of the 52nd Annual ACM SIGACT Symposium on Theory of Computing*; Association for Computing Machinery: New York, NY, USA, **2020**; p. 387–400.
148. Le Gall, F. Robust Dequantization of the Quantum Singular Value Transformation and Quantum Machine Learning Algorithms. *computational complexity* **2025**, *34*.
149. Sakurai, J.J.; Napolitano, J. *Modern quantum mechanics*, third edition ed.; Cambridge University Press: Cambridge, United Kingdom, **2021**.
150. Peruzzo, A.; McClean, J.; Shadbolt, P.; Yung, M.H.; Zhou, X.Q.; Love, P.J.; Aspuru-Guzik, A.; O'Brien, J.L. A variational eigenvalue solver on a photonic quantum processor. *Nature Communications* **2014**, *5*.
151. Wecker, D.; Hastings, M.B.; Troyer, M. Progress towards practical quantum variational algorithms. *Physical Review A* **2015**, *92*.
152. Cerezo, M.; Arrasmith, A.; Babbush, R.; Benjamin, S.C.; Endo, S.; Fujii, K.; McClean, J.R.; Mitarai, K.; Yuan, X.; Cincio, L.; et al. Variational quantum algorithms. *Nature Reviews Physics* **2021**, *3*, 625–644.
153. McClean, J.R.; Boixo, S.; Smelyanskiy, V.N.; Babbush, R.; Neven, H. Barren plateaus in quantum neural network training landscapes. *Nature Communications* **2018**, *9*.
154. Larocca, M.; Thanasilp, S.; Wang, S.; Sharma, K.; Biamonte, J.; Coles, P.J.; Cincio, L.; McClean, J.R.; Holmes, Z.; Cerezo, M. Barren plateaus in variational quantum computing. *Nature Reviews Physics* **2025**, *7*, 174–189.
155. Holmes, Z.; Sharma, K.; Cerezo, M.; Coles, P.J. Connecting Ansatz Expressibility to Gradient Magnitudes and Barren Plateaus. *PRX Quantum* **2022**, *3*, 010313.
156. Cerezo, M.; Larocca, M.; García-Martín, D.; Diaz, N.L.; Braccia, P.; Fontana, E.; Rudolph, M.S.; Bermejo, P.; Ijaz, A.; Thanasilp, S.; et al. Does provable absence of barren plateaus imply classical simulability? Or, why we need to rethink variational quantum computing. *arXiv* **2023**.
157. Farhi, E.; Goldstone, J.; Gutmann, S. A Quantum Approximate Optimization Algorithm, **2014**.
158. Bravo-Prieto, C.; LaRose, R.; Cerezo, M.; Subasi, Y.; Cincio, L.; Coles, P.J. Variational Quantum Linear Solver, **2019**.
159. Huang, H.Y.; Bharti, K.; Rebentrost, P. Near-term quantum algorithms for linear systems of equations, **2019**.
160. Lubasch, M.; Joo, J.; Moinier, P.; Kiffner, M.; Jaksch, D. Variational quantum algorithms for nonlinear problems. *Phys. Rev. A* **2020**, *101*, 010301.
161. Kubo, K.; Nakagawa, Y.O.; Endo, S.; Nagayama, S. Variational Quantum Simulations of Stochastic Differential Equations. *Physical Review A* **2021**, *103*, 052425.
162. Mitarai, K.; Negoro, M.; Kitagawa, M.; Fujii, K. Quantum circuit learning. *Phys. Rev. A* **2018**, *98*, 032309.
163. Bittel, L.; Kliesch, M. Training Variational Quantum Algorithms Is NP-Hard. *Phys. Rev. Lett.* **2021**, *127*, 120502.
164. Huembeli, P.; Dauphin, A. Characterizing the loss landscape of variational quantum circuits. *Quantum Science and Technology* **2021**, *6*, 025011.
165. Preskill, J. Beyond NISQ: The Megaquop Machine. *ACM Transactions on Quantum Computing* **2025**, *6*, 1–7.
166. Kadowaki, T.; Nishimori, H. Quantum annealing in the transverse Ising model. *Phys. Rev. E* **1998**, *58*, 5355–5363.
167. Farhi, E.; Goldstone, J.; Gutmann, S.; Sipser, M. Quantum Computation by Adiabatic Evolution, **2000**.

 doi:10.20944/preprints202511.1802.v2

168. Albash, T.; Lidar, D.A. Adiabatic quantum computation. *Rev. Mod. Phys.* **2018**, *90*, 015002.
169. Glover, F.; Kochenberger, G.; Du, Y. A Tutorial on Formulating and Using QUBO Models, **2018**.
170. Crosson, E.J.; Lidar, D.A. Prospects for quantum enhancement with diabatic quantum annealing. *Nature Reviews Physics* **2021**, *3*, 466–489.
171. Biamonte, J.D.; Love, P.J. Realizable Hamiltonians for universal adiabatic quantum computers. *Phys. Rev. A* **2008**, *78*, 012352.
172. Laarhoven, P.J.M.; Aarts, E.H.L. *Simulated annealing : theory and applications*; Mathematics and its applications, Reidel, **1987**.
173. Denchev, V.S.; Boixo, S.; Isakov, S.V.; Ding, N.; Babbush, R.; Smelyanskiy, V.; Martinis, J.; Neven, H. What is the Computational Value of Finite-Range Tunneling? *Phys. Rev. X* **2016**, *6*, 031015.
174. Kechedzhi, K.; Smelyanskiy, V.N. Open-System Quantum Annealing in Mean-Field Models with Exponential Degeneracy. *Phys. Rev. X* **2016**, *6*, 021028.
175. Cohen, E.; Tamir, B. D-Wave and predecessors: From simulated to quantum annealing. *International Journal of Quantum Information* **2014**, *12*, 1430002.
176. Streif, M.; Neukart, F.; Leib, M., Solving Quantum Chemistry Problems with a D-Wave Quantum Annealer. In *Quantum Technology and Optimization Problems*; Springer International Publishing, **2019**; pp. 111–122.
177. Ajagekar, A.; Humble, T.; You, F. Quantum computing based hybrid solution strategies for large-scale discrete-continuous optimization problems. *Computers and Chemical Engineering* **2020**, *132*, 106630.
178. Phillipson, F.; Bhatia, H.S., Portfolio Optimisation Using the D-Wave Quantum Annealer. In *Computational Science – ICCS 2021*; Springer International Publishing, **2021**; pp. 45–59.
179. Carugno, C.; Ferrari Dacrema, M.; Cremonesi, P. Evaluating the job shop scheduling problem on a D-wave quantum annealer. *Scientific Reports* **2022**, *12*.
180. An, D.; Liu, J.P.; Wang, D.; Zhao, Q. A Theory of Quantum Differential Equation Solvers: Limitations and Fast-Forwarding. *arXiv* **2023**.
181. Cochrane, J.H. *Asset Pricing*; Princeton University Press: s.l., **2009**.
182. Glasserman, P. *Monte Carlo Methods in Financial Engineering*; Applications of mathematics: stochastic modelling and applied probability, Springer, **2004**.
183. Bagherimehrab, M.; Nakaji, K.; Wiebe, N.; Aspuru-Guzik, A. Fast Quantum Algorithm for Differential Equations. *arxiv* **2023**.
184. Neal, R.M. Probabilistic inference using Markov chain Monte Carlo methods, 1993. Department of Computer Science, University of Toronto Toronto, ON, Canada, Last accessed: 20-05-2022.
185. de Mello, T.H.; Bayraksan, G. Monte Carlo sampling-based methods for stochastic optimization. *Surveys in Operations Research and Management Science* **2014**, *19*, 56–85.
186. Christian P. Robert, G.C. *Monte Carlo Statistical Methods*; Vol. 2, Springer, **2004**.
187. Chakrabarti, S.; Krishnakumar, R.; Mazzola, G.; Stamatopoulos, N.; Woerner, S.; Zeng, W.J. A Threshold for Quantum Advantage in Derivative Pricing. *Quantum* **2021**, *5*, 463.
188. Stamatopoulos, N.; Zeng, W.J. Derivative Pricing using Quantum Signal Processing. *Quantum* **2024**, *8*, 1322.
189. Plesch, M.; Brukner, i.c.v. Quantum-state preparation with universal gate decompositions. *Phys. Rev. A* **2011**, *83*, 032302.
190. Grover, L.; Rudolph, T. Creating superpositions that correspond to efficiently integrable probability distributions, **2002**.
191. Herbert, S. No quantum speedup with Grover-Rudolph state preparation for quantum Monte Carlo integration. *Phys. Rev. E* **2021**, *103*, 063302.
192. McArdle, S.; Gilyén, A.; Berta, M. Quantum state preparation without coherent arithmetic. *arXiv* **2022**.
193. Akhalwaya, I.Y.; Connolly, A.; Guichard, R.; Herbert, S.; Kargi, C.; Krajenbrink, A.; Lubasch, M.; Keever, C.M.; Sorci, J.; Spranger, M.; et al. A Modular Engine for Quantum Monte Carlo Integration. *arXiv* **2023**.
194. Gomes, N.; Mukherjee, A.; Zhang, F.; Iadecola, T.; Wang, C.Z.; Ho, K.M.; Orth, P.P.; Yao, Y.X. Adaptive Variational Quantum Imaginary Time Evolution Approach for Ground State Preparation. *Advanced Quantum Technologies* **2021**, *4*, 2100114.
195. Rattew, A.G.; Sun, Y.; Minssen, P.; Pistoia, M. The Efficient Preparation of Normal Distributions in Quantum Registers. *Quantum* **2021**, *5*, 609.
196. Zoufal, C.; Lucchi, A.; Woerner, S. Quantum Generative Adversarial Networks for learning and loading random distributions. *npj Quantum Information* **2019**, *5*.
197. Pereira, A.; Villarino, A.; Cortines, A.; Mugel, S.; Orus, R.; Beltran, V.L.; Scursulim, J.V.S.; Brito, S. Encoding of Probability Distributions for Quantum Monte Carlo Using Tensor Networks. *arXiv* **2024**.

 doi:10.20944/preprints202511.1802.v2

198. Herbert, S. Quantum Monte Carlo Integration: The Full Advantage in Minimal Circuit Depth. *Quantum* **2022**, *6*, 823.
199. Lanes, O.; Beji, M.; Corcoles, A.D.; Dalyac, C.; Gambetta, J.M.; Henriet, L.; Javadi-Abhari, A.; Kandala, A.; Mezzacapo, A.; Porter, C.; et al. A Framework for Quantum Advantage. *arXiv* **2025**.
200. Evans, L.C. *An introduction to stochastic differential equations*; American Mathematical Society: Providence, RI, **2014**.
201. Heath, D.; Jarrow, R.; Morton, A. Bond Pricing and the Term Structure of Interest Rates: A New Methodology for Contingent Claims Valuation. *Econometrica* **1992**, *60*, 77.
202. Heston, S.L. A Closed-Form Solution for Options with Stochastic Volatility with Applications to Bond and Currency Options. *Review of Financial Studies* **1993**, *6*, 327–343.
203. Wilmott, P. *Paul Wilmott Introduces Quantitative Finance*; Wiley & Sons, Incorporated, John, **2013**; p. 728.
204. Wilmott, P. *Paul Wilmott on Quantitative Finance*; Wiley & Sons, Incorporated, John, **2013**; p. 1500.
205. Feynman, R.P. Space-Time Approach to Non-Relativistic Quantum Mechanics. *Reviews of Modern Physics* **1948**, *20*, 367–387.
206. Kac, M. On distributions of certain Wiener functionals. *Transactions of the American Mathematical Society* **1949**, *65*, 1–13.
207. Del Moral, P., Feynman-Kac Formulae. In *Feynman-Kac Formulae*; Springer New York, 2004; pp. 47–93.
208. Mazumder, S. *Numerical methods for partial differential equations*; Academic Press, Imprint of Elsevier: London, **2016**.
209. Larson, M.G.; Bengzon, F. *The Finite Element Method: Theory, Implementation, and Applications*; Vol. 10, *Texts in Computational Science and Engineering*, Springer: Berlin, Heidelberg, **2013**.
210. Xu, S.; Zhao, J.; Wu, H.; Zhang, S.; Müller, J.D.; Huang, H.; Rahmati, M.; Wang, D. A Review of Solution Stabilization Techniques for RANS CFD Solvers. *Aerospace* **2023**, *10*, 230.
211. Clader, B.D.; Jacobs, B.C.; Sprouse, C.R. Preconditioned Quantum Linear System Algorithm. *Physical Review Letters* **2013**, *110*, 250504.
212. Shao, C.; Xiang, H. Quantum circulant preconditioner for a linear system of equations. *Phys. Rev. A* **2018**, *98*, 062321.
213. Tong, Y.; An, D.; Wiebe, N.; Lin, L. Fast inversion, preconditioned quantum linear system solvers, fast Green's-function computation, and fast evaluation of matrix functions. *Physical Review A* **2021**, *104*, 032422.
214. Nazareth, J.L. Conjugate Gradient Method. *WIREs Computational Statistics* **2009**, *1*, 348–353.
215. Chang, M.H. *Quantum stochastics*, first published 2015 ed.; Number 37 in Cambridge series on statistical and probabilistic mathematics, Cambridge University Press: New York, **2015**.
216. Jin, S.; Liu, N.; Wei, W. Quantum Algorithms for Stochastic Differential Equations: A Schrödingerisation Approach. *Journal of Scientific Computing* **2025**, *104*.
217. Gonzalez-Conde, J.; Rodriguez-Rozas, A.; Solano, E.; Sanz, M. Efficient Hamiltonian simulation for solving option price dynamics. *Physical Review Research* **2023**, *5*, 043220.
218. Hunacek, M. Lie groups: an introduction through linear groups, by Wulf Rossmann. Pp. 265, **2006**. ISBN 0 19 920251 6 (Oxford University Press). *The Mathematical Gazette* 2008, *92*, 380–382.
219. Jin, S.; Liu, N.; Yu, Y. Quantum simulation of partial differential equations: Applications and detailed analysis. *Physical Review A* **2023**, *108*, 032603.
220. McArdle, S.; Jones, T.; Endo, S.; Li, Y.; Benjamin, S.C.; Yuan, X. Variational ansatz-based quantum simulation of imaginary time evolution. *npj Quantum Information* **2019**, *5*.
221. Yeter-Aydeniz, K.; Moschandreou, E.; Siopsis, G. Quantum imaginary-time evolution algorithm for quantum field theories with continuous variables. *Physical Review A* **2022**, *105*, 012412.
222. Kolotouros, I.; Joseph, D.; Narayanan, A.K. Accelerating quantum imaginary-time evolution with random measurements. *Physical Review A* **2025**, *111*, 012424.
223. Jouzdani, P.; Johnson, C.W.; Mucciolo, E.R.; Stetcu, I. Alternative approach to quantum imaginary time evolution. *Physical Review A* **2022**, *106*, 062435.
224. Pavliotis, G.A. *Stochastic Processes and Applications: Diffusion Processes, the Fokker-Planck and Langevin Equations*; Springer New York, **2014**.
225. Nocedal, J.; Wright, S.J. *Numerical Optimization*, 2nd ed.; Springer, **2006**.
226. Boyd, S.; Vandenberghe, L. *Convex Optimization*; Cambridge University Press, **2004**.
227. Kirkpatrick, S.; Gelatt, C.D.; Vecchi, M.P. Optimization by Simulated Annealing. *Science* **1983**, *220*, 671–680.
228. Markowitz, H. Portfolio Selection. *The Journal of Finance* **1952**, *7*, 77–91.

 doi:10.20944/preprints202511.1802.v2

229. Shapiro, A.; Dentcheva, D.; Ruszczyński, A.P. *Lectures on stochastic programming : modeling and theory*, third edition. ed.; MOS-SIAM series on optimization, Society for Industrial and Applied Mathematics SIAM, **2021**.
230. N.M., et al. Quantum optimization using variational algorithms on near-term quantum devices. *Quantum Science and Technology* **2018**, *3*, 030503.
231. et al., A.K. Hardware-efficient variational quantum eigensolver for small molecules and quantum magnets. *Nature* **2017**, *549*, 242–246.
232. Guerreschi, G.G.; Smelyanskiy, M. Practical optimization for hybrid quantum-classical algorithms, **2017**.
233. Koch, T.; Neira, D.E.B.; Chen, Y.; Cortiana, G.; Egger, D.J.; Heese, R.; Hegade, N.N.; Cadavid, A.G.; Huang, R.; Itoko, T.; et al. Quantum Optimization Benchmark Library – The Intractable Decathlon, **2025**.
234. Hromkovič, J. *Algorithmics for hard problems: introduction to combinatorial optimization, randomization, approximation, and heuristics*; Springer Science & Business Media, **2013**.
235. Nemhauser, G.; Wolsey, L., Linear Programming. In *Integer and Combinatorial Optimization*; John Wiley and Sons, Ltd, 1988; chapter I.2, pp. 27–49.
236. Abbas, A.e.a. Challenges and opportunities in quantum optimization. *Nature Reviews Physics* **2024**, *6*, 718–735.
237. Kochenberger, G.; Hao, J.K.; Glover, F.; Lewis, M.; Lü, Z.; Wang, H.; Wang,Y. The Unconstrained Binary Quadratic Programming Problem: A Survey. *J. Comb. Optim.* **2014**, *28*, 58–81.
238. Okada, S.; Ohzeki, M.; Taguchi, S. Efficient partition of integer optimization problems with one-hot encoding. *Scientific Reports* **2019**, *9*.
239. Lucas, A. Ising formulations of many NP problems. *Frontiers in Physics* **2014**, *2*.
240. McClean, J.R.; Romero, J.; Babbush, R.; Aspuru-Guzik, A. The theory of variational hybrid quantum-classical algorithms. *New Journal of Physics* **2015**, *18*.
241. Rayleigh, J. In finding the correction for the open end of an organ-pipe. *Phil. Trans.* **1870**, *161*, 77.
242. Ritz, W. Uber eine neue Methode zur Losung gewisser Variationsprobleme der mathematischen Physik. . **1909**, *1909*, 1–61.
243. Tilly, J.; Chen, H.; Cao, S.; Picozzi, D.; Setia, K.; Li, Y.; Grant, E.; Wossnig, L.; Rungger, I.; Booth, G.H.; et al. The Variational Quantum Eigensolver: a review of methods and best practices, **2021**.
244. Rattew, A.G.; Hu, S.; Pistoia, M.; Chen, R.; Wood, S. A Domain-agnostic, Noise-resistant, Hardware-efficient Evolutionary Variational Quantum Eigensolver, **2019**.
245. Amaro, D.; Modica, C.; Rosenkranz, M.; Fiorentini, M.; Benedetti, M.; Lubasch, M. Filtering variational quantum algorithms for combinatorial optimization. *Quantum Science and Technology* **2022**, *7*, 015021.
246. Fujii, K.; Mizuta, K.; Ueda, H.; Mitarai, K.; Mizukami, W.; Nakagawa, Y.O. Deep Variational Quantum Eigensolver: a divide-and-conquer method for solving a larger problem with smaller size quantum computers, **2020**.
247. Motta, M.; Sun, C.; Tan, A.T.K.; O'Rourke, M.J.; Ye, E.; Minnich, A.J.; Brandão, F.G.S.L.; Chan, G.K.L. Determining eigenstates and thermal states on a quantum computer using quantum imaginary time evolution. *Nature Physics* **2019**, *16*, 205–210.
248. Gomes, N.; Zhang, F.; Berthusen, N.F.; Wang, C.Z.; Ho, K.M.; Orth, P.P.; Yao, Y. Efficient Step-Merged Quantum Imaginary Time Evolution Algorithm for Quantum Chemistry. *Journal of Chemical Theory and Computation* **2020**, *16*, 6256–6266.
249. Sun, S.N.; Motta, M.; Tazhigulov, R.N.; Tan, A.T.; Chan, G.K.L.; Minnich, A.J. Quantum Computation of Finite-Temperature Static and Dynamical Properties of Spin Systems Using Quantum Imaginary Time Evolution. *PRX Quantum* **2021**, *2*, 010317.
250. Huang, Y.; Shao, Y.; Ren, W.; Sun, J.; Lv, D. Efficient quantum imaginary time evolution by drifting real time evolution: an approach with low gate and measurement complexity, **2022**.
251. Yuan, X.; Endo, S.; Zhao, Q.; Li, Y.; Benjamin, S.C. Theory of variational quantum simulation. *Quantum* **2019**, *3*, 191.
252. Grimsley, H.R.; Economou, S.E.; Barnes, E.; Mayhall, N.J. An adaptive variational algorithm for exact molecular simulations on a quantum computer. *Nature Communications* **2019**, *10*.
253. Ryabinkin, I.G.; Yen, T.C.; Genin, S.N.; Izmaylov, A.F. Qubit Coupled Cluster Method: A Systematic Approach to Quantum Chemistry on a Quantum Computer. *Journal of Chemical Theory and Computation* **2018**, *14*, 6317–6326..
254. Poulin, D.; Qarry, A.; Somma, R.; Verstraete, F. Quantum Simulation of Time-Dependent Hamiltonians and the Convenient Illusion of Hilbert Space. *Phys. Rev. Lett.* **2011**, *106*, 170501.

 doi:10.20944/preprints202511.1802.v2

255. Alghassi, H.; Deshmukh, A.; Ibrahim, N.; Robles, N.; Woerner, S.; Zoufal, C. A variational quantum algorithm for the Feynman-Kac formula. *Quantum* **2022**, *6*, 730.
256. Galda, A.; Liu, X.; Lykov, D.; Alexeev, Y.; Safro, I. Transferability of optimal QAOA parameters between random graphs. In Proceedings of the 2021 IEEE International Conference on Quantum Computing and Engineering (QCE), **2021**, pp. 171–180.
257. Shaydulin, R.; Safro, I.; Larson, J. Multistart Methods for Quantum Approximate optimization. In Proceedings of the 2019 IEEE High Performance Extreme Computing Conference (HPEC), **2019**, pp. 1–8.
258. Shaydulin, R.; Hadfield, S.; Hogg, T.; Safro, I. Classical symmetries and the Quantum Approximate Optimization Algorithm. *Quantum Information Processing* **2021**, *20*.
259. Streif, M.; Leib, M. Training the Quantum Approximate Optimization Algorithm without access to a Quantum Processing Unit, **2019**.
260. Durr, C.; Hoyer, P. A Quantum Algorithm for Finding the Minimum, **1996**.
261. Zeng, Y.; Dong, Z.; Wang, H.; He, J.; Huang, Q.; Chang, S. A general quantum minimum searching algorithm with high success rate and its implementation. *Science China Physics, Mechanics and Astronomy* **2023**, *66*.
262. Boyer, M.; Brassard, G.; Høyer, P.; Tapp, A. Tight Bounds on Quantum Searching. *Fortschritte der Physik* **1998**, *46*, 493–505.
263. Gilliam, A.; Woerner, S.; Gonciulea, C. Grover Adaptive Search for Constrained Polynomial Binary Optimization. *Quantum* **2021**, *5*, 428.
264. Morapakula, S.N.; Deshpande, S.; Yata, R.; Ubale, R.; Wad, U.; Ikeda, K. End-to-End Portfolio Optimization with Quantum Annealing, **2025**.
265. Kim, S.; Ahn, S.W.; Suh, I.S.; Dowling, A.W.; Lee, E.; Luo, T. Quantum Annealing for Combinatorial Optimization: A Benchmarking Study, **2025**.
266. Guéry-Odelin, D.; Ruschhaupt, A.; Kiely, A.; Torrontegui, E.; Martínez-Garaot, S.; Muga, J. Shortcuts to adiabaticity: Concepts, methods, and applications. *Reviews of Modern Physics* **2019**, *91*.
267. Gomez-Tejedor, A.; Osaba, E.; Villar-Rodriguez, E. Addressing the Minor-Embedding Problem in Quantum Annealing and Evaluating State-of-the-Art Algorithm Performance, **2025**.
268. Ohzeki, M. Breaking limitation of quantum annealer in solving optimization problems under constraints, **2020**.
269. DWave. *minorminer documentation*. Accessed 06-08-2025.
270. DWave. Annealing Implementation and Controls, 2025. Accessed: 2025-08-04.
271. Sachdeva, N.; Hartnett, G.S.; Maity, S.; Marsh, S.; Wang, Y.; Winick, A.; Dougherty, R.; Canuto, D.; Chong, Y.Q.; Hush, M.; et al. Quantum optimization using a 127-qubit gate-model IBM quantum computer can outperform quantum annealers for nontrivial binary optimization problems. *arXiv* **2024**.
272. McGeoch, C.C.; Chern, K.; Farré, P.; King, A.K. A comment on comparing optimization on D-Wave and IBM quantum processors. *arXiv* **2024**.
273. del Campo, A. Shortcuts to Adiabaticity by Counterdiabatic Driving. *Physical Review Letters* **2013**, *111*.
274. Cadavid, A.G.; Dalal, A.; Simen, A.; Solano, E.; Hegade, N.N. Bias-field digitized counterdiabatic quantum optimization. *Physical Review Research* **2025**, *7*.
275. Visuri, A.M.; Cadavid, A.G.; Bhargava, B.A.; Romero, S.V.; Grabarits, A.; Chandarana, P.; Solano, E.; del Campo, A.; Hegade, N.N. Digitized counterdiabatic quantum critical dynamics, **2025**.
276. Romero, S.V.; Cadavid, A.G.; Nikačević, P.; Solano, E.; Hegade, N.N.; Lopez-Ruiz, M.A.; Girotto, C.; Yamada, M.; Barkoutsos, P.K.; Kaushik, A.; et al. Protein folding with an all-to-all trapped-ion quantum computer, **2025**.
277. Jordan, S.P. Quantum Computation Beyond the Circuit Model, **2008**.
278. Brandao, F.G.; Svore, K.M. Quantum Speed-Ups for Solving Semidefinite Programs. In Proceedings of the 2017 IEEE 58th Annual Symposium on Foundations of Computer Science (FOCS), **2017**, pp. 415–426.
279. Van Apeldoorn, J.; Gilyén, A.; Gribling, S.; de Wolf, R. Quantum SDP-Solvers: Better Upper and Lower Bounds. In Proceedings of the 2017 IEEE 58th Annual Symposium on Foundations of Computer Science (FOCS), **2017**, pp. 403–414.
280. Brandão, F.G.S.L.; Kalev, A.; Li, T.; Lin, C.Y.Y.; Svore, K.M.; Wu, X. Quantum SDP Solvers: Large Speed-Ups, Optimality, and Applications to Quantum Learning. In Proceedings of the 46th International Colloquium on Automata, Languages, and Programming (ICALP 2019); Baier, C.; Chatzigiannakis, I.; Flocchini, P.; Leonardi, S., Eds., Dagstuhl, Germany, **2019**; Vol. 132, *Leibniz International Proceedings in Informatics (LIPIcs)*, pp. 27:1–27:14.

 doi:10.20944/preprints202511.1802.v2

281. van Apeldoorn, J.; Gilyén, A. Improvements in Quantum SDP-Solving with Applications. In Proceedings of the 46th International Colloquium on Automata, Languages, and Programming (ICALP 2019); Baier, C.; Chatzigiannakis, I.; Flocchini, P.; Leonardi, S., Eds., Dagstuhl, Germany, **2019**; Vol. 132, *Leibniz International Proceedings in Informatics (LIPIcs)*, pp. 99:1–99:15.
282. Arkadi Nemirovski. Interior Point Polynomial Time Methods in Convex Programming (Lecture Notes), 2004. Accessed: 2025-08-07.
283. Nesterov, Y.; Nemirovskii, A. *Interior-Point Polynomial Algorithms in Convex Programming*; Society for Industrial and Applied Mathematics, **1994**.
284. Nannicini, G. Fast Quantum Subroutines for the Simplex Method. In Proceedings of the Integer Programming and Combinatorial Optimization; Singh, M.; Williamson, D.P., Eds., Cham, **2021**; pp. 311–325.
285. Kerenidis, I.; Prakash, A.; Szilágyi, D. Quantum algorithms for Second-Order Cone Programming and Support Vector Machines. *Quantum* **2021**, *5*, 427.
286. Jordan, S.P. Fast Quantum Algorithm for Numerical Gradient Estimation. *Phys. Rev. Lett.* **2005**, *95*, 050501.
287. Das Sarma, S.; Deng, D.L.; Duan, L.M. Machine learning meets quantum physics. *Physics Today* **2019**, *72*, 48–54.
288. Biamonte, J.; Wittek, P.; Pancotti, N.; Rebentrost, P.; Wiebe, N.; Lloyd, S. Quantum machine learning. *Nature* **2017**, *549*, 195–202.
289. Schuld, M.; Sinayskiy, I.; Petruccione, F. An introduction to quantum machine learning. *Contemporary Physics* **2014**, *56*, 172–185.
290. Lamichhane, P.; Rawat, D.B. Quantum Machine Learning: Recent Advances, Challenges, and Perspectives. *IEEE Access* **2025**, *13*, 94057–94105.
291. Dunjko, V.; Briegel, H.J. Machine learning & artificial intelligence in the quantum domain: a review of recent progress. *Reports on Progress in Physics* **2018**, *81*, 074001.
292. Schuld, M.; Killoran, N. Is Quantum Advantage the Right Goal for Quantum Machine Learning? *PRX Quantum* **2022**, *3*, 030101.
293. Lu, W.; Lu, Y.; Li, J.; Sigov, A.; Ratkin, L.; Ivanov, L.A. Quantum machine learning: Classifications, challenges, and solutions. *Journal of Industrial Information Integration* **2024**, *42*, 100736.
294. Wang, Y.; Liu, J. A comprehensive review of quantum machine learning: from NISQ to fault tolerance. *Reports on Progress in Physics* **2024**, *87*, 116402.
295. Shalev-Shwartz, S.; Ben-David, S. *Understanding Machine Learning: From Theory to Algorithms*; Cambridge University Press, **2014**.
296. Bishop, C.M. *Pattern Recognition and Machine Learning*; Springer-Verlag: Berlin, Heidelberg, **2006**.
297. An, Q.; Rahman, S.; Zhou, J.; Kang, J.J. A Comprehensive Review on Machine Learning in Healthcare Industry: Classification, Restrictions, Opportunities and Challenges. *Sensors* **2023**, *23*.
298. IBM. What Is Supervised Learning?, 2024. Accessed: 25-07-2025.
299. Lloyd, S.; Mohseni, M.; Rebentrost, P. Quantum algorithms for supervised and unsupervised machine learning. *arXiv* **2013**.
300. Macaluso, A. Quantum Supervised Learning. *KI - Künstliche Intelligenz* **2024**, *38*, 277–291.
301. Li, W.; Deng, D.L. Recent advances for quantum classifiers. *Science China Physics, Mechanics & Astronomy, 65, 220301 (2022)* **2021**, *65*.
302. Rebentrost, P.; Mohseni, M.; Lloyd, S. Quantum Support Vector Machine for Big Data Classification. *Physical Review Letters* **2014**, *113*, 130503.
303. Innan, N.; Khan, M.; Panda, B.; Bennai, M. Enhancing quantum support vector machines through variational kernel training. *Quantum Information Processing* **2023**, *22*.
304. Boser, B.E.; Guyon, I.M.; Vapnik, V.N. A training algorithm for optimal margin classifiers. In Proceedings of the Proceedings of the fifth annual workshop on Computational learning theory. ACM, **1992**, COLT92.
305. Suthaharan, S., Support Vector Machine. In *Integrated Series in Information Systems*; Springer US, **2016**; pp. 207–235.
306. Platt, J. Sequential Minimal Optimization: A Fast Algorithm for Training Support Vector Machines. Technical Report MSR-TR-98-14, Microsoft, **1998**.
307. Mehrotra, S. On the Implementation of a Primal-Dual Interior Point Method. *SIAM Journal on Optimization* **1992**, *2*, 575–601.
308. Hastie, T.; Tibshirani, R.; Friedman, J. *The Elements of Statistical Learning*, 2nd ed.; Springer Series in Statistics, Springer New York Inc.: New York, NY, USA, **2009**.

 doi:10.20944/preprints202511.1802.v2

309. Ben-Hur, A.; Weston, J., A User's Guide to Support Vector Machines. In *Data Mining Techniques for the Life Sciences*; Humana Press: Totowa, NJ, **2010**; pp. 223–239.
310. Suykens, J.; Vandewalle, J. Least Squares Support Vector Machine Classifiers. *Neural Processing Letters* **1999**, *9*, 293–300.
311. Liu, Y.; Arunachalam, S.; Temme, K. A rigorous and robust quantum speed-up in supervised machine learning. *Nature Physics* **2021**, *17*, 1013–1017.
312. Glick, J.R.; Gujarati, T.P.; Córcoles, A.D.; Kim, Y.; Kandala, A.; Gambetta, J.M.; Temme, K. Covariant quantum kernels for data with group structure. *Nature Physics* **2024**.
313. Shin, S.; Sweke, R.; Jeong, H. New perspectives on quantum kernels through the lens of entangled tensor kernels, **2025**.
314. Havlíček, V.; Córcoles, A.D.; Temme, K.; Harrow, A.W.; Kandala, A.; Chow, J.M.; Gambetta, J.M. Supervised learning with quantum-enhanced feature spaces. *Nature* **2019**, *567*, 209–212.
315. Neven, H.; Denchev, V.S.; Rose, G.; Macready, W.G. Training a Large Scale Classifier with the Quantum Adiabatic Algorithm. *arXiv* **2009**.
316. Pudenz, K.L.; Lidar, D.A. Quantum adiabatic machine learning. *Quantum Information Processing* **2012**, *12*, 2027–2070.
317. Shi, Y. Entropy lower bounds for quantum decision tree complexity. *Information Processing Letters* **2002**, *81*, 23–27.
318. Lu, S.; Braunstein, S.L. Quantum decision tree classifier. *Quantum Information Processing* **2013**, *13*, 757–770.
319. Heese, R.; Bickert, P.; Niederle, A.E. Representation of binary classification trees with binary features by quantum circuits. *Quantum* **2022**, *6*, 676.
320. Nishimura, H., A Survey: SWAP Test and Its Applications to Quantum Complexity Theory. In *Algorithmic Foundations for Social Advancement*; Springer Nature Singapore, **2025**; pp. 243–261.
321. Gentinetta, G.; Thomsen, A.; Sutter, D.; Woerner, S. The complexity of quantum support vector machines. *Quantum* **2024**, *8*, 1225.
322. Wang, X.; Du, Y.; Luo, Y.; Tao, D. Towards understanding the power of quantum kernels in the NISQ era. *Quantum* **2021**, *5*, 531.
323. Zalivako, I.V.; Gircha, A.I.; Kiktenko, E.O.; Nikolaeva, A.S.; Drozhzhin, D.A.; Borisenko, A.S.; Korolkov, A.E.; Semenin, N.V.; Galstyan, K.P.; Kamenskikh, P.A.; et al. Supervised binary classification of small-scale digit images and weighted graphs with a trapped-ion quantum processor. *Phys. Rev. A* **2025**, *111*, 052436.
324. Suzuki, T.; Hasebe, T.; Miyazaki, T. Quantum support vector machines for classification and regression on a trapped-ion quantum computer, **2024**.
325. He, H.; Xiao, Y. Probabilistic Quantum SVM Training on Ising Machine, **2025**.
326. Basheer, A.; Afham, A.; Goyal, S.K. Quantum *k*-nearest neighbors algorithm, **2021**.
327. Wiebe, N.; Kapoor, A.; Svore, K. Quantum Algorithms for Nearest-Neighbor Methods for Supervised and Unsupervised Learning, **2014**.
328. Peterson, L.E. K-nearest neighbor. *Scholarpedia* **2009**, *4*, 1883. revision #137311.
329. IBM. What is the k-nearest neighbors (KNN) algorithm? Last accessed: 24.03.2025.
330. Jiang, L.; Cai, Z.; Wang, D.; Jiang, S. Survey of Improving K-Nearest-Neighbor for Classification. In Proceedings of the Fourth International Conference on Fuzzy Systems and Knowledge Discovery (FSKD 2007), **2007**, Vol. 1, pp. 679–683.
331. Cunningham, P.; Delany, S.J. k-Nearest Neighbour Classifiers - A Tutorial. *ACM Comput. Surv.* **2021**, *54*.
332. Taunk, K.; De, S.; Verma, S.; Swetapadma, A. A Brief Review of Nearest Neighbor Algorithm for Learning and Classification. In Proceedings of the 2019 International Conference on Intelligent Computing and Control Systems (ICCS), **2019**, pp. 1255–1260.
333. Cover, T.; Hart, P. Nearest neighbor pattern classification. *IEEE Transactions on Information Theory* **1967**, *13*, 21–27.
334. Murphy, K. *Machine Learning: A Probabilistic Perspective*; Adaptive Computation and Machine Learning series, MIT Press, **2012**.
335. Basheer, A.; Afham, A.; Goyal, S.K. Quantum k-nearest neighbors algorithm, **2021**.
336. Zardini, E.; Blanzieri, E.; Pastorello, D. A quantum k-nearest neighbors algorithm based on the Euclidean distance estimation. *Quantum Machine Intelligence* **2024**, *6*.
337. Giovannetti, V.; Lloyd, S.; Maccone, L. Quantum Random Access Memory. *Phys. Rev. Lett.* **2008**, *100*, 160501.
338. Phalak, K.; Chatterjee, A.; Ghosh, S. Quantum Random Access Memory for Dummies. *Sensors* **2023**, *23*, 7462.

 doi:10.20944/preprints202511.1802.v2

339. Schuld, M.; Petruccione, F. *Supervised Learning with Quantum Computers*, 1st ed.; Springer Publishing Company, Incorporated, **2018**.
340. IBM. Data encoding. Last accessed: 24.03.2025.
341. Jaques, S.; Rattew, A.G. QRAM: A Survey and Critique. *arXiv* **2023**.
342. Giovannetti, V.; Lloyd, S.; Maccone, L. Architectures for a quantum random access memory. *Phys. Rev. A* **2008**, *78*, 052310.
343. Buhrman, H.; Cleve, R.; Watrous, J.; de Wolf, R. Quantum fingerprinting. *Phys. Rev. Lett.* **2001**, *87*, 167902.
344. Guerrero-Estrada, A.Y.; Quezada, L.F.; Sun, G.H. Benchmarking quantum versions of the kNN algorithm with a metric based on amplitude-encoded features. *Scientific Reports* **2024**, *14*, 16697.
345. Baldazzi, A.; Leone, N.; Sanna, M.; Azzini, S.; Pavesi, L. A linear photonic swap test circuit for quantum kernel estimation. *Quantum Science and Technology* **2024**, *9*, 045053.
346. Herman, D.; Googin, C.; Liu, X.; Galda, A.; Safro, I.; Sun, Y.; Pistoia, M.; Alexeev, Y. A Survey of Quantum Computing for Finance, **2022**.
347. Halder, R.K.; Uddin, M.N.; Uddin, M.A.; Aryal, S.; Khraisat, A. Enhancing K-nearest neighbor algorithm: a comprehensive review and performance analysis of modifications. *Journal of Big Data* **2024**, *11*, 113.
348. Myles, A.J.; Feudale, R.N.; Liu, Y.; Woody, N.A.; Brown, S.D. An introduction to decision tree modeling. *Journal of Chemometrics* **2004**, *18*, 275–285.
349. Yang, F.J. An Extended Idea about Decision Trees. In Proceedings of the 2019 International Conference on Computational Science and Computational Intelligence (CSCI), **2019**, pp. 349–354.
350. Younes, L. Introduction to Machine Learning, **2024**.
351. Breiman, L.; Friedman, J.H.; Olshen, R.A.; Stone, C.J. *Classification and Regression Trees*; Chapman and Hall/CRC, **1984**.
352. Shannon, C.E. A mathematical theory of communication. *The Bell System Technical Journal* **1948**, *27*, 623–656.
353. Nowozin, S. Improved Information Gain Estimates for Decision Tree Induction, **2012**.
354. Murthy, S.; Salzberg, S. Decision Tree Induction: How Effective is the Greedy Heuristic? In Proceedings of the KDD 1995 - Proceedings of the 1st International Conference on Knowledge Discovery and Data Mining; Fayyad, U.; Uthurusamy, R., Eds. AAAI Press, **1995**, pp. 222–227.
355. van der Linden, J.G.M.; Vos, D.; de Weerdt, M.M.; Verwer, S.; Demirović, E. Optimal or Greedy Decision Trees? Revisiting their Objectives, Tuning, and Performance, **2025**.
356. Khadiev, K.; Mannapov, I.; Safina, L. The Quantum Version Of Classification Decision Tree Constructing Algorithm C5.0, **2019**.
357. Ambainis, A. Understanding Quantum Algorithms via Query Complexity, **2017**.
358. Sharma, D.; Singh, P.; Kumar, A. Quantum-inspired attribute selection algorithms. *Quantum Sci. Technol.* **2025**, *10*, 015036.
359. Koren, M.; Peretz, O. A quantum procedure for estimating information gain in Boolean classification task. *Quantum Machine Intelligence* **2024**, *6*, 16.
360. Ahuja, A.; Kapoor, S. A Quantum Algorithm for finding the Maximum, **1999**.
361. Kumar, N.; Yalovetzky, R.; Li, C.; Minssen, P.; Pistoia, M. Des-q: a quantum algorithm to provably speedup retraining of decision trees. *Quantum* **2025**, *9*, 1588.
362. Wang, H.; Gupta, G. Superfast Selection for Decision Tree Algorithms, **2024**.
363. Zhang, G.; Gionis, A. Regularized impurity reduction: accurate decision trees with complexity guarantees. *Data Mining and Knowledge Discovery* **2023**, *37*, 434–475.
364. Cornelissen, A.; Mande, N.S.; Patro, S. Improved Quantum Query Upper Bounds Based on Classical Decision Trees. *Quantum* **2025**, *9*, 1777.
365. Pandya, R.; Pandya, J. C5.0 algorithm to improved decision tree with feature selection and reduced error pruning. *International Journal of Computer Applications* **2015**, *117*.
366. Kerenidis, I.; Landman, J.; Luongo, A.; Prakash, A. q-means: A quantum algorithm for unsupervised machine learning. In Proceedings of the Advances in Neural Information Processing Systems; Wallach, H.; Larochelle, H.; Beygelzimer, A.; d'Alché-Buc, F.; Fox, E.; Garnett, R., Eds. Curran Associates, Inc., **2019**, Vol. 32.
367. Li, Z.; Terashi, K. Quantum decision trees with information entropy, **2025**.
368. Rad, D.; Cuc, L.D.; Croitoru, G.; Gomoi, B.C.; Mazuru, L.; Bilți, R.S.; Rusu, S.; Sinaci, M.; Barbu, F.S. Modeling Investment Decisions Through Decision Tree Regression—A Behavioral Finance Theory Approach. *Electronics* **2025**, *14*.

 doi:10.20944/preprints202511.1802.v2

369. Grudniewicz, J.; Ślepaczuk, R. Application of machine learning in algorithmic investment strategies on global stock markets. *Research in International Business and Finance* **2023**, *66*, 102052.
370. Tu, J.; Wu, Z. Inherently interpretable machine learning for credit scoring: Optimal classification tree with hyperplane splits. *European Journal of Operational Research* **2025**, *322*, 647–664.
371. Luo, G.; Arshad, M.A.; Luo, G. Decision Trees for Strategic Choice of Augmenting Management Intuition with Machine Learning. *Symmetry* **2025**, *17*.
372. Černevičienė, J.; Kabašinskas, A. Explainable artificial intelligence (XAI) in finance: a systematic literature review. *Artificial Intelligence Review* **2024**, *57*, 216.
373. Bücker, M.; Szepannek, G.; Gosiewska, A.; Biecek, P. Transparency, auditability, and explainability of machine learning models in credit scoring. *Journal of the Operational Research Society* **2022**, *73*, 70–90.
374. Forensic Risk Alliance. Explainable AI: Building Confidence and Compliance, 2024. Accessed: 11-08-2025.
375. Montanaro, A. Almost all decision trees do not allow significant quantum speed-up, **2012**.
376. Shi, Y. Entropy lower bounds of quantum decision tree complexity, **2000**.
377. James, G.; Witten, D.; Hastie, T.; Tibshirani, R. *An introduction to statistical learning*; Springer, **2021**.
378. Altman, N.S. An Introduction to Kernel and Nearest-Neighbor Nonparametric Regression. *The American Statistician* **1992**, *46*, 175–185.
379. Seber, G.; Lee, A. *Linear regression analysis. 2nd edit.*; Wiley, **2003**.
380. Strang, G. *Introduction to Linear Algebra*, sixth ed.; Wellesley-Cambridge Press: Wellesley, MA, **2023**.
381. Aster, R.C.; Borchers, B.; Thurber, C.H. *Parameter Estimation and Inverse Problems (Third Edition)*, third edition ed.; Elsevier, **2019**.
382. Hoerl, A.E.; Kennard, R.W. Ridge Regression: Biased Estimation for Nonorthogonal Problems. *Technometrics* **1970**, *12*, 55–67.
383. Liu, S.; Dobriban, E. Ridge Regression: Structure, Cross-Validation, and Sketching, **2020**.
384. Golub, G.H.; Van Loan, C.F. *Matrix Computations - 4th Edition*; Johns Hopkins University Press: Philadelphia, PA, **2013**.
385. Song, Z.; Yin, J.; Zhang, R. Revisiting Quantum Algorithms for Linear Regressions: Quadratic Speedups without Data-Dependent Parameters, **2023**.
386. Chakraborty, S.; Morolia, A.; Peduri, A. Quantum Regularized Least Squares. *Quantum* **2023**, *7*, 988.
387. Schuld, M.; Killoran, N. Quantum Machine Learning in Feature Hilbert Spaces. *Phys. Rev. Lett.* **2019**, *122*, 040504.
388. Shawe-Taylor, J.; Cristianini, N. *Kernel Methods for Pattern Analysis*; Cambridge University Press, **2004**.
389. Welling, M. Kernel Ridge Regression. Lecture notes, University of Toronto, **2007**.
390. Rasmussen, C.E.; Williams, C.K.I. *Gaussian Processes for Machine Learning*; MIT Press: Cambridge, MA, **2006**.
391. Schnabel, J.; Roth, M. Quantum kernel methods under scrutiny: a benchmarking study. *Quantum Machine Intelligence* **2025**, *7*.
392. Schuld, M. Supervised quantum machine learning models are kernel methods, **2021**.
393. Li, T.; Chakrabarti, S.; Wu, X. Sublinear quantum algorithms for training linear and kernel-based classifiers, **2019**.
394. Huang, H.Y.; Broughton, M.; Mohseni, M.; Babbush, R.; Boixo, S.; Neven, H.; McClean, J.R. Power of data in quantum machine learning. *Nature Communications* **2021**, *12*.
395. Sabarad, V.; Varma, V.; Mahesh, T.S. Experimental Machine Learning with Classical and Quantum Data via NMR Quantum Kernels, **2025**.
396. Miyabe, S.; Quanz, B.; Shimada, N.; Mitra, A.; Yamamoto, T.; Rastunkov, V.; Alevras, D.; Metcalf, M.; King, D.J.M.; Mamouei, M.; et al. Quantum Multiple Kernel Learning in Financial Classification Tasks, **2023**.
397. Zhou, X.; Yu, J.; Tan, J.; Jiang, T. Quantum kernel estimation-based quantum support vector regression. *Quantum Information Processing* **2024**, *23*, 29.
398. Benedetti, M.; Garcia-Pintos, D.; Perdomo, O.; Leyton-Ortega, V.; Nam, Y.; Perdomo-Ortiz, A. A generative modeling approach for benchmarking and training shallow quantum circuits. *npj Quantum Information* **2019**, *5*.
399. Thanasilp, S.; Wang, S.; Cerezo, M.; Holmes, Z. Exponential concentration in quantum kernel methods. *Nature Communications* **2024**, *15*, 5200.
400. Shiota, T.; Ishihara, K.; Mizukami, W. Universal neural network potentials as descriptors: Towards scalable chemical property prediction using quantum and classical computers. *Digital Discovery* **2024**, *3*, 1714–1728.
401. Gurney, K. *An Introduction to Neural Networks*; An Introduction to Neural Networks, Taylor & Francis, **1997**.

 doi:10.20944/preprints202511.1802.v2

402. Schuld, M.; Sinayskiy, I.; Petruccione, F. The quest for a Quantum Neural Network. *Quantum Information Processing* **2014**, *13*, 2567–2586.
403. Goodfellow, I.; Bengio, Y.; Courville, A. *Deep Learning*; MIT Press, **2016**.
404. Abbas, A.; Sutter, D.; Zoufal, C.; Lucchi, A.; Figalli, A.; Woerner, S. The power of quantum neural networks. *Nature Computational Science* **2021**, *1*, 403–409.
405. Altaisky, M.V. Quantum neural network, **2001**.
406. Schuld, M.; Sweke, R.; Meyer, J.J. Effect of data encoding on the expressive power of variational quantum-machine-learning models. *Phys. Rev. A* **2021**, *103*, 032430.
407. Ding, X.; Song, Z.; Xu, J.; Hou, Y.; Yang, T.; Shan, Z. Scalable parameterized quantum circuits classifier. *Scientific Reports* **2024**, *14*, 15886.
408. Schuld, M.; Petruccione, F. *Machine Learning with Quantum Computers*; Quantum Science and Technology, Springer International Publishing, **2021**.
409. Beer, K.; Bondarenko, D.; Farrelly, T.; Osborne, T.J.; Salzmann, R.; Scheiermann, D.; Wolf, R. Training deep quantum neural networks. *Nature Communications* **2020**, *11*, 808.
410. Crooks, G.E. Gradients of parameterized quantum gates using the parameter-shift rule and gate decomposition, **2019**.
411. Paquet, E.; Soleymani, F. QuantumLeap: Hybrid quantum neural network for financial predictions. *Expert Syst. Appl.* **2022**, *195*.
412. Choudhary, P.K.; Innan, N.; Shafique, M.; Singh, R. HQNN-FSP: A Hybrid Classical-Quantum Neural Network for Regression-Based Financial Stock Market Prediction. *arXiv preprint arXiv:2503.15403* **2025**.
413. Tudisco, A.; Volpe, D.; Ranieri, G.; Curato, G.; Ricossa, D.; Graziano, M.; Corbelletto, D. Evaluating the Computational Advantages of the Variational Quantum Circuit Model in Financial Fraud Detection. *IEEE Access* **2024**, *12*, 102918–102940.
414. Innan, N.; Marchisio, A.; Bennai, M.; Shafique, M. QFNN-FFD: Quantum Federated Neural Network for Financial Fraud Detection, **2024**.
415. Bowles, J.; Ahmed, S.; Schuld, M. Better than classical? The subtle art of benchmarking quantum machine learning models, **2024**.
416. Gonon, L.; Jacquier, A. Universal Approximation Theorem and Error Bounds for Quantum Neural Networks and Quantum Reservoirs. *IEEE Transactions on Neural Networks and Learning Systems* **2025**, p. 1–14.
417. Kashif, M.; Marchisio, A.; Shafique, M. Computational Advantage in Hybrid Quantum Neural Networks: Myth or Reality?, **2025**.
418. Kashif, M.; Al-Kuwari, S. ResQNets: a residual approach for mitigating barren plateaus in quantum neural networks. *EPJ Quantum Technology* **2024**, *11*.
419. Krenn, M.; Landgraf, J.; Foesel, T.; Marquardt, F. Artificial intelligence and machine learning for quantum technologies. *Phys. Rev. A* **2023**, *107*, 010101.
420. Landman, J. Quantum Algorithms for Unsupervised Machine Learning and Neural Networks, **2021**.
421. Aïmeur, E.; Brassard, G.; Gambs, S. Quantum speed-up for unsupervised learning. *Mach. Learn.* **2013**, *90*, 261–287.
422. Wang, Y.J.; Yang, X.; Ju, C.; Zhang, Y.; Zhang, J.; Xu, Q.; Wang, Y.; Gao, X.; Cao, X.; Ma, Y.; et al. Quantum Computing in Community Detection for Anti-Fraud Applications. *Entropy* **2024**, *26*.
423. Lloyd, S. Least squares quantization in PCM. *IEEE Transactions on Information Theory* **1982**, *28*, 129–137.
424. Arthur, D.; Vassilvitskii, S. k-means++: the advantages of careful seeding. In Proceedings of the Proceedings of the Eighteenth Annual ACM-SIAM Symposium on Discrete Algorithms, USA, **2007**; SODA '07, p. 1027–1035.
425. Strohmer, T. K-Means Clustering. Lecture slides, University of California, Davis, **2017**.
426. Poggiali, A.; Berti, A.; Bernasconi, A.; Del Corso, G.M.; Guidotti, R. Quantum clustering with k-Means: A hybrid approach. *Theor. Comput. Sci.* **2024**, *992*, 114466.
427. Zubair, M.; Iqbal, A.; Shil, A.; Chowdhury, M.; Moni, M.A.; Sarker, I. An Improved K-means Clustering Algorithm Towards an Efficient Data-Driven Modeling. *Annals of Data Science* **2022**, *11*, 1525–1544.
428. Woodruff, D.P.; Zhong, P.; Zhou, S. Near-Optimal k-Clustering in the Sliding Window Model, **2023**.
429. Drineas, P.; Frieze, A.M.; Kannan, R.; Vempala, S.S.; Vinay, V. Clustering Large Graphs via the Singular Value Decomposition. *Machine Learning* **2004**, *56*, 9–33.
430. Shi, X.; Shang, Y.; Guo, C. Quantum inspired K-means algorithm using matrix product states, **2020**.
431. Park, D.; Petruccione, F.; Rhee, J. Circuit-Based Quantum Random Access Memory for Classical Data. *Scientific reports* **2019**, *9*.

 doi:10.20944/preprints202511.1802.v2

432. Abreu, D.; Moura, D.; Esteve Rothenberg, C.; Abelém, A. QuantumNetSec: Quantum Machine Learning for Network Security. *International Journal of Network Management* **2025**, *35*, e70018.
433. Li, Y. Quantum Machine Learning Based on K-Means to Optimize Cross-Border Intelligent Payment Supervision. In Proceedings of the Proceedings of the 2024 4th International Conference on Big Data, Artificial Intelligence and Risk Management, New York, NY, USA, **2025**; ICBAR '24, p. 676–681.
434. Tsai, Y.C.; Chen, S.Y.C. Quantum Feature Optimization for Enhanced Clustering of Blockchain Transaction Data, **2025**.
435. Ng, A.; Jordan, M.; Weiss, Y. On Spectral Clustering: Analysis and an algorithm. In Proceedings of the Advances in Neural Information Processing Systems; Dietterich, T.; Becker, S.; Ghahramani, Z., Eds. MIT Press, **2001**, Vol. 14.
436. Shi, J.; Malik, J. Normalized cuts and image segmentation. *IEEE Transactions on Pattern Analysis and Machine Intelligence* **2000**, *22*, 888–905.
437. Yan, D.; Huang, L.; Jordan, M.I. Fast approximate spectral clustering. In Proceedings of the Proceedings of the 15th ACM SIGKDD International Conference on Knowledge Discovery and Data Mining, New York, NY, USA, **2009**; KDD '09, p. 907–916.
438. Kerenidis, I.; Landman, J. Quantum spectral clustering. *Phys. Rev. A* **2021**, *103*, 042415.
439. Volya, D.; Mishra, P. Quantum Spectral Clustering of Mixed Graphs. In Proceedings of the 2021 58th ACM/IEEE Design Automation Conference (DAC), **2021**, pp. 463–468.
440. Creswell, A.; White, T.; Dumoulin, V.; Arulkumaran, K.; Sengupta, B.; Bharath, A.A. Generative Adversarial Networks: An Overview. *IEEE Signal Processing Magazine* **2018**, *35*, 53–65.
441. Coyle, B.; Mills, D.; Danos, V.; Kashefi, E. The Born supremacy: quantum advantage and training of an Ising Born machine. *npj Quantum Information* **2020**, *6*.
442. Kullback, S.; Leibler, R.A. On Information and Sufficiency. *The Annals of Mathematical Statistics* **1951**, *22*, 79–86.
443. Benedetti, M.; Lloyd, E.; Sack, S.; Fiorentini, M. Parameterized quantum circuits as machine learning models. *Quantum Science and Technology* **2019**, *4*, 043001.
444. Zoufal, C.; Lucchi, A.; Woerner, S. Variational quantum Boltzmann machines. *Quantum Machine Intelligence* **2021**, *3*.
445. Lloyd, S.; Weedbrook, C. Quantum Generative Adversarial Learning. *Phys. Rev. Lett.* **2018**, *121*, 040502.
446. Ackley, D.H.; Hinton, G.E.; Sejnowski, T.J. A learning algorithm for boltzmann machines. *Cognitive Science* **1985**, *9*, 147–169.
447. Aggarwal, C.C. *Neural Networks and Deep Learning*, second ed.; Springer Cham, **2023**; p. 497.
448. Hopfield, J.J. Neural Networks and Physical Systems with Emergent Collective Computational Abilities. *Proceedings of the National Academy of Sciences of the United States of America* **1982**, *79*, 2554–2558.
449. Rumelhart, D.E.; McClelland, J.L., Learning and Relearning in Boltzmann Machines. In *Parallel Distributed Processing: Explorations in the Microstructure of Cognition: Foundations*; MIT Press, **1987**; Vol. 1, pp. 282–317.
450. Haykin, S. *Neural Networks and Learning Machines*; Number v. 10 in Neural networks and learning machines, Pearson, **2009**.
451. Aarts, E.; Korst, J. *Simulated annealing and Boltzmann machines: a stochastic approach to combinatorial optimization and neural computing*; John Wiley & Sons, Inc., **1989**.
452. Carreira-Perpiñán, M.A.; Hinton, G. On Contrastive Divergence Learning. In Proceedings of the Proceedings of the Tenth International Workshop on Artificial Intelligence and Statistics; Cowell, R.G.; Ghahramani, Z., Eds. PMLR, 06–08 **2005**, Vol. R5, *Proceedings of Machine Learning Research*, pp. 33–40. Reissued by PMLR on 30 March 2021.
453. Rossi, R.J. *Mathematical Statistics: An Introduction to Likelihood Based Inference*; John Wiley & Sons, Ltd, **2018**.
454. Amin, M.H.; Andriyash, E.; Rolfe, J.; Kulchytskyy, B.; Melko, R. Quantum Boltzmann Machine. *Phys. Rev. X* **2018**, *8*, 021050..
455. Hebb, D. *The Organization of Behavior: A Neuropsychological Theory*, first ed.; Psychology Press, **2002**.
456. Wiebe, N.; Kapoor, A.; Svore, K.M. Quantum deep learning. *Quantum Info. Comput.* **2016**, *16*, 541–587.
457. Patel, D.; Koch, D.; Patel, S.; Wilde, M.M. Quantum Boltzmann machine learning of ground-state energies, **2024**.
458. Berner, N.; Fortuin, V.; Landman, J. Quantum Bayesian Neural Networks, **2021**.
459. Arjovsky, M.; Chintala, S.; Bottou, L. Wasserstein GAN, **2017**.
460. Dallaire-Demers, P.L.; Killoran, N. Quantum generative adversarial networks. *Phys. Rev. A* **2018**, *98*, 012324.

 doi:10.20944/preprints202511.1802.v2

461. Situ, H.; He, Z.; Wang, Y.; Li, L.; Zheng, S. Quantum generative adversarial network for generating discrete distribution. *Information Sciences* **2020**, *538*, 193–208.
462. Schuld, M.; Bergholm, V.; Gogolin, C.; Izaac, J.; Killoran, N. Evaluating analytic gradients on quantum hardware. *Physical Review A* **2019**, *99*, 032331..
463. Wierichs, D.; Izaac, J.; Wang, C.; Lin, C.Y.Y. General parameter-shift rules for quantum gradients. *Quantum* **2022**, *6*, 677.
464. Anoshin, M.; Sagingalieva, A.; Mansell, C.; Zhiganov, D.; Shete, V.; Pflitsch, M.; Melnikov, A. Hybrid Quantum Cycle Generative Adversarial Network for Small Molecule Generation. *IEEE Transactions on Quantum Engineering* **2024**, *5*, 1–14.
465. Cerezo, M.; Sone, A.; Volkoff, T.; Cincio, L.; Coles, P.J. Cost function dependent barren plateaus in shallow parametrized quantum circuits. *Nature Communications* **2021**, *12*.
466. Wang, S.; Fontana, E.; Cerezo, M.; Sharma, K.; Sone, A.; Cincio, L.; Coles, P.J. Noise-induced barren plateaus in variational quantum algorithms. *Nature Communications* **2021**, *12*.
467. Pajuhanfard, M.; Kiani, R.; Sheng, V.S. Survey of Quantum Generative Adversarial Networks (QGAN) to Generate Images. *Mathematics* **2024**, *12*.
468. Liu, J.G.; Wang, L. Differentiable learning of quantum circuit Born machines. *Physical Review A* **2018**, *98*.
469. Low, G.H.; Yoder, T.J.; Chuang, I.L. Quantum inference on Bayesian networks. *Physical Review A* **2014**, *89*.
470. Borujeni, S.E.; Nguyen, N.H.; Nannapaneni, S.; Behrman, E.C.; Steck, J.E. Experimental evaluation of quantum Bayesian networks on IBM QX hardware. In Proceedings of the 2020 IEEE International Conference on Quantum Computing and Engineering (QCE). IEEE, **2020**, pp. 372–378.
471. Moreira, C.; Wichert, A. Quantum-Like Bayesian Networks for Modeling Decision Making. *Frontiers in Psychology* **2016**, *7*.
472. Wichert, A.; Moreira, C.; Bruza, P. Balanced Quantum-Like Bayesian Networks. *Entropy* **2020**, *22*, 170.
473. F.R.S., K.P. LIII. On lines and planes of closest fit to systems of points in space. *Philosophical Magazine Series 1* **1901**, *2*, 559–572.
474. Hotelling, H. Analysis of a Complex of Statistical Variables Into Principal Components. *Journal of Educational Psychology*, **1933**, *24*.
475. Golub, G.H.; Reinsch, C. Singular value decomposition and least squares solutions. *Numerische Mathematik* **1970**, *14*, 403–420.
476. Tenenbaum, J.B.; de Silva, V.; Langford, J.C. A Global Geometric Framework for Nonlinear Dimensionality Reduction. *Science* **2000**, *290*, 2319–2323.
477. Lloyd, S.; Mohseni, M.; Rebentrost, P. Quantum principal component analysis. *Nature Physics* **2014**, *10*, 631–633.
478. Tang, E. Dequantizing algorithms to understand quantum advantage in machine learning. *Nature Reviews Physics* **2022**, *4*, 692–693.
479. Li, Z.; Chai, Z.; Guo, Y.; Ji, W.; Wang, M.; Shi, F.; Wang, Y.; Lloyd, S.; Du, J. Resonant quantum principal component analysis. *Science Advances* **2021**, *7*.
480. Wang, Y.; Luo, Y. Resource-efficient quantum principal component analysis. *Quantum Science and Technology* **2024**, *9*, 035031.
481. Nghiem, N.A. New Quantum Algorithm for Principal Component Analysis, **2025**
482. Hastings, M.B. Classical and Quantum Algorithms for Tensor Principal Component Analysis. *Quantum* **2020**, *4*, 237.
483. Hoyle, D.C.; Rattray, M. PCA learning for sparse high-dimensional data. *Europhysics Letters* **2003**, *62*, 117.
484. Wu, J.; Fu, H.; Zhu, M.; Zhang, H.; Xie, W.; Li, X.Y. Quantum circuit autoencoder. *Physical Review A* **2024**, *109*.
485. Sutton, R.S.; Barto, A.G. *Reinforcement Learning: An Introduction*; MIT Press, Cambridge, MA, 2018.
486. Ng, A. CS229 Lecture Notes: Machine Learning, 2023. Standford University, Accessed: 2025-07-05.
487. Kaelbling, L.P.; Littman, M.L.; Moore, A.W. Reinforcement Learning: A Survey, **1996**.
488. Ladosz, P.; Weng, L.; Kim, M.; Oh, H. Exploration in deep reinforcement learning: A survey. *Information Fusion* **2022**, *85*, 1–22.
489. Howard, R.A. *Dynamic Programming and Markov Processes*; MIT Press, **1960**.
490. Bertsekas, D.; Tsitsiklis, J. *Neuro-Dynamic Programming*; Vol. 27, Athena Scientific, **1996**.
491. Bellman, R.; Bellman, R.; Corporation, R. *Dynamic Programming*; Rand Corporation research study, Princeton University Press, **1957**.

 doi:10.20944/preprints202511.1802.v2

492. Murray, P.; Wood, B.; Buehler, H.; Wiese, M.; Pakkanen, M. Deep Hedging: Continuous Reinforcement Learning for Hedging of General Portfolios across Multiple Risk Aversions. In Proceedings of the Proceedings of the Third ACM International Conference on AI in Finance, New York, NY, USA, **2022**; ICAIF '22, p. 361–368.
493. Buehler, H.; Gonon, L.; Teichmann, J.; Wood, B.; Mohan, B.; Kochems, J. Deep Hedging: Hedging Derivatives Under Generic Market Frictions Using Reinforcement Learning. *SSRN Electronic Journal* **2019**.
494. Cherrat, E.A.; Raj, S.; Kerenidis, I.; Shekhar, A.; Wood, B.; Dee, J.; Chakrabarti, S.; Chen, R.; Herman, D.; Hu, S.; et al. Quantum Deep Hedging. *Quantum* **2023**, *7*, 1191.
495. Skolik, A.; Jerbi, S.; Dunjko, V. Quantum agents in the Gym: a variational quantum algorithm for deep Q-learning. *Quantum* **2022**, *6*, 720.
496. Mnih, V.; Kavukcuoglu, K.; Silver, D.; Rusu, A.A.; Veness, J.; Bellemare, M.G.; Graves, A.; Riedmiller, M.; Fidjeland, A.K.; Ostrovski, G.; et al. Human-level control through deep reinforcement learning. *Nature* **2015**, *518*, 529–533.
497. van Hasselt, H.; Doron, Y.; Strub, F.; Hessel, M.; Sonnerat, N.; Modayil, J. Deep Reinforcement Learning and the Deadly Triad, **2018**.
498. Jerbi, S.; Gyurik, C.; Marshall, S.C.; Briegel, H.J.; Dunjko, V. Parametrized quantum policies for reinforcement learning, **2021**.
499. Dong, D.; Chen, C.; Li, H.; Tarn, T.J. Quantum Reinforcement Learning. *IEEE Transactions on Systems, Man, and Cybernetics, Part B (Cybernetics)* **2008**, *38*, 1207–1220.
500. Paparo, G.D.; Dunjko, V.; Makmal, A.; Martin-Delgado, M.A.; Briegel, H.J. Quantum Speedup for Active Learning Agents. *Physical Review X* **2014**, *4*.
501. Meyer, N.; Ufrecht, C.; Yammine, G.; Kontes, G.; Mutschler, C.; Scherer, D.D. Benchmarking Quantum Reinforcement Learning, **2025**.
502. Chen, S.Y.C. Quantum Deep Q-Learning with Distributed Prioritized Experience Replay. In Proceedings of the 2023 International Conference on Quantum Computing and Engineering, 4 **2023**.
503. Lockwood, O.; Si, M. Reinforcement Learning with Quantum Variational Circuit. *Proceedings of the AAAI Conference on Artificial Intelligence and Interactive Digital Entertainment* **2020**, *16*, 245–251.
504. Preskill, J. Quantum Computing in the NISQ era and beyond. *Quantum* **2018**, *2*, 79.
505. Cerezo, M.; Verdon, G.; Huang, H.Y.; Cincio, L.; Coles, P.J. Challenges and opportunities in quantum machine learning. *Nature Computational Science* **2022**, *2*, 567–576.
506. Hohenfeld, H.; Heimann, D.; Wiebe, F.; Kirchner, F. Quantum Deep Reinforcement Learning for Robot Navigation Tasks. *IEEE Access* **2024**, *12*, 87217–87236.
507. Sutton, R.S.; McAllester, D.; Singh, S.; Mansour, Y. Policy gradient methods for reinforcement learning with function approximation. In Proceedings of the Proceedings of the 13th International Conference on Neural Information Processing Systems, Cambridge, MA, USA, **1999**; NIPS'99, p. 1057–1063.
508. Williams, R.J. Simple Statistical Gradient-Following Algorithms for Connectionist Reinforcement Learning. *Mach. Learn.* **1992**, *8*, 229–256.
509. Dawid, A.; Arnold, J.; Requena, B.; Gresch, A.; Płodzień, M.; Donatella, K.; Nicoli, K.A.; Stornati, P.; Koch, R.; Büttner, M.; et al. *Machine Learning in Quantum Sciences*; Cambridge University Press, **2025**.
510. Schulman, J.; Wolski, F.; Dhariwal, P.; Radford, A.; Klimov, O. Proximal Policy Optimization Algorithms, **2017**.
511. Arjona-Medina, J.A.; Gillhofer, M.; Widrich, M.; Unterthiner, T.; Brandstetter, J.; Hochreiter, S. RUDDER: Return Decomposition for Delayed Rewards, **2019**.
512. Pascanu, R.; Bengio, Y. Revisiting Natural Gradient for Deep Networks. *CoRR* **2013**, *abs/1301.3584*.
513. Pérez-Salinas, A.; Cervera-Lierta, A.; Gil-Fuster, E.; Latorre, J.I. Data re-uploading for a universal quantum classifier. *Quantum* **2020**, *4*, 226.
514. Chen, S.Y.C. An Introduction to Quantum Reinforcement Learning (QRL), **2024**.
515. Sequeira, A.; Santos, L.P.; Barbosa, L.S. Trainability issues in quantum policy gradients, **2024**.
516. Meyer, N.; Ufrecht, C.; Periyasamy, M.; Scherer, D.D.; Plinge, A.; Mutschler, C. A Survey on Quantum Reinforcement Learning, **2024**.
517. Jerbi, S.; Cornelissen, A.; Ozols, M.; Dunjko, V. Quantum Policy Gradient Algorithms, **2023**.
518. Dunjko, V.; Liu, Y.K.; Wu, X.; Taylor, J.M. Exponential improvements for quantum-accessible reinforcement learning, **2018**.
519. Katz, J.; Lindell, Y. *Introduction to Modern Cryptography*; Chapman and Hall/CRC, **2007**.

 doi:10.20944/preprints202511.1802.v2

520. Sahu, S.K.; Mazumdar, K. State-of-the-art analysis of quantum cryptography: applications and future prospects. *Frontiers in Physics* **2024**, *12*.
521. Thornhill, J. Time to get serious about the dangers of quantum computing, **2023**.
522. Raheman, F. The Q-Day Dilemma and the Quantum Supremacy/Advantage Conjecture, **2022**.
523. Rivest, R.L.; Shamir, A.; Adleman, L. A method for obtaining digital signatures and public-key cryptosystems. *Commun. ACM* **1978**, *21*, 120–126.
524. Diffie, W.; Hellman, M. New directions in cryptography. *IEEE Transactions on Information Theory* **1976**, *22*, 644–654.
525. Merkle, R.C. Secure communications over insecure channels. *Communications of the ACM* **1978**, *21*, 294–299.
526. Imam, R.; Areeb, Q.M.; Alturki, A.; Anwer, F. Systematic and Critical Review of RSA Based Public Key Cryptographic Schemes: Past and Present Status. *IEEE Access* **2021**, *9*, 155949–155976.
527. Paillier, P., Impossibility Proofs for RSA Signatures in the Standard Model. In *Topics in Cryptology – CT-RSA 2007*; Springer Berlin Heidelberg, **2006**; pp. 31–48..
528. Kleinjung, T.; Aoki, K.; Franke, J.; Lenstra, A.K.; Thomé, E.; Bos, J.W.; Gaudry, P.; Kruppa, A.; Montgomery, P.L.; Osvik, D.A.; et al. Factorization of a 768-Bit RSA Modulus. In Proceedings of the Advances in Cryptology – CRYPTO 2010; Rabin, T., Ed., Berlin, Heidelberg, **2010**; pp. 333–350.
529. Dritsas, E.; Trigka, M.; Mylonas, P. Performance and Security Analysis of the Diffie-Hellman Key Exchange Protocol. In Proceedings of the 2024 19th International Workshop on Semantic and Social Media Adaptation & Personalization (SMAP). IEEE, **2024**, pp. 166–171.
530. Sarkar, A.; Guha Roy, D.; Datta, P., An Overview of the Discrete Logarithm Problem in Cryptography. In *Proceedings of Third International Conference on Advanced Computing and Applications*; Springer Nature Singapore, **2024**; pp. 129–143.
531. KONOMA, C. The Computational Difficulty of Solving Cryptographic Primitive Problems Related to the Discrete Logarithm Problem. *IEICE Transactions on Fundamentals of Electronics, Communications and Computer Sciences* **2005**, *E88-A*, 81–88.
532. Kute, S.; Desai, C.; Jadhav, M. Analysis of RSA and Shor's algorithm for cryptography: A quantum perspective. In Proceedings of the ANNUAL SYMPOSIUM ON APPLIED AND INNOVATION TECHNOLOGICAL ENVIRONMENT 2023 (ASAITE2023): Smart Technology based on Revolution Industry 4.0 and Society 5.0. AIP Publishing, **2024**, Vol. 3222, p. 040004.
533. Irwan, N.F.I.B.A.; Zawawi, M.N.A.; Thabit, R.A.A.B. Investigating the Impact of Grover's Algorithm on AES S-Box. In Proceedings of the 2024 16th International Conference on Knowledge and System Engineering (KSE). IEEE, **2024**, pp. 379–385.
534. Olaoye, G. Quantum Cryptanalysis: Breaking Classical Encryption with Shor's and Grover's Algorithms, **2025**.
535. Hu, F.; Lamata, L.; Sanz, M.; Chen, X.; Chen, X.; Wang, C.; Solano, E. Quantum computing cryptography: Finding cryptographic Boolean functions with quantum annealing by a 2000 qubit D-wave quantum computer. *Physics Letters A* **2020**, *384*, 126214.
536. Zhang, A.; Feng, X. Applications of Quantum Annealing in Cryptography, **2022**.
537. Wang, F. The Hidden Subgroup Problem, **2010**.
538. Fowler, A.G.; Devitt, S.J.; Hollenberg, L.C.L. Implementation of Shor's Algorithm on a Linear Nearest Neighbour Qubit Array. *Quant. Info. Comput. 4, 237-251 (2004)* **2004**.
539. Albuainain, A.; Alansari, J.; Alrashidi, S.; Alqahtani, W.; Alshaya, J.; Nagy, N. Experimental Implementation of Shor's Quantum Algorithm to Break RSA. In Proceedings of the 2022 14th International Conference on Computational Intelligence and Communication Networks (CICN). IEEE, **2022**, pp. 748–752.
540. Kumar, M.; Mondal, B. Study on Implementation of Shor's Factorization Algorithm on Quantum Computer. *SN Computer Science* **2024**, *5*.
541. Gidney, C.; Ekerå, M. How to factor 2048 bit RSA integers in 8 hours using 20 million noisy qubits. *Quantum* **2021**, *5*, 433.
542. Gidney, C. How to factor 2048 bit RSA integers with less than a million noisy qubits. *arXiv* **2025**..
543. Ivezic, M. Q-Day Revisited – RSA-2048 broken by 2030, **2025**.
544. Sevilla, J.; Riedel, C.J. Forecasting timelines of quantum computing, **2020**.
545. Jiang, S.; Britt, K.A.; McCaskey, A.J.; Humble, T.S.; Kais, S. Quantum Annealing for Prime Factorization, **2018**.
546. Hong, C.; Pei, Z.; Wang, Q.; Yang, S.; Yu, J.; Wang, C. Quantum attack on RSA by D-Wave Advantage: a first break of 80-bit RSA. *Science China Information Sciences* **2025**, *68*.

 doi:10.20944/preprints202511.1802.v2

547. Zhang, A.; Feng, X. Applications of Quantum Annealing in Cryptography, **2022**.
548. Ding, J.; Spallitta, G.; Sebastiani, R. Effective Prime Factorization via Quantum Annealing by Modular Locally-structured Embedding, **2023**.
549. Mosca, M. *Post-Quantum Cryptography: 6th International Workshop, PQCrypto 2014, Waterloo, ON, Canada, October 1-3, 2014. Proceedings*; Springer International Publishing, **2014**.
550. Dam, D.T.; Tran, T.H.; Hoang, V.P.; Pham, C.K.; Hoang, T.T. A Survey of Post-Quantum Cryptography: Start of a New Race. *Cryptography* **2023**, *7*, 40.
551. Bavdekar, R.; Jayant Chopde, E.; Agrawal, A.; Bhatia, A.; Tiwari, K. Post Quantum Cryptography: A Review of Techniques, Challenges and Standardizations. In Proceedings of the 2023 International Conference on Information Networking (ICOIN). IEEE, **2023**, pp. 146–151.
552. Lohmiller, N.; Kaniewski, S.; Menth, M.; Heer, T. A Survey of Post-Quantum Cryptography Migration in Vehicles. *IEEE Access* **2025**, *13*, 10160–10176.
553. Boutin, C. NIST Announces First Four Quantum-Resistant Cryptographic Algorithms. *NIST* **2022**.
554. Alagic, G.; Apon, D.; Cooper, D.; Dang, Q.; Dang, T.; Kelsey, J.; Lichtinger, J.; Liu, Y.K.; Miller, C.; Moody, D.; et al. Status report on the third round of the NIST Post-Quantum Cryptography Standardization process. Technical Report NIST IR 8413, National Institute of Standards and Technology (U.S.), Gaithersburg, MD, **2022**.
555. Announcing Issuance of Federal Information Processing Standards (FIPS) FIPS 203, Module-Lattice-Based Key-Encapsulation Mechanism Standard, FIPS 204, Module-Lattice-Based Digital Signature Standard, and FIPS 205, Stateless Hash-Based Digital Signature Standard, National Institute of Standards and Technology **2024**.
556. Beck, B.; Benjamin, D.; O'Brien, D.; Adrian, D. Advancing Our Amazing Bet on Asymmetric Cryptography, **2024**.
557. iMessage with PQ3: The new state of the art in quantum-secure messaging at scale Apple Security Research, **2024**.
558. Ajtai, M.; Dwork, C. A Public-Key Cryptosystem with Worst-Case/Average-Case Equivalence, **1996**.
559. Overbeck, R.; Sendrier, N. Code-based cryptography. In *Post-Quantum Cryptography*; Bernstein, D.J.; Buchmann, J.; Dahmen, E., Eds.; Springer: Berlin, Heidelberg, **2009**; pp. 95–145.
560. Moody, D. The 2nd Round of the NIST PQC Standardization Process, **2019**.
561. Green, M. Hash-based Signatures: An illustrated Primer, **2018**.
562. Relyea, R. Post-quantum cryptography: Hash-based signatures, **2022**. publisher: Red Hat.
563. National Cyber Security Centre (NCSC). Cyber chiefs unveil new roadmap for post-quantum cryptography migration. Technical report, National Cyber Security Centre (NCSC), UK, **2025**. Accessed: 2025-08-14.
564. SIKE – Supersingular Isogeny Key Encapsulation. SIKE – Supersingular Isogeny Key Encapsulation. SIKE homepage, n.d. Accessed: 2025-08-14.
565. Costello, C.; Longa, P.; Naehrig, M.; Renes, J.; Virdia, F., Improved Classical Cryptanalysis of SIKE in Practice. In *Public-Key Cryptography – PKC 2020*; Springer International Publishing, **2020**; pp. 505–534.
566. Alagic, G.; Bros, M.; Ciadoux, P.; Cooper, D.; Dang, Q.; Dang, T.; Kelsey, J.; Lichtinger, J.; Liu, Y.K.; Miller, C.; et al. Status report on the fourth round of the NIST post-quantum cryptography standardization process, **2025**.
567. Castryck, W.; Decru, T. An efficient key recovery attack on SIDH, 2022. Publication info: Published by the IACR in EUROCRYPT **2023**.
568. Bennett, C.H.; Brassard, G. Quantum cryptography: Public key distribution and coin tossing. *Theoretical Computer Science* **1984**, *560*, 7–11.
569. Wolf, R. *Quantum Key Distribution: An Introduction with Exercises*; Springer International Publishing, **2021**.
570. Wootters, W.K.; Zurek, W.H. A single quantum cannot be cloned. *Nature* **1982**, *299*, 802–803.
571. Bennett, C.H.; Brassard, G.; Robert, J.M. Privacy Amplification by Public Discussion. *SIAM Journal on Computing* **1988**, *17*, 210–229.
572. Ekert, A.K. Quantum cryptography based on Bell's theorem. *Physical Review Letters* **1991**, *67*, 661–663.
573. Nurhadi, A.I.; Syambas, N.R. Quantum Key Distribution (QKD) Protocols: A Survey. In Proceedings of the 2018 4th International Conference on Wireless and Telematics (ICWT). IEEE, **2018**, pp. 1–5.
574. Cao, Y.; Zhao, Y.; Wang, Q.; Zhang, J.; Ng, S.X.; Hanzo, L. The Evolution of Quantum Key Distribution Networks: On the Road to the Qinternet. *IEEE Communications Surveys; Tutorials* **2022**, *24*, 839–894.
575. Dervisevic, E.; Tankovic, A.; Fazel, E.; Kompella, R.; Fazio, P.; Voznak, M.; Mehic, M. Quantum Key Distribution Networks - Key Management: A Survey. *ACM Computing Surveys* **2025**, *57*, 1–36.

 doi:10.20944/preprints202511.1802.v2

576. Padavic-Callaghan, K. China's city-wide quantum network. *New Scientist* **2023**, *259*, 13.
577. Wiesner, S. Conjugate coding. *ACM SIGACT News* **1983**, *15*, 78–88.
578. Jiang, Y.F.; Kent, A.; Pitalúa-García, D.; Yao, X.; Chen, X.; Huang, J.; Cowperthwaite, G.; Zheng, Q.; Li, H.; You, L.; et al. Experimental practical quantum tokens with transaction time advantage. *arXiv preprint* **2024**.
579. Ehara, Y.; Tada, M. How to generate transparent random numbers using blockchain. In Proceedings of the 2018 International Symposium on Information Theory and Its Applications (ISITA). IEEE, 2018, pp. 169–173.
580. Bartoletti, M.; Pompianu, L., An Empirical Analysis of Smart Contracts: Platforms, Applications, and Design Patterns. In *Financial Cryptography and Data Security*; Springer International Publishing, **2017**; pp. 494–509.
581. Chatterjee, K.; Goharshady, A.K.; Pourdamghani, A. Probabilistic Smart Contracts: Secure Randomness on the Blockchain. In Proceedings of the 2019 IEEE International Conference on Blockchain and Cryptocurrency (ICBC). IEEE, **2019**, pp. 403–412.
582. L'Ecuyer, P. Random Number Generation. Lecture notes / Technical report Chapter or Report, Département d'Informatique et de Recherche Opérationnelle, Université de Montréal, n.d. Accessed: 2025-08-14.
583. Komarov, A. Independent Functions or How to Create the Random Number Generator, **2019**. publisher: Serokell Labs.
584. L'Ecuyer, P., Random Number Generation. In *Handbook of Computational Statistics*; Springer Berlin Heidelberg, **2011**; pp. 35–71.
585. Blum, M.; Micali, S. *How to generate cryptographically strong sequences of pseudo random bits*; Association for Computing Machinery, **2019**.
586. L'Ecuyer, P.; Simard, R. TestU01: A C library for empirical testing of random number generators. *ACM Transactions on Mathematical Software* **2007**, *33*, 1–40.
587. Pironio, S.; Acín, A.; Massar, S.; de la Giroday, A.B.; Matsukevich, D.N.; Maunz, P.; Olmschenk, S.; Hayes, D.; Luo, L.; Manning, T.A.; et al. Random numbers certified by Bell's theorem. *Nature* **2010**, *464*, 1021–1024.
588. Aaronson, S.; Hung, S.H. Certified Randomness from Quantum Supremacy. In Proceedings of the Proceedings of the 55th Annual ACM Symposium on Theory of Computing. ACM, **2023**, STOC '23, pp. 933–944.
589. Acín, A.; Masanes, L. Certified randomness in quantum physics. *Nature* **2016**, *540*, 213–219.
590. Liu, M.; Shaydulin, R.; Niroula, P.; DeCross, M.; Hung, S.H.; Kon, W.Y.; Cervero-Martín, E.; Chakraborty, K.; Amer, O.; Aaronson, S.; et al. Certified randomness using a trapped-ion quantum processor. *Nature* **2025**, *640*, 343–348.
591. Gheorghiu, A.; Kapourniotis, T.; Kashefi, E. Verification of Quantum Computation: An Overview of Existing Approaches. *Theory of Computing Systems* **2018**, *63*, 715–808.
592. Carrasco, J.; Elben, A.; Kokail, C.; Kraus, B.; Zoller, P. Theoretical and Experimental Perspectives of Quantum Verification. *PRX Quantum* **2021**, *2*, 010102.
593. Kapourniotis, T.; Kashefi, E.; Leichtle, D.; Music, L.; Ollivier, H. Unifying quantum verification and error-detection: theory and tools for optimisations. *Quantum Science and Technology* **2024**, *9*, 035036.
594. Helm, T.; Low, A.; Townson, J. UK FinTech State of the Nation. Technical report, Department for International Trade, **2019**.
595. Ramamurthy, S.; Sironi, P. 2025 Global Outlook for Banking and Financial Markets. Technical report, IBM, **2025**.
596. Youssef, W.A.B.; Mansour, N. Finance in the Digital Age: The Challenges and Opportunities. In Proceedings of the Technology: Toward Business Sustainability; Alareeni, B.; Hamdan, A., Eds., Cham, **2024**; pp. 45–59.
597. International, K. Voices on 2030: Financial Services reinvented. Technical report, KPMG, **2022**.
598. Bueno, L.A.; Sigahi, T.F.; Rampasso, I.S.; Leal Filho, W.; Anholon, R. Impacts of digitization on operational efficiency in the banking sector: Thematic analysis and research agenda proposal. *International Journal of Information Management Data Insights* **2024**, *4*, 100230.
599. Bodie, Z.; Kane, A.; Marcus, A.J. *Investments*, 13th ed.; McGraw-Hill Education, **2023**.
600. Fama, E.F. Efficient Capital Markets: A Review of Theory and Empirical Work. *The Journal of Finance* **1970**, *25*, 383–417.
601. Hull, J. *Options, futures, and other derivatives*, eleventh edition, global edition ed.; Pearson4060 1 Online-Ressource (880 Seiten): Harlow, England, **2022**. Description based on publisher supplied metadata and other sources.
602. Orús, R.; Mugel, S.; Lizaso, E. Quantum computing for finance: Overview and prospects. *Reviews in Physics* **2019**, *4*, 100028.

 doi:10.20944/preprints202511.1802.v2

603. Föllmer, H.; Schied, A. *Stochastic finance*, fourth revised and extended edition ed.; De Gruyter graduate, De Gruyter: Berlin, **2016**. Literaturverzeichnis: Seite 576-586.
604. Gu, S.; Kelly, B.; Xiu, D. Empirical Asset Pricing via Machine Learning. *The Review of Financial Studies* **2020**, *33*, 2223–2273.
605. Vaheb, H. Asset Price Forecasting using Recurrent Neural Networks, **2020**.
606. Bausch, J. Recurrent Quantum Neural Networks. In Proceedings of the Advances in Neural Information Processing Systems; Larochelle, H.; Ranzato, M.; Hadsell, R.; Balcan, M.; Lin, H., Eds. Curran Associates, Inc., **2020**, Vol. 33, pp. 1368–1379.
607. Assouel, A.; Jacquier, A.; Kondratyev, A. A Quantum Generative Adversarial Network for distributions, **2021**.
608. Bao, J.; Rebentrost, P. Fundamental theorem for quantum asset pricing. *arXiv* **2022**.
609. Orrell, D. *Quantum economics and finance*, third edition ed.; Panda Ohana Publishing: New York City, NY, **2022**.
610. Accardi, L.; Boukas, A. The Quantum Black-Scholes Equation. *GJPAM, vol. 2, no. 2, pp. 155-170 (2006)* **2007**.
611. Insights, B.R. Derivatives Market Size, Share, Growth, Trends, Global Industry Analysis, 2025. Last accessed: 20-02-2025.
612. Wang, G.; Kan, A. Option pricing under stochastic volatility on a quantum computer. *Quantum* **2024**, *8*, 1504.
613. Chen, J.; Li, Y.; Neufeld, A. Quantum Monte Carlo algorithm for solving Black-Scholes PDEs for high-dimensional option pricing in finance and its complexity analysis, **2025**.
614. Fontanela, F.; Jacquier, A.; Oumgari, M. Short Communication: A Quantum Algorithm for Linear PDEs Arising in Finance. *SIAM Journal on Financial Mathematics* **2021**, *12*, SC98–SC114.
615. FIA. ETD Volume - January 2025, 2025. Last accessed: 20-02-2025.
616. SEC, U.S. Investor Bulletin: An Introduction to Options, 2015. Last accessed: 20-02-2025.
617. Chen, J. What Are Options? Types, Spreads, Example, and Risk, 2024. Last accessed: 20-02-2025.
618. Mikosch, T. *Elementary Stochastic Calculus, with Finance in View*; WORLD SCIENTIFIC, **1998**.
619. Rebentrost, P.; Gupt, B.; Bromley, T.R. Quantum computational finance: Monte Carlo pricing of financial derivatives. *Physical Review A* **2018**, *98*, 022321.
620. Stamatopoulos, N.; Egger, D.J.; Sun, Y.; Zoufal, C.; Iten, R.; Shen, N.; Woerner, S. Option Pricing using Quantum Computers. *Quantum* **2020**, *4*, 291.
621. Ramos-Calderer, S.; Pérez-Salinas, A.; García-Martín, D.; Bravo-Prieto, C.; Cortada, J.; Planagumà, J.; Latorre, J.I. Quantum unary approach to option pricing. *Physical Review A* **2021**, *103*, 032414.
622. Kaneko, K.; Miyamoto, K.; Takeda, N.; Yoshino, K. Quantum speedup of Monte Carlo integration with respect to the number of dimensions and its application to finance. *Quantum Information Processing* **2021**, *20*.
623. Beck, C.; Hutzenthaler, M.; Jentzen, A.; Kuckuck, B. An overview on deep learning-based approximation methods for partial differential equations. *Discrete Contin. Dyn. Syst. Ser. B 28 (2023), no. 6, 3697-3746* **2020**, *28*, 3697–3746.
624. Brunton, S.L.; Kutz, J.N. Promising directions of machine learning for partial differential equations. *Nature Computational Science* **2024**, *4*, 483–494.
625. Joo, J.; Moon, H. Quantum variational PDE solver with machine learning. *arXiv* **2021**.
626. Tavakoli, J.M. *Collateralized Debt Obligations and Structured Finance*; John Wiley & Sons, Ltd., 2004.
627. Tang, H.; Pal, A.; Wang, T.Y.; Qiao, L.F.; Gao, J.; Jin, X.M. Quantum computation for pricing the collateralized debt obligations. *Quantum Engineering* **2021**, *3*, e84.
628. Li, D.X. On Default Correlation. *The Journal of Fixed Income* **2000**, *9*, 43–54.
629. Barndorff-Nielsen, O.E. Normal Inverse Gaussian Distributions and Stochastic Volatility Modelling. *Scandinavian Journal of Statistics* **1997**, *24*, 1–13.
630. Chen, J. What Is a Swap?, 2025. Accessed: 2025-08-29.
631. Baker, L.; Haynes, R.; Roberts, J.; Sharma, R.; Tuckman, B. Risk Transfer with Interest Rate Swaps. *Financial Markets, Institutions; Instruments* **2020**, *30*, 3–28.
632. CFI Team. Netting, 2025. Accessed: 2025-08-29.
633. Schuldenzucker, S.; Seuken, S.; Battiston, S. The Computational Complexity of Financial Networks with Credit Default Swaps. *arXiv* **2017**.
634. Rosenberg, G.; Adolphs, C.; Milne, A.; Lee, A. Swap netting using a quantum annealer, 2016.
635. Boyd, S.; Johansson, K.; Kahn, R.; Schiele, P.; Schmelzer, T. Markowitz Portfolio Construction at Seventy, **2024**.

 doi:10.20944/preprints202511.1802.v2

636. DeMiguel, V.; Garlappi, L.; Nogales, F.J.; Uppal, R. A Generalized Approach to Portfolio Optimization: Improving Performance by Constraining Portfolio Norms. *Management Science* **2009**, *55*, 798–812.
637. Rosenberg, G.; Rounds, M. Long-Short Minimum Risk Parity Optimization Using a Quantum or Digital Annealer, 2018.
638. Benati, S.; Rizzi, R. A mixed integer linear programming formulation of the optimal mean/Value-at-Risk portfolio problem. *European Journal of Operational Research* **2007**, *176*, 423–434.
639. Mansini, R.; Ogryczak, W.; Speranza, M.G. Linear and Mixed Integer Programming for Portfolio Optimization. *Springer* **2015**.
640. Poon, H.K. Practical Portfolio Optimization with Metaheuristics:Pre-assignment Constraint and Margin Trading, **2025**.
641. Deng, W.; Polak, P.; Safikhani, A.; Shah, R. A Unified Framework for Fast Large-Scale Portfolio Optimization, **2023**.
642. Skolpadungket, P.; Dahal, K.; Harnpornchai, N. Portfolio optimization using multi-obj ective genetic algorithms. In Proceedings of the 2007 IEEE Congress on Evolutionary Computation, **2007**, pp. 516–523.
643. Owhadi-Kareshk, M.; Boulanger, P. Portfolio Optimization on Classical and Quantum Computers Using PortFawn, 2021.
644. Palmer, S.; Sahin, S.; Hernandez, R.; Mugel, S.; Orus, R. Quantum Portfolio Optimization with Investment Bands and Target Volatility, 2021.
645. Hodson, M.; Ruck, B.; Ong, H.; Garvin, D.; Dulman, S. Portfolio rebalancing experiments using the Quantum Alternating Operator Ansatz, publisher = arXiv, 2019.
646. Slate, N.; Matwiejew, E.; Marsh, S.; Wang, J.B. Quantum walk-based portfolio optimisation. *Quantum* **2021**, *5*, 513.
647. Rosenberg, G.; Haghnegahdar, P.; Goddard, P.; Carr, P.; Wu, K.; de Prado, M.L. Solving the Optimal Trading Trajectory Problem Using a Quantum Annealer. *IEEE Journal of Selected Topics in Signal Processing* **2016**, *10*, 1053–1060.
648. Mugel, S.; Kuchkovsky, C.; Sánchez, E.; Fernández-Lorenzo, S.; Luis-Hita, J.; Lizaso, E.; Orús, R. Dynamic portfolio optimization with real datasets using quantum processors and quantum-inspired tensor networks. *Phys. Rev. Research* **2022**, *4*, 013006.
649. Manouchehri, K.; Wang, J.B. Quantum Walks in an array of Quantum Dots, 2006.
650. Hadfield, S.; Wang, Z.; O'Gorman, B.; Rieffel, E.G.; Venturelli, D.; Biswas, R. From the Quantum Approximate Optimization Algorithm to a Quantum Alternating Operator Ansatz. *Algorithms* **2019**, *12*.
651. Cornuejols, G.; Fisher, M.L.; Nemhauser, G.L. Exceptional Paper—Location of Bank Accounts to Optimize Float: An Analytic Study of Exact and Approximate Algorithms. *Management Science* **1977**, *23*, 789–810.
652. Catalano, T.J. The Most Effective Hedging Strategies to Reduce Market Risk, 2024. Last accessed: 16-04-2025.
653. MARKOWITZ, H.M. Foundations of Portfolio Theory. *The Journal of Finance* **1991**, *46*, 469–477..
654. Kalra, A.; Qureshi, F.; Tisi, M. Portfolio Asset Identification Using Graph Algorithms on a Quantum Annealer. *SSRN Electronic Journal* **2018**.
655. Loader, D. The structure of clearing and settlement. In *Clearing, Settlement and Custody*; Loader, D., Ed.; Butterworth-Heinemann: Oxford, 2002; pp. 1–18..
656. McGill, R.; Patel, N., Clearing & Settlement. In *Global Custody and Clearing Services*; Palgrave Macmillan UK, **2008**; pp. 43–58.
657. Bakŭ161ys, D.; Sakalauskas, L. Modelling, Simulation and Optimisation of Interbank Settlements. *Information Technology and Control* **2007**, *36*. Accessed: 2025-08-29.
658. Braine, L.; Egger, D.J.; Glick, J.; Woerner, S. Quantum Algorithms for Mixed Binary Optimization Applied to Transaction Settlement. *IEEE Transactions on Quantum Engineering* **2021**, *2*, 1–8.
659. Huber, E.X.; Tan, B.Y.L.; Griffin, P.R.; Angelakis, D.G. Exponential qubit reduction in optimization for financial transaction settlement. *EPJ Quantum Technology* **2024**, *11*..
660. Ross, S. *Return, Risk and Arbitrage*; Vol. Vol. I, Rodney L. White Center for Financial Research, The Wharton School, **1977**.
661. Dybvig, P.H.; Ross, S.A., Arbitrage. In *The New Palgrave Dictionary of Economics*; Palgrave Macmillan UK, **2008**; pp. 1–12.
662. Aquilina, M.; Budish, E.; O'Neill, P. Quantifying the High-Frequency Trading 'Arms Race': A Simple New Methodology and Estimates. Technical report, Financial Conduct Authority, **2020**.
663. Borch, C.; Wosnitzer, R., Eds. *The Routledge handbook of critical finance studies*; Routledge international handbooks, Routledge, Taylor & Francis Group: New York, **2021**.

 doi:10.20944/preprints202511.1802.v2

664. Soon, W.; Ye, H.Q. Currency arbitrage detection using a binary integer programming model. In Proceedings of the 2007 IEEE International Conference on Industrial Engineering and Engineering Management, **2007**, pp. 867–870.
665. Bellman, R. On a routing problem. *Quarterly of Applied Mathematics* **1958**, *16*, 87–90..
666. Floyd, R.W. Algorithm 97: Shortest path. *Commun. ACM* **1962**, *5*, 345.
667. Karp, R.M., Reducibility among Combinatorial Problems. In *Complexity of Computer Computations*; Springer US, 1972; p. 85–103.
668. Deshpande, S.; Das, E.R.; Mueller, F. Currency Arbitrage Optimization using Quantum Annealing, QAOA and Constraint Mapping, **2025**.
669. Wu, W.; Wang, Y.; Yan, G.; Zhao, Y.; Zhang, B.; Yan, J. On Reducing the Execution Latency of Superconducting Quantum Processors via Quantum Job Scheduling. In Proceedings of the Proceedings of the 43rd IEEE/ACM International Conference on Computer-Aided Design. ACM, **2024**, ICCAD '24, p. 1–9.
670. Capponi, A.; (eds), C.A.L., NLP in Finance. In *Machine Learning and Data Sciences for Financial Markets: A Guide to Contemporary Practices*; Cambridge University Press, **2023**; p. 563–592.
671. Boleda, G. Distributional semantics and linguistic theory. *Annual Review of Linguistics* **2020**, *6*, 213–234.
672. Stein, J.; Christ, I.; Kraus, N.; Mansky, M.B.; Müller, R.; Linnhoff-Popien, C. Applying QNLP to Sentiment Analysis in Finance. In Proceedings of the 2023 IEEE International Conference on Quantum Computing and Engineering (QCE), **2023**, Vol. 02, pp. 20–25.
673. Steck, H.; Ekanadham, C.; Kallus, N. Is Cosine-Similarity of Embeddings Really About Similarity? In Proceedings of the Companion Proceedings of the ACM Web Conference 2024. ACM, **2024**, WWW '24, p. 887–890.
674. Mikolov, T.; Chen, K.; Corrado, G.; Dean, J. Efficient Estimation of Word Representations in Vector Space, 2013.
675. Mikolov, T.; Sutskever, I.; Chen, K.; Corrado, G.S.; Dean, J. Distributed Representations of Words and Phrases and their Compositionality. In Proceedings of the Advances in Neural Information Processing Systems; Burges, C.; Bottou, L.; Welling, M.; Ghahramani, Z.; Weinberger, K., Eds. Curran Associates, Inc., **2013**, Vol. 26.
676. Mikolov, T.; Yih, W.t.; Zweig, G. Linguistic regularities in continuous space word representations. In Proceedings of the Proceedings of the 2013 conference of the north american chapter of the association for computational linguistics: Human language technologies, **2013**, pp. 746–751.
677. Widdows, D.; Aboumrad, W.; Kim, D.; Ray, S.; Mei, J. Quantum Natural Language Processing. *KI - Künstliche Intelligenz* **2024**, *38*, 293–310.
678. Devlin, J.; Chang, M.W.; Lee, K.; Toutanova, K. BERT: Pre-training of Deep Bidirectional Transformers for Language Understanding, 2019.
679. Radford, A.; Narasimhan, K. Improving Language Understanding by Generative Pre-Training, 2018.
680. Otter, D.W.; Medina, J.R.; Kalita, J.K. A Survey of the Usages of Deep Learning for Natural Language Processing. *IEEE Transactions on Neural Networks and Learning Systems* **2021**, *32*, 604–624.
681. Devlin, J.; Chang, M.W.; Lee, K.; Toutanova, K. BERT: Pre-training of Deep Bidirectional Transformers for Language Understanding. In Proceedings of the Proceedings of the 2019 Conference of the North American Chapter of the Association for Computational Linguistics: Human Language Technologies, Volume 1 (Long and Short Papers), Minneapolis, Minnesota, **2019**; pp. 4171–4186.
682. Naseem, U.; Razzak, I.; Khan, S.K.; Prasad, M. A Comprehensive Survey on Word Representation Models: From Classical to State-of-the-Art Word Representation Language Models. *ACM Trans. Asian Low-Resour. Lang. Inf. Process.* **2021**, *20*.
683. Floridi, L.; Chiriatti, M. GPT-3: Its Nature, Scope, Limits, and Consequences. *Minds and Machines* **2020**, *110*.
684. Du, K.; Zhao, Y.; Mao, R.; Xing, F.; Cambria, E. Natural language processing in finance: A survey. *Information Fusion* **2025**, *115*, 102755.
685. OpenAI. Learning to reason with LLMs, 2024. [Accessed: 03.01.2025].
686. Strubell, E.; Ganesh, A.; McCallum, A. Energy and Policy Considerations for Deep Learning in NLP, 2019..
687. Bender, E.M.; Gebru, T.; McMillan-Major, A.; Shmitchell, S. On the Dangers of Stochastic Parrots: Can Language Models Be Too Big? In Proceedings of the Proceedings of the 2021 ACM Conference on Fairness, Accountability, and Transparency, New York, NY, USA, **2021**; FAccT '21, p. 610–623.
688. Sadrzadeh, M. High Level Quantum Structures in Linguistics and Multi-Agent Systems. In Proceedings of the AAAI Spring Symposia on Quantum Interactions (01/03/07); Bruza, P.; Lawless, W.; van Rijsbergen, C.J., Eds., **2006**.

 doi:10.20944/preprints202511.1802.v2

689. Coecke, B.; Sadrzadeh, M.; Clark, S. Mathematical Foundations for a Compositional Distributional Model of Meaning, 2010.
690. Coecke, B.; de Felice, G.; Meichanetzidis, K.; Toumi, A. Foundations for Near-Term Quantum Natural Language Processing, 2020.
691. Abramsky, S.; Coecke, B. Categorical quantum mechanics, 2008.
692. Coecke, B.; Duncan, R. Interacting quantum observables: categorical algebra and diagrammatics. *New Journal of Physics* **2011**, *13*, 043016.
693. Takaki, Y.; Mitarai, K.; Negoro, M.; Fujii, K.; Kitagawa, M. Learning temporal data with a variational quantum recurrent neural network. *Phys. Rev. A* **2021**, *103*, 052414.
694. de Felice, G.; Toumi, A.; Coecke, B. DisCoPy: Monoidal Categories in Python. *Electronic Proceedings in Theoretical Computer Science* **2021**, *333*, 183–197.
695. Lorenz, R.; Pearson, A.; Meichanetzidis, K.; Kartsaklis, D.; Coecke, B. QNLP in Practice: Running Compositional Models of Meaning on a Quantum Computer, 2021.
696. Meichanetzidis, K.; Toumi, A.; de Felice, G.; Coecke, B. Grammar-aware sentence classification on quantum computers. *Quantum Machine Intelligence* **2023**, *5*.
697. Meichanetzidis, K.; Gogioso, S.; de Felice, G.; Chiappori, N.; Toumi, A.; Coecke, B. Quantum Natural Language Processing on Near-Term Quantum Computers. *Electronic Proceedings in Theoretical Computer Science* **2021**, *340*, 213–229.
698. Majumder, A.; Zimmerman, C.; Zhu, D.; Alexander, A.; Widdows, D. Near-term advances in quantum natural language processing. *Ann. Math. Artif. Intell.* **2024**, *92*, 1249–1272.
699. Duneau, T.; Bruhn, S.; Matos, G.; Laakkonen, T.; Saiti, K.; Pearson, A.; Meichanetzidis, K.; Coecke, B. Scalable and interpretable quantum natural language processing: an implementation on trapped ions, 2024.
700. Zeng, W.; Coecke, B. Quantum Algorithms for Compositional Natural Language Processing. *Electronic Proceedings in Theoretical Computer Science* **2016**, *221*, 67–75..
701. Yang, X.; Zhu, J.; De Meo, P. A quantum-like zero-shot approach for sentiment analysis in finance. *Journal of Intelligent Information Systems* **2024**.
702. Zhou, J. Quantum Finance: Exploring the Implications of Quantum Computing on Financial Models. *Computational Economics* **2025**.
703. Maurer, T.; Nelson, A. The global cyber threat to financial systems, 2021.
704. Company, M.. The cyber clock is ticking: Derisking emerging technologies in financial services | McKinsey, 2024.
705. Hull, J. *Risk management and financial institutions*, sixth edition ed.; Wiley finance, Wiley: Hoboken, New Jersey, 2023.
706. National Cyber Security Centre. Cyber security risk management framework, 2023.
707. Wu, D.D.; Olson, D.L. Computational simulation and risk analysis: An introduction of state of the art research. *Mathematical and Computer Modelling* **2013**, *58*, 1581–1587.
708. Evrin, V. Risk Assessment and Analysis Methods: Qualitative and Quantitative, 2021.
709. Rumasukun, M.R.; Noch, M.Y. Exploring Financial Risk Management: A Qualitative Study on Risk Identification, Evaluation, and Mitigation in Banking, Insurance, and Corporate Finance. *Jurnal Manajemen Bisnis* **2024**, *11*, 1068–1083.
710. Woerner, S.; Egger, D.J. Quantum risk analysis. *npj Quantum Information* **2019**, *5*.
711. Laudagé, C.; Turkalj, I. Quantum Risk Analysis: Beyond (Conditional) Value-at-Risk, 2025.
712. Stamatopoulos, N.; Clader, B.D.; Woerner, S.; Zeng, W.J. Quantum Risk Analysis of Financial Derivatives, 2024.
713. Miyamoto, K. Quantum algorithm for calculating risk contributions in a credit portfolio. *EPJ Quantum Technology* **2022**, *9*, 20.
714. Wilkens, S.; Moorhouse, J. Quantum computing for financial risk measurement. *Quantum Information Processing* **2023**, *22*, 51.
715. Bank for International Settlements. MAR10 - Market Risk Terminologies, 2020. Accessed: 2025-04-26.
716. Basel Committee on Banking Supervision. Revisions to the Basel II Market risk framework, 2009. Accessed: 2025-04-26.
717. Jorion, P. *Value at risk*, 3. ed., [nachdr.] ed.; McGraw-Hill: New York, NY [u.a.], 2009. Literaturverz. S. 573 - 584.
718. Hong, L.J.; Hu, Z.; Liu, G. Monte Carlo Methods for Value-at-Risk and Conditional Value-at-Risk: A Review. *ACM Trans. Model. Comput. Simul.* **2014**, *24*.

 doi:10.20944/preprints202511.1802.v2

719. Egger, D.J.; García Gutiérrez, R.; Mestre, J.C.; Woerner, S. Credit Risk Analysis Using Quantum Computers. *IEEE Transactions on Computers* **2021**, *70*, 2136–2145..
720. Saunders, A.; Allen, L. *Credit risk measurement*, 2nd ed ed.; Number v.154 in Wiley Finance, John Wiley: New York, **2002**, p. 258-275.
721. Crouhy, M.; Galai, D.; Mark, R. *Risk management*, [reprint] ed.; McGraw-Hill: New York [u.a.], **2009**.
722. Thomas, L.C.; Edelman, D.; Crook, J.N. *Credit scoring and its applications*, second edition ed.; Number 2 in Mathematics in industry, SIAM, Society for Industrial and Applied Mathematics: Philadelphia, **2017**.
723. Teles, G.; Rodrigues, J.J.P.C.; Saleem, K.; Kozlov, S.; Rabêlo, R.A.L. Machine learning and decision support system on credit scoring. *Neural Computing and Applications* **2019**, *32*, 9809–9826.
724. Dastile, X.; Celik, T.; Potsane, M. Statistical and machine learning models in credit scoring: A systematic literature survey. *Applied Soft Computing* **2020**, *91*, 106263.
725. Ala'raj, M.; Abbod, M.F.; Majdalawieh, M.; Jum'a, L. A deep learning model for behavioural credit scoring in banks. *Neural Computing and Applications* **2022**, *34*, 5839–5866.
726. Bluhm, C.; Overbeck, L.; Wagner, C. *Introduction to Credit Risk Modeling*, second edition ed.; Chapman & Hall/CRC Financial Mathematics Series, CRC Press: Boca Raton, **2010**.
727. Dri, E.; Aita, A.; Giusto, E.; Ricossa, D.; Corbelletto, D.; Montrucchio, B.; Ugoccioni, R. A More General Quantum Credit Risk Analysis Framework. *Entropy* **2023**, *25*, 593.
728. Sironi, A.; Resti, A. *Risk management and shareholders' value in banking*; Wiley finance, Wiley: Chichester, West Sussex [England], **2007**, pages 759-770.
729. Rockafellar, R.T.; Uryasev, S. Optimization of conditional value-at-risk. *The Journal of Risk* **2000**, *2*, 21–41.
730. Glasserman, P. Measuring Marginal Risk Contributions in Credit Portfolios. *SSRN Electronic Journal* **2005**.
731. Tasche, D. Capital Allocation to Business Units and Sub-Portfolios: the Euler Principle. *arXiv* **2007**.
732. Rutkowski, M.; Tarca, S. Regulatory Capital Modelling for Credit Risk. *International Journal of Theoretical and Applied Finance* **2015**, *18*, 1550034.
733. World Bank Group. Credit Scoring Approaches Guidelines, 2019.
734. Dastile, X.; Çelik, T.; Potsane, M.M. Statistical and machine learning models in credit scoring: A systematic literature survey. *Appl. Soft Comput.* **2020**, *91*, 106263.
735. Wang, Y.; Hu, Z.; Sanders, B.C.; Kais, S. Qudits and High-Dimensional Quantum Computing. *Frontiers in Physics* **2020**, *8*.
736. Milne, A.; Rounds, M.; Goddard, P. Optimal feature selection in credit scoring and classification using a quantum annealer, 2017.
737. Mancilla, J.; Sequeira, A.; Tagliani, T.; Llaneza, F.; Beiza, C. Empowering Credit Scoring Systems with Quantum-Enhanced Machine Learning. *arXiv preprint* **2024**.
738. Schetakis, N.; Aghamalyan, D.; Boguslavsky, M.; Rees, A.; Rakotomalala, M.; Griffin, P.R. Quantum Machine Learning for Credit Scoring. *Mathematics* **2024**, *12*, 1391.
739. Minati, R.; Hema, D. Quantum Powered Credit Risk Assessment: A Novel Approach using hybrid Quantum-Classical Deep Neural Network for Row-Type Dependent Predictive Analysis. *arXiv* **2025**.
740. Chen, C.M.; Tso, G.K.F.; He, K. Quantum Optimized Cost Based Feature Selection and Credit Scoring for Mobile Micro-financing. *Computational Economics* **2023**, *63*, 919–950.
741. Finance, U. Annual Fraud Report, 2024. Accessed: 2024-10-07.
742. Government, U. Economic Crime and Corporate Transparency Act, 2023.
743. Yndurain, E.; Woerner, S.; Egger, D. Exploring quantum computing use cases for financial services, 2019. Last accessed: 20-05-2022.
744. Berkson, J. Application of the Logistic Function to Bio-Assay. *Journal of the American Statistical Association* **1944**, *39*, 357–365.
745. Balcan, M.F.; Sharma, D. Learning accurate and interpretable tree-based models, 2025.
746. Louppe, G. Understanding Random Forests: From Theory to Practice, 2015.
747. Moguerza, J.M.; Muñoz, A. Support Vector Machines with Applications. *Statistical Science* **2006**, *21*.
748. Chen, Y.; Zhao, C.; Xu, Y.; Nie, C. Year-over-Year Developments in Financial Fraud Detection via Deep Learning: A Systematic Literature Review, 2025.
749. Zhang, Z.; Zhou, X.; Zhang, X.; Wang, L.; Wang, P. A Model Based on Convolutional Neural Network for Online Transaction Fraud Detection. *Security and Communication Networks* **2018**, *2018*, 5680264.
750. Khalid, A.R.; Owoh, N.; Uthmani, O.; Ashawa, M.; Osamor, J.; Adejoh, J. Enhancing Credit Card Fraud Detection: An Ensemble Machine Learning Approach. *Big Data and Cognitive Computing* **2024**, *8*.

 doi:10.20944/preprints202511.1802.v2

751. Grossi, M.; Ibrahim, N.; Radescu, V.; Loredo, R.; Voigt, K.; Altrock, C.V.; Rudnik, A. Mixed Quantum-Classical Method For Fraud Detection with Quantum Feature Selection, 2022..
752. Marini, F.; Muthu, K.; Singh, K.; Capozi, M. How Deloitte Italy built a digital payments fraud detection solution using quantum machine learning and Amazon Braket, 2024.
753. Herr, D.; Obert, B.; Rosenkranz, M. Anomaly detection with variational quantum generative adversarial networks. *Quantum Science and Technology* **2021**, *6*, 045004.
754. Islam, M.; Turkeli, S.; Ozaydin, F. A Survey of Quantum Generative Adversarial Networks: Architectures, Use Cases, and Real-World Implementations, 2025.
755. Ezugwu, A.E.; Ikotun, A.M.; Oyelade, O.O.; Abualigah, L.; Agushaka, J.O.; Eke, C.I.; Akinyelu, A.A. A Comprehensive Survey of Clustering Algorithms: State-of-the-Art Machine Learning Applications, Taxonomy, Challenges, and Future Research Prospects. *Eng. Appl. Artif. Intell.* **2022**, *110*.
756. Implementing Technology Change, 2021.
757. of Standards, N.I.; Technology. Post-Quantum Cryptography. Accessed: 2025-09-11.
758. Dahmen-Lhuissier, S. Quantum-Safe Cryptography (QSC).
759. Gross, G. IETF launches post-quantum encryption working group, 2023. publisher: IETF.
760. Swayne, M. Quantum Economics: Could a New Economic Paradigm Be Guided by Quantum Models?, 2024. Last accessed: 01-07-2025.
761. Orrell, D.; Houshmand, M. Quantum Propensity in Economics. *Frontiers in Artificial Intelligence* **2022**, *4*.
762. Trisetyarso, A. Quantum Computational Economics. *Procedia Computer Science* **2023**, *216*, 3. 7th International Conference on Computer Science and Computational Intelligence 2022.
763. Holtfort, T.; Horsch, A. Quantum Economics: A Systematic Literature Review. *SocioEconomic Challenges* **2024**, pp. 62–77.
764. Varian, H.R. *Computational Economics and Finance Modeling And Analysis With Mathematica*; Springer, 2011; p. 482.
765. Samuelson, L. Game Theory in Economics and Beyond. *Journal of Economic Perspectives* **2016**, *30*, 107–130.
766. Cristelli, M.; Pietronero, L.; Zaccaria, A. Critical Overview of Agent-Based Models for Economics. *arXiv* **2011**.
767. Axtell, R.L.; Farmer, J.D. Agent-Based Modeling in Economics and Finance: Past, Present, and Future. *Journal of Economic Literature* **2025**, *63*, 197–287.
768. Seuring, S. A review of modeling approaches for sustainable supply chain management. *Decision Support Systems* **2013**, *54*, 1513–1520.
769. Aaronson, S. Quantum copy-protection and quantum money. *Proceedings of the 24th Annual IEEE Conference on Computational Complexity* **2009**, pp. 229–242.
770. Lutomirski, A.; Aaronson, S.; Farhi, E.; Gosset, D.; Hassidim, A.; Kelner, J.; Shor, P. Breaking and making quantum money: toward a new quantum cryptographic protocol. *Innovations in Computer Science - ICS 2010, Tsinghua University, Beijing, China, January 5-7, 2010. Proceedings, 20-31, 978-7-302-21752-7 Tsinghua University Press* **2009**..
771. Aaronson, S.; Christiano, P. Quantum money from hidden subspaces. In Proceedings of the Proceedings of the forty-fourth annual ACM symposium on Theory of computing. ACM, 2012, STOC'12, pp. 41–60.
772. Farhi, E.; Gosset, D.; Hassidim, A.; Lutomirski, A.; Shor, P. Quantum money from knots. In Proceedings of the Proceedings of the 3rd Innovations in Theoretical Computer Science Conference. ACM, **2012**, ITCS '12, pp. 276–289.
773. Zhandry, M. Quantum Lightning Never Strikes the Same State Twice. Or: Quantum Money from Cryptographic Assumptions. *Journal of Cryptology* **2021**, *34*.
774. Zhandry, M., Quantum Lightning Never Strikes the Same State Twice. In *Advances in Cryptology – EUROCRYPT 2019*; Springer International Publishing, **2019**; pp. 408–438.
775. Gavinsky, D. Quantum Money with Classical Verification. In Proceedings of the 2012 IEEE 27th Conference on Computational Complexity. IEEE, **2012**, pp. 42–52.
776. Mosca, M.; Stebila, D. Quantum Coins. *Error-Correcting Codes, Finite Geometries and Cryptography. Contemporary Mathematics, volume 523, pages 35-47. American Mathematical Society, 2010* **2009**.
777. Tokunaga, Y.; Okamoto, T.; Imoto, N. Anonymous quantum cash. In Proceedings of the ERATO Conference on Quantum Information Science, **2003**.
778. Ji, Z.; Liu, Y.K.; Song, F., Pseudorandom Quantum States. In *Advances in Cryptology – CRYPTO 2018*; Springer International Publishing, **2018**; pp. 126–152.
779. Behera, A.; Sattath, O. Almost Public Quantum Coins. *arXiv preprint* **2020**..

 doi:10.20944/preprints202511.1802.v2

780. Radian, R.; Sattath, O. Semi-Quantum Money. Cryptology ePrint Archive, Paper 2020/414, **2020**.
781. Amos, R.; Georgiou, M.; Kiayias, A.; Zhandry, M. One-shot signatures and applications to hybrid quantum/classical authentication. In Proceedings of the Proceedings of the 52nd Annual ACM SIGACT Symposium on Theory of Computing. ACM, **2020**, STOC '20, pp. 255–268.
782. Tapscott, D.; Tapscott, A. *The Blockchain Revolution*; Penguin USA, Inc. in New York, **2016**.
783. Coladangelo, A.; Sattath, O. A Quantum Money Solution to the Blockchain Scalability Problem. *Quantum* **2020**, *4*, 297.
784. Edwards, M.; Mashatan, A.; Ghose, S. A review of quantum and hybrid quantum/classical blockchain protocols. *Quantum Information Processing* **2020**, *19*.
785. Bilyk, A.; Doliskani, J.; Gong, Z. Cryptanalysis of three quantum money schemes. *Quantum Information Processing* **2023**, *22*.
786. Bozzio, M.; Orieux, A.; Trigo Vidarte, L.; Zaquine, I.; Kerenidis, I.; Diamanti, E. Experimental investigation of practical unforgeable quantum money. *npj Quantum Information* **2018**, *4*.
787. Bozzio, M.; Diamanti, E.; Grosshans, F. Semi-device-independent quantum money with coherent states. *Physical Review A* **2019**, *99*, 022336.
788. Kent, A.; Lowndes, D.; Pitalúa-García, D.; Rarity, J. Practical quantum tokens without quantum memories and experimental tests. *npj Quantum Information* **2022**, *8*.
789. Liberto, D. Economic Forecasting: Definition, Use of Indicators, and Example, 2024. Accessed: 2025-08-29.
790. Hamilton, J.D. *Time series analysis*; Princeton University Press: Princeton, N.J, **1994**.
791. Kirchgässner, G.; Wolters, J.; Hassler, U. *Introduction to Modern Time Series Analysis*, second edition ed.; SpringerLink, Springer: Berlin, Heidelberg, **2013**.
792. Gohel, P.; Joshi, M. Quantum time series forecasting. In Proceedings of the Sixteenth International Conference on Machine Vision (ICMV 2023); Osten, W., Ed. SPIE, **2024**, p. 39.
793. Granger, C.W.J.; Newbold, P.; Shell, K. *Forecasting Economic Time Series*, 2. aufl. ed.; Economic theory, econometrics, and mathematical economics, Elsevier Reference Monographs: [s.l.], **2014**.
794. Ryan Tibshirani. ARIMA Models Lecture Notes, 2023. Accessed: 2025-08-29.
795. Kontopoulou, V.I.; Panagopoulos, A.D.; Kakkos, I.; Matsopoulos, G.K. A Review of ARIMA vs. Machine Learning Approaches for Time Series Forecasting in Data Driven Networks. *Future Internet* **2023**, *15*, 255.
796. Francq, C.; Zakoïan, J.M. *GARCH models*, second edition ed.; ProQuest Ebook Central, Wiley: Hoboken, NJ, **2019**. Aus dem Französischen übersetzt.
797. Khodarahmi, M.; Maihami, V. A Review on Kalman Filter Models. *Archives of Computational Methods in Engineering* **2022**, *30*, 727–747.
798. Daskin, A. A walk through of time series analysis on quantum computers. *arXiv* **2022**.
799. Emmanoulopoulos, D.; Dimoska, S. Quantum Machine Learning in Finance: Time Series Forecasting. *arXiv preprint* **2022**.
800. Hirth, A.; Droguett, E.L. State of Quantum RNNs for Time-Series Forecasting. In Proceedings of the 2025 Annual Reliability and Maintainability Symposium (RAMS). IEEE, 2025, pp. 1–6.
801. Jones, C.; Kraus, N.; Bhardwaj, P.; Adler, M.; Schrödl-Baumann, M.; Manrique, D.Z. Benchmarking Quantum Models for Time-Series Forecasting. In Proceedings of the 2024 IEEE International Conference on Quantum Computing and Engineering (QCE). IEEE, 2024, pp. 22–27.
802. Lu, Y.; Shen, M.; Wang, H.; Wang, X.; van Rechem, C.; Fu, T.; Wei, W. Machine Learning for Synthetic Data Generation: A Review, 2025.
803. Assefa, S.A.; Dervovic, D.; Mahfouz, M.; Tillman, R.E.; Reddy, P.; Veloso, M. Generating synthetic data in finance: opportunities, challenges and pitfalls. In Proceedings of the Proceedings of the First ACM International Conference on AI in Finance, New York, NY, USA, 2021; ICAIF '20.
804. Ramzan, F.; Sartori, C.; Consoli, S.; Reforgiato Recupero, D. Generative Adversarial Networks for Synthetic Data Generation in Finance: Evaluating Statistical Similarities and Quality Assessment. *AI* **2024**, *5*, 667–685.
805. Potluru, V.K.; Borrajo, D.; Coletta, A.; Dalmasso, N.; El-Laham, Y.; Fons, E.; Ghassemi, M.; Gopalakrishnan, S.; Gosai, V.; Kreačić, E.; et al. Synthetic Data Applications in Finance, 2024.
806. Figueira, A.; Vaz, B. Survey on Synthetic Data Generation, Evaluation Methods and GANs. *Mathematics* **2022**, *10*..
807. Chen, J.; Hull, J.C.; Poulos, Z.; Rasul, H.; Veneris, A.G.; Wu, Y. A Variational Autoencoder Approach to Conditional Generation of Possible Future Volatility Surfaces. *SSRN Electronic Journal* **2023**.
808. Acciaio, B.; Eckstein, S.; Hou, S. Time-Causal VAE: Robust Financial Time Series Generator, 2024.
809. Cont, R.; Cucuringu, M.; Xu, R.; Zhang, C. Tail-GAN: Learning to Simulate Tail Risk Scenarios, 2025.

 doi:10.20944/preprints202511.1802.v2

810. Chen, L. Risk Management with Feature-Enriched Generative Adversarial Networks (FE-GAN), 2024.
811. Na, A.; Zhang, M.; Wan, J. Computing Volatility Surfaces using Generative Adversarial Networks with Minimal Arbitrage Violations, 2023.
812. Marti, G. CORRGAN: Sampling Realistic Financial Correlation Matrices Using Generative Adversarial Networks. In Proceedings of the ICASSP 2020 - 2020 IEEE International Conference on Acoustics, Speech and Signal Processing (ICASSP), 2020, pp. 8459–8463.
813. Milena Vuletić, F.P.; Cucuringu, M. Fin-GAN: forecasting and classifying financial time series via generative adversarial networks. *Quantitative Finance* **2024**, *24*, 175–199..
814. Guo, X.; Chen, Y. Generative AI for Synthetic Data Generation: Methods, Challenges and the Future, 2024.
815. Takahashi, S.; Chen, Y.; Tanaka-Ishii, K. Modeling financial time-series with generative adversarial networks. *Physica A: Statistical Mechanics and its Applications* **2019**, *527*, 121261.
816. Caprioli, S.; Cagliero, E.; Crupi, R. Quantifying Credit Portfolio sensitivity to asset correlations with interpretable generative neural networks, 2023.
817. Vieloszynski, A.; Cherkaoui, S.; Ahmad, O.; Laprade, J.F.; Nahman-Lévesque, O.; Aaraba, A.; Wang, S. LatentQGAN: A Hybrid QGAN with Classical Convolutional Autoencoder, 2024.
818. Ganguly, S. Implementing Quantum Generative Adversarial Network (qGAN) and QCBM in Finance, 2023.
819. Coopmans, L.; Benedetti, M. On the sample complexity of quantum Boltzmann machine learning. *Communications Physics* **2024**, *7*.
820. Salloum, H.; Salloum, A.; Mazzara, M.; Zykov, S. Quantum Annealing in Machine Learning: QBoost on D-Wave Quantum Annealer. *Procedia Computer Science* **2024**, *246*, 3285–3293. 28th International Conference on Knowledge Based and Intelligent information and Engineering Systems (KES 2024)..
821. Maheshwari, D.; Sierra-Sosa, D.; Garcia-Zapirain, B. Variational Quantum Classifier for Binary Classification: Real vs Synthetic Dataset. *IEEE Access* **2022**, *10*, 3705–3715.
822. Pires, O.M.; Nooblath, M.Q.; Silva, Y.A.C.; da Silva, M.H.F.; Galvão, L.Q.; Albino, A.S. Synthetic data generation with hybrid quantum-classical models for the financial sector. *The European Physical Journal B* **2024**, *97*, 178.
823. Guryanova, L.S.; Gvozdytskyi, V.S.; Dymchenko, O.V.; Rudachenko, O.A. Models of Forecasting in the Mechanism of Early Informing and Prevention of Financial Crises in Corporate Systems. *Financial and credit activity problems of theory and practice* **2018**, *3*, 303–312.
824. Greenwood, R.; Hanson, S.G.; Shleifer, A.; Sørensen, J.A. Predictable Financial Crises, 2021.
825. Elliott, M.; Golub, B.; Jackson, M.O. Financial Networks and Contagion. *American Economic Review* **2014**, *104*, 3115–3153.
826. Ding, Y.; Gonzalez-Conde, J.; Lamata, L.; Martín-Guerrero, J.D.; Lizaso, E.; Mugel, S.; Chen, X.; Orús, R.; Solano, E.; Sanz, M. Toward Prediction of Financial Crashes with a D-Wave Quantum Annealer. *Entropy* **2023**, *25*, 323.
827. Orús, R.; Mugel, S.; Lizaso, E. Forecasting financial crashes with quantum computing. *Phys. Rev. A* **2019**, *99*, 060301.
828. Fellner, M.; Ender, K.; ter Hoeven, R.; Lechner, W. Parity Quantum Optimization: Benchmarks, 2021.
829. National Quantum Computing Centre (NQCC). Quantum Computing Scalability Conference 2025, 2025. Accessed: 2025-05-07.
830. Aharonov, D.; Ben-Or, M. Fault-Tolerant Quantum Computation With Constant Error Rate, 1999.
831. Knill, E.; Laflamme, R.; Zurek, W.H. Resilient Quantum Computation. *Science* **1998**, *279*, 342–345.
832. Kitaev, A. Fault-tolerant quantum computation by anyons. *Annals of Physics* **2003**, *303*, 2–30..
833. von Neumann, J., Probabilistic Logics and the Synthesis of Reliable Organisms From Unreliable Components. In *Automata Studies. (AM-34), Volume 34*; Princeton University Press, 2016; pp. 43–98.
834. Ryan-Anderson, C.; Bohnet, J.; Lee, K.; Gresh, D.; Hankin, A.; Gaebler, J.; Francois, D.; Chernoguzov, A.; Lucchetti, D.; Brown, N.; et al. Realization of Real-Time Fault-Tolerant Quantum Error Correction. *Physical Review X* **2021**, *11*, 041058.
835. Google Quantum AI. Suppressing quantum errors by scaling a surface code logical qubit. *Nature* **2023**, *614*, 676–681.
836. Bluvstein, D.; Evered, S.J.; Geim, A.A.; Li, S.H.; Zhou, H.; Manovitz, T.; Ebadi, S.; Cain, M.; Kalinowski, M.; Hangleiter, D.; et al. Logical quantum processor based on reconfigurable atom arrays. *Nature* **2023**, *626*, 58–65.

 doi:10.20944/preprints202511.1802.v2

837. Liao, H.; Hartnett, G.S.; Kakkar, A.; Tan, A.; Hush, M.; Mundada, P.S.; Biercuk, M.J.; Baum, Y. Achieving computational gains with quantum error correction primitives: Generation of long-range entanglement enhanced by error detection. *arXiv* **2024**.
838. Bravyi, S.; Cross, A.W.; Gambetta, J.M.; Maslov, D.; Rall, P.; Yoder, T.J. High-threshold and low-overhead fault-tolerant quantum memory. *Nature* **2024**, *627*, 778–782.
839. Department for Science, Innovation and Technology. National Quantum Strategy Missions, 2023. Accessed: 2025-05-07.
840. Couteau, C. Quantum computing using photons. *The European Physical Journal A* **2025**, *61*.
841. Kaggle. Datasets, n.d. Retrieved May 7, 2025.
842. Davis, T.A.; Hu, Y. The university of Florida sparse matrix collection. *ACM Transactions on Mathematical Software* **2011**, *38*, 1–25.
843. Kolodziej, S.; Aznaveh, M.; Bullock, M.; David, J.; Davis, T.; Henderson, M.; Hu, Y.; Sandstrom, R. The SuiteSparse Matrix Collection Website Interface. *Journal of Open Source Software* **2019**, *4*, 1244.
844. GQI, G.Q.I. Midstack Focus Report with Classiq, 2023.
845. GQI, G.Q.I. Midstack Focus Report with QuantrolOX, 2023.
846. GQI, G.Q.I. Midstack Focus Report with QEDMA, 2023.
847. Faro, I.; Sitdikov, I.; Valiñas, D.G.; Fernandez, F.J.M.; Codella, C.; Glick, J. Middleware for Quantum: An orchestration of hybrid quantum-classical systems. In Proceedings of the 2023 IEEE International Conference on Quantum Software (QSW). IEEE, 2023..
848. Ostrander, A.J. Quantum Algorithms for Differential Equations. phdthesis, University of Maryland, College Park, United States – Maryland, 2019.
849. Jordan, S.P.; Shutty, N.; Wootters, M.; Zalcman, A.; Schmidhuber, A.; King, R.; Isakov, S.V.; Khattar, T.; Babbush, R. Optimization by Decoded Quantum Interferometry, 2025.
850. Zeitgeist, Q. Exploring QRAM: The Daring Quest For Quantum Memory Persistence, 2024.
851. Physics World. On the path towards a quantum economy, 2025. Accessed: 2025-05-08.
852. Ciceri, A.; Cottrell, A.; Freeland, J.; Fry, D.; Hirai, H.; Intallura, P.; Kang, H.; Lee, C.K.; Mitra, A.; Ohno, K.; et al. Enhanced fill probability estimates in institutional algorithmic bond trading using statistical learning algorithms with quantum computers. *arXiv* **2025**.
853. Agliardi, G.; Alevras, D.; Kumar, V.; Nardo, R.L.; Compostella, G.; Kumar, S.; Proissl, M.; Mehta, B. Portfolio construction using a sampling-based variational quantum scheme. *arXiv* **2025**.
854. Markham, C.; Grassie, R. Quantum computing applications in financial services. Technical report, Financial Conduct Authority, 2025.
855. Hughes, A.C.; Srinivas, R.; Löschnauer, C.M.; Knaack, H.M.; Matt, R.; Ballance, C.J.; Malinowski, M.; Harty, T.P.; Sutherland, R.T. Trapped-ion two-qubit gates with >99.99% fidelity without ground-state cooling, 2025.
856. Abanin, D.A.; et al. Observation of constructive interference at the edge of quantum ergodicity. *Nature* **2025**, *646*, 825–830.
857. Foundation, T.N. Nobel Prize in Physics 2025 - Press Release, 2025. Last accessed: 27-10-2025.
858. Eisert, J.; Preskill, J. Mind the gaps: The fraught road to quantum advantage *arXiv* **2025**.